ADSORPTION OF BILE ACIDS BY

ION-EXCHANGE RESINS

by

Danièle LEONARD

A Thesis Submitted to the Faculty of Graduate Studies and Research in Partial Fulfillment of the Requirements for the Degree of Doctor of Philosophy

Department of Chemistry
McGill University
Montréal, Québec, Canada

December, 1989

Ph.D **Chemistry**

D. Léonard

Adsorption of Bile Acids by Ion-Exchange Resins

Abstract

The interactions of cholestyramine with bile acids in aqueous buffer solutions were studied by ***in vitro*** adsorption experiments. Application of the Donnan theory, which is based on ion partitioning between two phases, indicates that the adsorption is an ion-exchange process - the bile acid anion displaces the chloride counter-ion of cholestyramine. Donnan considerations indicate that the bile acid in the resin phase exists in two forms, bound and unbound, but at higher Ceq the bound form is increasingly favoured. Since the concentrations of bound bile acid in the resin phase are above the critical micellar concentration, micelle-type ordering is occurring. It is also possible that the unbound bile acid in the resin phase aggregates to form "regular" micelles. The micellization promotes the partitioning of glycocholic acid into the resin phase, explaining the ability of cholestyramine to adsorb glycocholic acid significantly, ***in vitro***.

Ion-exchange resins were prepared by solid phase peptide synthesis with active sites chosen to resemble those of cholestyramine. They were produced by coupling 4-(aminomethyl)benzoic acid, 4-aminophenylacetic acid or 4-(aminomethyl)phenylacetic acid to the backbone. The ion-exchange resins were prepared both as primary amines and in the quaternized form. The cholestyramine-like sorbents were synthesized with systematic changes in the structure, e.g., change from a hydrophobic to a hydrophilic backbone; the incorporation of an ala_3 spacer between the backbone and the active site; the

change in the position of the methylene group from being between the phenyl ring and the amino group to being between the phenyl ring and the carbonyl group; the change of primary amines to quaternary ammonium groups; the change in functionality, to determine which structural parts of cholestyramine are involved in the adsorption process. As compared to cholestyramine, both sets of resins were remarkably ineffective in adsorbing bile acids ***in vitro***. It was found that the nature of the backbone determines the accessibility to the active site; that the resins with the methylene group positioned between the phenyl group and the amino group have higher adsorption capacity for glycocholic acid; and that quaternization increases the adsorption capacity. The two latter observations indicate the importance of the basicity of the active site. Therefore, in cholestyramine, the backbone is such that it permits the transfer of ionic species and the quaternary ammonium group is involved in the interaction with bile acids. These results confirm that ion-exchange is the mode of interaction.

Computer modelling showed that the cholestyramine pendants are close to one another and are separated by benzene rings, thus leaving too little space between them to allow a bile acid molecule to interact with the benzene rings. Therefore, the bile acids must interact with the quaternary ammonium group, leaving the bile acid molecule inside the cavity where they interact with one another to form micelles. The possible modes of interactions of bile acids with the synthesized resins are more numerous since the pendants are not as close together. Thus, interactions with both the amino group and with the hydrophobic part of the pendant are possible.

Ph.D **Chimie**

D. Léonard

L'Adsorption des Acides Biliaires par des Résines Echangeuses d'Ions

Résumé

Les interactions, ***in vitro***, entre la cholestyramine et les acides biliaires, en solutions aqueuses tamponnées, ont été étudiées par des expériences d'adsorption. Les résultats indiquent que la cholestyramine interagit avec les acides biliaires par un mécanisme d'échange d'ions; le contre-ion de la cholestyramine est échangé pour un acide biliaire. Ce phénomène peut être expliqué par la théorie de Donnan. Les acides biliaires dans la résine sont soit liés au pendant de la cholestyramine ou soit non-liés, mais à des concentrations à l'équilibre plus élevées, la forme liée étant favorisée. La concentration des acides biliaires liés dans la résine est dans la région de celle où ils peuvent interagir entre eux pour former des micelles. Le même phénomène est aussi possible pour les acides biliaires non-liés. La micellisation encourage l'entrée des ions glycocholate dans la résine, expliquant ainsi la capacité élevée de la cholestyramine pour les acides biliaires, ***in vitro***.

Des résines échangeuses d'ions ont été préparées par la synthèse de peptides en phase solide. Elles avaient soit un support de polyacrylamide réticulé hydrophile ou un support polymérique de Merrifield hydrophobe. Les chaînes sur le support polymérique étaient soit l'acide 4-(aminométhyle)benzoique, l'acide 4-aminophénylacétique ou l'acide 4-(aminométhyle)phénylacétique. Ces résines ont été premièrement obtenues dans leur forme d'amine primaire; elles furent quaternisées pour obtenir l'amine quaternaire. En comparant les résines qui ne

sont différentes que par une caractéristique (par exemple: le support polymérique utilisé; la présence de trois alanines entre la chaîne et le support polymérique; la position du groupe méthylène; l'amine primaire ou l'amine quaternaire; la variation de la fonctionnalité), il est possible de déterminer quelles sont les parties structurales de la cholestyramine qui sont responsables de l'interaction avec les acides biliaires. Toutes ces résines ont été étudiées pour leur adsorption, ***in vitro***, des acides biliaires et ces adsorptions étaient basses. Il a été conclu que la nature du support polymérique influence l'accessibilité au site actif; la présence du groupe méthylène entre le groupement phényl et l'amine augmente l'adsorption; et que les résines avec l'amine quaternaire adsorbent mieux que celles avec l'amine primaire. Ces deux dernière observations indiquent l'importance de la basicité du groupe actif. Donc, la cholestyramine est efficace à adsorber les acides biliaires grâce à son support polymérique qui permet le transfert des ions et grâce à la présence de l'amine quaternaire. De ces résultats, le mécanisme d'échange d'ions a été réaffirmé.

Les interactions entre la cholestyramine ou les résines synthétisées et les acides biliaires furent aussi étudiées qualitativement à l'aide de modèles moléculaires. Il a été trouvé que les groupes actifs de la cholestyramine sont près les uns des autres et sont séparés par des groupements phényles, ce qui laisse peu de place entre eux pour permettre des interactions avec les acides biliaires. Alors, les acides biliaires interagissent avec les amines quaternaires les laissant dans la cavité de la cholestyramine permettant ainsi des interactions entre eux pour former des micelles. Les résines synthétisées peuvent interagir avec les acides biliaires par leurs groupements amines et aussi par des interactions hydrophobes puisque les groupes actifs ne sont pas aussi près les uns des autres.

à mes parents

ACKNOWLEDGEMENTS

I would like to give my greatest thanks to my research director Dr. G R. Brown for all of the guidance, and continual understanding throughout my stay in his laboratory.

I would also like to thank:

The Chemistry Department of McGill University, for teaching assistantship;

FCAR for financial assistance in the form of a post-graduate scholarship;

Dr. L.E. St-Pierre, for his advice and encouragement;

Dr. S.-D. Clas, for many valuable discussions and her friendship;

Dr. A.M. Scallan, of the Pulp and Paper Research Institute of Canada in Pointe-Claire, for suggesting the possibility of using Donnan theory and helping me reach a better understanding of it;

Dr. J.F. Britton, for introducing me to the basic concepts of molecular modelling;

Dr. X.X. Zhu, for the use of the computer program for the analysis of the bile acid data;

My co-workers, past and present, for their friendship, patience and helpful discussions.

A special thanks to my best friend, Dr. Franco Sandrin, for helping me through all these years and for always believing in me.

Finalement, je veux remercier de tout coeur mes parents pour leur compréhension, leur patience, leur aide et pour m'avoir toujours encouragée.

TABLE OF CONTENTS

APPENDICES

LIST OF FIGURES

CHAPTER 1

CHAPTER 2

CHAPTER 3

CHAPTER 4

CHAPTER 6

LIST OF TABLES

CHAPTER 2

CHAPTER 3

CHAPTER 4

LIST OF ABBREVIATIONS AND SYMBOLS

The abbreviations and symbols for the physical and chemical terms and units used in this thesis are in accordance with those adopted by IUPAC (International Union of Pure and Applied Chemistry), IUPAP (International Union of Pure and Applied Physics) and IUB (International Union of Biochemistry), published in the Handbook of Chemistry and Physics. Some of the abbreviations and symbols used are listed below.

a	activity
ala	alanine
B^+	fixed ionic group
BA	fixed ionic group bound to bile acid
BCl	fixed ionic group bound to chloride
t-Boc	di-tert-butyl-dicarbonate
BOH	fixed ionic group bound to hydroxyl group
c	concentration by volume
C	concentration of fixed ionic groups
Ceq, A	concentration at equilibrium
CA	cholic acid
CA Cl	cholestyramine with chloride as counter-ion
CA I	cholestyramine with iodide as counter-ion
CMC	critical micellar concentration
CMT	critical micellar temperature
Corr	correlation
DCC	dicyclohexylcarbodiimide
DCM	dichloromethane
DCU	dicyclohexylurea
DEPT	distortionless enhancement by polarization transfer
DG	diglyceride
DIEA	diisopropyl ethylamine
dL	deciliter (10^{-1} L)
DMF	dimethylformamide

eq pndnt	equivalent of pendant
f(x), E_s	potential energy
F	Faraday's constant
FA	fatty acids
g	gram
GCA	glycocholic acid
HDL	high-density lipoprotein
HMG-CoA reductase	3-hydroxy-3-methylglutaryl-coenzyme A reductase
HPLC	high pressure (or performance) liquid chromatography
HSA	human serum albumin
3α-HSD	3α-hydroxysteroid dehydrogenase
K_1	dissociation constant
K_a	acidity constant
K_b	basicity constant
k_f	measure of the capacity of adsorption
K_f	formation constant
k_i	site binding constant
k_i'	site binding constant from the modified Scatchard model
K_i	stoichiometric binding constant
K_i'	stoichiometric binding constant from the modified Scatchard model
kcal	kilocalorie
K_w	ionization constant of water
LDL	low-density lipoprotein
M	concentration in molarity (mole/liter solution)
mg	miligram (10^{-3} g)
MG	monoglycerol
mM	millimole/liter
mol	mole
mmol	millimole (10^{-3} mol)
mp	melting point
MW	molecular weight

n	number of available sites
	number of Faradays of charge passing through a membrane
N	concentration in normality (normal/liter solution)
NaC	sodium cholate
NADH	reduced nicotinamide adenine dinucleotide
NaGCA	sodium glycocholate
nm	nanometer (10^{-9} m)
NMR, nmr	nuclear magnetic resonance
ODS	octadecylsilyl
p	measure of the strength of adsorption
P	phosphate
PP	pyrophosphate
ppm	parts per million (unit for nmr chemical shift)
r	mole of bound adsorbate per unit weight of adsorbent
R	measure of the fit
	gas constant (8.3143 $JK^{-1}mol$)
RIA	radioimmunoassay
RT	retention time
SPPS	solid phase peptide synthesis
T	temperature
TG	triacylglycerol
THF	tetrahydrofuran
TLC, tlc	thin layer chromatography
TNH_2	tris-(hydroxymethyl)aminomethane
TPNH	hydrogen triphosphopyridine nucleotide
Tris-HCl	tris-(hydroxymethyl)aminomethane
UV	ultraviolet
V	volume
VLDL	very-low-density lipoprotein
X	mole of bound bile acid per equivalent of pendant
$[\alpha]$	specific optical rotation
Φ	electrostatic potential
λ	Donnan partition coefficient

μ	electrochemical potential
μL	microliter (10^{-6} L)

1 INTRODUCTION

Cardiovascular diseases are a major cause of death among North American adults (1-6). However, increased awareness of the role of cholesterol has resulted in a gradual decrease in the death rate due to heart problems. It is now well recognized that a high level of cholesterol (hypercholesterolemia) is associated with coronary artery diseases, which may lead to angina, myocardial infarction, and peripheral vascular diseases (6). Serum cholesterol levels can be reduced in part by careful attention to the diet, and in addition, use can be made of drugs such as orally ingested bile acid binding resins and cholesterol-lowering drugs.

1.1 METABOLISM OF CHOLESTEROL

Cholesterol, a fat like substance (lipid) (Figure 1.1), is a structural component in cellular and extracellular membranes (7), giving them stiffness and better protection from natural deformation (8), and is found in all vertebrates It is synthesized in all cells and is vital for their function and growth. The synthesis follows a lengthy biochemical pathway, shown schematically in Figure 1.2, and occurs chiefly in liver cell microsomes (9-11). Twenty-six separate enzymatic reactions are involved in this biochemical conversion of acetate to cholesterol, the major intermediates being mevalonic acid and squalene (12).

Cells are able to regulate their cholesterol synthesis as well as their uptake, release and storage to maintain the optimum cholesterol concentration for their functions. In some cells this regulation is very efficient. However, under certain conditions, such as a higher concentration of cholesterol in the blood than necessary for a cell to function, it becomes less effective and this external factor can override the internal mechanism of the cell. Thus, the metabolism of

cholesterol is subject to a delicate balance which, if disturbed, can cause an accumulation of cholesterol (in their ester form) in artery walls, subsequently causing coronary artery problems.

When dietary cholesterol is available, the liver uses that source of sterol. However, when there is insufficient cholesterol in the diet, the liver synthesizes its own (14, 15), by increasing the activity of a rate controlling enzyme, 3-hydroxy-3-methylglutaryl coenzyme A reductase (E.C. 1.1.1.3.4 HMG CoA reductase) (16, 17).

Cholesterol is eliminated either by conversion, in the liver, to bile acids and sterol hormones, e.g., progesterone, or by secretion into the bile. The conversion of cholesterol to bile acids is the main process by which the body eliminates cholesterol (8).

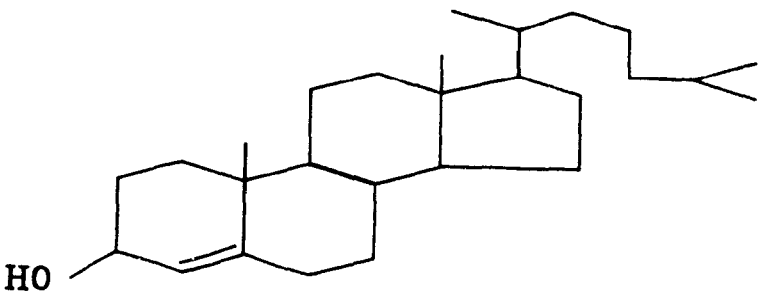

Figure 1.1 Structure of Cholesterol

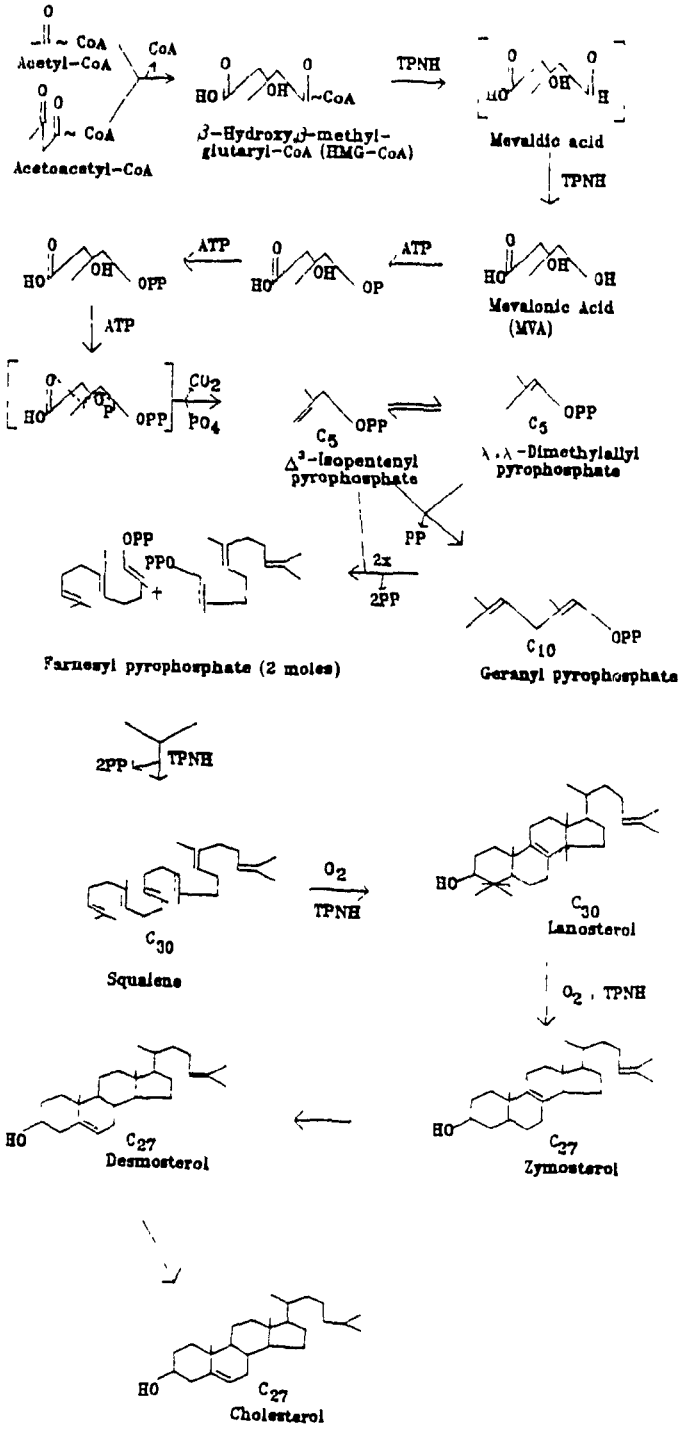

Figure 1.2 Biosynthesis of Cholesterol (13). (P: phosphate, PP: pyrophosphate, TPNH: hydrogen triphosphopyridine nucleotide)

1.2 METABOLISM OF BILE ACIDS

Bile acids are carboxylic acids containing 22-28 carbon atoms. All are derivatives of cyclopentanophenanthrene and the carboxylic acid group terminates a branched C_3-C_9 side-chain. In nature, the common bile acids are saturated C_{24} acids derived from 5β-cholanic acid (Figure 1.3). Normally the bile acids are present in the bile and are excreted into the duodenum as conjugates of taurine or glycine.

The bile acids may be divided into two groups (Figure 1.4) according to the original source in the body: the primary bile acids, cholic and chenodeoxycholic acids, are derived directly from cholesterol; the secondary bile acids, deoxycholic and lithocholic acids are derived from the primary acids during the enterohepatic circulation.

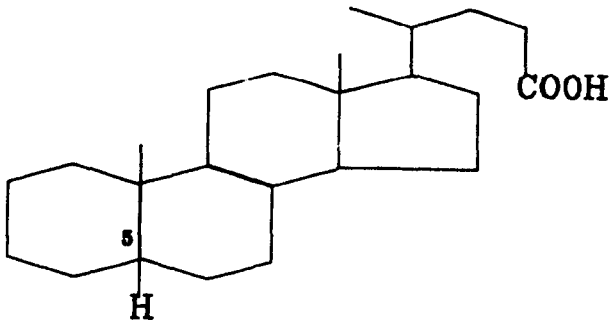

Figure 1.3. Structure of 5β-cholanic acid (18)

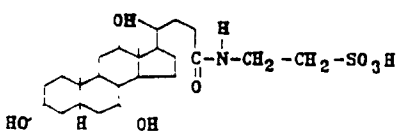

Taurocholic Acid

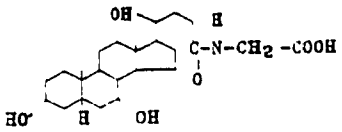

Glycocholic Acid

Primary Bile Acids

C | Deconjugation + 7α-dehydroxylation

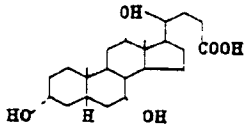

Deoxycholic Acid
Secondary Bile Acid

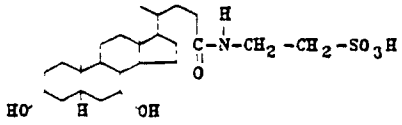

Taurochenodeoxycholic Acid

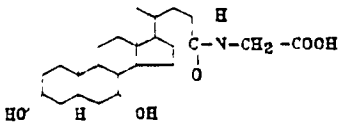

Glycochenodeoxycholic Acid

Primary Bile Acids

C | Deconjugation + 7α-dehydroxylation

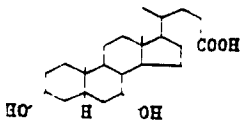

Lithocholic Acid
Secondary Bile Acid

C Catalyzed by Microbial Enzymes

Figure 1.4 Structures of primary and secondary bile acids (19)

1.2.1 Synthesis of Primary Bile Acids

Bile acids are synthesized in only one organ, the liver. The first and rate-limiting step of this synthesis (20) is the 7α-hydroxylation of cholesterol (I) (Figure 1.5). The 7α–hydroxy-cholesterol (II) undergoes oxidation of the 3β-hydroxyl group and an isomerization of the double bond at position 5 to position 4 to yield 7α-hydroxy-4-cholesten-3-one (III), which is the common precursor of all primary bile acids. In turn, it is converted to 7α,12α-dihydroxy-4-cholesten-3-one (IV), by hydroxylation at the 12α position. Then, both 7α-hydroxy-4-cholesten-3-one (III) and 7α,12α-dihydroxy-4-cholesten-3-one (IV) undergo the following reactions: (i) reduction of the 4 double bond and of the 3-keto group, and (ii) oxidation of the C_{26} side-chain. The 26-hydroxylated compounds are then oxidized to the corresponding carboxylic acids, which, in turn, are hydroxylated at C_{24}, followed by an oxidation of the 24-hydroxyl group to give cholic and chenodeoxycholic acids (21-24).

The primary bile acids are then conjugated by enzymatic catalysis, also in the liver, with either glycine or taurine, the ratio being 3 to 1 (21).

1.2.2 Enterohepatic Circulation

Bile acids, in their conjugated forms, are secreted by the liver, together with free cholesterol, phospholipids and other minor constituents of bile. During fasting, bile is diverted into the gallbladder where it is concentrated and stored until the gallbladder contracts, in response to feeding, causing secretion of the bile into the duodenum through the common bile duct (Figure 1.6). After participating in the absorption of fats and phospholipids in the jejunum, the bile salts pass down the ileum where at least 95% (18) of the total is re-absorbed (25, 26), the un-absorbed fraction being eliminated into the feces. The re-absorbed

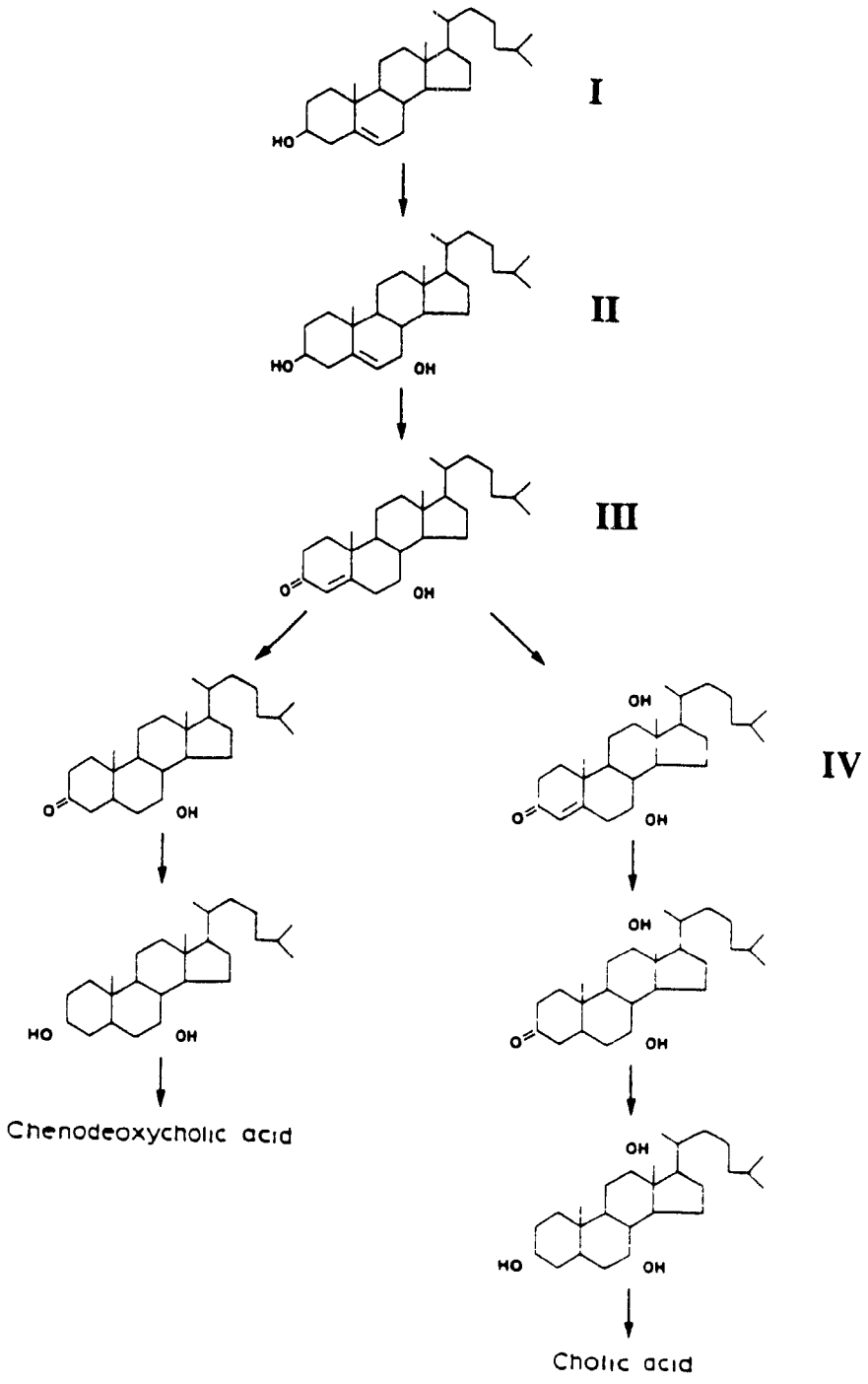

Figure 1.5 Biosynthesis of the primary bile acids (29) from cholesterol (I)

portion is bound to albumin (27) and returned to the liver, to be re-used (Figure 1.6). This cycle is referred to as the enterohepatic circulation. In the steady state, the bile salt pool (3-5 g) participating in the enterohepatic circulation is maintained by synthesis of an amount of primary bile acid equal to the fecal loss (ca. 500 mg/day) (28).

In the lower ileum and colon some of the conjugated bile acids will be acted upon by enzymes of the intestinal flora, with deconjugation and 7α-dehydroxylation as major reactions, giving rise to secondary bile acids: deoxycholic acid from cholic acid and lithocholic acid from chenodeoxycholic acid (Figure 1.4) (18). A portion of the secondary bile acids formed is re-absorbed, eventually re-appearing in the bile.

1.2.3 Function and Physiology

The major functions of bile acids are: (i) they induce the formation of bile; (ii) due to their amphiphilic nature, they transport lipids; and (iii) they regulate their own biosynthesis from cholesterol (31). Formation of bile acids from cholesterol may in itself be regarded as a contribution to the homeostatic regulation of the amount of cholesterol in the body.

The amphiphilic nature gives bile acids detergent properties, enabling them to maintain cholesterol and phospholipids in solution in the bile, by forming water-soluble micelles. These micelles also include fatty acids and glycerides, after fat absorption, and are referred to as "mixed micelles" (32). The water-soluble micelles transport components to plasma membranes to be transferred, and the bile acids then move down the intestine where they are re-absorbed (33).

Thus, the bile acids are not only a means by which cholesterol can be eliminated, but also play an important role in the solubilization, transport and absorption of fat and non-polar lipids, e.g., vitamins D and K.

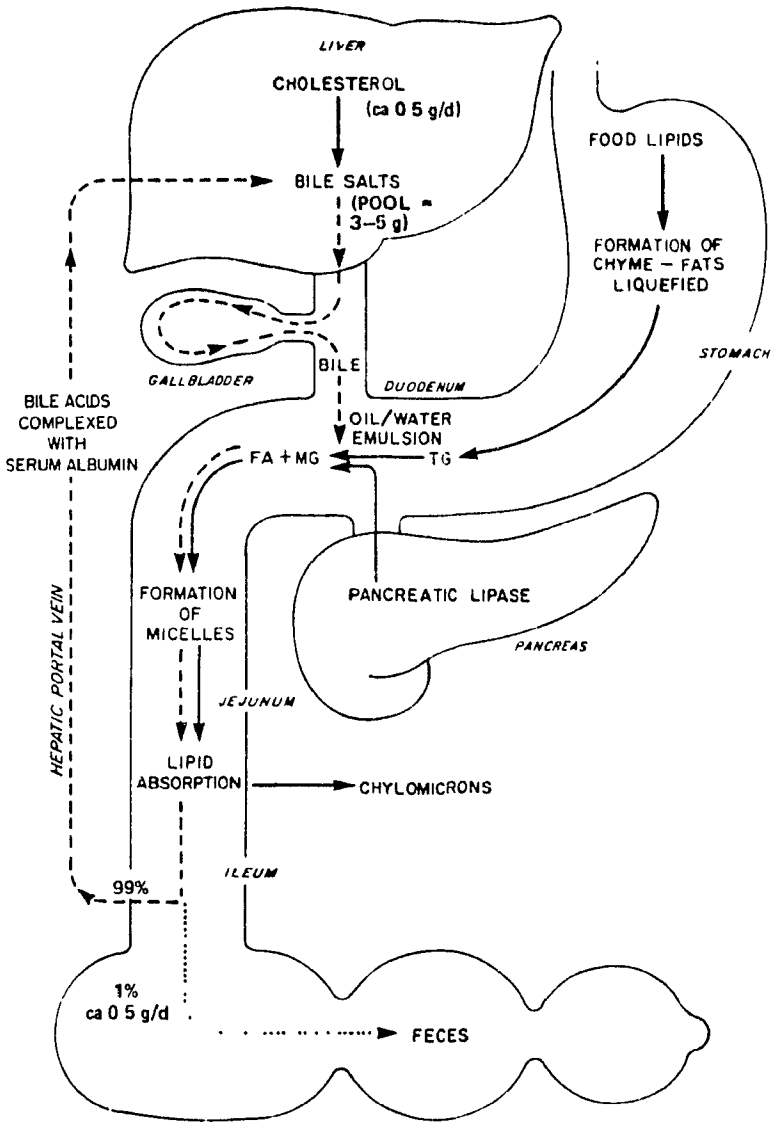

Figure 1.6 The Enterohepatic Circulation (30). (TG: triacylglycerol, FA: long-chain fatty acids, MG: monoglycerol, DG: diglycerides)

1.3 PROPERTIES OF BILE ACIDS

1.3.1 Structure

The most common bile acids found in man have a saturated cyclopentanophenanthrene skeleton, containing a four-ring steroidal nucleus and a five-carbon side-chain branched at carbon-21 that terminates in a carboxylic acid group (Figures 1.4, 1.7). The A/B ring has a cis-junction (34, 35), while the B/C and C/D rings have trans-junctions; the hydrogen at carbon-5 is in the α-position (Figure 1.7). Hydroxyl groups can be found at positions 3, 7, and 12, and are also in the α-position (35, 36). In nature, the carboxylic acid group of the side-chain is conjugated with either glycine or taurine by a peptide linkage. The primary bile acids in humans are cholic acid (3α,7α,12α-trihydroxy-5ß-cholan-24-oic acid) and chenodeoxycholic acid (3α,7α-dihydroxycholan-24-oic acid), conjugated to either glycine or taurine (Figure 1.4).

The steroidal nucleus of the bile acid molecule exhibits planar polarity, with the hydrophilic groups being situated below the equator of the molecule, and most of the steroid skeleton with its protruding methyl groups lying above it (Figure 1.7). When ionized, the short, mobile side-chain at carbon-17 lies in the α-axial position with respect to the plane of the molecule, causing the polar carboxylic acid group to be in the same plane as the hydroxyl groups. When it is un-ionized it lies parallel to the steroidal nucleus (37-39). Thus, in its ionized form the side-chain provides a major contribution to the polarity of the under surface of the molecule. The bile acids then have two distinct domains, one that is mainly hydrophobic and the other mainly hydrophilic, and are referred to as amphiphiles.

A:

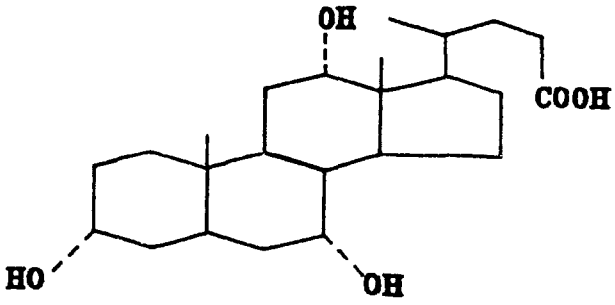

B:

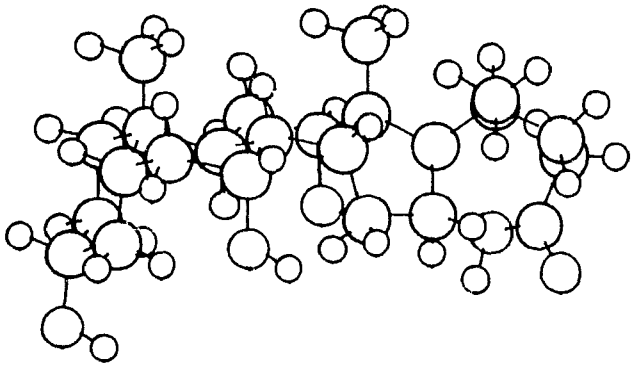

C:

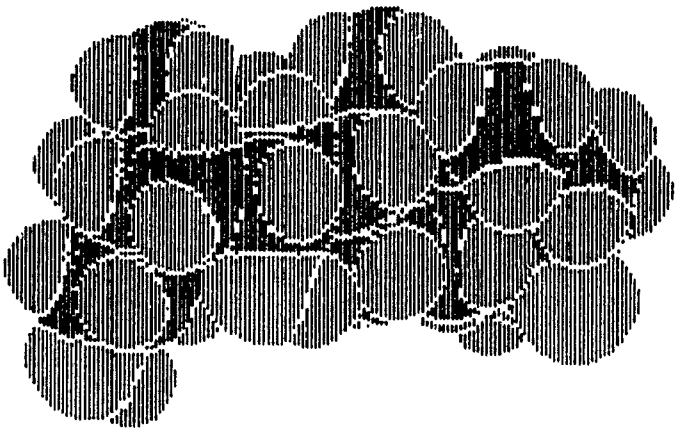

Figure 1.7 Structure of cholic acid represented in the conventional way (A), in a perspective structural formula (B) and as a spacefill model (C) (43). (black:carbon, blue:hydrogen, red:oxygen)

Depending on the position and number of hydroxyl groups, the polarity of the bile acid will change in the order:

monohydroxy < dihydroxy < trihydroxy

For the monohydroxy bile salts, the polarity falls in the following order (40):

3-OH > 7-OH > 12-OH

The taurine conjugated bile salts are more hydrophilic than the corresponding glycine conjugate or the unconjugated bile salt (34, 41).

In general, the molecule of a free bile salt is about 2-2.1nm long and is nearly circular in cross-section with a diameter of 0.6-0.7nm (42). The molecular volume of a bile salt anion is about 0.53nm^3 (42). The distance between the hydroxyl groups in the α-position is about 0.5nm (42).

Some bile acids form crystalline polymorphs (44-46) and most dihydroxy bile acids form stable crystalline solvates with a wide variety of solvent molecules (45, 47-49). More details on the physical states and properties of bile acids are found in Appendix 1.

1.3.2 Solubility

Small (50) classified bile acids as insoluble amphiphiles and bile salts as soluble amphiphiles. However, in the literature the two terms "bile acid" and "bile salt", are often used interchangeably and both refer to bile salts since, at physiological pH, the bile acids are in their unprotonated form. On account of the undissociated carboxylic acid group, the aqueous solubility of bile acids is limited (51), but the bile salts have appreciable aqueous solubility as monomers (5×10^{-8} - 6×10^{-3}) (52), and their solubility is greatly enhanced by the formation of micelles (44).

The solubility of bile salts is complicated since it depends not only on the ionization of the carboxylic acid group of the side-chain, but also on the number of hydroxyl groups and on the presence of micelles in solution. Therefore, conjugation of the bile acid also alters its solubility since protonation of the free acid occurs at pH 9, glycine conjugates at pH 8 and taurine conjugates at pH 4 (53). The unconjugated bile acids have pKa's in the region of 5-6.5, the glycine conjugates in the region of 4-5 and the taurine conjugates have pKa's of about 1.9 (43).

1.3.3 Micelle Formation

Bile salts are amphiphilic and undergo a rapid dynamic association-dissociation equilibrium to form micelles as the total concentration of bile salt increases to the critical micellar concentration, (CMC), at a critical micellar temperature, (CMT) (42, 43, 54, 55). Because bile salt micelles are often small, i.e. dimers (42), and self-aggregation continues to proceed with increasing concentration (56-60), the detection of the lowest concentration at which the first aggregate forms depends particularly upon the sensitivity of the technique (60) and on the physico-chemical conditions (42, 43, 49). This, at least in part, explains the large array of results which have been obtained to date. Interplay of the effects of the number and orientations of the various ring hydroxyl groups, the length and polarity of the side-chain and any conjugation affect the CMC of the bile salt.

Micelles of pure bile salt are essentially spherical (18) and are highly hydrated (61). The average size and the distribution of micellar size are important physico-chemical characteristics of a bile salt solution (42). The size increases with decreased hydrophilicity for unconjugated bile salt (56, 58, 60) It was

found that, upon conjugation, the micellar size and growth potential increase from free to glycine-conjugates to taurine-conjugates (62).

The primary micelles of bile salts aggregate as their concentration increases, the interactions being mainly between the hydrophobic hydrocarbon parts of the molecules; the core of the micelle is then hydrophobic with the hydrophilic groups pointing outwards (Figure 1.8) (62, 63). The hydrophobic interaction is due to the agglomeration of hydrophobic surfaces in a back-to-back way so as to maximize Van der Waals contacts between the alicyclic steroid rings on this side of the bile salt molecule (62). This interaction can also be affected by the side-chain length of the bile salt molecule (52).

Secondary micelles will also form (62) from the aggregation of primary micelles, the interaction taking place between some of the exposed hydrophilic parts of the bile salts (Figure 1.8). This intermicellar hydrogen bonding interaction possibly helps to stabilize these large aggregates (62, 64). The interaction in secondary micelles is weaker than in the primary micelles (43).

The number of bile salts in a primary micelle is referred to as the aggregation number. This number varies from one bile salt to the other, since it depends upon the molecular structure, the molecular weight, the position of the hydroxyl groups, the total concentration, the pH, the temperature, the nature and concentration of counter-ions, the length of the side-chain and the state of conjugation. In general, the aggregation number varies between 2 and 9, but can be even higher (42, 43, 55, 62). It increases in the following order for some of the bile acids, going from 3 for cholic acid to 22 for taurodeoxycholic acid (61):

cholic < glycocholic < taurocholic < taurochenodeoxycholic < taurodeoxycholic.

The CMC also varies according to the above factors.

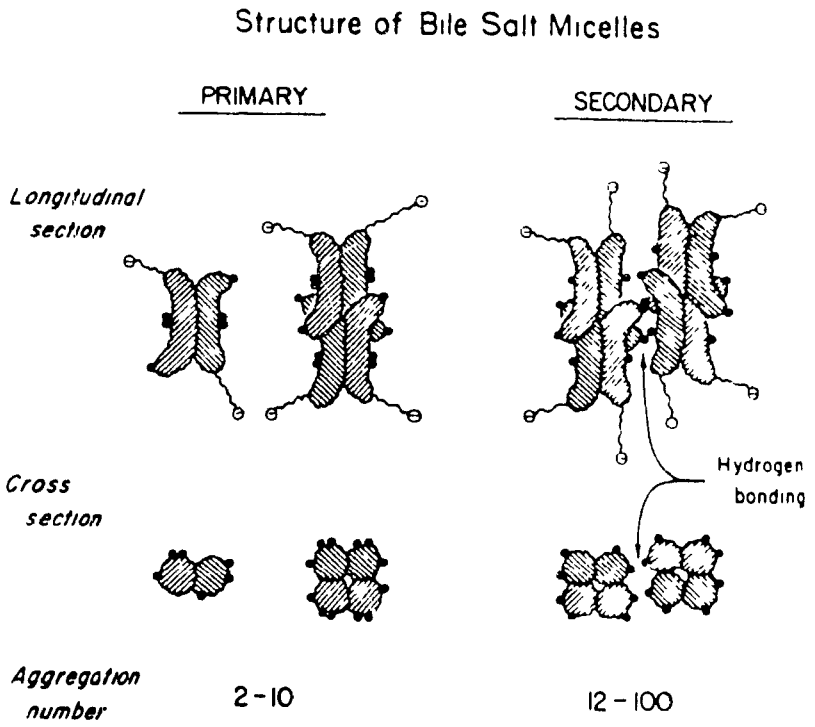

Figure 1.8 Structure of primary and secondary bile salt micelles (43)

It has been of interest to try to elucidate the structure of bile salt micelles. Several models have been proposed. For example, the micellar association in aqueous solution of sodium deoxycholate has been explained by intermolecular hydrophobic interaction and hydrophilic interactions with the aqueous environment (65, 66). It has been proposed that the micelles of sodium deoxycholate and rubidium deoxycholate exist as helices stabilized by hydrogen-bonding (67-69) (Figure 1.9). Further studies, including analysis of the micelles with proton and carbon-13 NMR (67, 71), X-ray crystallography (67-69, 72, 73), and electron-spin-resonance (72), seem to support this helical model (70-73). The micelles of sodium taurodeoxycholate have also been studied (74, 75) and, although not all of the above techniques have been applied yet, the helical model

is also indicated. In a recent paper (76) sodium glycodeoxycholate was studied by X-ray crystallography and the helical model was also proposed. The authors suggest that bile salt micelles, in general, are helical.

Because the primary micelles of bile salt have a hydrophobic core, it is possible to incorporate hydrophobic domains of other molecules, to form mixed micelles. The requirement for a mixed micelle is that it is composed of more than one lipid-like species, and that at least one of these species must be able to form micelles alone in aqueous solution (62). Bile salt micelles have been studied for their interactions with hydrocarbons, such as naphthalene (77), with acyl alcohol (78) and others but the most studied is with lecithin (79-82). The bile salt-lecithin mixed micelle is of physiological importance since it allows the transport and solubilization of fats and lipids during the enterohepatic circulation.

Figure 1.9 Helices of RbDC (A) viewed along and perpendicular to the helical axis (72) and NaTDC (B) viewed along the helical axis (76)

1.4 ANALYSIS AND IDENTIFICATION OF BILE ACIDS

A variety of analytical procedures may be used for qualitative and quantitative assay of bile acids. Several of these methods require hydrolysis or solvolysis of the conjugates as part of the procedure. The primary interest is to separate the different forms of bile acids, mainly the free and the conjugated bile acids, and to identify them.

1.4.1 Analysis of Bile Acids

1.4.1.1 Chromatographic Methods

Gas liquid chromatography (GLC) (83-88) is a sensitive and precise method for the individual quantification of the main free primary and secondary bile acids in one operation. However, the conjugated bile acids must be hydrolyzed prior to analysis, so that it is not possible to separate them. For routine purposes, GLC is inconvenient since it requires extraction, hydrolysis, and also derivatization prior to injection.

Thin-layer chromatography (TLC) can also be used to separate bile acids (89-97). It requires the use of time-consuming elution procedures and the resolution of glycine- and taurine-conjugates is not satisfactory. Recently, a two-dimensional TLC technique has been applied (89) giving better resolution of some glycine- and taurine-conjugated bile acids.

Of all the chromatographic techniques, high-pressure-liquid chromatography (HPLC) is the most widely used. Separation can be done on straight-phase, or affinity, and reversed-phase columns. In affinity HPLC, the bile acids are eluted in the order of decreasing number of hydroxyl groups on the steroid nucleus; it can resolve glycine- and taurine-conjugated chenodeoxycholic and deoxycholic acids (98, 99).

The chemically bonded stationary phase, octadecysilyl (ODS) reversed-phase column is the most suitable and widely used column for the resolution of bile acids (100-106). The separation of bile acids can be done either with or without prior derivatization and hydrolysis, depending on the method of detection that is used. The detectors that are widely used are differential refractometers, the ultraviolet detectors and fluorimeters.

Differential refractometers are widely used for the detection of compounds, such as bile acids, which do not exhibit strong UV absorption or fluorescence properties (101, 105, 107). However, the sensitivity obtained with refractometers is not always sufficient, especially when used for the analysis of bile acids in biological fluids (108).

Ultraviolet (UV) detectors are more commonly used (100, 102-104, 109, 110); they use light in the 190-210 nm region to detect bile acids. This technique is applicable to the determination of glycine- and taurine-conjugates in bile but the sensitivity is not sufficient for the measurement of unconjugated bile acids in serum. To improve the sensitivity, use can be made of an ion-pair reagent, such as Hyamine 1622 (111), to produce the UV-absorbing ion-pair that is monitored at 254 nm. However, it is required that the acidic moiety of the bile acid be dissociated prior to ion-pairing This detection method can be used to distinguish between unconjugated and conjugated bile acids and between glycine- and taurine-conjugates by adjusting the pH of the mobile phase.

The bile acids can also be modified by an enzymatically catalyzed reaction prior to UV-detection or fluorimetry. One enzyme that is widely used is 3α-hydroxysteroid dehydrogenase (3α-HSD), which is capable of transforming the 3α–hydroxyl group of the 5α-steroid into a 3-oxo group in presence of NAD^+ under alkaline conditions (112-116). The NAD^+ is converted to NADH, which has UV-absorption and fluorescence. The difficulty with this method is that it is

hard to obtain reproducible results since the enzymatic reaction is not always reliable.

Derivatization of the carboxyl and the hydroxyl groups, widely used for biological substances which do not have UV absorption nor fluorescence, can also be used to enhance UV-absorption of bile acids. This can be achieved by labelling the carboxylic acid group with a chromophore or a fluorophore. There are many derivatization compounds (110, 117-120), but in general 1-p-nitro-3-p-tolyltraze or O-p-nitrobenzyl-N,N'-diisopropylisourea are used for UV detection giving rise to the p-nitrobenzyl ester of the bile acid. For fluorescence purposes 4-bromomethyl-7-methoxycoumarin and bromacetyl pyrene are widely used (121, 122). The disadvantages of this method are that: (i) it results in poor resolution of chenodeoxycholic and deoxycholic acids, and (ii) it requires that the taurine-conjugates be deconjugated prior to analysis.

When analyzing for bile acids, it is important to keep in mind the purpose of the separation and the bile acids that are to be identified so that the best method of detection can be used.

1.4.1.2 Other Methods

Other methods are available for the isolation and analysis of bile acids. Radioimmunoassay (RIA) (123-126) is extremely sensitive and rapid but is limited by the availability of specific antibodies. There are also enzymatic methods (127-129) which use 3α-HSD; it is a direct, simple procedure and is available for bile acid quantitation. However, it does not discriminate between different bile acids.

Conducting organic salt electrodes, which readily oxidise NADH (130), have been proposed for the analysis of bile acids (131). In the presence of the enzyme 3α-HSD the following chemistry takes place (131):

$$NAD^+ + R_1R_2CHOH \xrightarrow{3\alpha\text{-HSD}} R_1R_2CO + NADH$$

$$NADH \xrightarrow{\text{electrode}} NAD^+ + H^+ + 2\acute{e}$$

where R_1 and R_2 stands for the groups adjacent to the hydroxyl group in bile acid.

A linear response between the current and the concentration of bile acids (in the 0-0.2 mM range) was obtained (131). Currently, further work is being carried out to apply this system to the analysis of bile acids (132).

1.4.2 Identification of Bile Acids

Various spectroscopic techniques have been used to identify and characterize bile acid molecules. Nuclear magnetic resonance (nmr) has been used to study bile salts as monomers and in their micellar forms. Proton nmr distinguishes the main structural features and functional groups of bile acids, although little information is obtained about skeletal parts containing the methylene groups, since all of these protons resonate in the 1-2.5 ppm region. The main peaks are those due to the protons of the methyl groups at carbon-18, -19, -21, and the geminal hydrogen of the hydroxyl group (39, 65). The resonance of the remaining hydrogens are found between 1.0 and 2.35 ppm. Work done previously in this laboratory (133), using DEPT and 2D-correlation experiments, enabled an elucidation of the proton nmr spectra of some bile acids.

Carbon-13 nmr has also been applied to bile acids. The methyl carbons resonate between 7-24 ppm, the methylenes between 23-40 ppm, and the ring junctions from 34 to 55 ppm; the carbons bearing the hydroxyl groups resonate at 65-80 ppm and the one for the carboxyl group resonates at about 175 ppm (67, 134-136). Carbon-13 and proton 2-D correlation nmr experiments have also been done to obtain a complete assignment for sodium cholate and sodium

deoxycholate (137). Again, work by Zhu (133) was done to elucidate the complete assignment of carbon-13 nmr of some bile salts using DEPT and 2D-correlation nmr.

NMR spectroscopy can be used to study the micellization process of bile acids by monitoring the peaks of the hydrogens at carbon-18 and -19 which broaden, due to the hydrophobic interactions, upon micelle formation (35, 58, 67). It can also be applied to the study of the interactions in mixed micelles. A specific study (138) elucidated the interactions of bile salt and lecithin, using the spin echo technique, which monitors the aggregate self-diffusion coefficient. The interactions can also be studied by monitoring the chemical shifts of specific protons (139).

X-ray crystallography is another method by which bile acids have been studied. The first report (140) confirmed the expected conformation and stereochemistry for the 6-membered ABC rings of the steroid nucleus. It showed the flexible regions of the molecules as being the 5-membered D ring (which is, however, restricted to a narrow range of conformations) and the side chain attached at C-17. Examination of inter-molecular interactions and crystal packing reveals a tendency for these compounds to form bilayers with a hydrophobic core and a hydrophilic exterior (36, 67, 141, 142).

Mass spectroscopy has also been used to characterize bile acids. The general fragmentation of a hydroxylated bile acid is the loss of an angular methyl group, followed by loss of the side-chain and ring cleavage of either C or D or C/D rings (87, 143-145).

1.5. HYPERCHOLESTEROLEMIA AND BILE ACIDS

1.5.1 Hypercholesterolemia

Although atherosclerosis is recognized as a multifactorial disease, it is now well established that the main cause is the accumulation of free or esterified cholesterol in the artery wall (1, 146, 147). The cholesterol is transported in lipoproteins, such as low-density lipoproteins (LDL) and very low-density lipoproteins (VLDL) (VLDL are secreted by the liver and transformed into LDL) to the artery wall. But it is also possible for the cholesterol to be transported away by means of the high-density lipoproteins (HDL). Thus, it can be said that it is the disturbance in the balance of deposition and removal of the cholesterol in the artery wall which will lead to the growth of atherosclerosis.

Hypercholesterolemia is the term used to refer to a condition in which excess cholesterol is found in the body, that may lead to the development of atherosclerosis. This condition, when identified, can be treated in several ways: low-cholesterol and low-fat diets and administration of cholesterol-lowering drugs. The primary treatment, in conditions where the excess cholesterol is not too high (about 200-239 mg/dL), is a change in diet to lower the cholesterol intake (6). Changes in diet alone can lower cholesterol by 4-6% (6, 148). However, diet changes alone are generally insufficient to lower the cholesterol level sufficiently when it is higher than 240 mg/dL (6), so that other methods of treatment are required.

1.5.2 Treatments of Hypercholesterolemia and Bile Acids

From the literature, it appears that the most frequently employed forms of treatment of hypercholesterolemia involve three mechanisms of action: 1. Binding of bile acids by a non-absorbable agent during the enterohepatic

circulation; 2. Increased utilization of the LDL-cholesterol; and 3. Inhibition of cholesterol synthesis in the liver.

The binding of bile acids occurs in the intestinal lumen (Figure 1.6). During the enterohepatic circulation, a constant bile acid pool is necessary to make the process efficient. Upon binding of the bile acids to a non-absorbable agent, an increased amount is eliminated through the feces, reducing the percentage returning to the liver. To maintain a constant pool, the liver synthesizes more bile acids. This decreases the amount of cholesterol in the liver, as well as the cholesterol contained in LDL, since it is also used for the synthesis. Thus, binding of bile acids affects both hepatic cholesterol and LDL-cholesterol.

The inhibition of the cholesterol synthesis is another method by which the cholesterol level can be reduced. It can be achieved through the use of a competitive inhibitor of HMG CoA reductase, the rate-limiting enzyme of cholesterol synthesis. The inhibition of the cholesterol synthesis decreases the amount of cholesterol present in the liver. Because the liver needs a certain concentration of cholesterol, it then uses the LDL-cholesterol to attain the desired concentration.

Although these mechanisms are treated separately, they all come down to the decrease in LDL-cholesterol, which is desirable, since it transports cholesterol to the artery wall where it can accumulate.

In the following pages, a brief survey of common cholesterol-lowering agents and drugs will be presented. Dietary fibers have been reported extensively as a natural means by which cholesterol can be lowered. Neomycin, nicotinic acid, fibric acid derivatives and probucol are some of the drugs which can be used for lowering cholesterol and which are commonly surveyed in the literature. 3-Hydroxy-3-methylglutaryl co-enzyme A (HMG CoA) reductase inhibitors are a new class of drugs which are efficient in lowering cholesterol but because of their

novelty no long term study has yet been completed and their use is still limited. The bile acid binding resins, which are discussed last, are the most widely used and also the better known of the cholesterol-lowering drugs. They have been studied extensively and their ability to bind bile acids is of interest in the present work.

1.5.2.1 Dietary Fibers

The cholesterol-lowering action of some dietary fibers is well documented (149). Dietary fibers are composed of a diverse group of substances, generally derived from plant cell walls, which are not metabolized by the intestinal secretion. Bile acid binding by a number of types of fibers has been demonstrated both ***in vitro*** (150-156) and ***in vivo*** (152, 156). The most common types of fibers studied are wheat bran (157-165), oat bran (166, 167), pectin (168) and soyabean (169). Guar gum and lignin are the most effective adsorbents, ***in vitro***, while alfalfa, bran and cellulose are less effective (154, 155, 170, 171).

The extent of bile acid binding is a function of pH, osmolarity, type of bile acid and fiber, and the degree of micellization. Binding is greater at acid pH and increased bile acid concentration, but is inhibited by micelle formation, particularly at higher pH (153). The extent of adsorption differs for the various individual bile acids and a consistent pattern, based on the number of hydroxyl groups or on the state of conjugation, has not been identified (149-152, 172).

The mechanisms proposed to account for the lowering cholesterol effect of the dietary fibers, include the binding of bile acids (173), alteration of the bile acid metabolism (174) and alteration of the solubilization and absorption of intestinal cholesterol (175).

1.5.2.2 Neomycin

Neomycin is a non-absorbable aminoglycoside antibiotic (176). With a daily dose of 1-2 grams, it can decrease LDL-cholesterol by 20-25% (6). Its

mode of action would appear to be inhibition of the re-absorption of bile acids by precipitating the micellar sterol in the intestines, thus increasing its fecal elimination (177-179). Side-effects of neomycin are mostly gastrointestinal, such as diarrhea and abdominal cramps.

1.5.2.3 Nicotinic acid

Nicotinic acid is a water-soluble vitamin-B (Figure 1.10) (180, 181). It lowers both total and LDL-cholesterol by about 25%, and increases the HDL-cholesterol levels (182). Its primary mechanism of action is thought to be that it inhibits the secretion of VLDL, which in turn will decrease the production of LDL (183). It is relatively safe, causing side effects like cutaneous flushing and rashes in some patients, and is relatively cheap since the daily dose is about 100-250 mg (183). Nicotinic acid is considered one of the most effective drugs for lowering cholesterol (184).

1.5.2.4 Fibric Acid Derivatives

The fibric acid derivatives currently used to treat hypercholesterolemia are gemfibrozil (5-(2,5-dimethylphenoxy)-2,2-dimethylpentanoic acid (Figure 1.10)) and clofibrate (2-(4-chlorophenoxy)-2-methylpropanoic acid ethyl ester (Figure 1.10)). A long-term study (4) showed that gemfibrozil increases HDL-cholesterol and decreases both total and LDL-cholesterol. A new generation of these derivatives, such as bezafibrate and fenofibrate, used in Europe appear to be more potent than their parent compounds (185-188). Gemfibrozil and clofibrate also seem to decrease the cholesterol level by promoting the catabolism of VLDL (189). Their side-effects are of gastrointestinal nature.

1.5.2.5 Probucol

Probucol (Figure 1.10) is modestly effective in lowering cholesterol. It decreases total and LDL-cholesterol by 8-15% (6, 190), but it also reduces HDL-

cholesterol by 20-25% (6, 191). Side-effects are mostly of gastrointestinal nature, although no long-term study has been carried out.

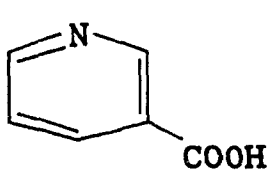

Nicotinic Acid

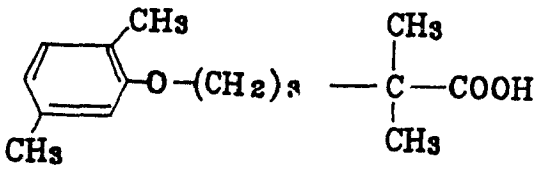

Gemfibrozil

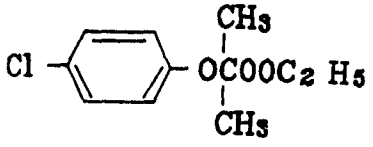

Clofibrate

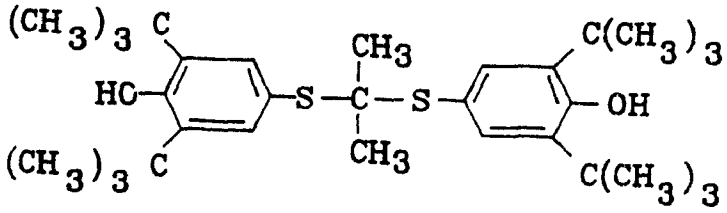

Probucol

Figure 1.10 Chemical Structures of some cholesterol lowering drugs (192)

1.5.2.6 HMG CoA Reductase Inhibitor

One of the most promising groups of drugs that has recently been developed is lovastatin and its analogue, compactin. They are prototypes of a chemical class of fungal derivatives that inhibit the action of 3-hydroxy-3-methylglutaryl co-enzyme A (HMG CoA) reductase, the rate-limiting enzyme in cholesterol biosynthesis (193). Compactin is butanoic acid, 2-methyl-1,2,3,7,8,8a-hexahydro-7-methyl-8-[2-(tetrahydro-4-hydroxy-6-oxo-2-H-pyran-2-

yl)ethyl]-1-naphthalenyl ester (Figure 1.11). Lovastatin, also referred to as mevinolin, differs from compactin by the presence of a second methyl group on the naphthalene ring (Figure 1.11), but its affinity for the enzyme is about twice that of compactin.

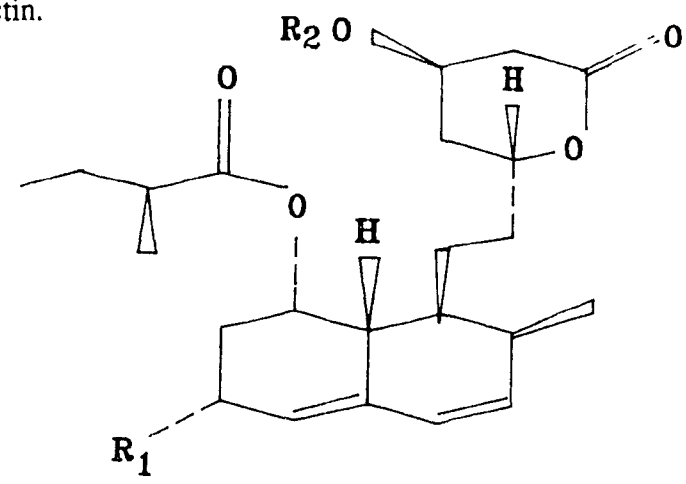

a) R_1 = Me, R_2 = H

b) R_1 = R_2 = H

Figure 1.11 Structural formulas of a) mevinolin and b) compactin (194)

They can effectively decrease LDL-cholesterol by 25-45% with daily doses of 20-80 mg (1 mg/kg of body weight of compactin or 0 5 mg/kg of body weight of lovastatin) (6, 178). It is thought (195) that they inhibit cholesterol synthesis by occupying two sites on the enzyme: one is the HMG-binding domain of the active site and the other is a hydrophobic pocket located adjacent to the active site. Thus, by blocking endogenous sterol production in the liver, the drug limits the availability of cholesterol necessary for normal bile acid synthesis and for biliary sterol secretion. Consequently, the hepatic LDL-receptor activity is increased, decreasing the concentration of LDL-cholesterol and of the circulating cholesterol (178).

Lovastatin is generally well tolerated. Skin rashes and other allergic manifestation do occur (in 1-2% of patients). However, the most serious side-effect would appear to be the development of lenticular opacities, even though it has been noted only in a small percentage of patients and that opacities often disappear (196).

Although they effectively reduce cholesterol, their effects on coronary heart disease and their long-term safety have not yet been established.

1.5.2.7 Bile Acid-Binding Resins

The first choice of drug for the treatment of hypercholesterolemia is a bile acid binding resin that can be administered orally. The two currently used clinically are cholestyramine and colestipol.

Cholestyramine is a strongly basic anion exchanger; it is a co-polymer of styrene and divinyl benzene onto which are attached quaternary ammonium groups with chloride counter-ions (Figure 1.12). Its equivalent weight is 230 and its molecular weight is above 1 x 10^6. Colestipol is a N-(2-aminoethyl)-1,2-ethanediamine polymer with (chloromethyl)oxirane. Its functional groups are secondary and tertiary amines making it a weaker basic ion-exchanger than cholestyramine. Although its backbone is water-swellable, which should improve its biocompatability, it has a lower binding capacity for bile acids than cholestyramine (197). Because cholestyramine has been known for more than thirty years (186, 198, 199), and is more effective, it has received more attention.

Bile acid binding resins lower both total and LDL-cholesterol. Their action is to bind bile acids in the intestinal lumen where it decreases their re-absorption, reducing the amount of bile acids returning to the liver. As mentioned earlier, a constant pool of bile acid is required. Thus, the lost bile acids are replenished by synthesis of bile acids from cholesterol, utilizing both hepatic and

LDL-cholesterol. Because these resins are not absorbed or digested, they produce no toxic effects on short term administration.

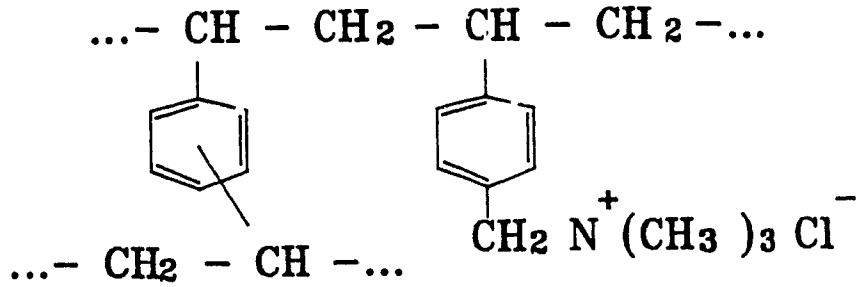

Figure 1.12 Structure of cholestyramine

It has been shown, in a long-term study (1), that cholestyramine statistically lowers LDL-cholesterol (15-30%, with daily doses of 16-24 g) and the incidence of coronary heart disease. The most common side-effects were shown to be gastrointestinal in nature, e.g., constipation, bloating, nausea; however they were not found in all patients. It may also interfere with the absorption of other anionic drugs, e.g., digitoxin and warfarin, when these are taken concurrently.

Although cholestyramine requires patient education to achieve effective adherence, due to the large dose required and the fact that it is not very palatable, it remains the first choice in drug therapy to lower cholesterol since its effectiveness has been shown in clinical trials and its long-term safety has been established.

1.5.2.8 Other Treatments

Many other classes of drugs have been tested for lowering cholesterol, including antacids (200-203), activated charcoal (204, 205) and chitosan (which is currently receiving more attention) (175), just to name a few. They show poor to relatively poor effectiveness in lowering cholesterol.

However, the most promising treatment is the combination of two drugs with complementary mechanisms. Among these are colestipol and probucol (206-208), colestipol and bezafibrate (185), cholestyramine and nicotinic acid or HMG CoA reductase inhibitor (184) or probucol (190). It would appear that the best of these combinations would be an anion-exchange resin and HMG CoA reductase inhibitor (184).

1.5.3 Binding of Bile Acids

As mentioned previously, drugs such as cholestyramine lower the cholesterol level by binding bile acids. The mode of interaction has been postulated as being primarily electrostatic (209-211), the interaction taking place between the negatively charged carboxylic acid group of the bile acid and the positively charged quaternary ammonium group of cholestyramine. Johns and Bates postulated that a secondary mode of interaction also existed, between the hydrophobic regions of the bile acid and of cholestyramine. To verify the latter, they studied (210) the interactions between cholestyramine and fatty acids of various chain lengths. As the chain length increases the hydrophobicity also increases. They reported that with such an increase the affinity of binding also increases. Also, because cholestyramine is a quaternary ammonium salt, it was proposed that there could be an ion-exchange process between the anionic bile acid and the chloride anion (212).

Other studies have involved the binding of bile acids with proteins, such as human serum albumin (HSA) (213, 214), which plays a role in the transport of bile acids back to the liver during the enterohepatic circulation. Little information was found about the relative contribution of electrostatic and hydrophobic forces in the binding process, but it was found that bile acids induced a conformational change in HSA upon binding (215).

Glutathione-S-transferase has also been identified as a protein which binds bile acids (216-219). However, its mode of interaction has not yet been identified.

1.6 PRESENT STUDY

Short peptide chains grafted onto a polymeric backbone have been shown to adsorb bilirubin (220, 221) and bile acids (133). The interactions between bile salts and the polymeric resins was proposed as being primarily ionic. It was suggested that hydrophobic interactions could also play a role in the binding. This was concluded following adsorption studies and nmr experiments (133).

The present work focused on elucidating the interactions between bile salt and ion-exchange resins. Cholestyramine, the bile acid binding resin, was first studied. It is known to be effective in lowering the plasma cholesterol level. Therefore, it was of interest to obtain a better understanding of the mechanism of action of this drug as to permit the design of improved sorbents in the future. The adsorption of bile acids by cholestyramine was studied, ***in vitro***, under various experimental conditions.

These results were studied quantitatively by applying different binding models, but they were found unsatisfactory. The ion-exchange mechanism was then proposed and treated with the Donnan theory. It was suggested that the

interaction between cholestyramine and bile acid was an ion-exchange process, a finding also cited in Zhu's thesis (133).

A series of cholestyramine-like sorbents were then prepared by solid phase peptide synthesis with systematic changes in the structure. These differences in structure permitted to determine how they would affect the adsorption of bile acid. The adsorption of bile acids by these resins were studied and from the results it was possible to determine which structural parts of cholestyramine are important for the binding of bile acids and to verify if indeed ion-exchange is the mechanism of interaction.

Molecular modelling was used as to offer a qualitative approach to the interaction of cholestyramine or ion-exchange resin and the bile acids . It helped to determine how the resin and the bile acid can interact with one another and to verify if what was proposed by the Donnan theory is plausible.

1.7 REFERENCES

1. The Lipid Research Clinics Coronary Primary Prevention Trial Results, *J. Am. Med. Assoc.*, **251**, 351. 1984
2. R. Ross, *N. Eng. J. Med.*, **314**, 488, 1986
3. M.J. Martin, S.B. Hulley, W.S. Browner, L.H. Kuller and D. Wentworth, *Lancet*, **2**, 933, 1986
4. The Helsinki Heart Study, *N. Engl. J. Med.*, **317**, 1237, 1987
5. W.P. Castelli, *Am. J. Obstet. Gynecol* , **158**, 1553, 1988
6. The Expert Panel, *Arch. Intern Med.*, **148**, 38, 1988
7. E. Anderson, *Acta Med. Scand., [Suppl]*, **643**, 1, 1980
8. K.E. Suckling and P.H.E. Groot, *Chem. ir. Britain*, **24**, 436, 1988
9. J. Hok and C.B. Taylor, *Arch. Pathol.*, **90** 83, 1970
10. G. Popjak and J.W. Cornforth, *Adv Enzymol.*, **22**, 281, 1960
11. J.L. Gaylor, *Adv. Lipid Res.*, **10**, 89, 1972
12. M.D. Siperstein and M.J. Griest, *J. Clin Invest* , **39**, 642, 1960
13. M.D. Siperstein, *Curr. Top Cell Regul* , **2**, 65, 1970
14. J.M. Dietschy and J.D. Wilson, *N. Engl. J Med* **282**, 1128; 1179, 1271; 1970
15. V.W. Rodwell, J.L. Nordstrom and J J. Mitschelen, *Adv. Lipid Res* , **14**, 1, 1976
16. M.S. Brown and J.L.Goldstein, *J. Lipid Res.*, **21**, 505, 1980
17. A. Cantarow and B. Schepartz, **Chap. 18, Metabolism of Lipids**, p 491, in *Biochemistry*, 3rd edition, W.B. Saunders Co., Philadelphia, 1962
18. R. Coleman, *Biochem. Soc. Trans.*, **15**, 68S, 1987
19. P.A. Mayes, **Chap. 27, Cholesterol Synthesis, Transport and Excretion**, p 249, in *Harper's Biochemistry*, 21st edition, R.K. Murray, D.K. Granner, P.A. Mayes, V.W Rodwell eds., Appleton and Lange, California, 1988
20. H. Danielsson, K. Einarsson and G. Johansson, *Eur. J Biochem* , **2**, 44, 1967
21. F. Magne, J. Saric and C. Balabaud, *Nouv. Presse Med.*, **9**, 2561, 1980
22. T.B. Van Itallie and S.A. Hashim, *Med. Clin. N Amer.*, **47**, 629, 1963
23. I. Bjorkem and H. Danielsson, **Chap. 13, Biosynthesis and Metabolism of Bile Acids in Man,** p 215-291, in *Progress in Liver Disease*, vol. 5, H. Popper, F. Schaffner eds., Grune and Stratton Publishers, New-York, London, 1976
24. E.H. Mosbach, *Arch. Intern. Med.*, **130**, 478, 1972
25. I. Bjorkhem, **Chap. 9, Mechanism of Bile Acids Biosynthesis in Mammalian Liver**, p 236, in *Sterols and Bile Acids*, H. Danielsson and J. Sjovall eds., Elsevier, Amsterdam, 1985
26. M.C. Carey and M.J. Cahalane, **Chap. 33, Enterohepatic Circulation**, in *The Liver, Biology and Pathobiology*, 2nd edition, I.M. Arias, W.B. Jakoby, H. Popper, D. Schachter, D.A. Shafritz eds., Raven Press, New-York, 1988

27. A.F. Hofmann, *Clin. Gastroenterol.*, **6**, 3, 1977

28. R. Coleman, *Biochem. J.*, **244**, 249, 1987

29. D.M. Small, *Arch. Int. Med.*, **130**, 552, 1972

30. A.F. Hoffmann, *AJR* , **151**, 5, 1988

31. A.F Hofmann, **Chap. 1, Fat Digestion**, in *Lipid Absorption*, K. Rommeland and H. Goebell eds., MTP Press, Lancaster, 1976

32. A.B.R Thomson, **Chap. 2, Intestinal Absorption of Lipids**, in *Disturbances in Lipids and Lipoprotein Metabolism*, J.M. Dietschy, A.M. Gotto, Jr., J.A. Ontkoeds, Clinical Physiology Series, American Physiology Society, Bethesda, 1978

33. P.A. Mayes, **Chap. 44, Digestion/Absorption in the Gastrointestinal Tract**, p 626, in *Harper's Review of Biochemistry*, 20th edition, D.W. Martin Jr., P.A. Mayes, V.W. Rodwell, Lange Medical Publication, Los Altos, California, 1985

34. G.A.D. Haslewood, p 1-16, in *Bile Salts*, R. Peters, F.G. Young eds., Methuen, London, 1967

35. S. Barnes and M. Geckles, *J. Lipid Res* , **23**, 161, 1982

36. R.E. Cobbledick and F.W.B. Einstein, *Acta Cryst.*, **B36**, 287, 1980

37. M.C. Carey, J-C. Montet, M.C. Phillips, M.J. Armstrong and N.A. Mazer, *Biochemistry*, **20**, 3637, 1981

38. P. Joos and R. Ruyssen, *Chem. Phys Lipids*, **3**, 8390, 1969

39. S. Barnes, *Hepatology*, **4**, 98S, 1984

40. W.H. Elliot and R. Shaw, p 1, in *Steroid Analysis by HPLC*, M.P. Kautsky, ed., Marcel Dekker, N.Y., 1981

41. M.J. Armstrong and M.C. Carey, *J Lipid Res* , **23**, 70, 1982

42. D.M. Small, **Chap. 8, The Physical Chemistry of Cholanic Acids**, in *The Bile Acids, Chemistry, Physiology and Metabolism* vol 1, P.P. Nair, D. Kritchevsky, eds., Plenum Press, New-York, 1971

43. A.F. Hofmann, *Acta Chem Scand.*, **171**, 173,1963

44. T. Iida and F.C. Chang, *J Org Chem* , **43**, 2786, 1981

45. G.P. Van Berge-Henegowen, A.F. Hofmann and T.S. Gaginella, *Gastroenterology*, **73**, 291, 1977

46. T. Iida and F.C. Chang, *J. Org Chem* , **47**, 2966, 1982

47. F C. Chang, N.F. Wood and W.G. Holton, *J. Org. Chem.*, **30**, 1718, 1965

48. T. Iida, H.R. Tanya and F.C. Chang, *Lipids*, **16**, 863, 1981

49. M.C. Carey and D.M. Small, *Arch. Intern Med.*, **130**, 506, 1972

50. D.M. Small, *J. Am. Oil Chem. Soc.*, **45**, 108, 1968

51. H. Igimi and M.C. Carey, *J Lipid Res* , **21**, 72, 1980

52. A. Roda, A.F. Hofmann and K.J. Mysels, *J Biol. Chem.*, **258**, 6362, 1983

53. M.C. Carey, *Hepatology*, **4**, 66S, 1984

54. A.F. Hofmann and D.M. Small, *Annu Rev Med.*, **18**, 333, 1967

55. M C. Carey and D.M. Small, *Am. J Med.*, **49**, 590, 1970

56. A. Norman, *Acta Chem. Scand* , **14**, 1300, 1960

57. D.F. Evans, R. DePalma, J. Nadas and J. Thomas, *J. Sol. Chem.*, **1**, 377, 1972

58. B. Lindman, N Kamenka, H. Fabre, J Ulmius and T Wieloch, *J Colloid Interface Sci* , **73**, 556, 1980

59. T. Djavanbakht, K.M. Kale and R. Zana, *J. Colloid Interface Sci* , **59**, 139, 1977

60. P. Mukerjee and J.R. Cardinal, *J. Pharm Sci.*, **65**, 882, 1976

61. M.C. Carey, **Chap. 13, Physical-Chemical Properties of Bile Acids and their Salts**, in *Sterols and Bile Acids*, H. Danielsson, J. Sjovall, eds., Elsevier, Amsterdam, 1985

62. D.M. Small, *Adv Chem. Ser.*, **84**, 31, 1968

63. D.M. Small and S.A. Penkett, *Biochem Biophys. Acta*, **173**, 178, 1969

64. N.A. Mazer, M.C. Carey, R.F. Kwasnick and G.B. Benedek, *Biochemistry*, **18**, 3064, 1979

65. D.M. Small, S.A Penkett and D.Chapman, *Biochim Biophys Acta*, **176**, 178, 1969

66. B.M. Fung and M.C. Pedin, *Biochim Biophys Acta*, **437**, 273, 1976

67. G. Conte R. DiBlasi, E. Giglio, A. Parretta and N.V. Pavel, *J Phys. Chem* , **885**, 720, 1984

68. A.R. Campanelli, D Ferro, E. Giglio, P. Imperatori and V Piacente, *Thermochim Acta*, **67**, 223, 1983

69. A.R. Campanelli, S. Candeloro De Sanctis, E. Giglio and S. Petriconi, *Acta Crystallogr , Sect. C*, **C40**, 631, 1984

70. M. D'Alagni, M.L. Forallese and E. Giglio, *Colloid Polym Sci* , **263**, 160, 1985

71. G. Esposito, A. Zanobi, E. Giglio, N.V. Pavel and I.D. Campbell, *J Phys Chem* , **91**, 83, 1987

72. G. Esposito, E. Giglio, N.V. Pavel and A. Zanobi, *J Phys Chem* , **91**, 356, 1987

73. E. Giglio, S. Loreti and N.V. Pavel, *J Phys Chem* , **92**, 2858, 1988

74. A.R. Campanelli, S. Candeloro De Sanctis, E. Giglio and L Scaramuzza, *J Lipid Res* , **28**, 483, 1987

75. M. D'Alagni, E. Giglio and S. Petriconi, *Colloid Polym Sci* , **265**, 517, 1987

76. A.R. Campanelli, S. Candeloro De Sanctis, E Chiessi, M. D'Alagni, E. Giglio and L Scaramuzza, *J Phys Chem* , **93**, 1536, 1989

77. J.-C. Montet, C. Merienne and C. Bram, *Tetrahedron*, **38**, 1159, 1982

78. C.H. Spink and S. Colgan, *J Colloid Interface Sci* , **97**, 41, 1984

79. N.A. Mazer, G.B. Benedek and M.C Carey, *Biochemistry*, **19**, 601, 1980

80. W. Shankland, *Chem Phys. Lipids*, **4**, 109, 1970

81. R.O. Zimmerer Jr. and S. Lindenbaum, *J Pharm Sci* , **68**, 581, 1979

82. K. Muller, *Biochemistry*, **20**, 404, 1981

83. G.P Van Berge-Henegouwen, A. Ruben and K.H. Brandt, *Clin. Chim. Acta*, **54**, 249, 1974

84. N. Kaplowitz, E. Kok and N.B. Javett, *J Am Med Assoc* , **225**, 292, 1973

85. P.P. Nair and C. Garcia, *Anal Biochem* , **29**, 164, 1969

86. P.E. Ross, C.R. Pennington and A.D Bouchier, *Anal. Biochem.*, **80**, 458, 1977

87. J. Sjovall, P Eneroth and R. Ryhage, **Chap. 7, Mass Spectrometry of Bile Acids,** in *The Bile Acids, Chemistry, Physiology and Metabolism*, vol.1, P.P Nair, D. Kritchevsky, eds., Plenum Press, New-York, 1971

88. P. Child, M. Aloe and D. Mee, *J Chromatogr* , **415**, 13, 1987

89. L. Lepri, D. Heimler and P.G. Desideri, *J. Chromatogr.*, **288**, 461, 1984

90. M.J.G. Bolt, *J. Lipid Res.*, **28**, 1013, 1987

91. J.M. Street, D.J.H. Trafford and H.L.J. Makin, *J. Lipid Res.*, **24**, 491, 1983

92. A.K. Batta, G. Salen and S. Schefer, *J. Chromatogr* , **168**, 557, 1979

93. R. Beke, G A. De Weerdt and F. Barbier, *J. Chromatogr.*, **193**, 504, 1980

94. A.K. Batta, S. Schefer and G. Salen, *J Lipid Res.*, **22**, 712, 1981

95. G. Szepesi, K. Dudas, A. Pap, Z. Vegh, E. Micsovics and T. Tyihak, *J. Chromatogr.*, **336**, 249, 1984

96. A.F. Hofmann, *Gastroenterology*, **52**, 752, 1967

97. P.N. Maton, G.M. Murphy and R.H Dowling, *Lancet*, **2**, 1297, 1977

98. R. Shaw and W.H. Elliot, *Anal Biochem* , **74**, 273, 1976

99. R.W.R. Baker, J. Ferret and G.M Murphy, *J. Chromatogr* , **146**, 137, 1978

100. S.S. Rossi, J.L. Converse and A.F. Hofmann, *J. Lipid Res.*, **28**, 589, 1987

101. K. Shimada, M. Hasegawa, J. Goto and T. Nambara, *J.Chromatogr.*, **152**, 431, 1978

102. P.S. Tietz, J.L. Thistle, L.J. Miller and N.F. LaRusso, *J Chromatogr* , **336**, 249, 1984

103. S. Terabe, K. Yamamoto and T Ando, *J. Chromatogr* , **239**, 515, 1982

104. A.T. Ruben and, G.P. Van Berge-Henegouwen, *Clin. Chim Acta*, **119**, 41, 1982

105. R. Shaw, M. Rivetna and W.E. Elliott, *J Chromatogr* , **202**, 347, 1980

106. W. Svobodnik, Y.Y. Zhang, U. Klueppelberg, P. Janowitz, J.G. Wechsler, P. Fuerst and H Dirschinert, *J. Chromatogr* , **423**, 75, 1987

107. A.D. Reid and P.R. Baker, *J. Chromatogr* , **247**, 149, 1982

108. N.A. Parris, *J. Chromatogr* , **133**, 273, 1977

109. M. Paciotti, L. Perinati, F. Gori and P Rampazzo, *J. Chromatogr.*, **270**, 402, 1983

110. S. Okuyama, D. Uemura and Y. Hirata, *Chem Lett.*, 679, 1976

111. N. Parris, *Anal Biochem.*, **100**, 260, 1979

112. S. Okuyama, N. Kokubeen, S. Higashidate, D Uemura and Y. Hirata, *Chem. Lett.*, 1443, 1979

113. K. Arisue, Z. Ogawa, K. Kohda, C. Hayashi and Y. Ishida, Jpn. *J. Clin. Chem* , **9**, 104, 1980

114. S. Onishi, S. Itoh and Y. Ishida, *Biochem. J* , **204**, 135, 1982

115. S. Hasegawa, R. Uenoyama, F Takeda, J. Chuma and S. Baba, *J. Chromatogr* , **278**, 25, 1983

116. S. Riva, R. Bovara, P. Pasta and G. Carrea, *Ann N Y Acad Sci.*, **542**, 413, 1988

117. B. Shaik, N.J. Pontzer, J.E. Molina and M.I Kesley, *Anal Biochem.*, **85**, 47, 1978

118. F.S. Stellard, D.L. Hachey and P.D. Klein, *Anal. Biochem.*, **87**, 359, 1978

119. G. Mingrove, A.V. Greco and S. Passe, *J. Chromatogr* , **183**, 277, 1980

120. T. Iida, Y. Ohnuki, F.C Chang, J. Goto and T. Mambara, *Lipids*, **20**, 187, 1985

121. S. Okuyama, D. Uemura and Y. Hirata, *Chem Lett.*, 461, 1979

122. S. Kamada, M. Maeda and A. Tsuji, *J Chromatogr.*, **272**, 29, 1983

123. L. Demers and G. Hepner, *Clin. Chem* , **22**, 602, 1976

124. A.A. Mehas, J.G. Spenney, B I. Hirshowitz and R.G. Gibson, *Clin Chim. Acta*, **76**, 389, 1977

125. S.W. Schalm, G.P. Van Berge-Henegouwen, A F. Hofmann, A.E. Cowen and J. Turcotte, *Gastroenterology*, **73**, 285, 1977

126. W.J. Simmonds, M.G. Korman, W. Gove and A.F. Hofmann, *Gastroenterology*, **65**, 705, 1973

127. D. Fausa, *Scand. J. Gastroent.*, **10**, 747, 1975

128. G.M. Murphy, B.H.Billing and D.N. Baron, *J. Clin Pathol.*, **23**, 594, 1970

129. H.P. Schwarz, K. VonBergmann and G. Paugmgartner, *Clin. Chim Acta*, **50**, 197, 1974

130. W.J. Albery and P.N. Bartlett, *J Chem Soc , Chem Commun* , 234, 1984

131. W.J. Albery, P.N. Bartlett and A.E.G. Cass, *Phil. Trans. R Soc. London*, **B316**, 107, 1987

132. W.J. Albery, P.N. Bartlett, R.B. Lennox, D. Armstrong, G.M. Murphy and H. Dowling, paper submitted to *J. Electroanal Chem*

133. X.X. Zhu, **Ph.D. Thesis**, McGill University, 1988

134. D. Leibfritz and J.D. Roberts, *J Am Chem Soc* , **95**, 4996, 1973

135. J.W. Blunt and J B. Stothers, *Org Magn Reson* , **9**, 439, 1977

136. Y. Murata, G. Sugihara, F. Fukushima, M. Tanaka and K. Matsushita, *J Phys Chem* , **86**, 4690, 1982

137. M Campredon, V. Quiroa, A. Thevand, A. Allouche and G. Pouzara, *Magn Reson Chem* , **24**, 624, 1986

138. P. Schurtenberger and B. Lindman, *Biochemistry*, **24**, 7161, 1985

139. E. Kolehmainen, *J Colloid Interf Sci* , **105**, 273, 1985

140. J.P Schaefer and L.L Reed, *Acta Cryst* , **B38**, 1743, 1972

141. P.F. Lindley, M.M.Mahmoud, F.E. Watson and W.A Jones, *Acta Cryst* , **B36**, 1893, 1980

142. L. Lessinger, *Cryst. Struct Commun* , 11, 1787, 1982

143. T. Iida, F.C. Chang, T. Matsumoto and T. Tamura, *Biomed Mass Spectrom* , **9**, 473, 1982

144. K.R.R. Setchell and A. Matsui, *Clin Chim. Acta*, **127**, 1, 1983

145. J.M. Street, D.J.H Trafford and H.J L. Makin, *J. Lipid Res.*, **27**, 208, 1986

146. W.B. Kanne, W.P. Castelli, T. Gordon and P M. McNamara, *Ann. Intern Med* , **74**, 1, 1971

147. J.P Kane and R.J. Havel, *Ann Rev Med* , **37**, 427, 1986

148 . G. Kolata, *Science*, **223**, 381, 1984

149. T.A. Miettinen, *Adv. Lipid Res* , **18**, 65, 1981

150. T. Midvedt and A. Norman, *Acta Pathol. Microbiol. Scand*, **80**, 202, 1972

151. F. Kern Jr., J.J. Birkner and V Ostower, *Am. J. Clin. Nutr.*, **31**, S175, 1978

152. G.W Kuron and D.M. Tennent, *Fed Proc.*, **20**, 268, 1961

153. M.A. Eastwood and L. Mowbray, *Am J Clin Nutr*, **29**, 1461, 1976

154. D. Kritchevsky, *Am J. Clin Nutr.*, **30**, 979, 1977

155. G.V. Vahouny, R. Tombes, M M. Cassidy, D. Kritchevsky and L.L Gallo, *Lipids*, **15**, 1012, 1980

156. G.V. Vahouny, T. Roy, L.L Gallo, J.A. Story, D. Kritchevsky and M M. Cassidy, *Am. J. Clin. Nutr*, **33**, 2182, 1980

157. M A. Eastwood, T. Hamilton, J.R. Kirkpatrick and W.D. Mitchell, *Proc. Nutr Soc*, **32**, 22A, 1973

158. M.A. Eastwood, J.R. Kirkpatrick, W.D Mitchell, A. Bone and T. Hamilton, *Br. Med. J*, **4**, 392, 1973

159. W.E. Bell, E.A. Emkin, L.M. Klevay and H.H. Scandstead, *Am J. Clin Nutr*, **34**, 1071, 1981

160. R.M. Kay and A.S. Triswell, *Br J. Nutr*, **37**, 227, 1977

161. A.W. Huijbregts, G.P. VanBerge-Henegouwen, M.P. Hectors, A. Van Schaik and S D. Van der Welf, Eur. *J Clin Invest.*, **10**, 451, 1980

162. R.L. Walters, I.M. Baird, P.S. Davies, M.J. Hill, B.S. Draser, D.A.T. Southgate, J. Green and B. Morgan, *Br. Med J*, **2**, 536, 1975

163. J.H. Cummings, M.J. Hill, D J.A Jenkins, J.R. Pearson and H.S. Weggers, *Am. J Clin Nutr.*, **29**, 1468, 1976

164. J.H. Cummings, M.J. Hill, T. Jivraj, H. Houston W.J Branch and D.J.A. Jenkins, *Am J Clin Nutr*, **32**, 208, 1979

165. D.J.A. Jenkins, M.J. Hill and J.H Cummings, *Am J Clin Nutr*, **28**, 1408, 1975

166. R.W Kveby, J.W. Anderson, B. Sieling, E.D. Rees, J. Chen, R.E. Miller and E.M. Kay, *Am. J Clin. Nutr*, **34**, 824, 1981

167. M.M. Stanley, D. Paul, D. Gacke and J. Murphy, *Gastroenterology*, **65**, 889, 1973.

168. J.K. Ross and J.E. Leklem, *Am J Clin Nutr*, **34**, 2068, 1981

169. T. F. Schweizer, A.R. Bekhichi, B. Koellreuter, S. Reimann, D. Pometta and B.A. Baron, *Am. J. Clin. Nutr.*, **38**, 1, 1983

170. J.A. Story, *Proc Soc Exp Biol Med*, **180**, 447, 1985

171. D. Gallaher and B.O. Schneeman, *Am. J Physiol.*, **250**, G420, 1986

172. D. Kritchevsky, *Cancer*, **58**, 1830, 1986

173. H.J. Birkner and F. Kern Jr., *Gastroenterology*, **67**, 237, 1974

174. D. Kritchevsky, F Tipper and J.A. Story, *J Food Sci*, **40**, 8, 1975

175. G.V. Vahouny, *Adv Exp Med Biol.*, **183**, 265,1985

176. T.A. Kesaniemi and S.M. Grundy, *Arteriosclerosis*, **4**, 41, 1984

177. J.M. Hoeg, M.B. Maher, E. Bou, L.A. Zech, K.R. Bailey, R.E. Gregg, D.L. Sprecher, J.K. Susser, A.M. Perkus and H.B. Brewer Jr., *Circulation*, **70**, 1004, 1984

178. J. Shepherd and C.J. Packard, *Biochem. Soc. Trans* , **15**, 199, 1987

179. H. Eyssen, P. Claes, W. Wuijts, H. Van der Haegne and P. de Somer, *Biochem Pharmacol.*, **24**, 1593, 1975

180. P.L. Canner, K.G. Berge and N.K. Wenger, *J. Am. Coll. Cardiol* , **8**, 1245, 1986

181. The Lipid Research Clinic s Coronary Primary Prevention Trial Results, *J Am Med Assoc* , **255**, 512, 1986

182. H.T.I. Mor and S.M. Grundy, *Gastroenterology*, **73**, 1235, 1977

183. J.P Kane and M.J. Malloy, *Med Clin North Am.*, **66**, 537, 1982

184. D.R. Illingworth, *Clin. Chem* , **34**, B123, 1988

185. L. Klosiewicz-Latoszek, G Nawicka, W.B Szostak and M. Naruszewicz, *Atherosclerosis*, **63**, 203, 1987

186. C.J. Packard and J. Shepherd, *J Lipid Res* , **23**, 1081, 1982

187. J.M. Stewart, C.J. Packard, A R. Lorimer, D.E. Boag and J Shepherd, *Atherosclerosis*, **44**, 355, 1982

188. J. Shepherd, C.J. Packard, J.M. Stewart, R.F. Atmeh, R.S. Clark, D.E Boag, K. Carr, A R Lorimer, D. Ballantyne, H.G. Morgan and T.D.V. Laurie, *J Clin. Invest* , **74**, 2164, 1984

189. C. East, D.W. Bilheimer and S.M. Grundy, *Ann. Intern Med* , **25**, 109, 1988

190. D. Sommariva, D. Bonfiglioli, M. Tirrito, I. Poghaghi, A. Branchi and E Cabini, *Int J Clin. Pharmacol. Ther. Toxicol* , **24**, 505, 1986

191. M. Naruszewicz, T.E Carew, R.C Pittman, J.L. Witztum et al, *J Lipid Res* , **25**, 1206, 1984

192. **The Merck Index**, pp 935, 626, 338, 1116, 10th edition, M. Windholz ed , Merck and Co Inc., Rahway, New-Jersey, USA, 1983

193. D.R. Illingworth, *Ann. Intern. Med.*, **101**, 598, 1984

194. A. Yamamoto, H. Sudo and A Endo, *Atherosclerosis*, **35**, 259, 1980

195. C.E. Nakamura and R.H. Abeles, *Biochemistry*, **24**, 1364, 1985

196. J.R. DiPalma, *AFP*, **36**, 189, 1987

197. P.W. Stacpoole and J. Alig, *Cardiovasc Clin.*, **18**, 267, 1987

198. M. Thale and O. Faergeman, *Scand J Gastroenterol* , **13**, 353, 1978

199. D.M. Tennent, H. Siegel, M.E. Zanetti, G.W. Kuron, W.H. Ott and F.J. Woll, *J Lipid Res* , **1**, 469, 1960

200. D.M. Tennent, S.A. Hashim and T.B Van Itallie, , *Fed Proc* , **21**, 77, 1962

201. G.D. Cousar and T.R. Gadacz,, *Arch Surg* , **119**, 1018, 1984

202. J.E. Clain, J.R. Malagelada, V S. Chadwick and A.F Hofmann, *Gastroenterology*, **73**, 556, 1977

203. Z. Gregus, A. Barth, E. Fischer, J. Zaunseil, W Klinger and F Varga, *Acta Biol Med Ger* , **39**, 705, 1980.

204. S.A. Kocoshis, C N. Ghent andJ.D. Gryboski, *Dig Dis Sci* , **29**, 1148, 1984

205. J.C. Krasopoulos, V A de Barie and M A. Needle, *Lipids*, **15**, 365, 1980

206. N.I. Nakano, S. Funada, Y. Honda and M Nakano, *Chem Pharm Bull* , **32**, 4096, 1984

207. C.A. Dujvone, P. Krehbiel and S.B. Chemoff, *Am. J. Cardiol.*, **57**, 36H, 1986

208. C.J. Glueck, *Ann. Intern. Med.*, **96**, 475, 1982

209. J.L. Witztum, D. Simmons, D. Steinberg, W.F. Beltz, R. Weinseb, S.G. Young, P. Lester, N. Kelly and J. Juliano, *Circulation*, **79**, 16, 1989

210. W.H. Johns and T.R. Bates, *J Pharm Sci.*, **58**, 179, 1969

211. W.H. Johns and T.R. Bates, *J. Pharm. Sci.*, **59**, 329, 1970

212. W.H. Johns and T.R. Bates, *J. Pharm Sci.*, **59**, 789, 1970

213. A. Kuksis, **Chap 6, Ion-Exchange Chromatography of Bile Acids**, in *The Bile Acids, Chemistry, Physiology and Metabolism vol 1*, P.P Nair, D. Kritchevsky eds., Plenum Press, New-York 1971

214. H. Takikawa, Y. Sugiyama, M. Hanano, M. Kurita, H. Yoshida and T. Sugimoto, *Biochem. Biophys. Acta*, 926, 145, 1987

215. H. Takikawa, A. Stolz, M. Sugimoto, Y. Sugiyama and N. Kaplowitz, *J. Lipid Res.*, **27**, 652, 1986

216. A.F. Hofmann and D.M. Small, *Ann Rev Med.*, **18**, 333, 1967

217. A. Stolz, Y. Sugiyama, J. Kuhlenkamp and N. Kaplowitz, *FEBS Lett.*, **177**, 31, 1984

218. H. Takikawa, Y. Sugiyama and N. Kaplowitz, *J. Lipid Res.*, **27**, 955, 1986

219. J.D. Hayes, R.C. Strange and I.W. Percy-Robb, *Biochem J*, **197**, 491, 1981

220. Y. Sugiyama, T. Yamada and N. Kaplowitz, *J Biol. Chem*, **258**, 3602, 1983

221. D. Henning, **Ph.D. Thesis**, McGill University, 1985

222. M. Bouvier, **Ph.D. Thesis**, McGill University, 1988

2 ADSORPTION OF BILE ACIDS BY CHOLESTYRAMINE

It has been suggested that the binding of bile acids by cholestyramine is mainly due to ionic interactions between the negatively charged carboxylic acid group of the bile acid and the positively charged quaternary ammonium group of cholestyramine, although a secondary mode of interaction was also suggested (1-3). However, the ionic interaction is not specific for bile acids so that other species, such as fatty acids (2, 4) also interact competitively with cholestyramine, leading to a decrease in the binding capacity for bile acids. Thus, clinically excess amounts of cholestyramine are administered so that it will be effective in lowering plasma cholesterol levels. Since the use of cholestyramine is also accompanied by unpleasant side-effects, it is of interest to develop more selective, i.e., specific, and consequently more efficient bile acid binding resins. This would decrease adsorption of species other than bile acids and thereby permit a decrease in administered dose which would, in turn, minimize the side effects. A better understanding of the interactions between cholestyramine and the bile acids is needed to determine the factors that are important and responsible for the binding.

This chapter presents results for the adsorption of bile acids by cholestyramine, ***in vitro***, under various experimental conditions. A model is developed, based on these results, to explain the interactions, giving insight and conclusions about cholestyramine and its binding affinity for bile acids.

2.1 EXPERIMENTAL

2.1.1 Treatment of Cholestyramine

Cholestyramine (Dowex 1x2-200, 2% crosslinked, 100-200 dry mesh, Aldrich) as received contains various impurities. To remove them, it was added to a 1:1 mixture of water and glacial acetic acid which was refluxed for 2-3 hours, or was left to stir overnight at room temperature. The mixture was filtered and the filtrate was analyzed spectrophotometrically at 246 nm for UV-absorbing impurity. This procedure was repeated, with fresh solution, until there was no trace of the UV-absorbing impurity in the filtrate. The cholestyramine was then washed with water, methanol and finally with a saturated aqueous sodium chloride solution to convert the counter-ions to the chloride ion. Finally, it was rinsed with anhydrous diethyl ether and dried ***in vacuo*** for several days at room temperature.

To obtain cholestyramine with iodide as the counter-ion, the same procedure was followed except that the final rinse was done with saturated aqueous sodium iodide solution.

The functionalities of cholestyramine, determined by potentiometric titrations using silver nitrate ($AgNO_3$) as titrant and potassium nitrate (KNO_3) as the solution to "drive out" the counter-ion, was found to be 3.16 (± 2%) mmole of chloride ion per gram of resin and 2.76 (± 5%) mmole of iodide per gram of resin. These titrations were done twice each and gave reproducible results. For the iodide containing cholestyramine, a functionality of 2.45 mmole per gram is expected based on the weight difference and the functionality of 3.16 mmol/g for the chloride form; the difference is about 11%, and suggests that not all of the chloride was displaced by the iodide anion.

2.1.2 Adsorption Experiments

Studies of the adsorption of bile acids were done with aqueous solutions, both buffered and non-buffered. Tris-HCl (tris(hydroxymethyl)aminomethane, Aldrich) and phosphate (KH_2PO_4-NaOH, potassium dihydrogen phosphate, Fisher), were used as buffers. These buffers have a pH range of 7-9 for Tris-HCl and 5.80-8 for the phosphate buffer, corresponding to the pH range of the gastrointestinal tract, which has a pH range of 7-8 (5). For most of the experiments, the Tris HCl buffer at pH 7.00 was used.

A stock solution of bile salt (10-50 mg/dL) was prepared, either in water or in aqueous buffer, and from it a series of standard solutions were prepared by dilution. These solutions of known concentrations were then added to a weighed amount of cholestyramine (4-10 mg). The mixtures were shaken for 20-24 hours at room temperature (18-20°C) using a mechanical shaker or with a reciprocal shaker in a water bath at a specific temperature, moving at 100 oscillations per minute. The solutions containing the resin were then filtered by gravity and the peak areas of the bile salt before and after adsorption were determined by HPLC.

The bile salts used in this study were either sodium cholate (Sigma) or sodium glycocholate (Sigma), since the most commonly occurring primary bile salt in bile is cholic acid and its glycine conjugate is the most abundant conjugate (6). By choosing the bile acid and its conjugate, it was possible to study the effect of the conjugation on the binding by cholestyramine.

2.1.3 Analysis of Bile Acids

The bile acid concentrations were determined by high-pressure-liquid-chromatography (HPLC) using a C-6 (5 microns) siloxane hexyl reverse phase column (CSC). The mobile phase, 70:30/methanol:acetic acid (0.1 N), was pumped at a flow rate of 1 ml per minute using a dual piston pump (Eldex AA-94

Dual HP Pump). A Rheodyne (model 7125) injector with a 200 μL loop was used. The detector was a Waters 410 Differential Refractometer that was interfaced to a Varian Datapack (Model DS-604).

The choice of the buffer for the adsorption was also influenced by its performance with the HPLC since, according to the manufacturer, the optimal pH range of the column is between 2-7.5. The composition of the mobile phase was adjusted to give good resolution for both cholic and glycocholic acids. Figure 2.1 shows a typical chromatogram for these two bile acids.

The experimentally obtained peak areas were then analyzed, using a computer program developed by Zhu (7), based on calibration data prepared daily with bile salts solutions of known concentrations. It calculated the bile acid concentration in the solutions at equilibrium and the amount of bile salt adsorbed. From these, adsorption isotherms were obtained.

2.2 ADSORPTION OF BILE ACIDS BY CHOLESTYRAMINE

2.2.1 Comparison Between Buffers

Figure 2.2 shows the adsorption isotherms for cholestyramine, with chloride as the counter-ion, and sodium glycocholate in water, in Tris-HCl and in phosphate buffer. There is an increase in the extent of adsorption, especially at low equilibrium concentrations, on going from phosphate buffer to Tris-HCl to water, although the latter two seem to approach the same "plateau" value.

For the phosphate buffer, at pH 7.0, the ions HPO_4^{2-} and $H_2PO_4^-$ are present in the solution in the ratio of 3 to 5. These anions, especially HPO_4^{2-}, compete with the bile acid anions for the binding sites on cholestyramine (8), which explains why the adsorption isotherm does not exceed 0.1 mole of bound bile acid per equivalent of pendant.

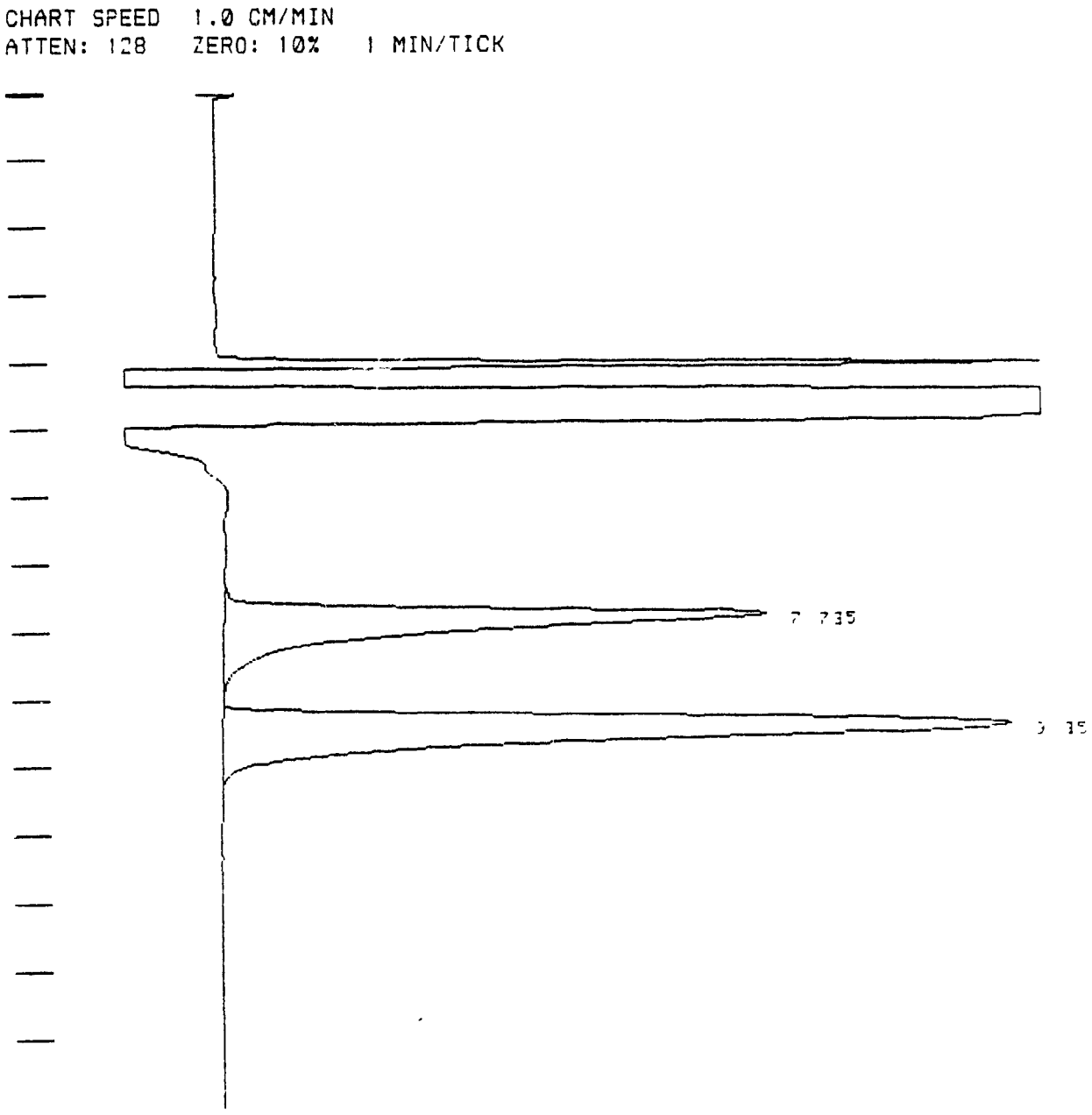

Figure 2.1 HPLC chromatogram showing the peaks of cholic (9.355 minutes) and glycocholic (7.735 minutes) acids. The large peaks eluting before the bile acid are the buffer peaks

However, with Tris-HCl, such a competition does not occur, since the anion of the buffer is also chloride, i.e., it is identical to the counter-ion of cholestyramine. In Tris-HCl the capacity of cholestyramine attains a value of about 1.1 mole of bile acid anions bound per equivalent of pendant. Previous results from this laboratory (7) (Figure 2.2), are limited to low concentrations and appear to be slightly lower. This may be due to the fact that the cholestyramine was not treated in the same way as that used for the present study, which would affect the purity of cholestyramine.

The adsorption isotherm for glycocholic acid in water shows an abrupt increase and reaches maximum adsorption at about 1.2 mole per equivalent. This rapid increase can be attributed to the absence of other anions in the system, which facilitates the interaction. In Figure 2.3 the results for the adsorption of bile salt by cholestyramine (CA Cl) in water are compared with those obtained by Johns and Bates (1), as taken from their diagram. Their isotherm, plotted on a mass basis, is lower than that obtained in the present study. Their cholestyramine was of pharmaceutical grade and they do not indicate whether it was purified. Therefore, the difference may be due to the presence of impurities. Furthermore, neither the functionality nor the extent of cross-linking were reported, both of which would affect the capacity.

For further experiments, Tris-HCl was chosen as the operating medium to keep a constant pH, because it showed minimal lowering compared to the isotherm obtained in water.

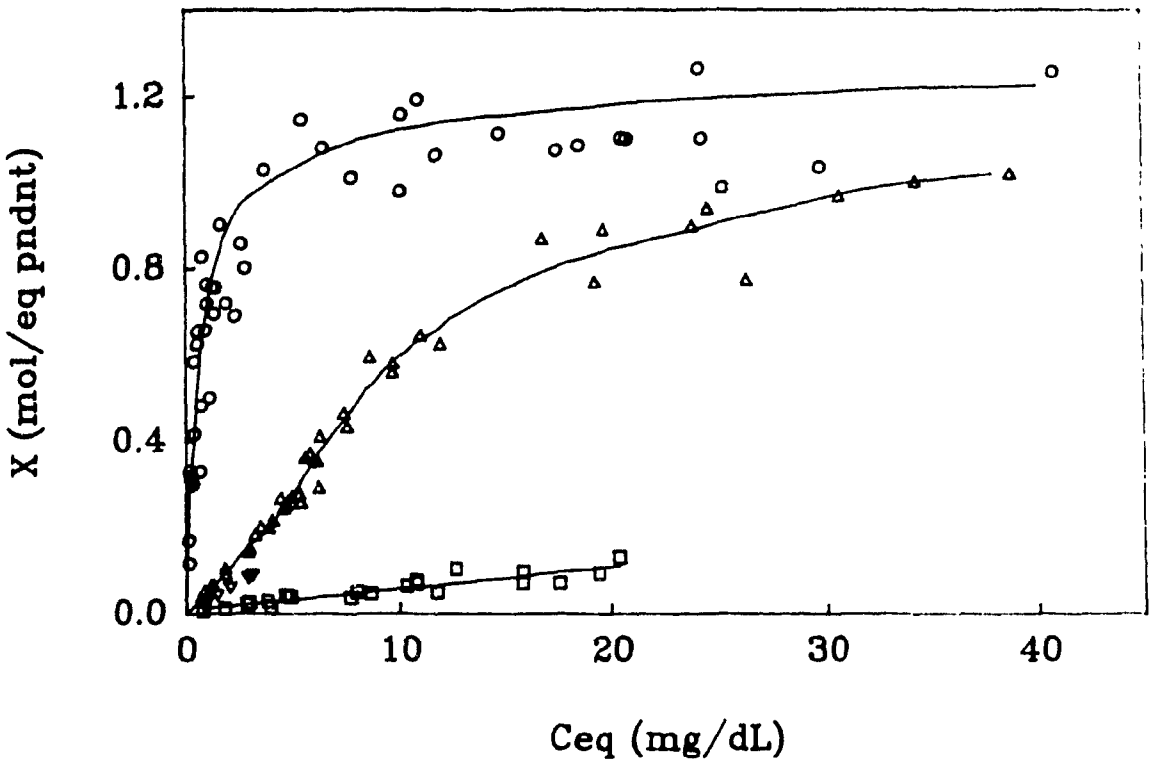

Figure 2.2 Isotherms (T = 20°C) for the adsorption of glycocholic acid by cholestyramine (Cl) in different buffers. Δ in 0.0026 M Tris-HCl (present results); ∇ 0.005M Tris-HCl (previous results (7)); ❑ in 0.0027 M phosphate buffer; ○ in water.

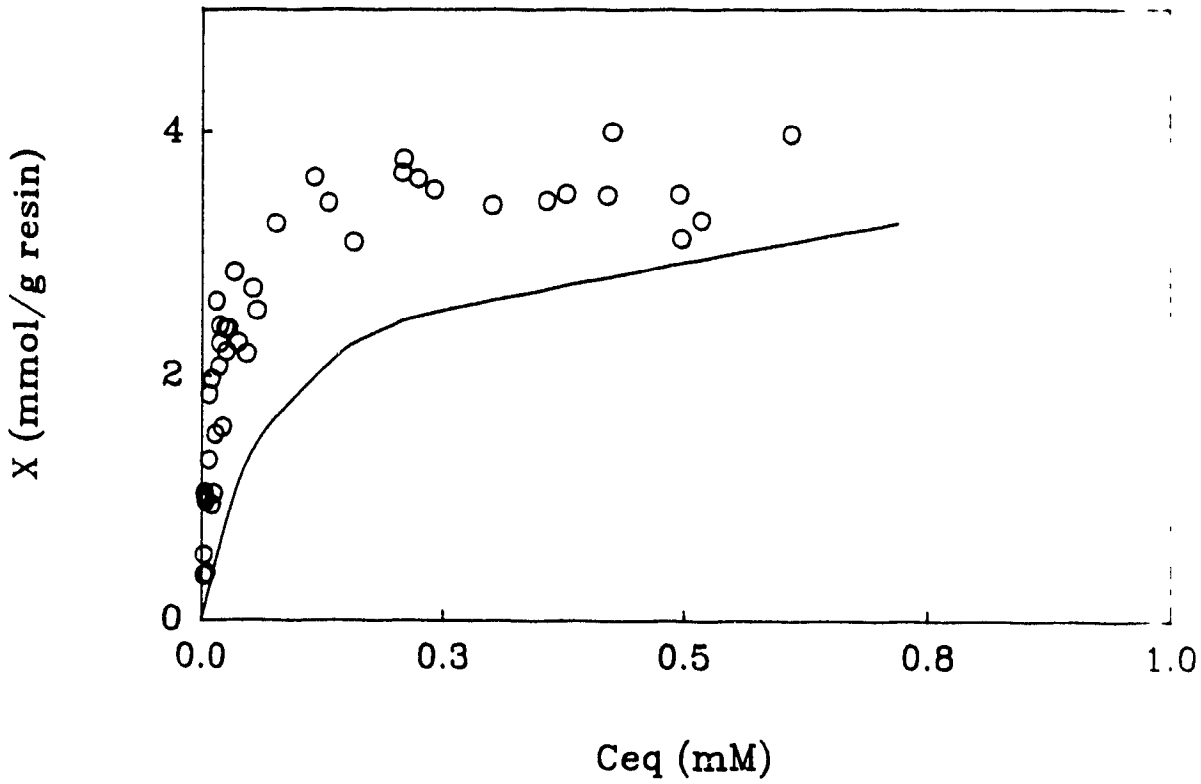

Figure 2.3 Isotherms for the adsorption of sodium glycocholate in water by cholestyramine (Cl). Comparison of the present results with the literature (1). ○ present results (T = 20°C); — Johns and Bates (T = 25°C) (1)

2.2.2 Comparison Between Counter-Ions

Changing the counter-ion of cholestyramine from chloride to iodide markedly reduces its ability to bind sodium glycocholate (Figure 2.4). The adsorption isotherm for the iodide reaches a "plateau" at about 0.5 mole per equivalent of pendant, or about one half the value of 1.1 obtained with the chloride counter-ion. This suggests that the chloride ion is displaced from cholestyramine more easily than is the iodide ion. Thus, the iodide ion interacts more favorably with cholestyramine than the chloride, which is in keeping with reports in the literature (9). This was also seen when the chloride ion was replaced by the iodide ion (Section 2.1.1). The iodide is thought (10) to bind somewhat better than the chloride ion, such that when bile salt anions are present they will displace the chloride ion more readily.

The chloride containing cholestyramine was chosen for further experiments because it was expected that any variations could be more prominent when the adsorbent of higher adsorption capacity was used.

2.2.3 Comparison Between Bile Acids

The isotherms for the adsorption, using cholestyramine with chloride counter-ion (CA Cl), of different bile acids in aqueous tris-buffer are given in Figure 2.5. Cholic and glycocholic acid anions have similar binding characteristics with cholestyramine, both having maximum adsorption at about 1.1 mole per equivalent of pendant; thus cholestyramine shows little, if any, specificity.

Previous results, obtained by Zhu (7), for the adsorption of cholic acid by cholestyramine (Cl) are also shown in Figure 2.5. It can be seen that they are slightly lower, as seen before in Section 2.2.1.

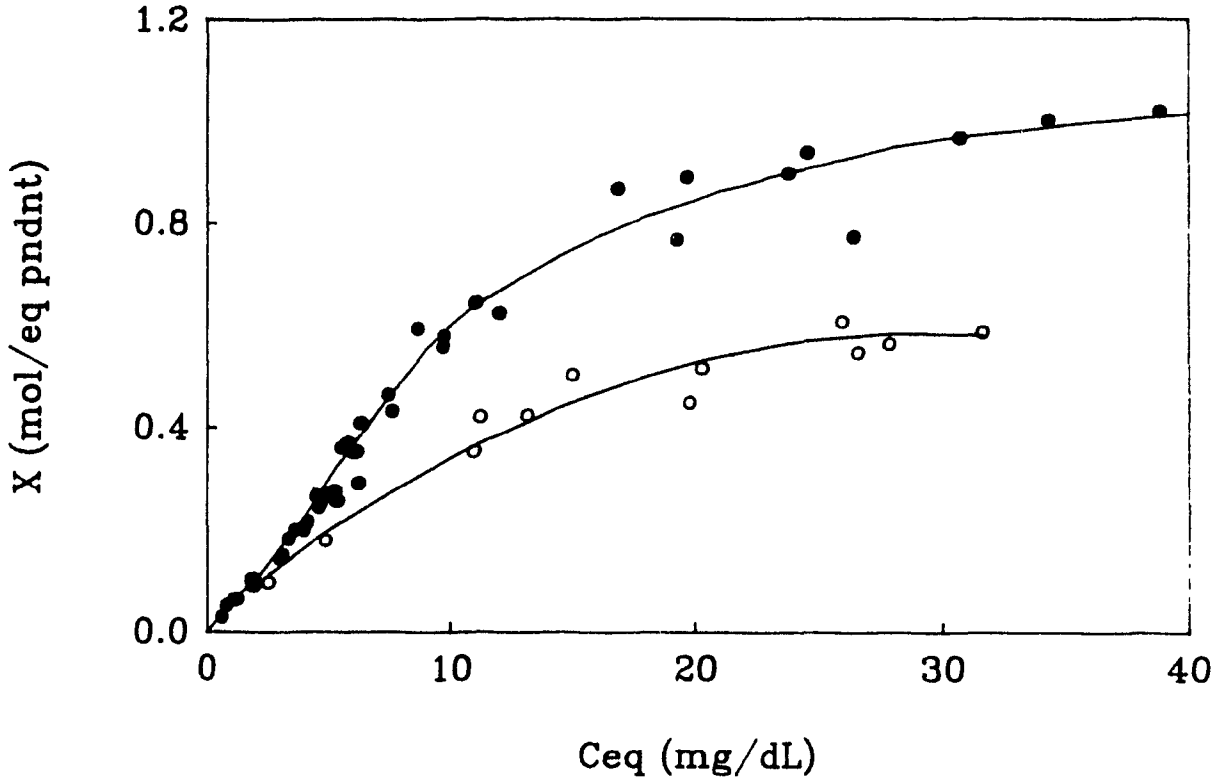

Figure 2.4 Isotherms (T = 20°C) for the adsorption of glycocholic acid by cholestyramine with different counter-ions, in Tris-HCl (0.0026 M). ○ iodide; ● chloride

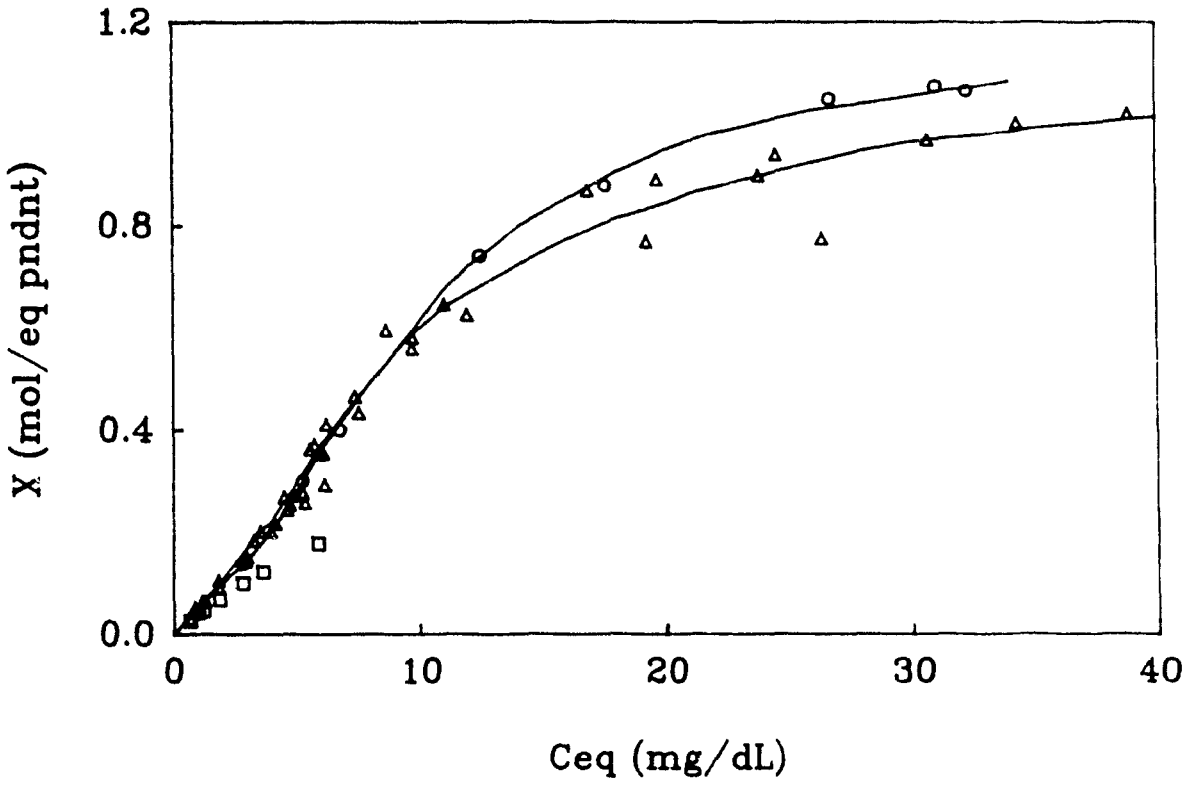

Figure 2.5 Isotherms (T = 20°C) for the adsorption of different bile acids by cholestyramine (Cl), in Tris-HCl (0.0026 M). ○ cholic acid (present results); ❑ cholic acid (previous results (7)); Δ glycocholic acid

2.2.4 Temperature Effect

The adsorption of cholic and glycocholic acids was studied at four different temperatures, 6, 25, 37 and 65°C. For glycocholic acid in Tris-buffer, identical adsorption isotherms are obtained at all temperatures other than 6°C (Figure 2.6). However, a significant decrease in adsorption capacity is observed in the 6°C isotherm. Similar behaviour is seen for cholic acid (Figure 2.7). For both bile acids a maximum of about 1.1 mole per equivalent is reached so that, within experimental error, the isotherms other than those for adsorption at 6°C correspond to that obtained at room temperature. This is in agreement with observations by Johns and Bates (1) who found that, for adsorption at 25 and 37°C, the process is not temperature dependent.

Consideration of the anomalous isotherm at 6°C suggested that it might reflect a change in the kinetics of adsorption. All solutions had been left to stir for a fixed period of 20-24 hours. It seemed possible that the adsorption process might be much slower at 6°C and, consequently, it had not reached equilibrium at 24 hours. Therefore, experiments were carried out to determine the concentration of bile acid in the solution at different adsorption times. The results (Figures 2.8, 2.9) clearly show that saturation is attained within 10 hours, i.e., well within the allotted time of 20-24 hours.

Clearly the behaviour observed for the adsorption is not consistent with a normal temperature dependence. The general pattern of the isotherms appears to be an increase in adsorption with an increase in temperature until an ultimate capacity is reached somewhere between 6 and 25°C. Further increase in temperature has essentially no effect on the adsorption isotherms.

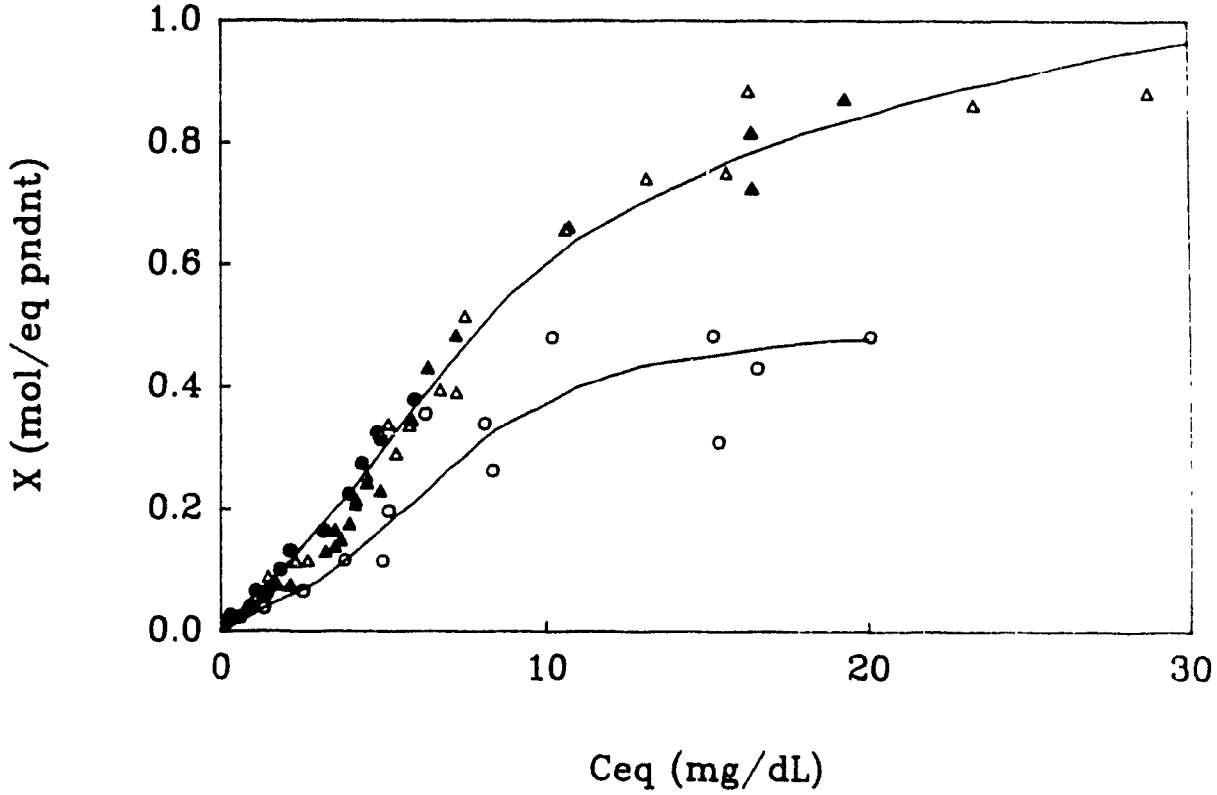

Figure 2.6 Isotherms for the adsorption of glycocholic acid by cholestyramine (Cl) in Tris-HCl (0.0027 M) at various temperatures. ○ 6°C; ● 25°C; Δ 37°C; ▲ 65°C

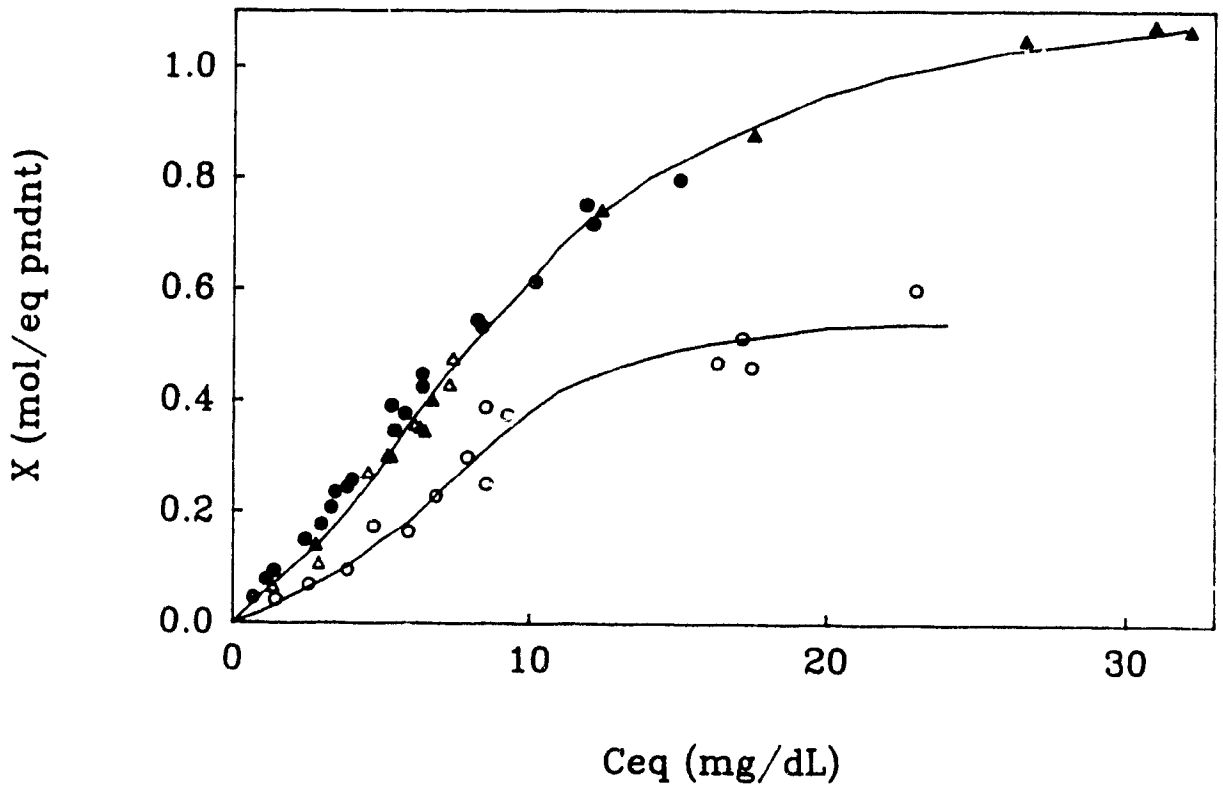

Figure 2.7 Isotherms for the adsorption of cholic acid by cholestyramine (Cl) in Tris-HCl (0.0026 M) at various temperatures. ○ 6°C; ▲ 25°C; ● 37°C; Δ 65°C.

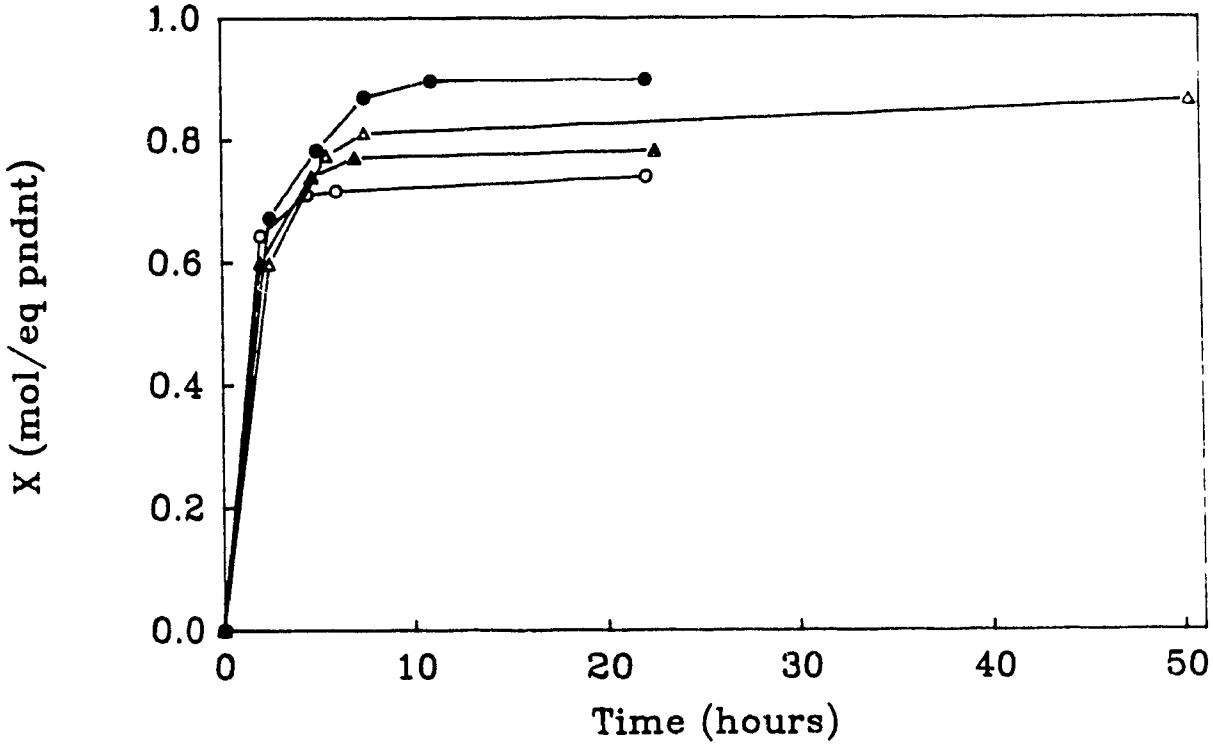

Figure 2.8 Kinetic experiments showing the amount of glycocholic acid adsorbed with time by cholestyramine (Cl), at different temperatures. ○ 6°C; ● 25°C; Δ 37°C; ▲ 65°C

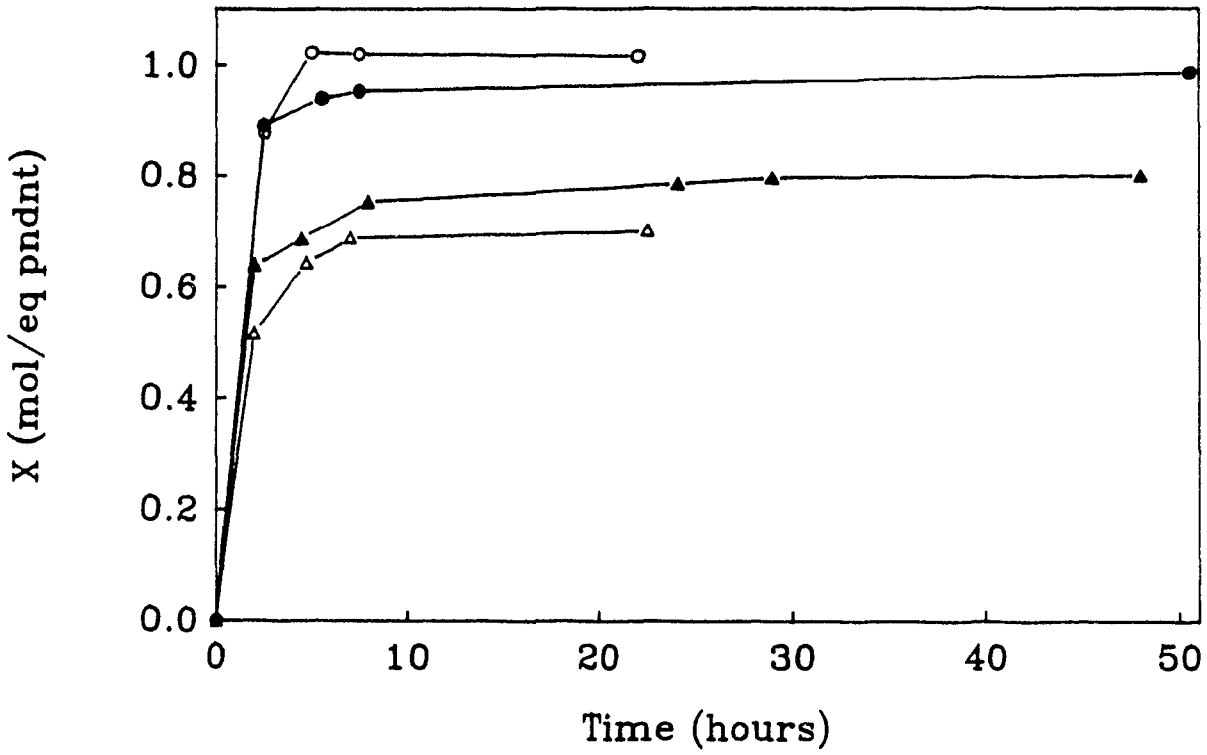

Figure 2.9 Kinetic experiments showing the amount of cholic acid adsorbed by cholestyramine (Cl) with time at different temperatures. ▲ 6°C; ○ 25°C; ● 37°C; Δ 65°C.

One explanation for such behaviour is that the solubility of the bile acid increases with a decrease in temperature leading to lower adsorption; however, this has not been verified. The process of bile acid anions entering the cholestyramine pores involves the transfer from an aqueous to a less polar environment. Generally, such a transfer process is endothermic (11, 12) so that as the temperature is increased this transfer becomes more favourable. Thus, an increase in temperature would result in an increase in adsorption. However, it is also expected that an increase in temperature would increase the solubility of bile acids in aqueous buffer (13), leading to a decrease in adsorption. On the other hand, as proposed earlier, a reverse temperature dependence for the solubility of bile acids could take place. These qualitative arguments do not yield a satisfactory explanation. Later in the chapter, a model is proposed, and a hypothesis is brought forward to explain the results obtained for different temperatures.

2.2.5. Challenges for a Chosen Model

From the results presented it can be seen that there are a number of questions which need to be answered. The model proposed to describe the adsorption behaviour should show not only the fit isotherms but should also explain other experimental observations. Thus, for example, the model should explain why the adsorption from Tris-HCl buffer and from water are different even though neither has competitive ions for the interaction with cholestyramine. Also, it should explain why iodide is not displaced as well as chloride. Furthermore, the model should offer a reasonable explanation for the temperature effect seen for the adsorption of bile acids by cholestyramine.

2.3 ADSORPTION ISOTHERMS

Adsorption isotherms reflect the binding affinity of an adsorbent for an adsorbate. Quantitatively, these affinities are expressed as binding constants that can be derived by use of various mathematical models. Generally each model results in its own binding constant, i.e., binding constants can differ from one model to the other because the concepts on which they are based are different. Many models are presented in the literature, of which some of the most commonly used will be discussed here.

2.3.1 Freundlich Model

The Freundlich model (14, 15), which does not have a strictly theoretical foundation, is expressed as:

$$r = k_f C^p \qquad \textbf{(Equation 2.1)}$$

where r is the moles of bound adsorbate per unit weight of adsorbent, k_f and p are constants. The constant k_f is generally a measure of the capacity of adsorption, p is a measure of the strength of adsorption and C is the concentration of adsorbate in solution at equilibrium.

The most common use of the Freundlich model is to simply obtain a fit to adsorption isotherms. The constants which are obtained are empirical and generally do not give an explanation of the adsorption data. Therefore, this model will not be used to develop an explanation for the present data.

2.3.2 Langmuir Isotherms

The Langmuir-type equation (equation 2.2) (16) has been used extensively to explain adsorption (17). It is expressed as:

$$1/r = (1/(nk))(1/C) + 1/n \qquad \textbf{(Equation. 2.2)}$$

where r is the moles of bound adsorbate per unit weight of adsorbent, n is the number of available sites, k is an intrinsic binding constant and C is the concentration of adsorbate in the equilibrium solution.

The Langmuir isotherm was originally applied to the adsorption of a gas on a solid surface. Subsequently, it has been modified and extended to other types of adsorption, such as liquid-liquid adsorption and liquid-solid adsorption. It presents a good fit for chemisorption but when the interaction is more physical (physi-sorption) the fit is not always good. However, in some cases a good fit of the data is obtained even though the assumptions of the model are not met (18-22). It cannot be fit to isotherms with an "S"-shape, indicating interaction (cooperativity) between sites.

The assumptions of the Langmuir model are: i) the adsorbent contains a fixed number of adsorbing sites and, at any temperature or presssure, there exist both occupied and unoccupied sites; ii) each site can accommodate **only one** adsorbate molecule; iii) the heat of adsorption is the same for all the sites and does not depend on the number of sites which are occupied; and iv) there are no interactions between molecules on different sites.

Equation 2.2 was used by Ihara (23-25) to interpret the data for the adsorption of fatty acids by ion-exchange resins and also by Johns and Bates (1-3) for the study of the adsorption of bile acids by cholestyramine.

The data obtained in this study for the adsorption of bile salts by cholestyramine (CA) under various conditions, as shown in Section 2.2, were fitted using Equation 2.2. The Langmuir isotherms are shown in Figures 2.10-2.14. Table 2.1 gives the values obtained for the number of available sites, n, and

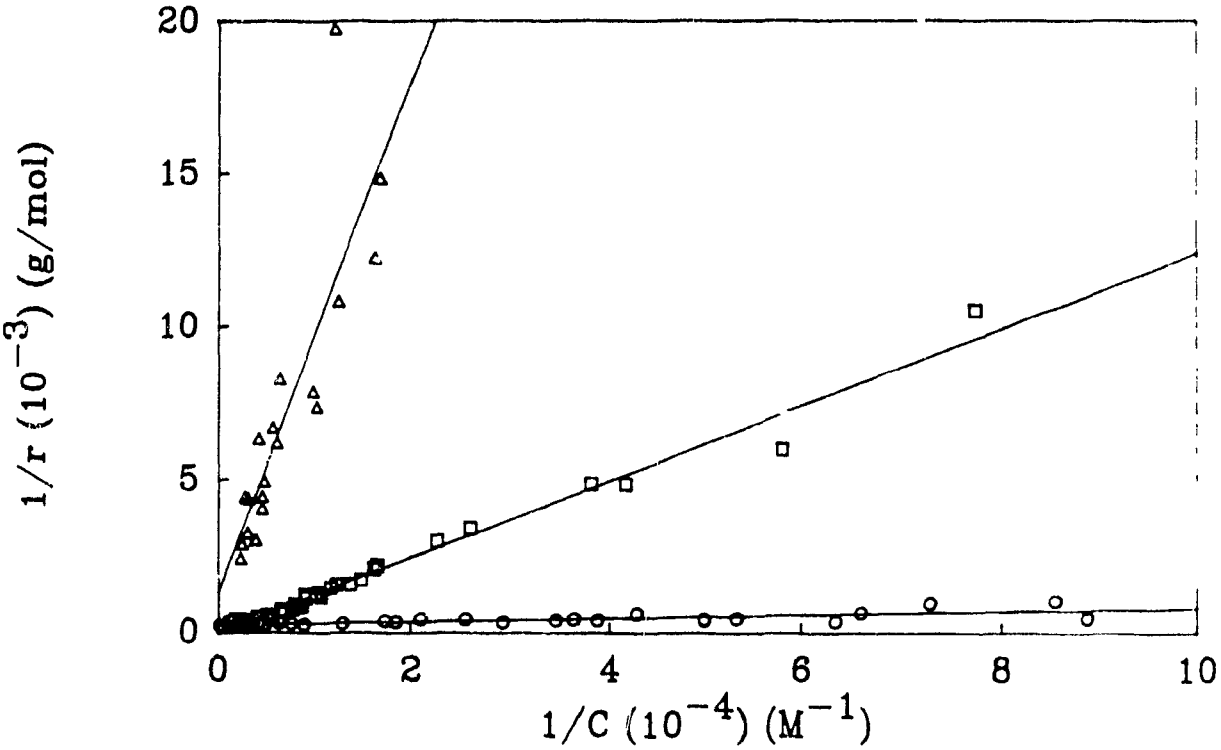

Figure 2.10 Langmuir isotherms for the adsorption of glycocholic acid by cholestyramine (Cl), in different buffers. ○ water; Δ phosphate buffer (0.0027M); ❑ Tris-HCl (0.0026M)

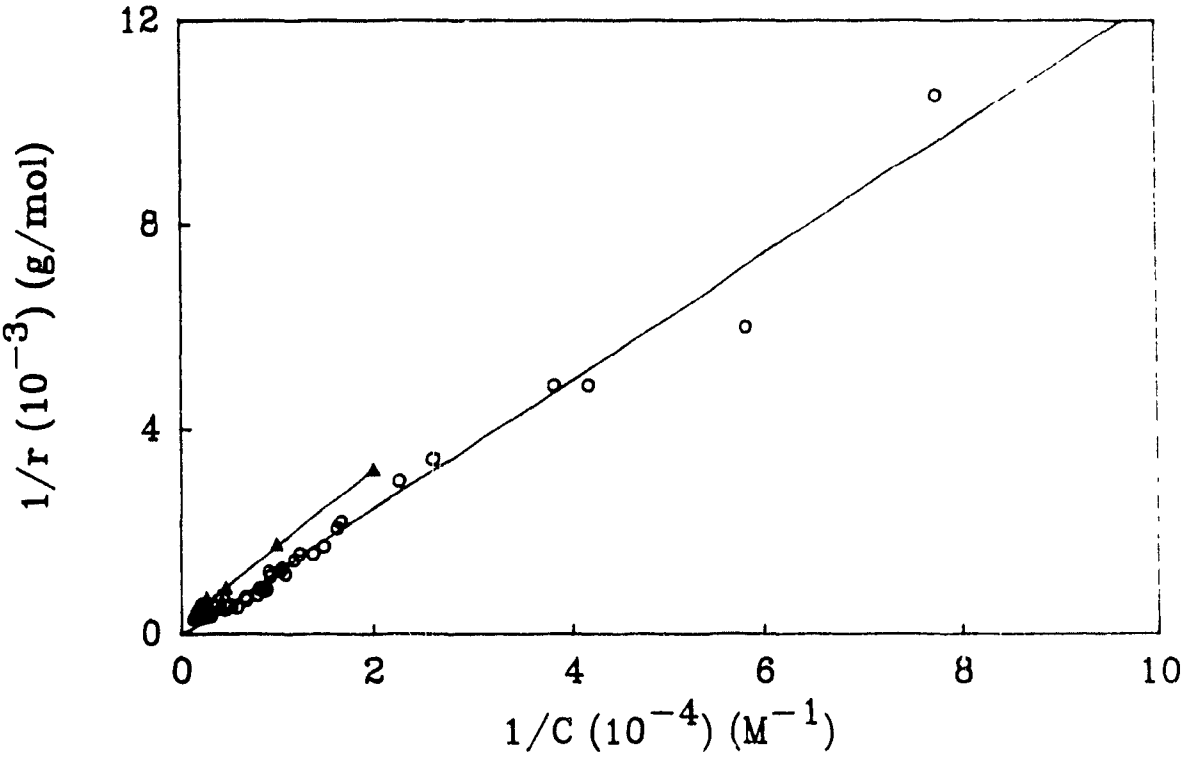

Figure 2.11 Langmuir isotherms for the adsorption of glycocholic acid by cholestyramine with different counter-ions, in Tris-HCl ○ chloride; Δ iodide

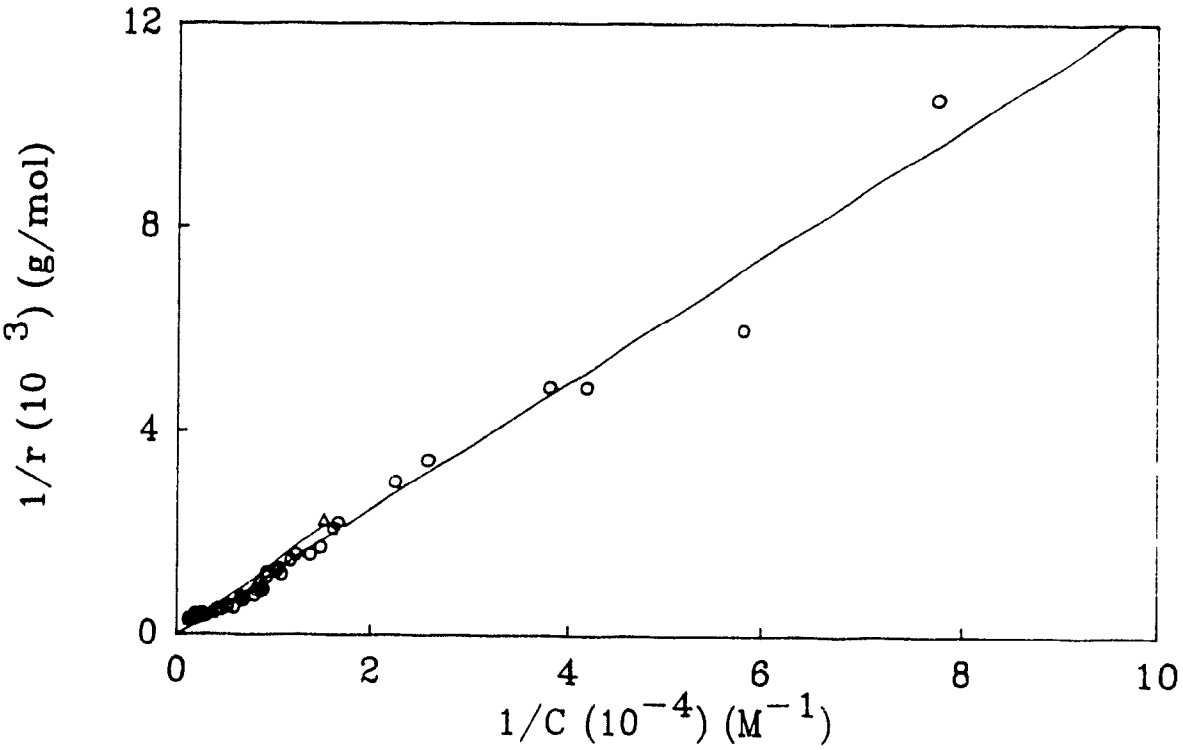

Figure 2.12 Langmuir isotherms for the adsorption of different bile acids by cholestyramine (Cl), in Tris-HCl. ○ glycocholic acid; Δ cholic acid

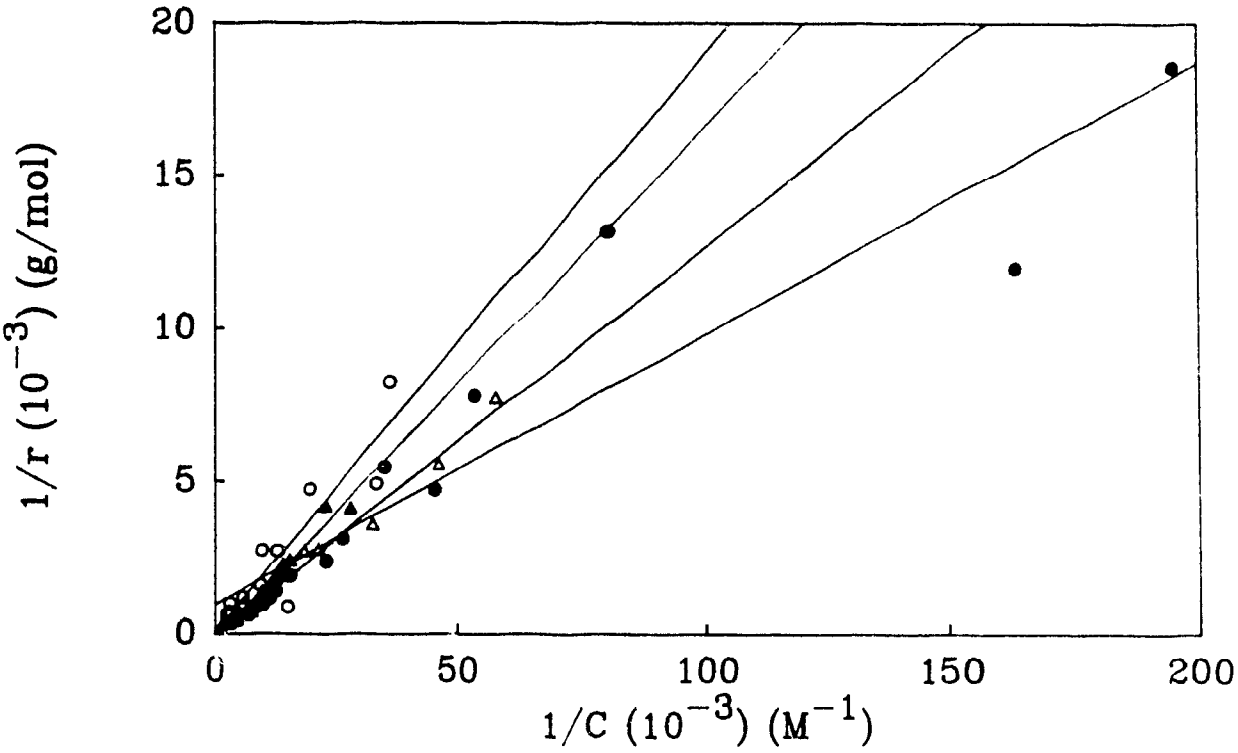

Figure 2.13 Langmuir isotherms for the adsorption of glycocholic acid by cholestyramine (Cl), in Tris-HCl, at various temperatures ○ 6°C; ● 25°C; Δ 37°C; ▲ 65°C

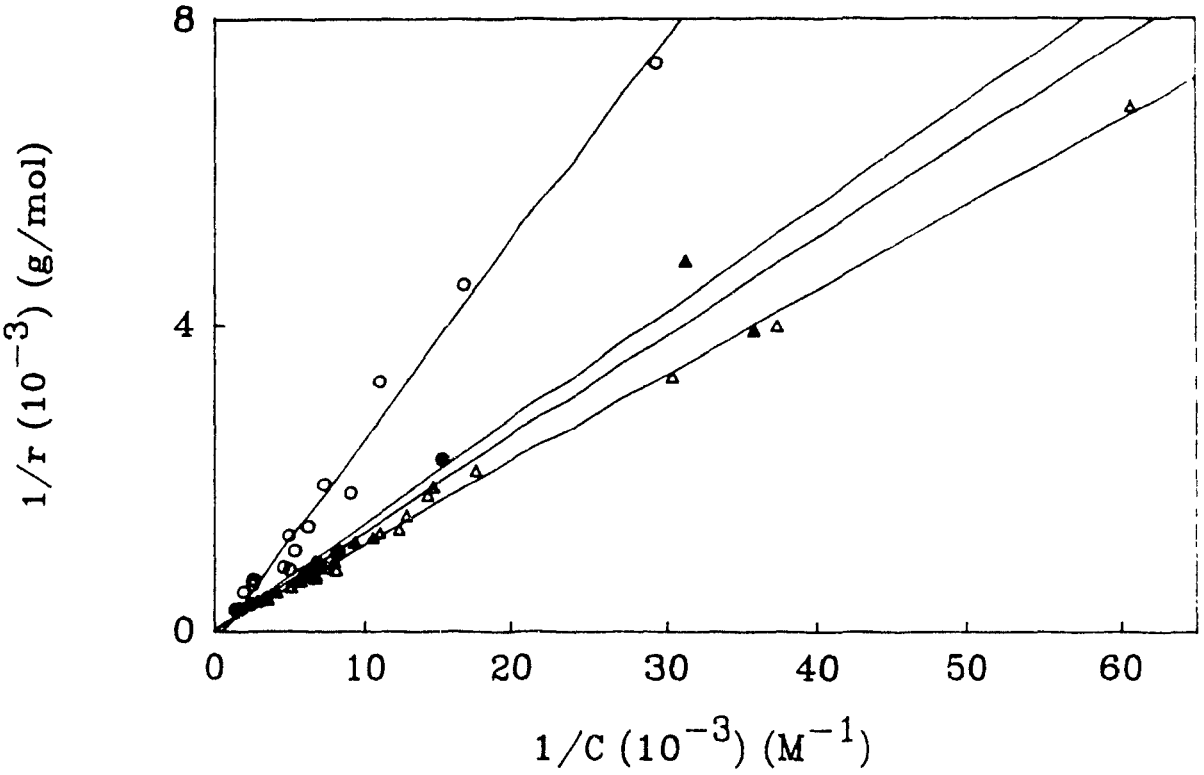

Figure 2.14 Langmuir isotherms for the adsorption of cholic acid by cholestyramine (Cl), in Tris-HCl, at various temperatures. ○ 6°C; ● 25°C; Δ 37°C; ▲ 65°C

the intrinsic binding constants, k, for the various systems as obtained from the intercept and the slope of the Langmuir isotherms. The lines represent the best fit obtained by linear regression of the data.

Superficial analysis of the data in Table 2.1 shows that the binding constant for the adsorption by cholestyramine (CA Cl) of glycocholic acid in water is higher than the one in phosphate buffer, as expected from the general shape of the isotherm (Figure 2.2). Furthermore, the values of n, the number of available sites, are also consistent with the trend. The results for cholestyramine (CA I) adsorbing glycocholic acid and cholestyramine (CA Cl) adsorbing cholic acid, are also consistent with the trends seen in the isotherms (Figures 2.4, 2.5)

However, further examination of the data reveals that: (i) the fits, as measured by the correlation coefficient, are generally poor; (ii) values are obtained for n that exceed the number of available sites or, in some cases, take negative values, which clearly has no physical meaning. Furthermore, in a number of cases, e.g., Figure 2.12, there is clear evidence for curvature near the intercept, which suggests some form of interaction which would render the Langmuir treatment meaningless. Indeed, in most cases the negative values of n reflect curvature in the Langmuir plot.

At best some of the values derived from these Langmuir isotherms show trends, but they do not give meaningful quantitative results. The negative values cannot be used, so that the Langmuir model is only of limited, if any, value for these systems.

Table 2.1 Values of the number of available sites, n, and the intrinsic binding constant, k, obtained by the Langmuir isotherms; the quality of the fit is shown by the correlation (Corr.).

	n (mol/g resin) (10^3)	k (M^{-1}) (10^{-3})	nk (mol/g M^{-1})	Corr.
CA Cl + GCA/Tris	-45	-0.18	0.80	0.990
KH_2PO_4	0.66	1.9	0.12	0.977
H_2O	3.5	60	21	0.821
CA I + GCA/Tris	4.0	1.8	0.68	0.996
CA Cl + CA/Tris	37	0.20	0.72	0.990
CA Cl + GCA/Tris				
6°C	23	0.23	5.3	0.922
25°C	1.0	11	11	0.938
37°C	-21	-0.38	7.8	0.994
65°C	-4.0	-1.5	59	0.980
CA Cl + CA/Tris				
6°C	-7.5	-0.51	3.8	0.991
25°C	37	0.20	7.2	0.990
37°C	35	0.26	9.0	0.999
65°C	63	0.12	7.8	0.970

2.3.3 Stoichiometric and Site Binding Models

The models used to obtain binding constants are of two general types: stoichiometric models and the site oriented approach (26, 27) In the stoichiometric model a molecule is viewed as binding n ligand(s) in a stepwise manner, i.e., it forms stepwise associations. The n associations are considered to occur sequentially, and no assumptions are made about the sites. The second type of model considers the addition of a ligand to a specific site to obtain a site binding constant. While no assumptions are required to obtain the stoichiometric binding constants, certain assumptions are necessary to determine site binding constants, such as that the binding sites are grouped into classes. Confusion about

the physical meaning of the stoichiometric binding constants (27, 28) tends to make the site oriented approach a preferred model.

2.3.3.1 One Binding Site per Pendant

Generally, when an interaction occurs between a single adsorbate molecule and one pendant, which represents a single binding site, the Scatchard equation (29) is then used:

$$X = \frac{k_1 [A]}{1 + k_1 [A]} = \frac{K_1 [A]}{1 + K_1 [A]} \qquad \textbf{(Equation 2.3)}$$

where [A] is the equilibrium concentration of free ligand, X is the number of moles bound per mole of active site and k_1 and K_1 are the site and stoichiometric binding constants, respectively. Binding to a single site is characterised by a linear Scatchard plot (X/[A] as a function of X) (29) with a slope equal to $-k_1 = -K_1$, i.e., a single binding constant is obtained.

The one binding site model was applied only to the data for isotherms that showed maximum adsorption lower than one mole of bile acid bound per equivalent of pendant. In these cases the fits, obtained by non-linear regression, shown in Figures 2.15-2.18, are quite satisfactory, although significant deviations tend to occur at low concentrations. This is particularly clear in Figure 2.18, for an isotherm that appears to have some "S" character. Furthermore, for isotherms of low binding, for which the best fit is obtained, the isotherms never approach one mole of bound bile acid per pendant within realistic equilibrium concentrations.

Table 2.2 shows the stoichiometric binding constants which were obtained using the one binding site model, along with a measure of the fit (R) which gets smaller as the fit improves. It can be seen that the values of the binding constants and of R are in accord with the observed trend.

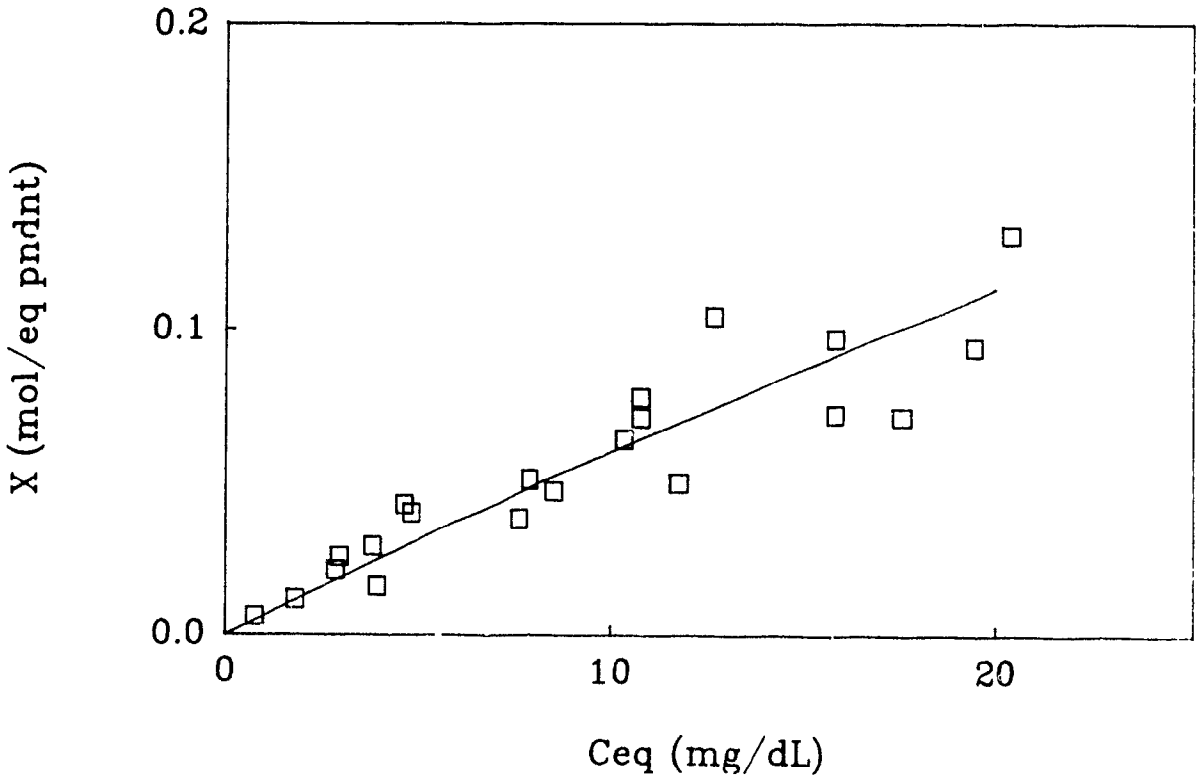

Figure 2.15 Isotherm (T= 20°C) for the adsorption of glycocholic acid by cholestyramine (Cl), in phosphate buffer, fitted according to the one binding site model. Experimental ❑ , fit —

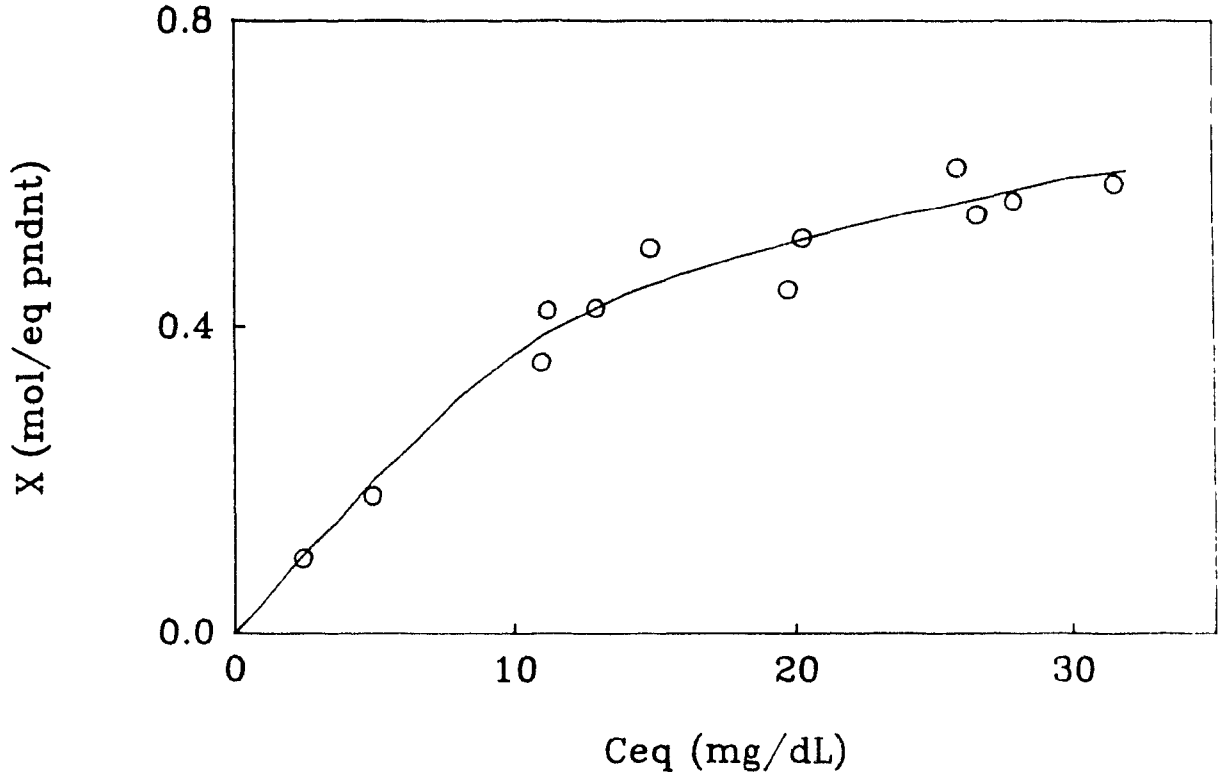

Figure 2.16 Isotherm (T = 20°C) for the adsorption of glycocholic acid by cholestyramine (I), in Tris-HCl, fitted according to the one binding site model Experimental ○ , fit —

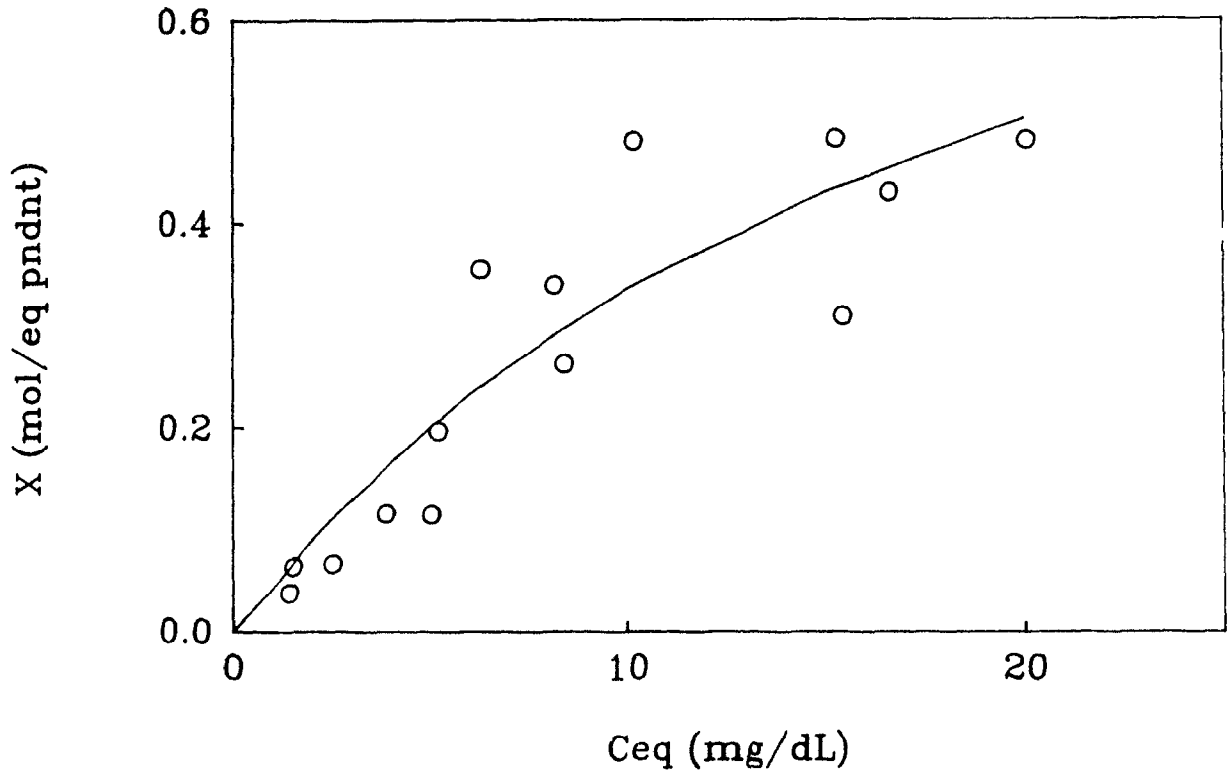

Figure 2.17 Isotherm (T = 6°C) for the adsorption of glycocholic acid by cholestyramine (Cl), in Tris-HCl, fitted according to the one binding site model.Experimental O , fit —

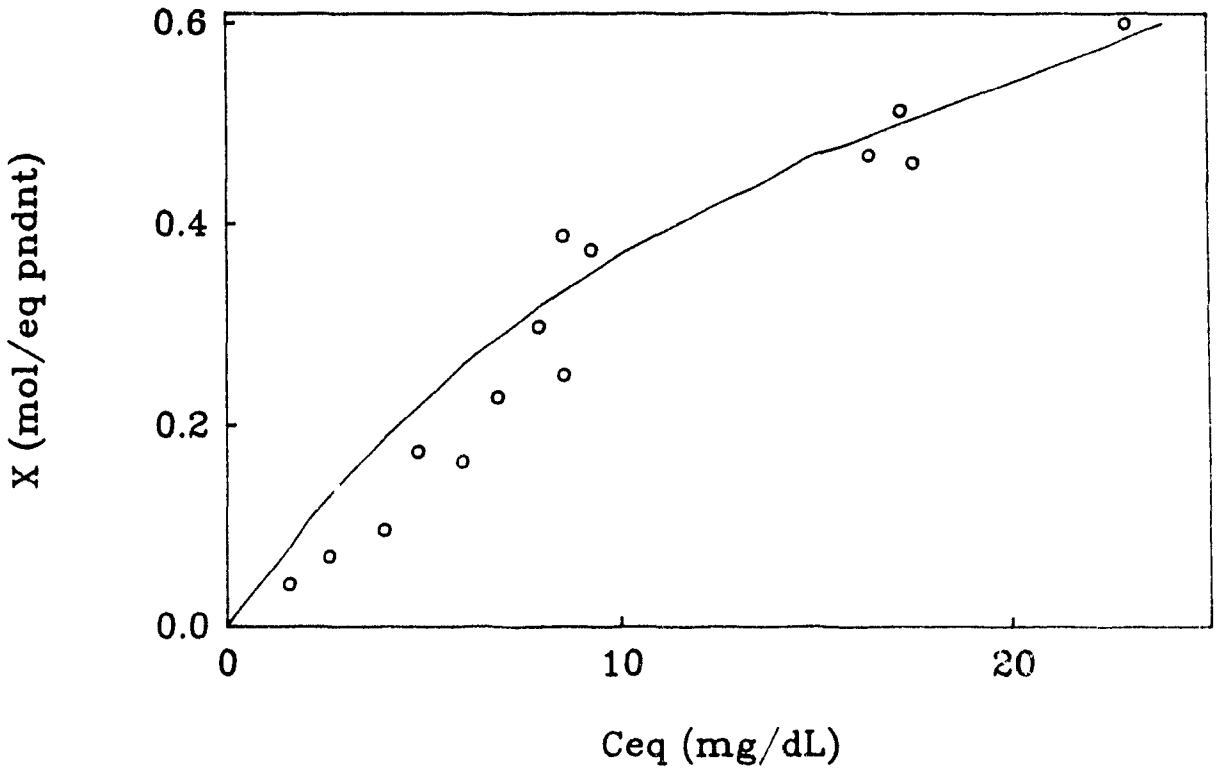

Figure 2.18 Isotherm (T = 6°C) for the adsorption of cholic acid by cholestyramine (Cl), in Tris-HCl, fitted according to the one binding site model.Experimental O , fit —

Table 2.2 Stoichiometric Binding Constants for the Adsorption of Bile Acid by Cholestyramine, using the One Binding Site Model. R is the measure of the fit

	$K_1(M^{-1})$ (10^{-3})	R
CA Cl + GCA/KH_2PO_4	0.31	0.0036
CA I + GCA/Tris	2.7	0.010
CA Cl + GCA/Tris 6°C	2.5	0.10
CA Cl + CA/Tris 6°C	2.5	0.033

The binding constants obtained are indicative of moderate to weak binding, particularly in the presence of phosphate buffer. Although the one binding site model does not apply to all of the isotherms, it is generally satisfactory for cases where X<1, except for cholestyramine (Cl) adsorbing cholic acid, in Tris-HCl at 6°C. Another model is required to explain the other results.

2.3.3.2 Two Binding Sites per Pendant

Consideration of the isotherms not included in the calculations described in Section 2.3.3.1 shows that: 1. "plateau" values exceeding one mole of bile acid per equivalent of pendant, and 2. some "S" character at low concentrations. These features suggest multiple binding at each pendant with some interaction between bound species. If specific binding is assumed, it seems unlikely that the polymer would have binding sites other than the pendants. Consequently, a model with more than one ligand per pendant is indicated, i.e., more than one binding site per pendant.

Both the site and stoichiometric models can be applied in the case where there is adsorption of two ligands per pendant, i.e., two sites per pendant. The site binding model assumes that the two binding sites are initially equivalent and

interacting, i.e., they are not independent. The expression to calculate the binding constants is shown in Equation 2.4 (28):

$$X = \frac{2k_1[A] + 2k_1k_2[A]^2}{1 + 2k_1[A] + k_1k_2[A]^2} \qquad \textbf{(Equation 2.4)}$$

where k_1 and k_2 are the site binding constants for the binding of the ligands on the first and second binding sites on the pendant. Equation 2.4 can be expressed as a quadratic equation:

$$[A]^2 + \frac{2[A](1-X)}{k_2(2-X)} + \frac{X}{k_1k_2(2-X)} = 0 \qquad \textbf{(Equation 2.5)}$$

Solving for the concentration at equilibrium, [A] yields:

$$[A] = \frac{X - 1 + \delta}{k_2(2-X)} \qquad \textbf{(Equation 2.6)}$$

where:

$$\delta = \{1 + 2(\varepsilon - 1)X - (\varepsilon - 1)X^2\}^{1/2} \qquad \textbf{(Equation 2.7)}$$

and:

$$\varepsilon = k_2/k_1 \qquad \textbf{(Equation 2.8)}$$

Then, a modified Scatchard equation is obtained:

$$X/[A] = \frac{k_2X(2-X)}{X - 1 + \varepsilon} \qquad \textbf{(Equation 2.9)}$$

As X approaches 0, $X/[A] = 2k_1$ and when X = 1, or at half-saturation, $X/[A] = (k_1k_2)^{1/2}$ (30, 31).

For the stoichiometric model, the following equation is obtained for a two site binding model (32):

$$X = \frac{K_1[A] + 2K_1K_2[A]^2}{1 + K_1[A] + K_1K_2[A]^2} \qquad \textbf{(Equation 2.10)}$$

Comparison of equations 2.4 and 2.10 gives rise to the following relationship between the binding constants (27, 33):

$$K_1 = 2k_1 \qquad \textbf{(Equation 2.11a)}$$

$$K_2 = 1/2k_2 \qquad \textbf{(Equation 2.11b)}$$

Application of equation 2.10 to the experimental data for the adsorption of bile acids by cholestyramine under various experimental conditions is shown in Figures 2.19-2.23. Table 2.3 shows the first and second stoichiometric binding constants obtained from the two binding site model along with the measure of the fit (R). It can be seen that the fits are reasonably good. For the isotherms with low adsorption, e.g., CA Cl + GCA/ KH_2PO_4; CA I + GCA/Tris; CA Cl + GCA/Tris 6°C, the second binding constant is zero, indicating that the one binding site model adequately describes the adsorption. Indeed, the binding constants obtained for these isotherms are very similar to those obtained by the one site calculations (Table 2.2). For the other isotherms, the first stoichiometric binding constant is larger than the second, indicating that the binding of the bile acid to the first site is better than the binding to the second The magnitude of the binding constants, in general, indicates only moderate binding affinity. Only in the case of adsorption from water is the binding constant large.

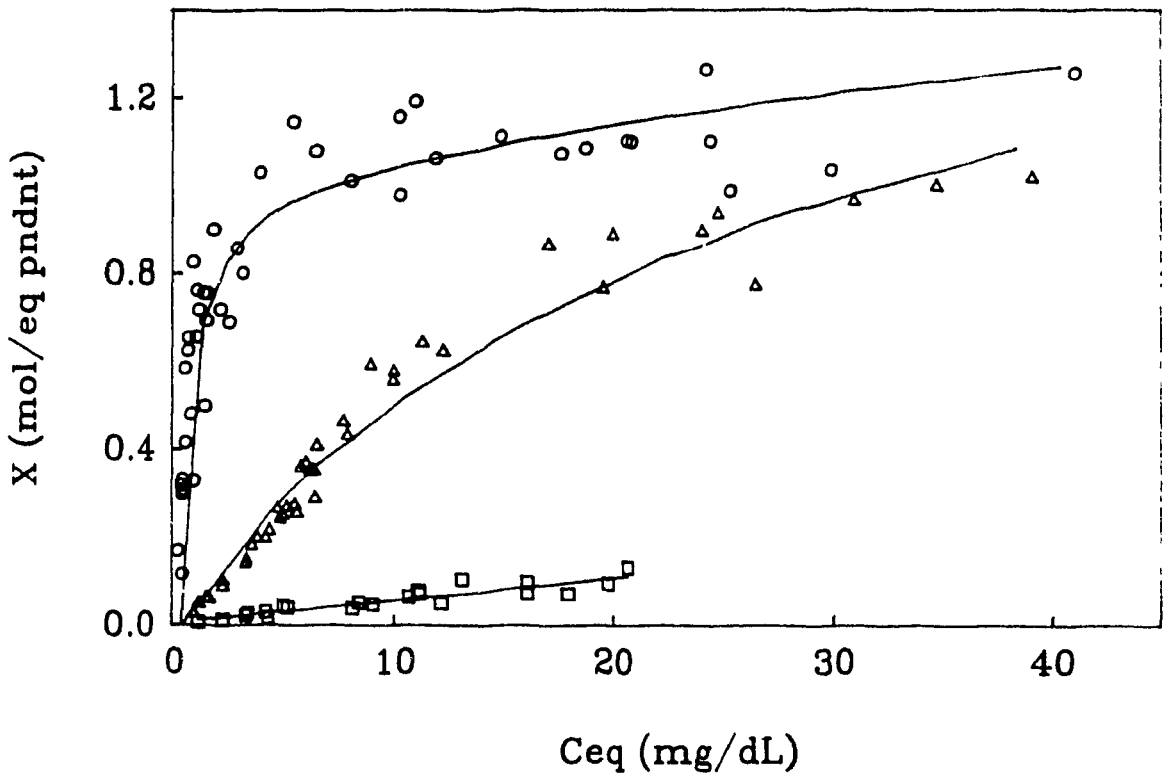

Figure 2.19 Isotherms (T = 20°C) for the adsorption of glycocholic acid by cholestyramine (Cl) in different buffers, fitted according to the two binding site model. Tris HCl:experimental Δ , best fit —; phosphate buffer:experimental ❑ , best fit — ; water:experimental ○ , best fit —

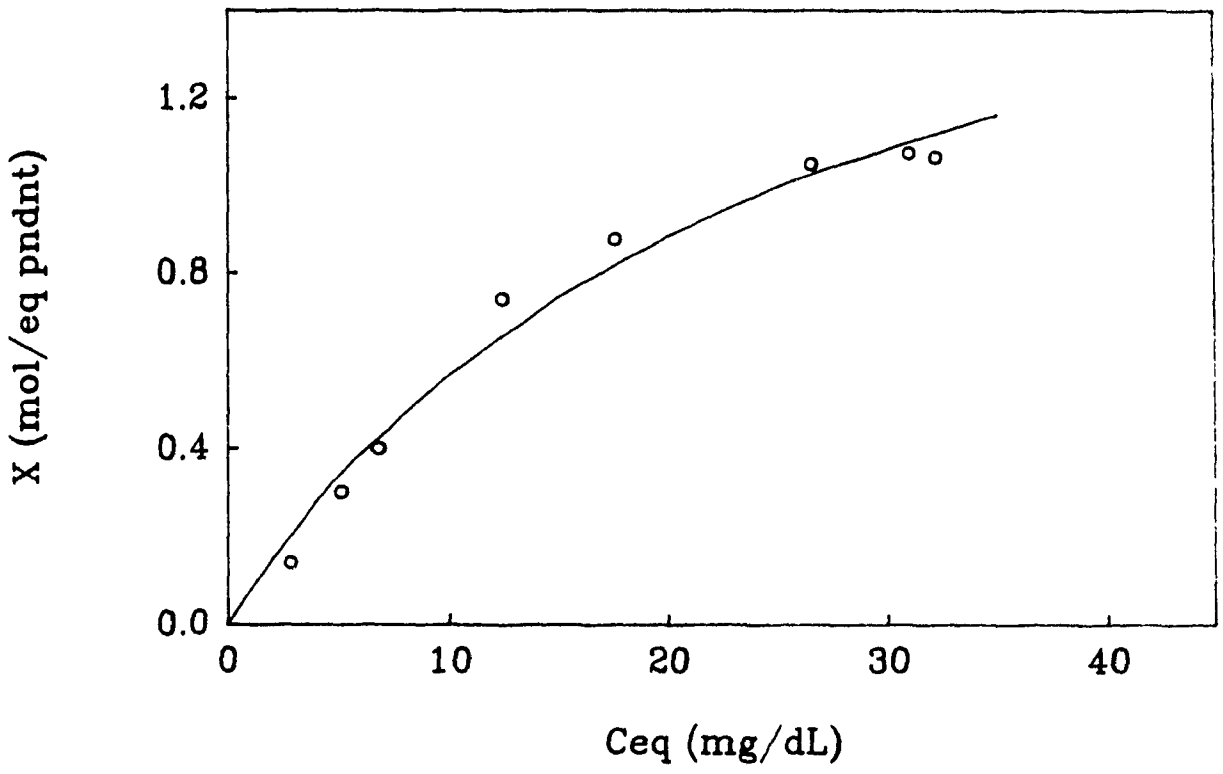

Figure 2.20 Isotherm (T =20°C) for the adsorption of cholic acid by cholestyramine (Cl), in Tris-HCl, fitted according to the two binding site model. Experimental O ; best fit —

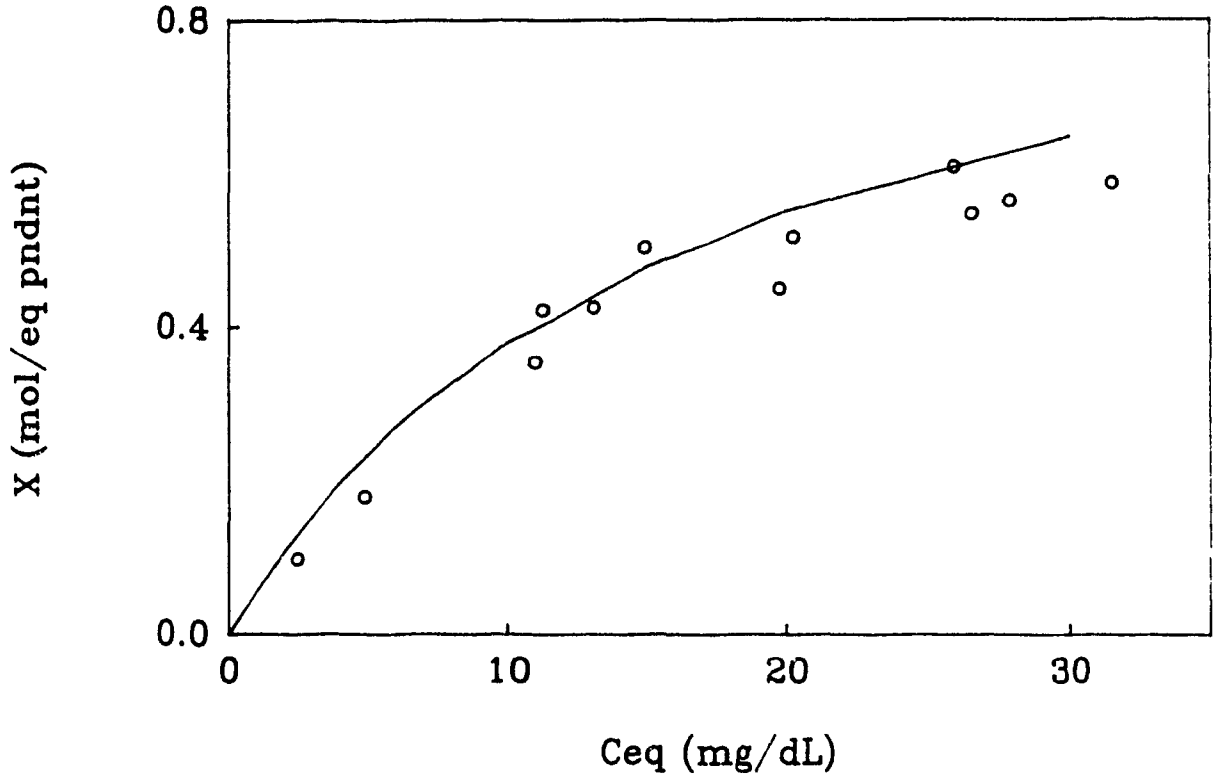

Figure 2.21 Isotherm (T = 20°C) for the adsorption of glycocholic acid by cholestyramine (I), in Tris-HCl, fitted according to the two binding site model. Experimental: O , best fit —

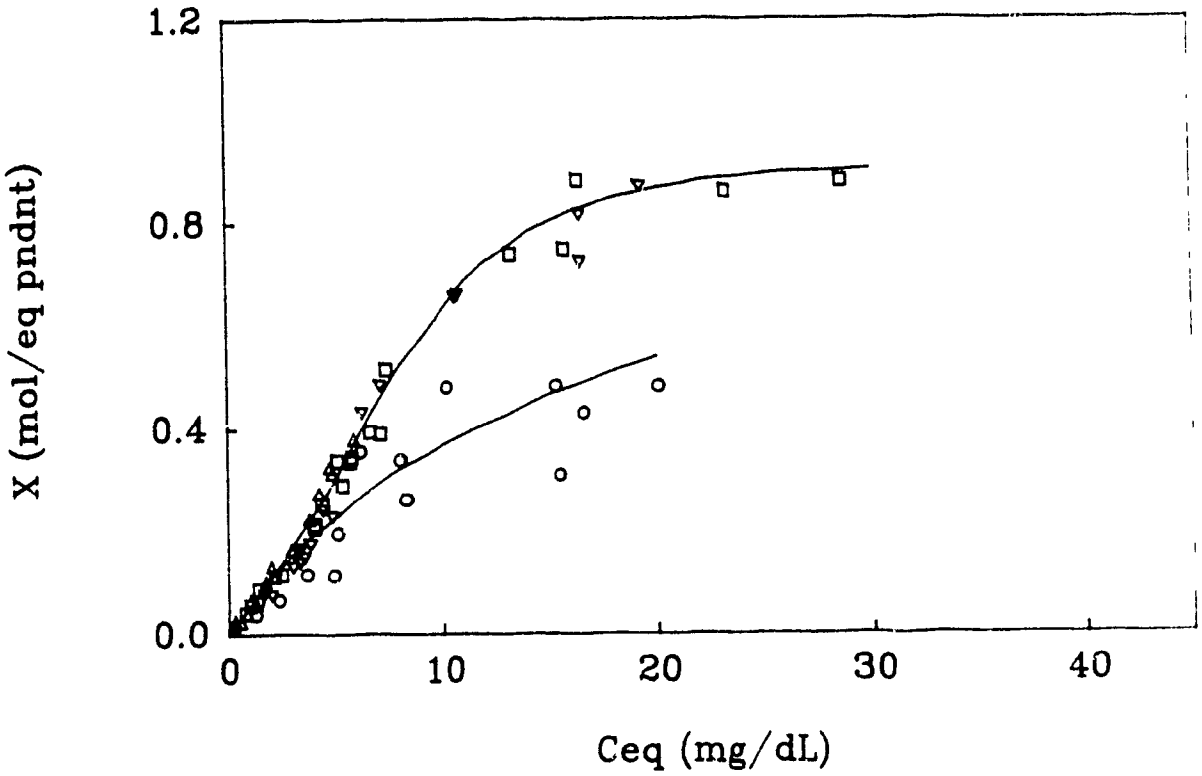

Figure 2.22 Isotherms for the adsorption of glycocholic acid by cholestyramine (Cl), in Tris-HCl, at different temperatures, fitted according to the two binding site model. 6°C:experimental ○ , best fit —; 25°C Δ ; 37°C ❑ ; 65°C ∇ ; best fit (25, 37, 65°C) —

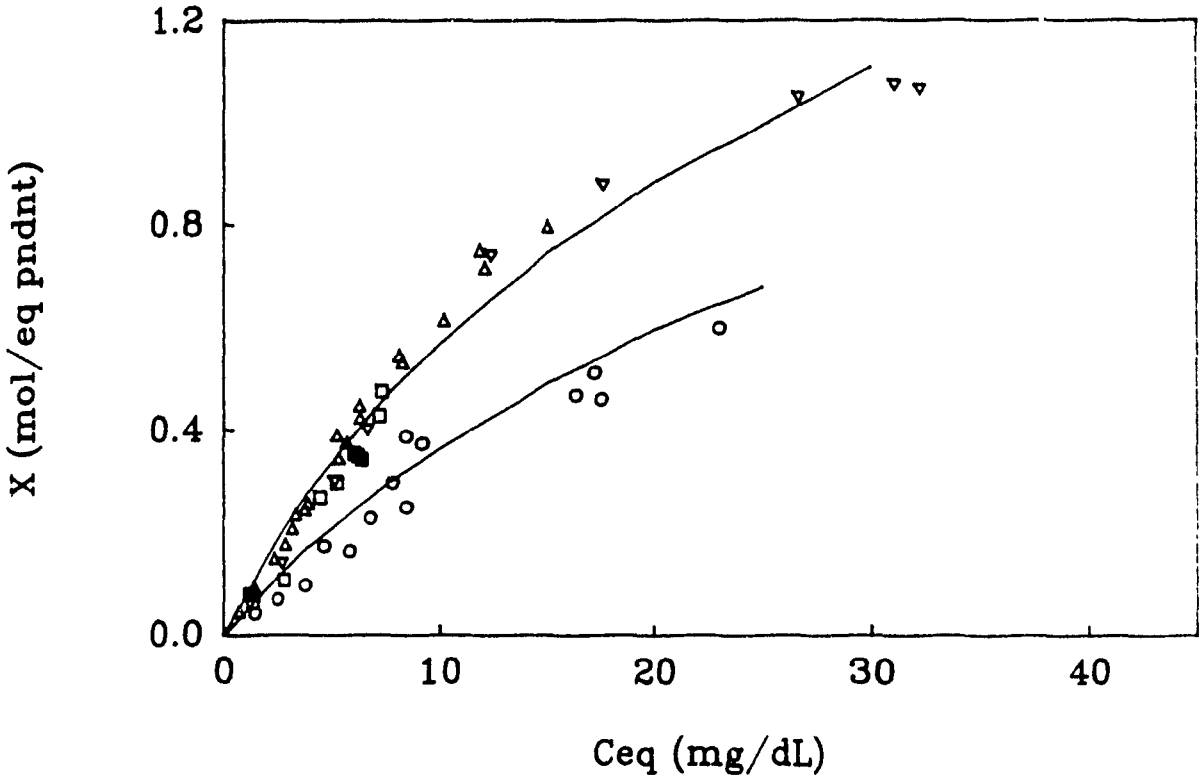

Figure 2.23 Isotherms for the adsorption of cholic acid by cholestyramine (Cl), in Tris-HCl, at different temperatures, fitted according to the two binding site model. 6°C:experimental ○ , best fit —; 25°C ▽ ; 37°C △ ; 65°C □ ; best fit (25, 37, 65°C) —

This treatment of the data appears to give reasonable values for the binding constants, with $K_1 \approx 6K_2$, in most cases. However, based on molecular models it is difficult to explain how the cholestyramine pendants could have two binding sites; mainly how is it sterically possible for two bile acids to bind to the benzylammonium pendant. Also the experimental isotherms tend to reach a "plateau" value of about 1.1 mol/eq. pendant, and with no indication that they tend to reach a value of 2. Therefore, this model is not entirely satisfactory. To obtain further insight regarding the binding, further calculations were made.

Table 2.3 Stoichiometric Binding Constants for the Adsorption of Bile Acid by Cholestyramine using the Two Site Binding Model. R is the measure of the fit.

	$K_1(M^{-1})$ (10^{-3})	$K_2(M^{-1})$	R
CA Cl + GCA/Tris	3.7	630	0.090
/KH_2PO_4	0.34		0.0041
/H_2O	103	480	0.25
CA Cl + CA/Tris	3.4	850	0.020
CA I + GCA/Tris	3.0		0.089
CA Cl + GCA/Tris			
6°C	2.9		0.11
25, 37, 65°C	3.7	630	0.090
CA CA + CA/Tris			
6°C	2.0	350	0.025
25, 37, 65°C	3.4	850	0.020

2.3.4 Modified Scatchard Model

To adequately describe adsorption for isotherms with "S" character, indicative of cooperativity, two binding constants are required, even though saturation occurs at 1 mole of ligand per site (X=1). A model that has been

proposed (34, 35) to be used for such a system is based on two assumptions: the sites are initially equivalent and the pendants bind a maximum of one ligand. Sites on separate pendants are assumed to be sufficiently close so that binding of a ligand on one site affects the affinity of a subsequent ligand binding on an adjacent site (34, 35). Thus, the cooperativity nature of the binding is between adjacent pendants, each having one binding site.

The site binding constants can be obtained by the following equation (35):

$$X' = \frac{k'_1[A] + k'_1k'_2[A]^2}{1 + 2k'_1[A] + k'_1k'_2[A]^2} \qquad \textbf{(Equation 2.12)}$$

where X' is equal to 2X, as defined by equation 2.4. This is done to account for the interaction between two adjacent pendants, which effectively decreases the substitution on the polymer support by half, i.e., it is assumed that initially adjacent pendants interact with one another making the number of available sites less than the functionality; k'_1 and k'_2 are site binding constants for the binding of the first ligand on one pendant and for the binding of the second ligand on the adjacent pendant, respectively.

The modified Scatchard equation (34, 35) can then be expressed as follows:

$$X'/[A] = \frac{2k'_2 X'(1-X')}{2X' - 1 + \delta'} \qquad \textbf{(Equation 2.13)}$$

where:

$$\delta' = \{1 + 4(\varepsilon' - 1)X' - 4(\varepsilon' - 1)X'^2\}^{1/2} \qquad \textbf{(Equation 2.14)}$$

$$\varepsilon' = k'_2k'_1 \qquad \textbf{(Equation 2.15)}$$

Then k'_1 and k'_2 can be evaluated from a Scatchard plot of X'/[A] as a function of X', since as X' approaches 0, X'/[A] = k'_1 and at X' = 0.5, X'/[A] = 1/2 $(k'_1k'_2)^{1/2}$.

This model has been used previously to explain the binding of bilirubin by polymers containing various peptide pendants (34-36). Application to the adsorption of bile acids to cholestyramine, under various experimental conditions gives the results shown in Figures 2.24-2.28. In a number of cases, e.g., adsorption of glycocholic acid by cholestyramine (Cl), in Tris-HCl, at 20-65°C and adsorption of cholic acid by cholestyramine (Cl), in Tris-HCl,at 20-65°C, a much improved fit is obtained. However, although an "S" shape is evident in the 6°C isotherms, it is not fitted by the model, possibly because of scatter in the original data. Furthermore, as required by the model, in cases of adsorption more than one mole of bile acid per equivalent of pendant the fit is not good at high Ceq, since it cannot exceed X=1 (e.g., the isotherm for the adsorption of glycocholic acid by cholestyramine (Cl) in water).

Table 2.4 shows the stoichiometric binding constants (which are related to the site binding constants, k'_1 and k'_2, by Equation 2.11a,b) obtained by this model along with the measure of the fit (R). It can be seen that for the adsorption of glycocholic acid by cholestyramine (Cl) in phosphate buffer and Tris-HCl at 6°C, the second binding constant is zero. For cholestyramine (I) adsorbing glycocholic acid and cholestyramine (Cl) adsorbing cholic acid at 6°C, both in Tris-HCl, the first binding constant is larger than the second ($K_1>K_2$) and for the other experiments, the opposite was observed ($K_1<K_2$). When $K_1>K_2$, the second bile acid is bound less effectively than the first, and it is referred to as negative cooperativity. When $K_1<K_2$, positive cooperativity is indicated, meaning that the second bile acid is bound more strongly than the first. The measure of the fit R shows that the fits are best when X<1. The presence of the first bile acid

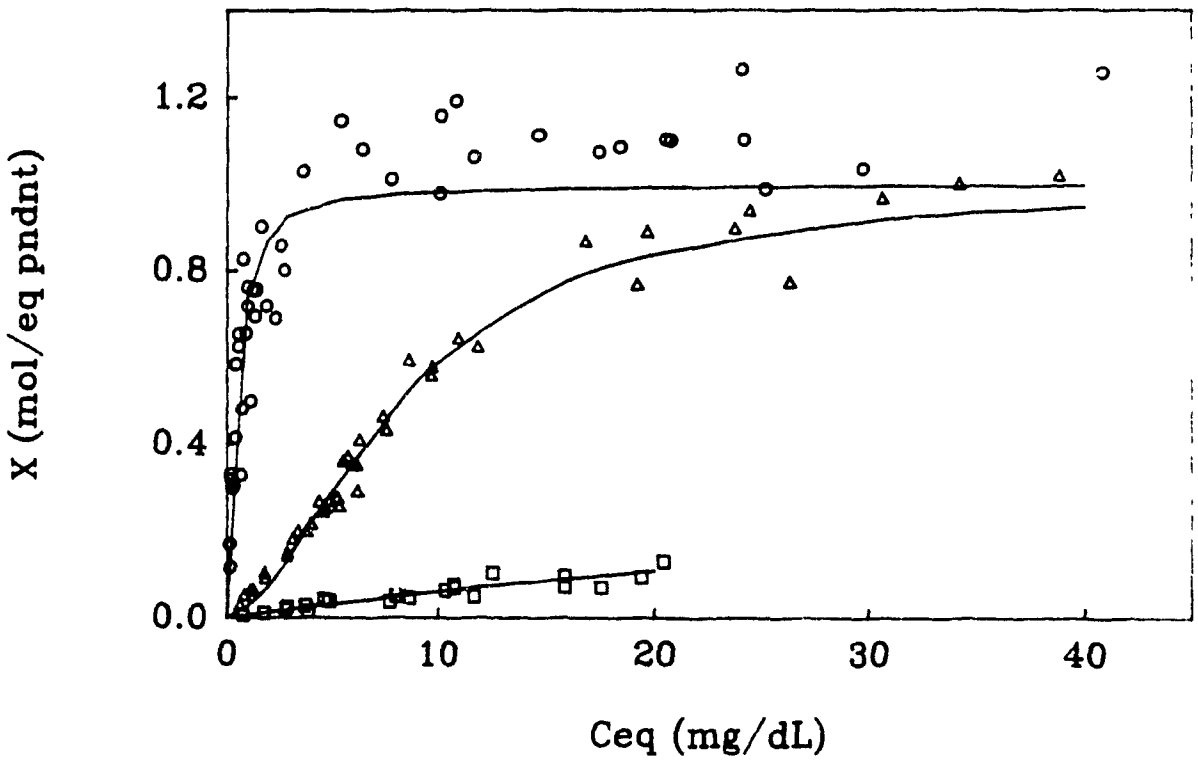

Figure 2.24 Isotherms (T = 20°C) for the adsorption of glycocholic acid by cholestyramine (Cl) in different buffers, fitted according to the modified Scatchard model. Tris-HCl:experimental Δ , best fit — ; phosphate buffer:experimental ❑ , best fit — ; water:experimental ○ , best fit —

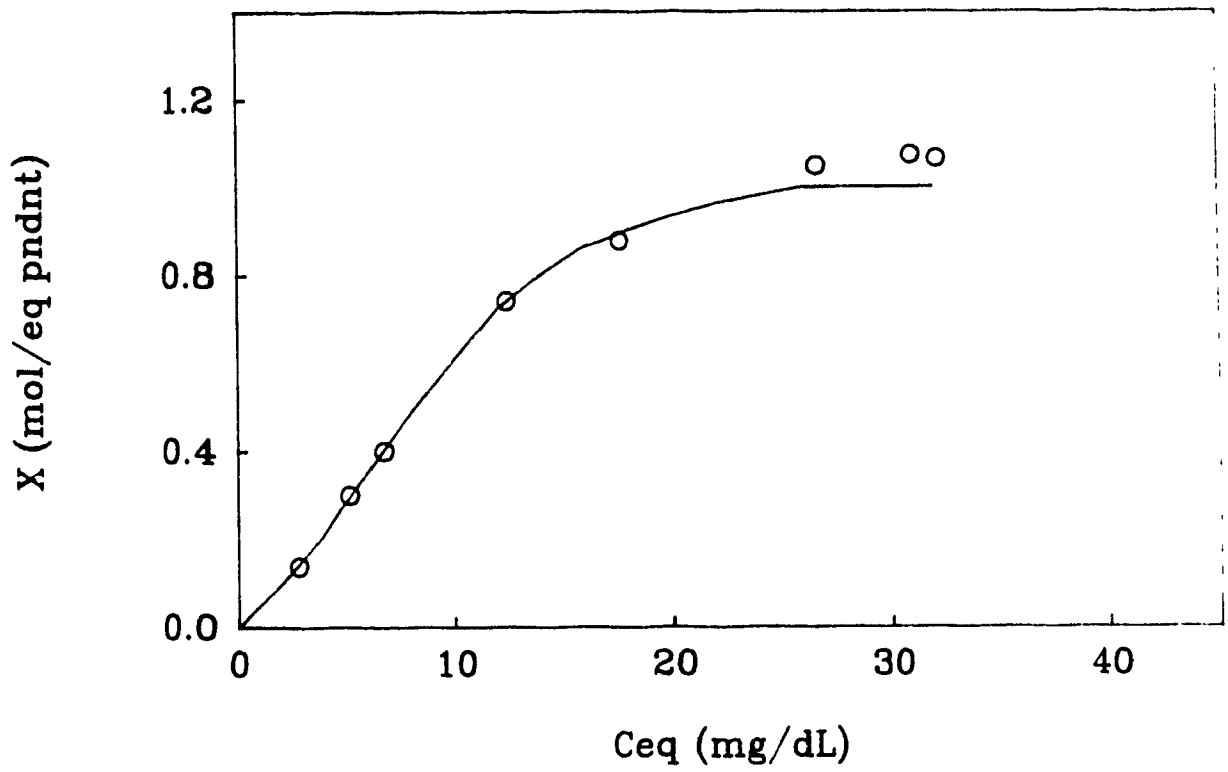

Figure 2.25 Isotherm (T = 20°C) for the adsorption of cholic acid by cholestyramine (Cl), in Tris-HCl, fitted according to the modified Scatchard model. Experimental O , best fit —

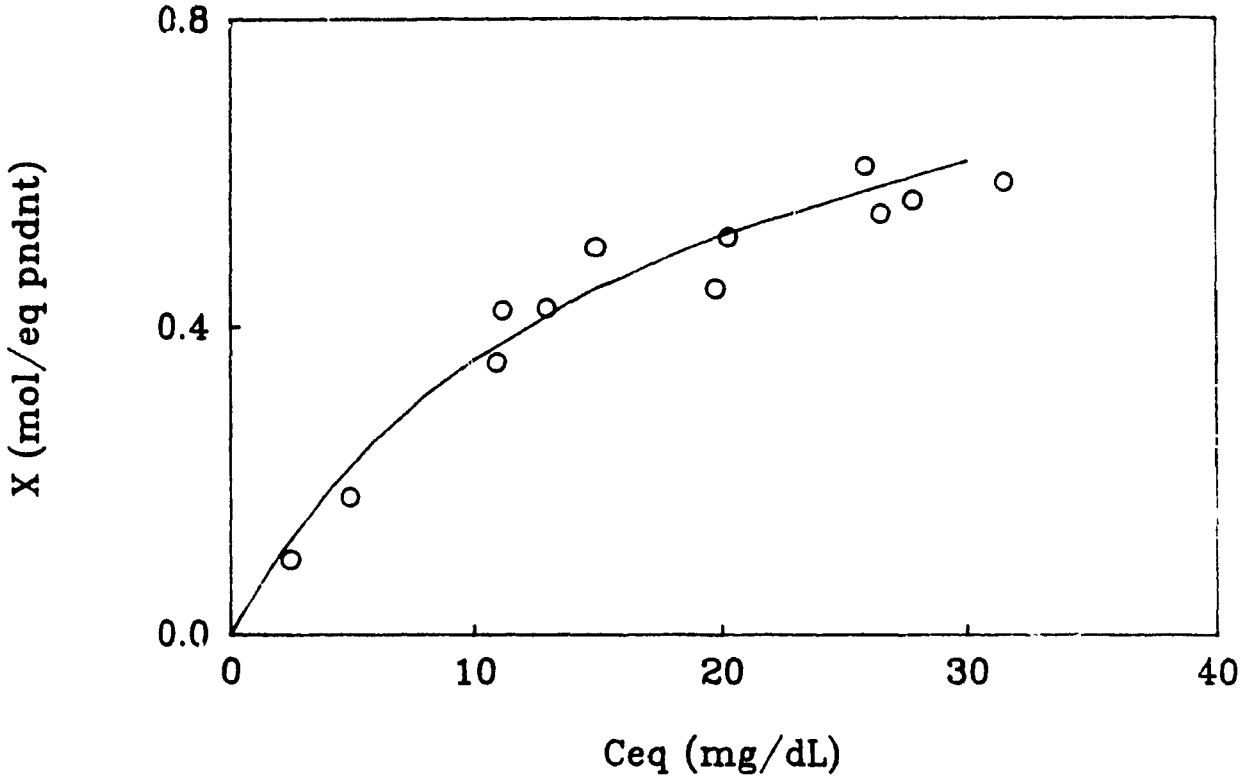

Figure 2.26 Isotherm (T = 20°C) for the adsorption of glycocholic acid by cholestyramine (I), in Tris-HCl, fitted according to the modified Scatchard model. Experimental O , best fit —

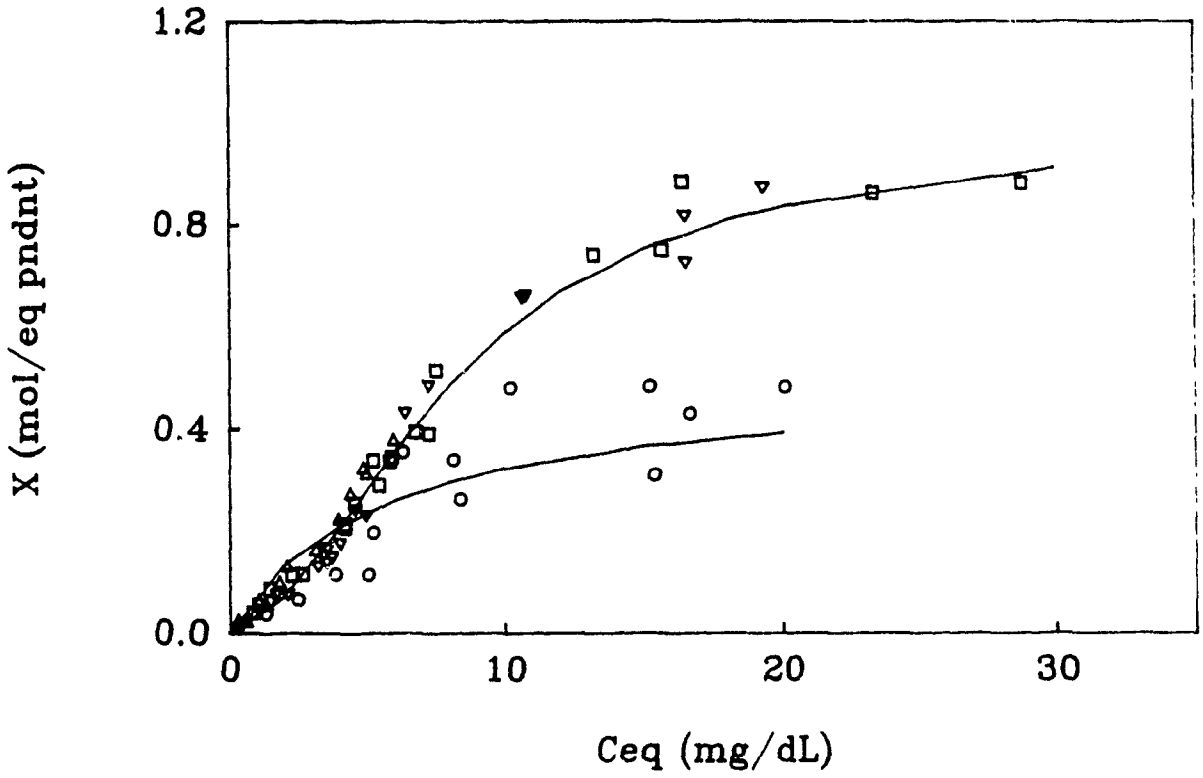

Figure 2.27 Isotherms for the adsorption of glycocholic acid by cholestyramine (Cl), in Tris-HCl, at different temperatures, fitted according to the modified Scatchard model. 6°C:experimental ○ , best fit —; 25°C Δ ; 37°C □ ; 65°C ∇ ; best fit (25, 37, 65°C) —

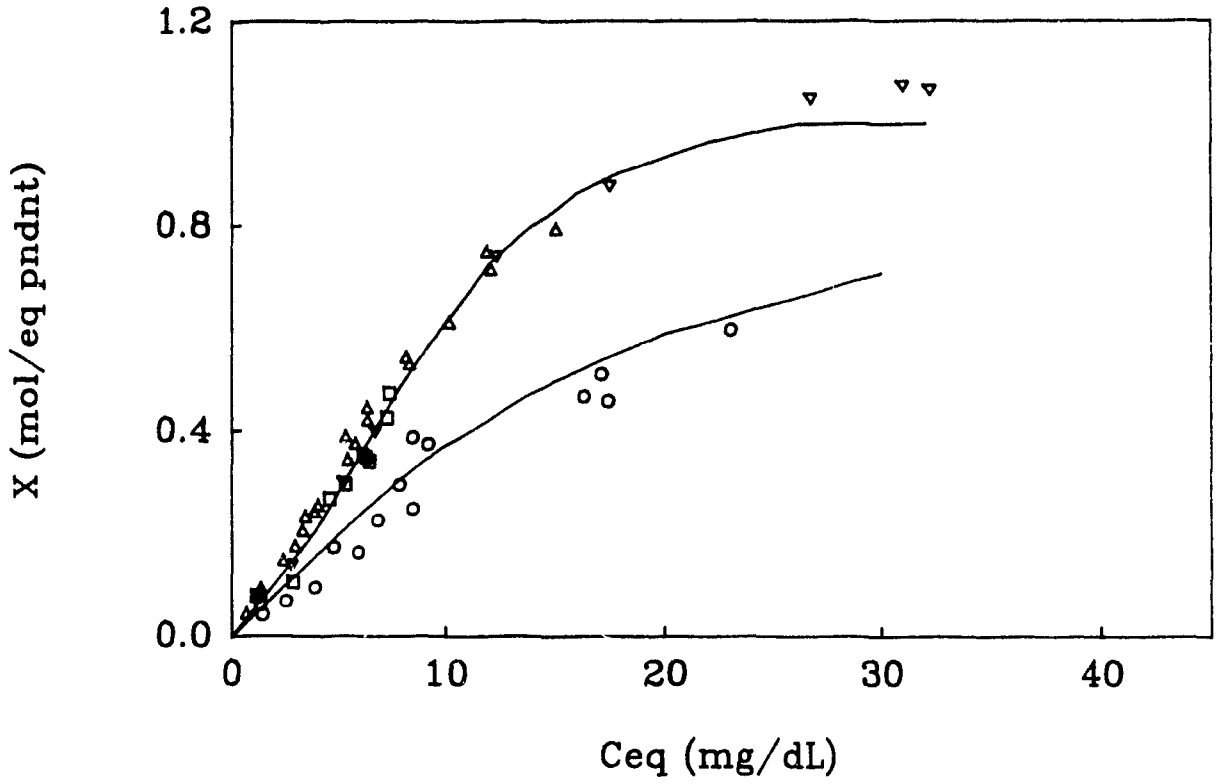

Figure 2.28 Isotherms for the adsorption of cholic acid by cholestyramine (Cl), in Tris-HCl, at different temperatures, fitted according to the modified Scatchard model. 6°C:experimental O , best fit —; 25°C ∇ ; 37°C Δ ; 65°C □ ; best fit (25, 37, 65°C) —

molecule apparently assists the binding of the second, perhaps by some hydrophobic interactions as observed in the formation of bile acid micelles.

Table 2.4 Stoichiometric Binding Constants for the Adsorption of Bile Acid by Cholestyramine, using the Modified Scatchard Model. R is the measure of the fit

	$K_1(M^{-1})$ (10^{-3})	$K_2(M^{-1})$ (10^{-3})	R
CA Cl + GCA/Tris	0.93	38	0.53
/KH_2PO_4	0.69		0.014
/H_2O	7.0	139	0.96
CA Cl + CA/Tris	0.87	40	0.45
CA I + GCA/Tris	5.8	1.2	0.040
CA Cl + GCA/Tris			
6°C	8.9		0.43
25, 37, 65°C	0.93	38	0.53
CA Cl + CA/Tris			
6°C	3.2	2.6	0.089
25, 37, 65°C	0.87	40	0.45

With the modified Scatchard model, good fits are obtained for some isotherms. However,there are some anomalies. For example, it is difficult to explain why cholestyramine (Cl) adsorbing cholic acid at 6°C shows a negative cooperativity while at higher temperatures, it is positive. Although the experimental conditions differ, the interaction between the pendant and the bile acid should be similar Also this model assumes interactions between active sites, and in the case of cholestyramine, this may not be possible, as illustrated in Figure 2.29. This matter will be discussed in more detail in Chapter 4.

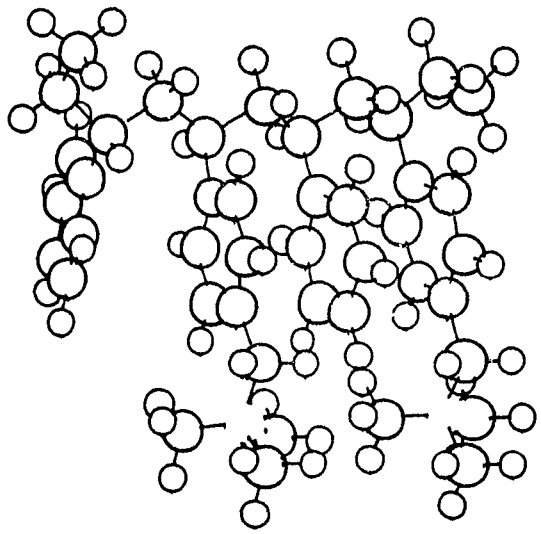

Figure 2.29 Structure of Cholestyramine showing two pendants bearing the quaternary ammonium group. (black:carbon, blue:hydrogen, yellow:nitrogen)

2.3.5 Summary

For isotherms saturating at a value of less than one mole bound of bile acid per equivalent of pendant, the one binding site model gives a satisfactory fit, and this was corroborated by use of the two binding site model which gave the second binding constant as being zero. However, in the use of the modified Scatchard model, although the adsorption of glycocholic acid by cholestyramine is found to have a $K_1 > K_2$, indicating negative cooperativity, an adsorption of less than one mole of bound bile acid per equivalent of pendant is observed. The two binding site model for the other isotherms fits some of the data, although the isotherms with an "S" shape could not be explained; the modified Scatchard model fits the latter.

It is difficult to understand why different models are needed to account for the various isotherms. It appears unlikely that cholestyramine would have two binding sites per pendant. The limitations of the modified Scatchard model, are in its saturation to X=1 and that interactions between adjacent pendant are required.

These calculations show that in most cases some interaction is occurring between sites. However, these treatments do not give an explanation that accounts for the global patterns.

2.4 ION-EXCHANGE

Ion-exchangers are insoluble solid materials which carry exchangeable counter-ions, cations or anions. They consist of a framework, held together by chemical bonds or lattice energy, that carries a positive or negative electric charge surplus which is compensated by counter-ions. The counter-ions are free to move within the framework and can be replaced by other ions of the same sign This

replacement can take place when the ion-exchanger is in contact with an electrolyte solution.

Electroneutrality must be preserved within the ion-exchange resin; thus a counter-ion can leave the framework only when another counter-ion simultaneously enters. The counter-ion content of the ion-exchanger, the ion-exchange capacity, is a constant which is given solely by the magnitude of the framework charge and is independent of the nature of the counter-ion.

The most important class of ion-exchanger are organic ion-exchange resins. Their framework, or matrix, consists of an irregular macromolecular three-dimensional network of hydrocarbon chains and carries ionic groups, such as $-SO_3^-$, $-COO^-$, $-NH_3^+$, $-NR_3^+$, to show a few.

The chemical, thermal and mechanical stability and the ion-exchange behaviour of the resins depend chiefly on the structure and the degree of cross-linking of the matrix and on the nature and number of fixed ionic groups. The degree of cross-linking determines the mesh width of the matrix, and thus the swelling ability of the resin, and in turn the mobilities of counter-ions. The latter determines the rate of ion-exchange and other processes.

The nature of the fixed ionic group determines the acid or base strength of the ion-exchanger. For example, weak base groups such as $-NH_3^+$ lose a proton forming $-NH_2$ at high pH, but strong base groups such as $-NR_3^+$ remain ionized. Thus, the ion-exchange capacity of weak base resins will be more pH dependent than that of strong base resins. The nature of the fixed ionic group also affects the selectivity of the resin. Counter-ions which tend to associate with the fixed ionic groups by forming ion-pairs or complexes are preferred by the resin.

The basicity of the resin plays a role in the ion-exchange. It has been found that, for weak base resins, the interaction between the fixed ionic group and the counter-ion is primarily electrostatic (37). However, for strong base resins the

interaction depends not only on electrostatic forces but also on a selectivity sequence. The selectivity, defined as the ability of ion-exchange resin to distinguish between various counter-ions, depends primarily on electrostatic interactions as well as on other interactions, like coulombic, polarization, and hydration of the counter-ion (37). An order of strength of the binding of various anions has been determined (10):

$OH^{-a)}$> SO_4^{-2}> CrO_4^{-2}>citrate^{-3}> tartrate^{-2}> NO_3^-> AsO_4^{-3}> PO_4^{-3}> molybdate> acetate, I^-, Br^-> Cl^-> F^-> $OH^{-b)}$,

where a) is the position of the hydroxyl group for weak base resins, and b) is its position for strong base resins (10, 38, 39).

Thus, when an ion-exchanger is in dilute solution of electrolyte, there will be a displacement of the original counter-ion if the electrolyte ion is better "liked" by the resin:

$$A^+_r + B^+_s \rightleftharpoons A^+_s + B^+_r,$$

where r and s refer to the resin and solution phases, respectively. This process is referred to as ion-exchange.

Ion-exchange is mainly a statistical redistribution of counter-ions between the pores of the resin and the external solution. It limits the maximum adsorption to the number of stoichiometric equivalents of the ionic group of the resin, since if more, then other interactions would be taking place in the resin pores.

The primary interaction in ion-exchange is electrostatic, and depends on the size and the valence of the counter-ion; there are also other forces which exist between the ions and their environment. In addition, some large counter-ions

may be excluded from the resin pores by steric hindrance, although the resin can expand or swell. The swelling of the resin will depend upon such factors as the polarity of the solvent, the degree of cross-linking, the solvation tendency of the fixed ionic group, the valence of the counter-ions and others. The ion-exchange process depends upon the mobilities of the counter-ions, making it dependent upon the diffusion through the resin pores.

The ion-exchange process has been reviewed extensively in the literature and many mathematical models have been applied to explain it. Early attempts to formulate a theory were based on the law of mass action (40). The ion-exchange process has also been considered as an adsorption process, by applying the Freundlich and the Langmuir isotherms. Although these can fit the data, they do not provide a true representation of the process (23-25, 41).

2.5 DONNAN THEORY

Beginning in 1911, Donnan reported the study of the distribution of electrolytes in a system consisting of a membrane freely permeable to low molecular weight ions but impermeable to colloidal ions present only on one side of the membrane (42-44). This theory was then extended to systems of electrolytes of which at least one species of ions is restrained in any way from diffusing to other parts of the system. The Donnan theory has been applied extensively to ion-exchange.

Since one of the ionic species is restrained to one part of the solution, either by a membrane or by being fixed to a polymer matrix, an unequal distribution of ions will ensue. Migration of both cations and anions will take place between the two regions giving rise to an electric potential. The force by which equilibrium is re-established between the two phases is referred to as the Donnan potential and the attained equilibrium as the Donnan equilibrium. The

Donnan equilibrium is then obtained when the action of the Donnan potential balances the tendency of the counter-ions to diffuse out into solution.

The theory of Donnan can be explained using the following example: Solutions of sodium chloride and a compound referred to as NaA are put together, but the anion A^- is restricted to one side by the presence of a semi-permeable membrane. The sodium and chloride ions are able to diffuse through the membrane (Figure 2.30). For charge conservation in both phases, an ion can pass through the membrane only if : i) an ion of the same sign simultaneously strikes the other side of the membrane, or ii) an ion of opposite sign strikes the same side at the same time. These requirements follow since, at equilibrium, electroneutrality must exist in both phases.

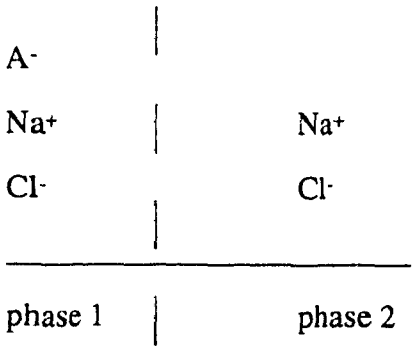

Figure 2.30 Representation of the equilibrium existing between two solutions separated by a semi-permeable membrane

At equilibrium, the electrochemical potential of an ion on one side must equal the electrochemical potential of the same ion on the other side of the membrane:

$$\underline{\mu}_{Na^+} = \underline{\mu}'_{Na^+} \qquad \textbf{(Equation 2.16)}$$

where ' refers to phase 1.

The electrochemical potential of sodium ions in phase 2 can be defined by:

$$\underline{\mu}_{Na^+} = \mu_{Na^+} + nF\Phi, \qquad \textbf{(Equation 2.17)}$$

where μ_{Na+} is the chemical potential of the sodium ion, Φ is the electrostatic potential of phase 2, n is the number of Faradays of charge passing through the membrane and F is Faraday's constant.

At equilibrium:

$$\mu_{Na^+} + nF\Phi = \mu'_{Na^+} + nF\Phi'. \qquad \textbf{(Equation 2.18)}$$

But:

$$\mu_{Na^+} = \mu^o_{Na^+} + RT \ln a_{Na^+}. \qquad \textbf{(Equation 2.19)}$$

Then:

$$\mu^o_{Na^+} + RT \ln a_{Na^+} + nF\Phi = \mu^o_{Na^+} + RT \ln a'_{Na^+} + nF\Phi', \qquad \textbf{(Equation 2.20)}$$

or:

$$\Delta\Phi = (RT/nF) \ln (a'_{Na^+}/a_{Na^+}). \qquad \textbf{(Equation 2.21)}$$

If the solutions are dilute, activities can be approximated with concentrations:

$$\Delta\Phi = (RT/nF) \ln (C'_{Na^+}/C_{Na^+}) \qquad \textbf{(Equation 2.22)}$$

Then, for a system that contains more than one ionic species, it can be written:

$$\Delta\Phi = (RT/nF) \ln (C'_{Na^+}/C_{Na^+}) = (RT/nF) \ln (C_{Cl^-}/C'_{Cl^-}). \quad \textbf{(Equation 2.23)}$$

Thus, the Donnan equilibrium can be defined by:

$$\lambda = C'_{Na^+}/C_{Na^+} = C_{Cl^-}/C'_{Cl^-}, \quad \textbf{(Equation 2.24a)}$$

or:

$$\lambda = [Na^+]_1/[Na^+]_2 = [Cl^-]_2/[Cl^-]_1 \quad \textbf{(Equation 2.24b)}$$

where λ is known as the Donnan distribution coefficient. This relationship will hold for any number of ions that are present in the system (45).

The Donnan theory has been applied to a variety of experiments of ion-exchange processes (46-48), in textile research, particularly dying processes (49-53), in the study of the interactions between amino acids and ion-exchangers (54) and between drugs and receptor sites (55), as well as in swelling of gels (56).

2.5.1 Simplified Donnan Model

Haynes (54) used a simple form of the Donnan theory to study the interaction between amino acids and a strong cation exchange resin in the hydrogen form that could interact with the amino acid as follows:

$$RSO_3^-H^+ + A^+ \rightleftharpoons RSO_3^-A^+ + H^+,$$

where RSO_3^- refers to the fixed ionic group within the resin and A^+ the amino acid in its cationic form. The internal volume of the resin (solvent volume/gram of resin) was referred to as V_1, which initially has a hydrogen ion concentration of C_1; thus $C_1V_1 = n$, the initial number of moles of hydrogen cations per gram of resin. From the Donnan equation, at equilibrium:

$$[H^+]_1/[H^+]_2 = [A^+]_1/[A^+]_2 \qquad \textbf{(Equation 2.25)}$$

where 1 and 2 refer to the resin and external phases, respectively.

The concentrations of the cations in the resin phase can be expressed as follows:

$$[H^+]_1 = C_1 - (X/V_1) \qquad \textbf{(Equation 2.26)}$$

and:

$$X/V_1 = [A^+]_1 \qquad \textbf{(Equation 2.27)}$$

where X is the number of moles of cation A in phase 1. Substitution of equations 2.26 and 2.27 in equation 2.25 gives the following equation:

$$\frac{C_1 - X/V_1}{[H^+]_2} = \frac{X/V_1}{[A^+]_2} \qquad \textbf{(Equation 2.28)}$$

Upon rearrangement:

$$X = \frac{C_1V_1}{1 + [H^+]_2/[A^+]_2} \qquad \textbf{(Equation 2.29)}$$

The dissociation of the amino acid cation can be expressed as:

$$A^+ \underset{}{\overset{K_1}{\rightleftharpoons}} A^{\pm} + H^+$$

and:

$$K_1 = \frac{[A^{\pm}][H^+]}{[A^+]} \qquad \textbf{(Equation 2.30)}$$

Then equation 2.29 can be rewritten as:

$$X = \frac{n[A^{\pm}]_2/K_1}{1 + [A^{\pm}]_2/K_1} \qquad \textbf{(Equation 2.31)}$$

It was assumed that, since only the amino acid and the hydrogen cations are present, the pH remains constant in phase 2 and is such that the amino acid is in its dipolar form, i.e., $A^{\pm}$. Then, the dipolar amino acid $A^{\pm}$ corresponds to the total concentration in phase 2 (the external solution) and can be expressed as C_a; $1/K_1$ will be made equal to α so that equation 2.31 can be rewritten as:

$$X = \frac{n\alpha C_a}{1 + \alpha C_a} \qquad \textbf{(Equation 2.32)}$$

Upon rearrangement, a general expression was derived to analyse the data and it is:

$$X/C_a = \alpha n - \alpha X, \qquad \textbf{(Equation 2.33)}$$

Thus, by plotting X/C_a as a function of X, it was possible to obtain n and K_1.

Attempts were made to apply this simplified approach of the Donnan theory to the adsorption of bile acids by cholestyramine. The interaction between cholestyramine and the bile acid anion can be expressed as:

$$RN(CH_3)_3^+Cl^- + R'COO^- \rightleftharpoons RN(CH_3)_3^+R'COO^- + Cl^-,$$

where $RN(CH_3)_3^+$ is the fixed ionic group of cholestyramine. Then equation 2.33 was applied:

$$X/C_a = \alpha n - \alpha X \qquad \textbf{(Equation 2.33)}$$

where X is the amount of bile acid bound by cholestyramine, C_a is the bile acid concentration at equilibrium, n is the number of exchangeable chloride ions and $\alpha = 1/K_a$, K_a being the dissociation constant for the bile acid:

$$R'COOH \overset{K_a}{\rightleftharpoons} R'COO^- + H^+$$

The plots of X/C_a as a function of X for the adsorption of glycocholic acid by cholestyramine with chloride and iodide as counter-ions are shown in Figures 2.31 and 2.32 respectively. Attempts to fit the plots by linear regression resulted in correlation coefficients of 0.67 and 0.81, respectively, i.e., the data obviously do not give a linear correlation. Failure to give satisfactory results for the present results possibly reflects pH changes in the external solution. Furthermore, the strongest deviations occur at low values of X (0-1 range), while the data of Haynes show no data points in this region and are all in the range of 1-6 mole of adsorbate per gram of resin. Clearly, a more refined approach is needed.

2.5.2 The Donnan Theory applied to the Adsorption of Bile Acids by Cholestyramine

Previous work by Scallan (56) forms the basis for the development of the Donnan theory for the ion-exchange system used in this study. This system involves the adsorption of bile acids by cholestyramine which contains bound basic quaternary ammonium groups, with chloride as counter-ion. Because the basic group cannot move out of the resin phase, this can be referred to as a Donnan system. All the other ions, namely sodium, the bile salt in its anionic form, chloride, hydronium and hydroxyl groups are free to move between the resin and the external solution phases. It is of interest to obtain the amount of bile salt anion which will interact directly with the quaternary ammonium group.

Figure 2.33 shows the constituents of the two phases of the system, with the broken line that represents a hypothetical membrane. At equilibrium, the mobile ions are present in both phases, at a certain concentration. The $-NR_3^+$ represents the fixed ionic groups and its molar concentration is expressed by $[B^+]$.

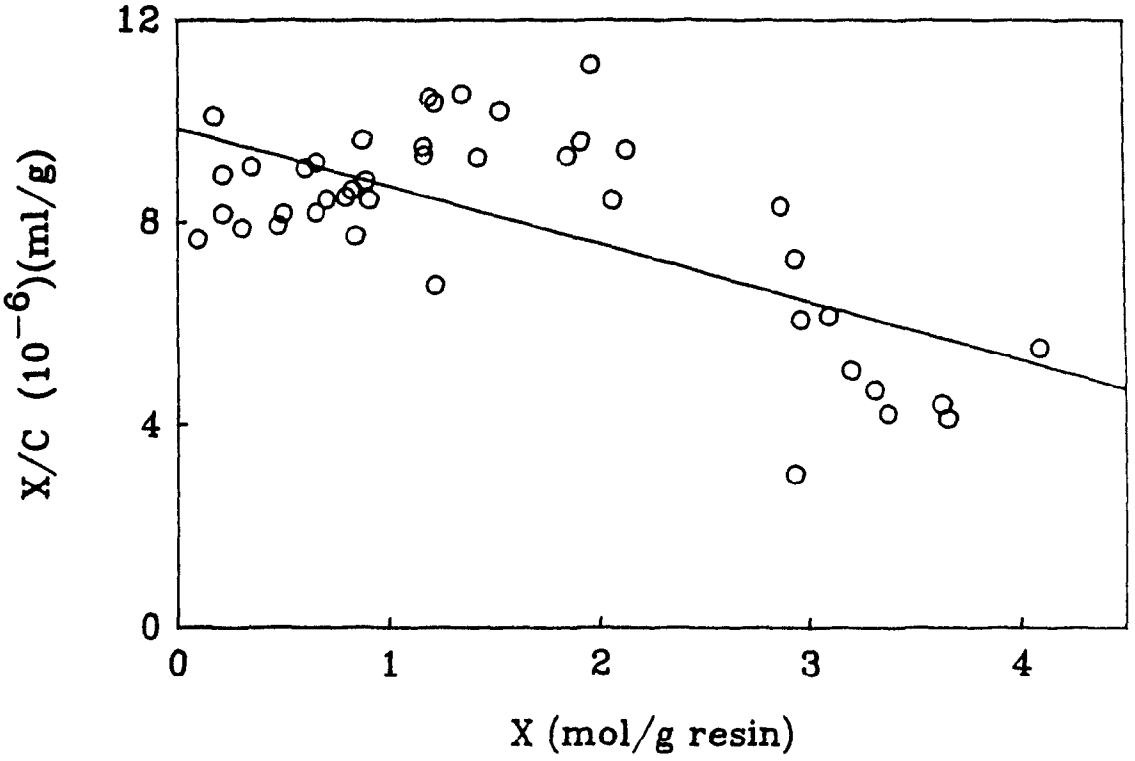

Figure 2.31 Isotherm for the adsorption of glycocholic acid by cholestyramine (Cl), in Tris-HCl, fitted with the simplified Donnan model

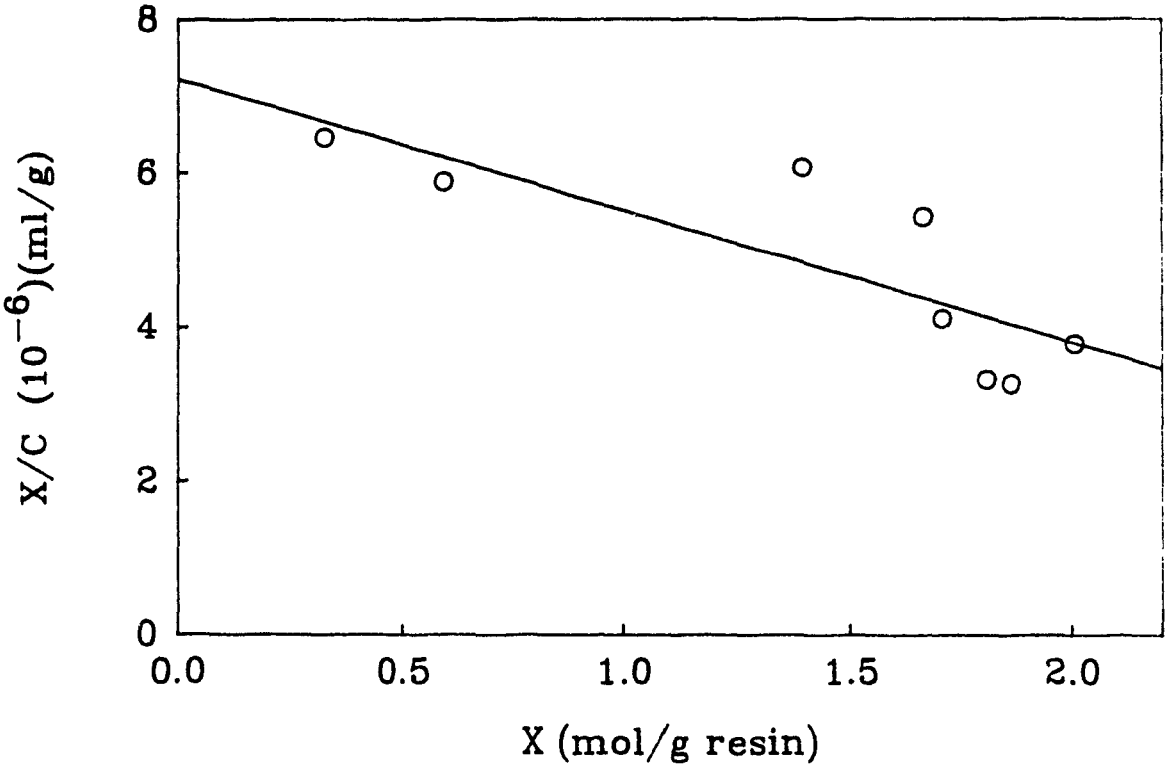

Figure 2.32 Isotherm for the adsorption of glycocholic acid by cholestyramine (I), in Tris-HCl, fitted with the simplified Donnan model

In principle, the quaternary ammonium ($-NR_3^+$) group can bind the chloride, hydroxide and bile acid anions to form species with respective molar concentrations of [BCl], [BOH] and [BA]. All of the other ions are shown using their symbols. The bile acid anion is shown as $R'COO^-$.

At equilibrium, electroneutrality must be preserved in both phases. Therefore, for the solution phase:

$$[Cl^-]_s + [R'COO^-]_s + [OH^-]_s = [Na^+]_s + [H^+]_s \qquad \textbf{(Equation 2.34)}$$

and for the resin phase:

$$[Cl^-]_r + [R'COO^-]_r + [OH^-]_r = [Na^+]_r + [H^+]_r + [B^+], \qquad \textbf{(Equation 2.35)}$$

where s and r refer to the external solution and resin phases, respectively.

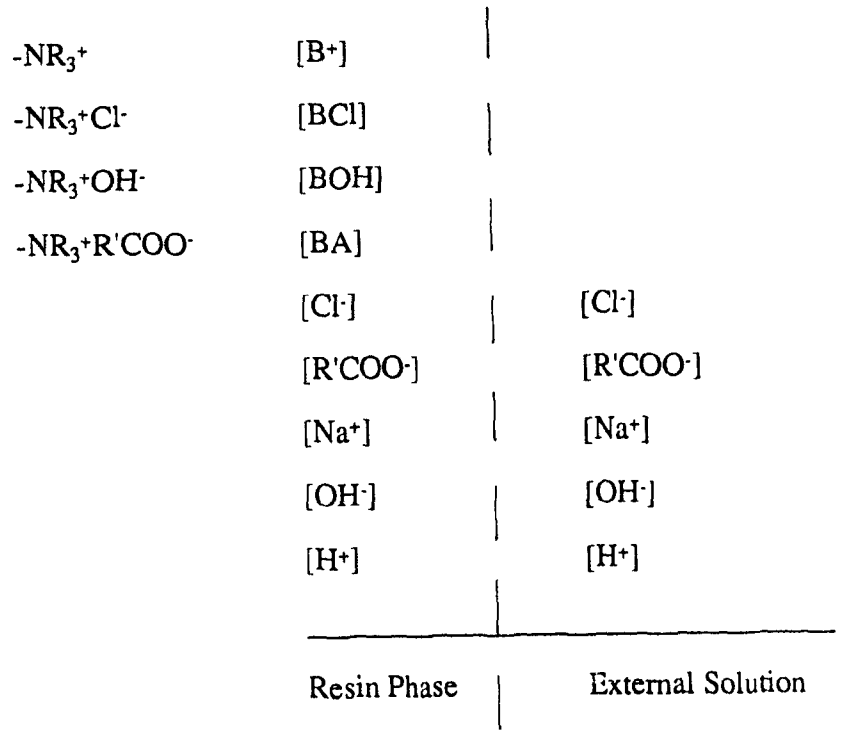

Figure 2.33 Representation of the equilibria existing when bile acids are in solution with cholestyramine

The total concentration of fixed groups in the resin phase [C], which corresponds to the functionality, can be expressed as follows:

$$[C] = [B^+]_r + [BCl]_r + [BOH]_r + [BA]_r. \qquad \textbf{(Equation 2.36)}$$

However, because cholestyramine is a strong anion exchange resin it may be assumed that the quaternary ammonium salt is completely ionized, i.e., $[BCl]_r = 0$ (9). Then:

$$[C] = [B^+]_r + [BOH]_r + [BA]_r, \qquad \textbf{(Equation 2.37a)}$$

or, in terms of moles:

$$C = B^+_r + BOH_r + BA_r \text{ (moles)} \qquad \textbf{(Equation 2.37b)}$$

and:

$$C = Cl^-_s + Cl^+_r \text{ (moles).} \qquad \textbf{(Equation 2.38)}$$

The concentration of bile salt anion can be determined experimentally, both for the external solution phase and for the resin phase, where it can be in the bound and the unbound forms. Conservation of mass requires that:

$$R'COONa_i = R'COO^-_r + R'COO^-_s + BA_r \text{ (moles)} \qquad \textbf{(Equation 2.39)}$$

where $R'COONa_i$ is the number of moles of bile salt present in the initial solution. Furthermore, in terms of the sodium ions:

$$R'COONa_i = Na^+_s + Na^+_r \text{ (moles)} \qquad \textbf{(Equation 2.40)}$$

For a Donnan equilibrium, it can be said that:

$$\lambda = \frac{[Na^+]_r}{[Na^+]_s} = \frac{[H^+]_r}{[H^+]_s} = \frac{[Cl^-]_s}{[Cl^-]_r} = \frac{[OH^-]_s}{[OH^-]_r} = \frac{[R'COO^-]_s}{[R'COO^-]_r} \qquad \textbf{(Equation 2.41)}$$

Taking the inverse of λ and adding the last three ratios yields:

$$1/\lambda = \frac{[Cl^-]_r + [OH^-]_r + [R'COO^-]_r}{[Cl^-]_s + [OH^-]_s + [R'COO^-]_s} \qquad \textbf{(Equation 2.42)}$$

From electroneutrality:

$$1/\lambda = \frac{[Na^+]_r + [H^+]_r + [B^+]}{[Na^+]_s + [H^+]_s} \qquad \textbf{(Equation 2.43)}$$

From equation 2.41:

$$1/\lambda = \frac{[Na^+]_r + [H^+]_r + [B^+]}{([Na^+]_r/\lambda)+([H^+]_r/\lambda)} \qquad \textbf{(Equation 2.44)}$$

and:

$$\lambda = \left(1 + \frac{[B^+]}{[Na^+]_r + [H^+]_r}\right)^{-1/2} \qquad \textbf{(Equation 2.45)}$$

This series of equations, together with experimentally determined concentrations, can be used to obtain the concentration of each ionic species in both phases along with the amount of bound bile salt and hydroxyl anions. A knowledge of the latter permits a determination of the basicity constant for the bound hydroxyl group and the formation constant for the bound bile acid groups:

$$-NR_3^+OH^- \overset{K_b}{\rightleftharpoons} -NR_3^+ + OH^-$$

$$K_b = \frac{[-NR_3^+][OH^-]}{[-NR_3^+OH^-]} \qquad \textbf{(Equation 2.46)}$$

and:

$$-NR_3^+ + R'COO^- \overset{K_r}{\rightleftharpoons} -NR_3^+R'COO^-$$

$$K_r = \frac{[-NR_3^+R'COO^-]}{[-NR_3^+][R'COO^-]} \qquad \textbf{(Equation 2.47)}$$

This model can also be extended to the adsorption of bile acids from Tris-HCl buffer. The only difference is the presence of an additional cation in the system, the cation from the Tris-buffer, $(HOCH_2)_3CNH_3^+$ which will be referred as TNH_3^+. Figure 2.34 shows the equilibrium that would exist. Because Tris-HCl is a buffer, the following equilibrium must be included:

$$TNH_3^+ \rightleftharpoons TNH_2 + H^+$$

This equilibrium will exist in both phases explaining why TNH_2 is shown in Figure 2.34. Even though TNH_2 is not an ionic species, it will partition between the two phases.

At equilibrium. the electroneutrality can be expressed for the solution phase:

$$[Cl^-]_s + [R'COO^-]_s + [OH^-]_s = [Na^+]_s + [H^+]_s + [TNH_3^+]_s, \qquad \textbf{(Equation 2.48)}$$

and for the resin phase:

$$[Cl^-]_r + [R'COO^-]_r + [OH^-]_r = [Na^+]_r + [H^+]_r + [TNH_3^+]_r. \qquad \textbf{(Equation 2.49)}$$

Equations 2.36, 2.37, 2.39 and 2.40 are still applicable but Equation 2.38 becomes:

$$Cl^-_s + Cl^-_r = C + TNH_3Cl, \text{ (moles)} \qquad \textbf{(Equation 2.50)}$$

since there will be chloride ions coming from the Tris-HCl buffer.

Equation 2.41 can be expressed as:

$$\lambda = \frac{[Na^+]_r}{[Na^+]_s} = \frac{[H^+]_r}{[H^+]_s} = \frac{[TNH_3^+]_r}{[TNH_3^+]_s} = \frac{[Cl^-]_s}{[Cl^-]_r} = \frac{[OH^-]_s}{[OH^-]_r} = \frac{[R'COO]_s}{[R'COO^-]_r}$$

(Equation 2.51)

and:

$$\lambda = \left(1 + \frac{[B^+]}{[Na^+]_r + [TNH_3^+]_r + [H^+]_r}\right)^{-1/2}$$

(Equation 2.52)

The basicity and formation constants for the binding of the hydroxide and bile acid ions can then be determined by equations 2.46 and 2.47, respectively.

$-NR_3^+$	$[B^+]$		
$-NR_3^+Cl^-$	$[BCl]$		
$-NR_3^+OH^-$	$[BOH]$		
$-NR_3^+R'COO^-$	$[BA]$		
	$[Cl^-]$		$[Cl^-]$
	$[TNH_3^+]$		$[TNH_3^+]$
	$[TNH_2]$		$[TNH_2]$
	$[R'COO^-]$		$[R'COO^-]$
	$[Na^+]$		$[Na^+]$
	$[OH^-]$		$[OH^-]$
	$[H^+]$		$[H^+]$
	Resin Phase		External Solution

Figure 2.34 Representation of the equilibria existing when bile acids are in a Tris-HCl buffer solution with cholestyramine

2.6 APPLICATION OF THE DONNAN MODEL

2.6.1 Experimental

The initial experiments were carried out with the idea that it would be easier to determine the concentrations of mobile ions in the external solution rather than in the resin phase. Also water was used as the medium for the adsorbate. This facilitates the determination of the chloride concentrations in both phases since cholestyramine (Cl) is the only source of chloride anions.

Then the following parameters had to be measured: the bile salt anion concentrations, before and after adsorption, the chloride anion and the sodium cation concentrations in solution and the pH at equilibrium. To determine the bile salt anion concentrations (glycocholate) the usual HPLC technique was used (see Section 2.1.3).

Measurements of the chloride ion concentrations in solution were first attempted by potentiometric titration with silver nitrate ($AgNO_3$) and subsequently by conductimetry. The latter technique was found to yield better results for the present system. The conductimetry experiments were carried out as follows: A known volume of the external solution was filtered to retain the resin; it was titrated with a standardized silver nitrate ($AgNO_3$) solution (0.05162M). The conductivity during the titration was measured using 2 hydrogen/platinum electrodes (Sargent Welch), with a conductance meter (YSI Scientific, model 35). From the plot of conductance as a function of the volume of $AgNO_3$ the end-point was determined and gave the chloride ion concentration in the external solution. Figure 2.35 shows an example of the titration curve for this type of titration.

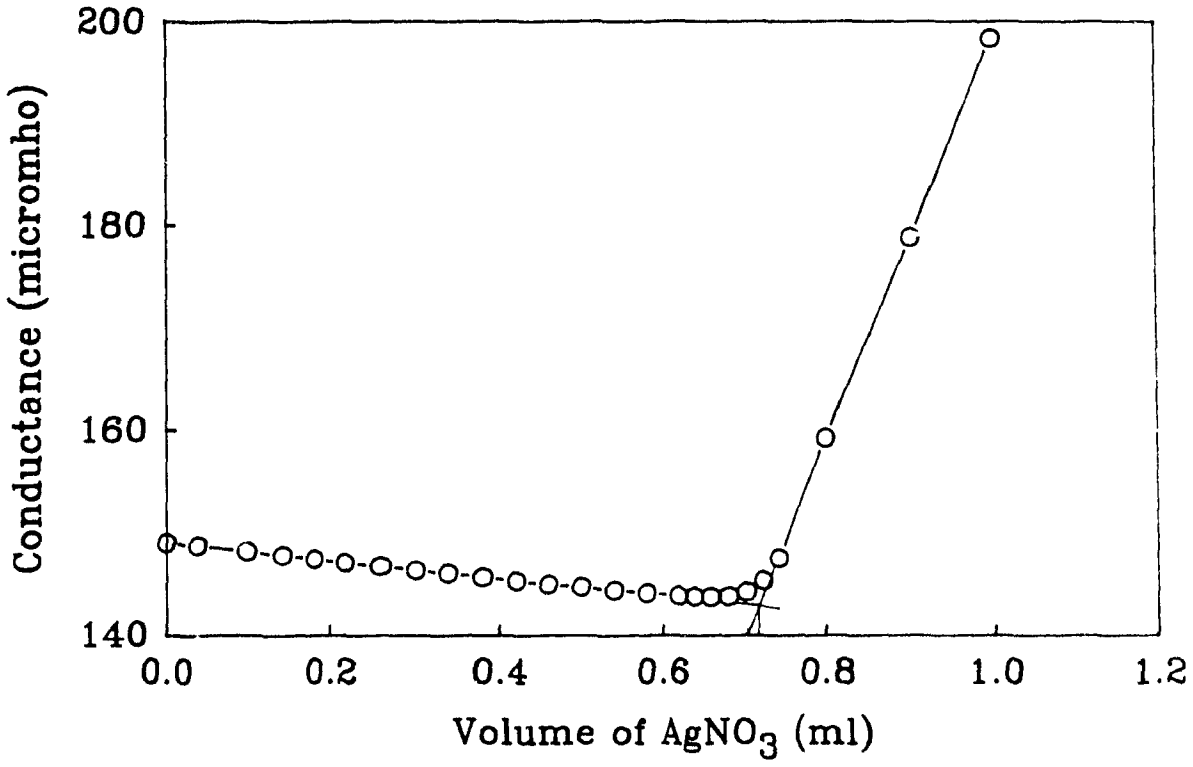

Figure 2.35 Typical data, obtained by conductance, for the titration of the chloride anions by silver nitrate $AgNO_3$)

Measurements of the sodium cation concentrations were tried initially by flame atomic emission spectroscopy. These indicated that the difference between the sodium ion concentration before and after adsorption was either zero, or in some cases it appeared to be larger after adsorption. Measurements with a sodium selective electrode (Corning) also indicated that the concentrations before and after adsorption were equal. Therefore, it would appear that the change in sodium concentration due to adsorption is small and difficult to quantify.

Measurements of the pH of the solutions were made with a pH meter (Corning, 220) equipped with a general purpose combination electrode (Corning).

All of the above measurements were carried out following adsorption experiments between sodium glycocholate and cholestyramine in aqueous solution (950 ml), at room temperature, as was explained earlier (see Section 2.1.2).

The wet swollen volume of cholestyramine was determined as follows: 5 ml of water were added to 3.09 g of cholestyramine (Dowex 1x2, Aldrich). It was left to "sit" for two hours to ensure complete swelling. The resin was filtered by gravity and added to a known volume (10 ml) of cyclohexane (A and C); the increase in volume was noted (1.50 ml). Thus, the density of the swollen cholestyramine was found to be 0.687 g/ml.

2.6.2 Results and Discussion

From the experimental determinations of the concentrations of the bile acid anions and of the chloride anions in solution, it is possible to obtain the total concentration of bile acid, in both the unbound and bound forms, and of the chloride concentration in the resin phase. From the knowledge of the chloride concentrations in both phases, λ can be evaluated. Based on this value of λ, and the measured concentrations in the solution phase, it is possible to determine the

concentrations of the other ions in the resin phase, using the equations shown previously. The following Results section will show how these concentrations were determined.

2.6.2.1 Results

Table 2.5 shows the experimentally determined concentrations of chloride anions in the external solution. Since it is assumed, in the model, that the basic quaternary ammonium groups are all ionized, it is possible to obtain the moles of chloride ion in the resin phase by use of equation 2.53.

$$Cl^-_r = C - Cl^-_s \text{ (moles)} \qquad \textbf{(Equation 2.53)}$$

where C in the functionality, determined previously as 3.16 mmole of active sites per gram of resin. The moles of chloride anion in the resin phase are converted to the molar concentrations, using the density of 0.687 g/ml to obtain the volume of the resin, and are presented in Table 2.5.

Table 2.5 Experimental values of the chloride $[Cl^-]_s$ anion equilibrium concentrations in the external solution and the calculated values of the chloride $[Cl^-]_r$ concentrations in the resin phase. Calculated values of the Donnan distribution coefficient λ

Sample	$[Cl^-]_s$ (M) (10^4)	$[Cl^-]_r$ (M)	λ (10^4)
1	1.70	1.75	0.973
2	3.23	1.38	2.33
3	4.54	1.08	4.21
4	6.30	0.43	14.7

Based on these chloride ion concentrations in both phases, values of λ can be calculated by equation 2.41, and are shown in Table 2.5. These values of λ are significantly concentration dependent, similar to those reported by Scallan for anionic resins (56).

The experimentally measured values for the concentrations of glycocholate in the external solution and the **total** bile acid content in the resin phase are given in Table 2.6. The amounts of unbound glycocholate in the resin phase, as calculated by equation 2.41 using λ and the concentrations of glycocholate in solution, are also given in Table 2.6. This indicates that the majority of the glycocholate in the resin phase is not ionized, i.e., it is in a bound state. It is of interest that on a molar basis, the concentrations of free glycocholate in the resin phase are rather high, probably exceeding the CMC.

Table 2.6 Experimental values for the concentration of glycocholate anions $[R'COO^-]_s$ in the external solution and calculated concentrations of ionized $[R'COO^-]_r$ and bound [BA] glycocholate in the resin phase

Sample	$[R'COO^-]_s$ (M) (10^5)	$[R'COO^-]_r$ (M) (10^2)	[BA] (M)
1	0.287	2.95	0.225
2	1.37	5.90	0.656
3	2.34	5.56	1.03
4	5.76	3.93	1.70

Figure 2.36 shows the smoothed curve representing the adsorption isotherm for cholestyramine adsorbing glycocholic acid in water, as reported previously in Section 2.2.1. Data points are shown representing the total concentration of bile acid in the resin phase, which take into account both the unbound and bound forms of the bile acid anions. When the actual concentration

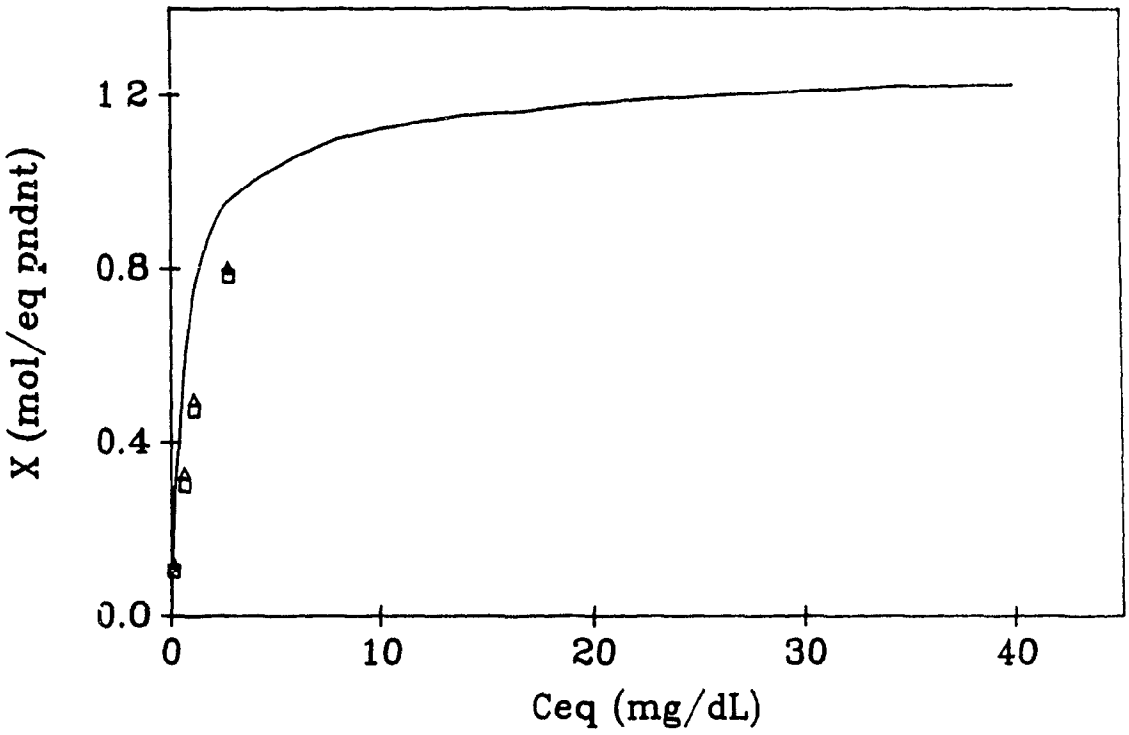

Figure 2.36 Isotherm for the adsorption of glycocholic acid by cholestyramine (Cl) in water. — original isotherm, Δ total bile acid in the resin phase, ❑ bile acid bound in the resin phase

of bound bile acid ([BA]) is put onto the isotherm. It can be seen that the points, which represent the amount of bile acid bound to the resin, are slightly below the smoothed isotherm, the difference decreasing with increasing Ceq.

Experiments to determine the sodium concentration in the resin phase indicated that it is present only in small quantity. Since the experiments were not sufficiently sensitive to detect the loss of sodium cation from the aqueous phase, $[Na^+]_r$ is a calculated value based on the sodium ion concentration in solution obtained by:

$$[Na^+]_r = \lambda[Na^+]_s \qquad \textbf{(Equation 2.54)}$$

and:

$$[Na^+]_r = \lambda[\{(R'COONa)_i - Na^+_s\}/V_r] \qquad \textbf{(Equation 2.55)}$$

Since the number of moles of sodium cation lost to the resin phase is very small, the sodium ion concentration in the external phase can be approximated by:

$$[Na^+]_r = \lambda[R'COONa]_i \qquad \textbf{(Equation 2.56)}$$

The results, given in Table 2.7, confirm that most of the sodium cation is in the external solution phase and that the quantity in the resin phase is negligible compared to the concentrations of other cations.

As mentioned in the Experimental section, attempts to determine the pH of the external solution after adsorption resulted in readings that were not very stable but seemed to level off at pH 6-6.5. However, in view of the uncertainties in the experimental data, the pH of the solution is determined from the electroneutrality equation:

$$[Cl^-]_s + [R'COO^-]_s + [K_w/H^+]_s = [Na^+]_s + [H^+]_s \qquad \textbf{(Equation 2.57)}$$

$$[H^+]_s^2 + [H^+]_s([Na^+]_s - [Cl^-]_s - [R'COO^-]_s) - K_w = 0 \qquad \textbf{(Equation 2.58)}$$

Solving the above quadratic equation yields the hydrogen ion concentrations shown in Table 2.7, as the pH. There is an increase in pH as the initial concentration of bile acid increases.

Table 2.7 Calculated concentrations of sodium cations, $[Na^+]_s$ and $[Na^+]_r$ and the pH in both phases

Sample	$[Na^+]_s$ (10^4 M)	$[Na^+]_r$ (10^7 M)	pH_s	pH_r
1	1.05	0.10	4.17	8.18
2	3.06	0.71	4.52	8.15
3	4.74	2.0	5.45	8.83
4	6.86	10	5.99	8.82

Based on the pH of the external solution and the value of λ, it is then possible to evaluate the pH in the resin phase (Table 2.7). It is of particular interest that the resin phase is considerably basic even though the solution phase is distinctively acidic. Similar distinct differences in pH have been verified experimentally by Scallan, by measuring the rates of acid catalyzed reactions in the presence of anionic sorbents.

The concentration of free fixed ionic groups in cholestyramine, $[B^+]$, can be obtained by application of equation 2.35, and the concentration of bound hydroxyl groups, [BOH], is determined by equation 2.37 (Table 2.8). Knowing both [BOH] and the concentrations of bound glycocholate, basicity constants for BOH and formation constants for $-NR_3^+R'COO^-$ can be evaluated, using equations 2.47 and 2.48 respectively, and are reported in Table 2.9.

Table 2.8 The calculated concentrations of free fixed ionic groups [B^+], and bound hydroxyl groups [BOH].

Sample	[B^+] (M)	[BOH] (10^2 M)
1	1.78	17.0
2	1.44	7.48
3	1.14	0.85
4	0.47	0.28

Table 2.9 The values of the formation constants of bound glycocholate (K_f) and the basicity constant of bound hydroxyl groups(K_b).

Sample	K_f (M^{-1})	K_b (10^4 M^{-1})
1	4.3	0.16
2	7.7	0.27
3	16	9.1
4	92	11

The equilibrium constants for the binding of glycocholic acid to cholestyramine pendant increase with increasing equilibrium concentrations. Such behaviour may indicate some form of positive cooperativity, i.e., as more bile acid is bound subsequent binding of bile acids is facilitated. On the other hand, these changes may also reflect variations in the dielectric of the medium, i.e., inside the resin. Certainly, the basicity constant, K_b, shows a simultaneous increase. This behaviour is considered in more detail in the Discussion.

2.6.2.2 Discussion

Application of Donnan theory to the adsorption of glycocholic acid by cholestyramine (Cl) yields interesting results that require further analysis. The assumptions were: 1. Complete ionization of the quaternary ammonium groups with the chloride counter-ion in cholestyramine. This appears to be a reasonable assumption. 2. Concentrations rather than activities were used in the Donnan equation (Equation 2.41). In the external phase, the concentrations of the ions are in the range of 10^{-4}-10^{-10}M (Table 2.5-2.7), which certainly can be considered as a dilute solution, so that the use of concentrations is acceptable. However, for the ion concentrations of the resin phase, particularly the chloride and glycocholate anion concentrations (Table 2.5, 2.6), the solutions are not dilute and activity effects may be significant. This may, in fact, contribute to the change in the formation constant with equilibrium concentration.

The values of λ, determined from the ratio of the chloride anion concentration in the solution to that in the resin phase, increase with increasing concentration of bile salt anion in solution (Table 2.5, Figure 2.37) and reflect a "neutralization" of charge as a result of strong binding of glycocholate to the resin sites. The values of λ are less than one, as expected for a strong base ion-exchange resin (56), since the concentrations of mobile cations in the resin phase are less than in the external solution, while the opposite trend is seen for the anion concentrations.

According to the experimental results, the amount of chloride displaced from the resin phase to the external solution phase increases with increasing equilibrium concentration of glycocholate in solution (Figure 2.38). However, at low Ceq, the amount displaced is larger than the amount of bile salt anion, bound plus unbound, that enters the resin phase, i.e., it is not a stoichiometric displacement. The difference between the concentration of

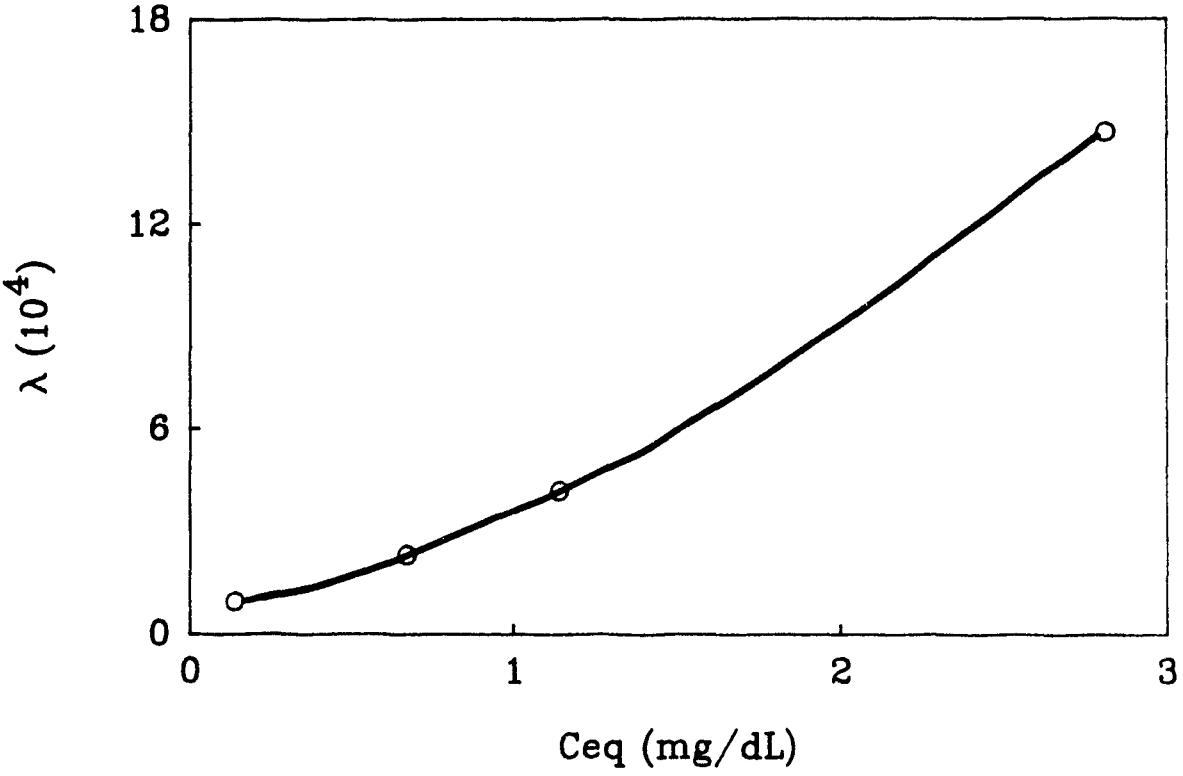

Figure 2.37 Variation of the Donnan partition coefficient, λ, with increasing Ceq

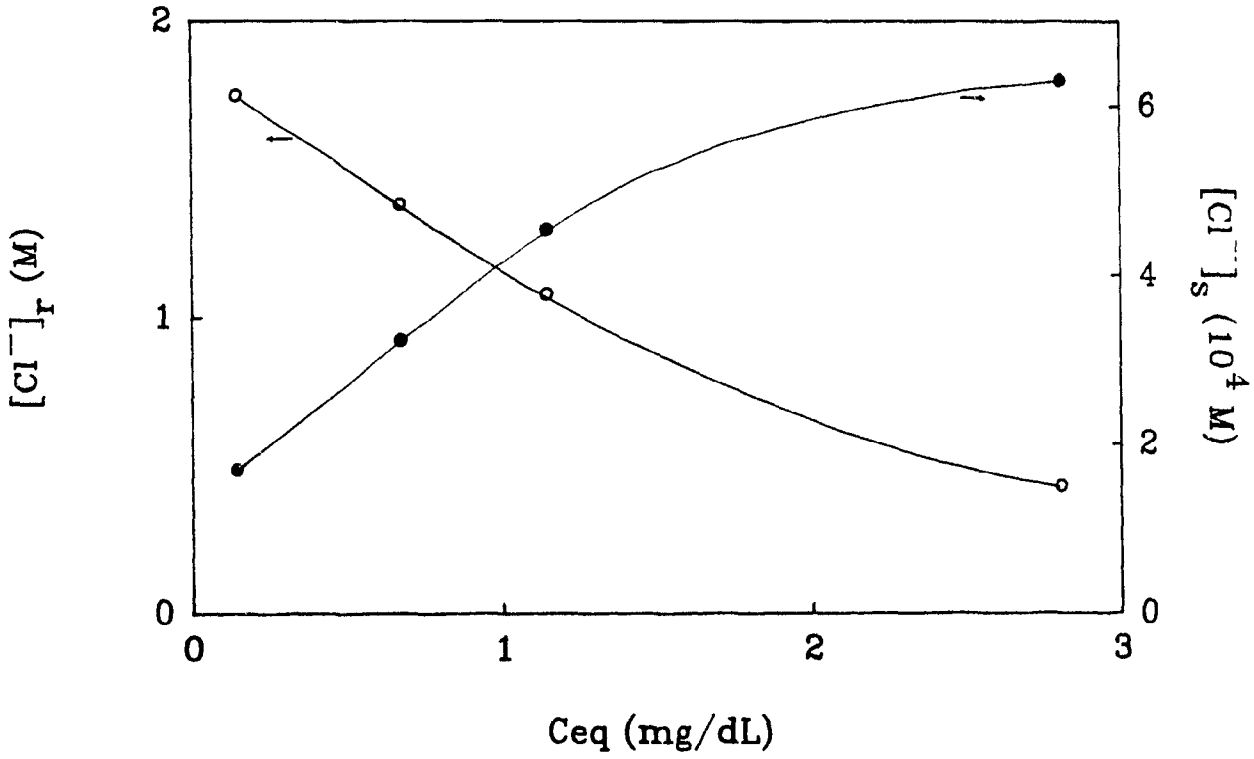

Figure 2.38 Variation of the concentration of chloride anions in the solution ● and resin phase ○, with increasing Ceq

chloride ion displaced to the external solution and the total concentration of bile acid anion entering the resin phase, in the bound and unbound forms, corresponds to the total concentration of hydroxyl anion in the bound (BOH) and unbound (OH^-) forms, in the resin phase. This difference decreases with increasing equilibrium concentration of glycocholate and becomes negligible for Ceq>2 mg/dL (Figure 2.39).

An experiment in which cholestyramine was added to water only, according to the procedure used for the usual adsorption experiment, gave no chloride ion in the external solution. Thus, the chloride is not displaced by the hydroxyl group, which follows the selectivity sequence (section 2.4). However, upon addition of bile salts, the chloride ion was displaced to the external solution.

The glycocholate in the resin phase exists both in the bound and unbound forms. The concentration of unbound glycocholate initially increases with increasing concentration of glycocholate in the external solution, reaches a maximum and then starts to decrease (Figure 2.39). On the other hand, the concentration of bound glycocholate increases smoothly (Figure 2.40). At low Ceq, the bile acid anion enters the resin phase, displacing excess chloride anions, and establishes an equilibrium between the unbound and the bound forms. As the concentration of bile acid in the resin increases, a maximum in glycocholate is attained at about the same Ceq where the excess chloride displaced becomes negligible. Concomitantly, there is a sharp increase in the pH inside the resin (Figure 2.41). Further increase in glycocholate results in a stoichiometric chloride displacement and the binding of bile acid appears to be favoured, decreasing the concentration of unbound glycocholate. The overall behaviour indicates a discontinuity, similar to that seen on reaching the CMC.

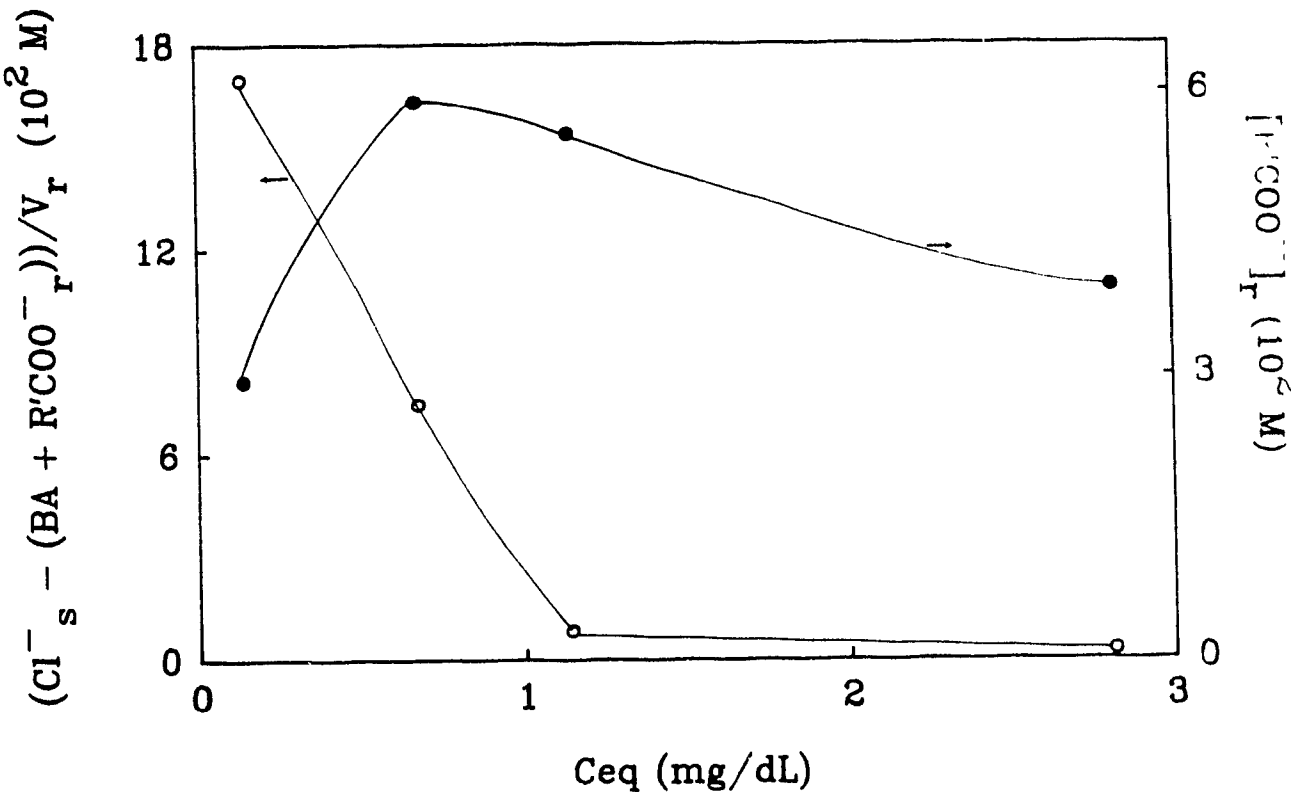

Figure 2.39 Variation of the difference between the concentration of chloride anions in the solution phase and the total bile acid concentration in the resin phase ○, and the variation of the concentration of unbound bile acid, [R'COO-], in the resin phase ●, with increasing Ceq

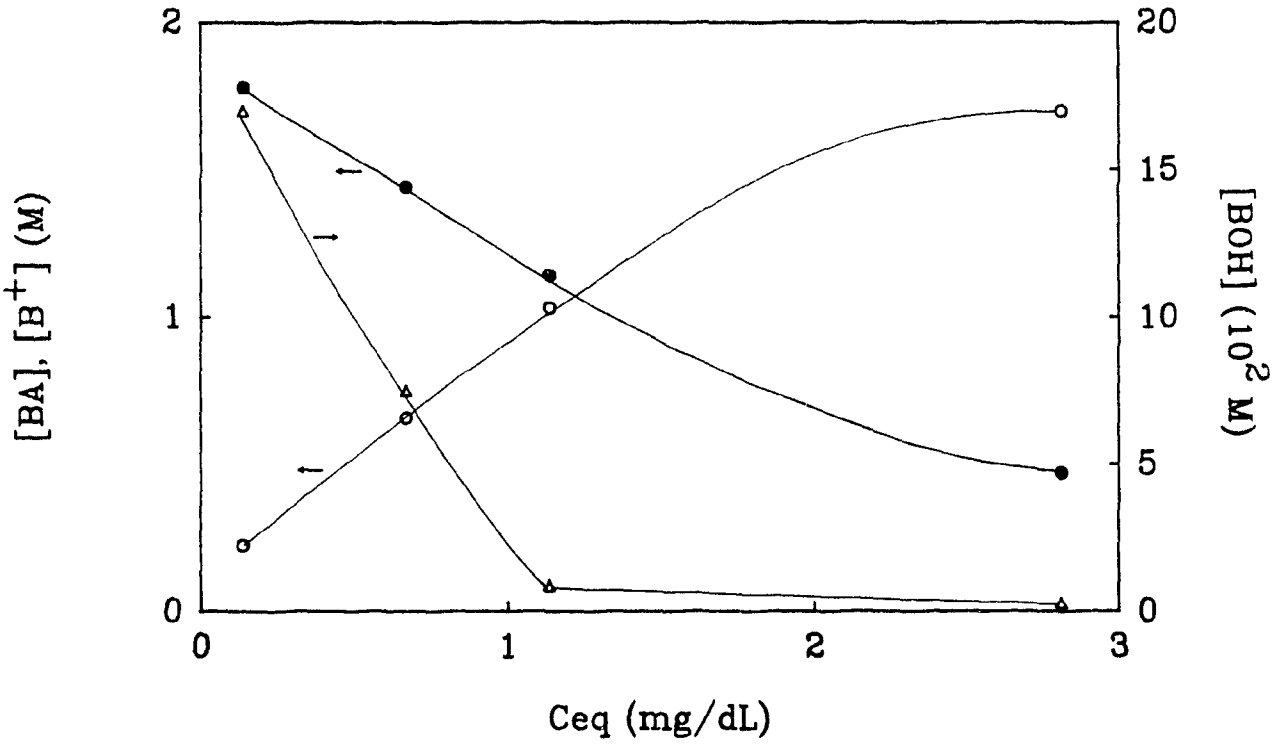

Figure 2.40 Variation of the concentration of bound bile acid, [BA] O, of bound hydroxyl group, [BOH] Δ, and of free fixed ionic group, [B+] ●, in the resin phase, with increasing Ceq

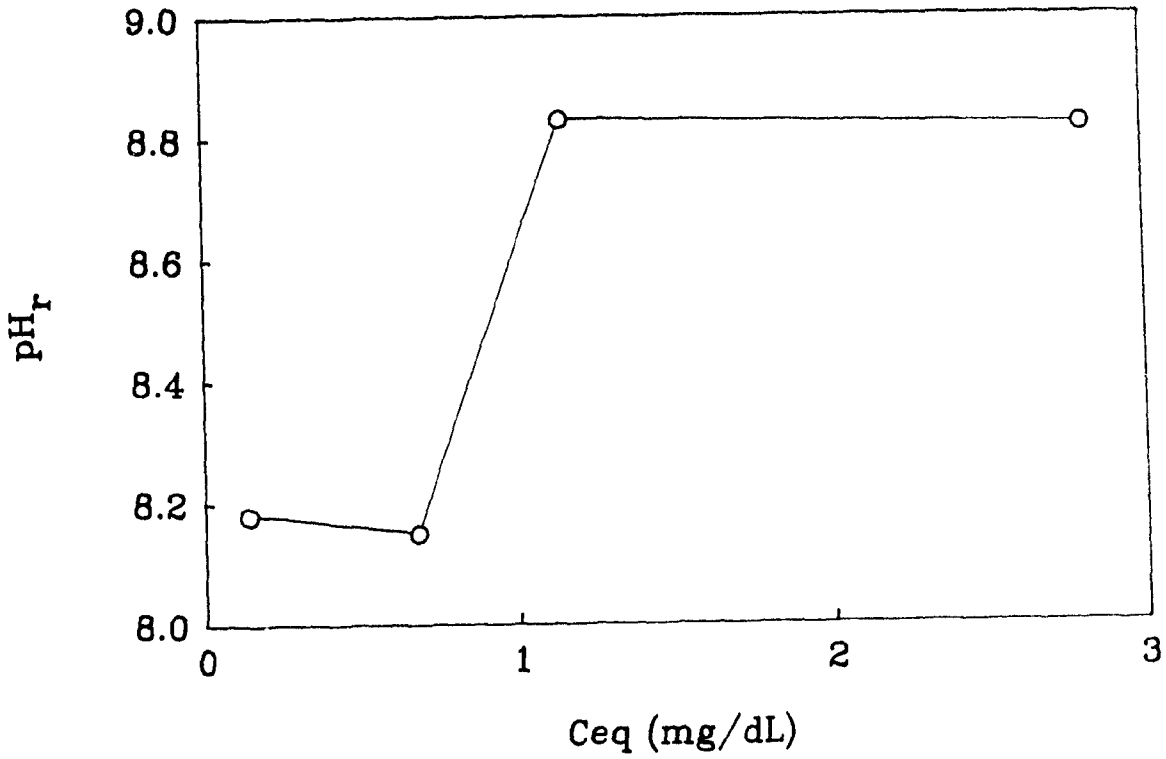

Figure 2.41 Variation of the pH of the resin phase with increasing Ceq

Without question the concentrations of bound glycocholate are well above the range where aggregation should take place. Because the pendants of cholestyramine are relatively close to one another (Figure 2.29), interactions can occur between bound bile acid molecules at adjacent sites. Such interaction, involving either the hydrophilic or hydrophobic faces of the glycocholate, cause a degree of ordering of the bile acid, similar to that observed in the formation of mixed micelles. It is well known that the quaternary amines are effective in forming such micelles (57). The electrostatic interaction of glycocholate with the pendant favours the formation of mixed micelles. An important consequence of this ordering is that, in addition to the electrostatic interaction between the glycocholate and the pendant, interaction between glycocholate ions at adjacent sites will have a synergistic effect on the binding. This effect, which represents a form of positive cooperativity, will be reflected by an increase in K_f with increasing Ceq.

At all Ceq, the concentrations of **unbound** glycocholate in the resin phase (Table 2.6) are also in a range such that aggregation could take place (58), especially dimerization. Such aggregation would favour the partition of bile acid into the resin phase. The concentration of unbound glycocholate in the resin reaches a maximum with an increase in Ceq and then begins to decrease where the ordering of bound glycocholate leads to a situation of positive cooperativity. Since the ordering favours additional binding of bile acid, it will be the preferred form in the resin phase. Thus, the glycocholate will then tend to be bound rather than be unbound, which explains the decrease in the concentration of unbound bile acid with an increase in Ceq.

From calculations, the sodium ion concentration in the resin phase is of the order of 10^{-8}-10^{-7} M (Table 2.7). The fact that few sodium cations enter the resin phase can be explained by co-ion exclusion.

The pH of the external solution, as determined by calculation, shows a smooth increase in [OH^-], from 4.17 to 5.99, as Ceq increases from 0.14 to 2 81 mg/dL (Table 2.7, Figure 2.42). The increase in the concentration of the hydroxyl anion can be explained by the hydrolysis of the glycocholate anion, $R'COO^-$, i.e.,:

$$R'COO^- + H_2O \rightleftharpoons R'COOH + OH^-$$

As the concentration of bile acid increases, the hydrolysis process will become more important, such that the concentration of the hydroxyl anion in the external solution will increase and, in turn, so will the pH.

The pH of the resin phase shows a sudden increase from 8.15 to 8.83 (Table 2.7, Figure 2.41) at a Ceq which corresponds approximately to the point where the concentration of the unbound form of bile acid in the resin phase begin to decrease (Figure 2.39). As was proposed above, this may be attributed to the fact that the binding of bile acid becomes more favourable at higher Ceq. If binding of bile acid becomes favoured, it will compete with the binding of the hydroxyl groups:

$$-NR_3^+ + R'COO^- \rightleftharpoons -NR_3^+R'COO^-$$

$$-NR_3^+ + H_2O \rightleftharpoons -NR_3^+OH^- + H^+$$

Binding of the hydroxyl group, by hydrolysis, releases a proton thus decreasing the pH. At low Ceq, hydrolysis of the resin pendant keeps the pH at a relatively lower value. However, as more bile acid enters the resin phase, the concentration of bound hydroxyl group decreases, thus the contribution of the hydrolysis process is diminished, leading to a sudden increase in pH.

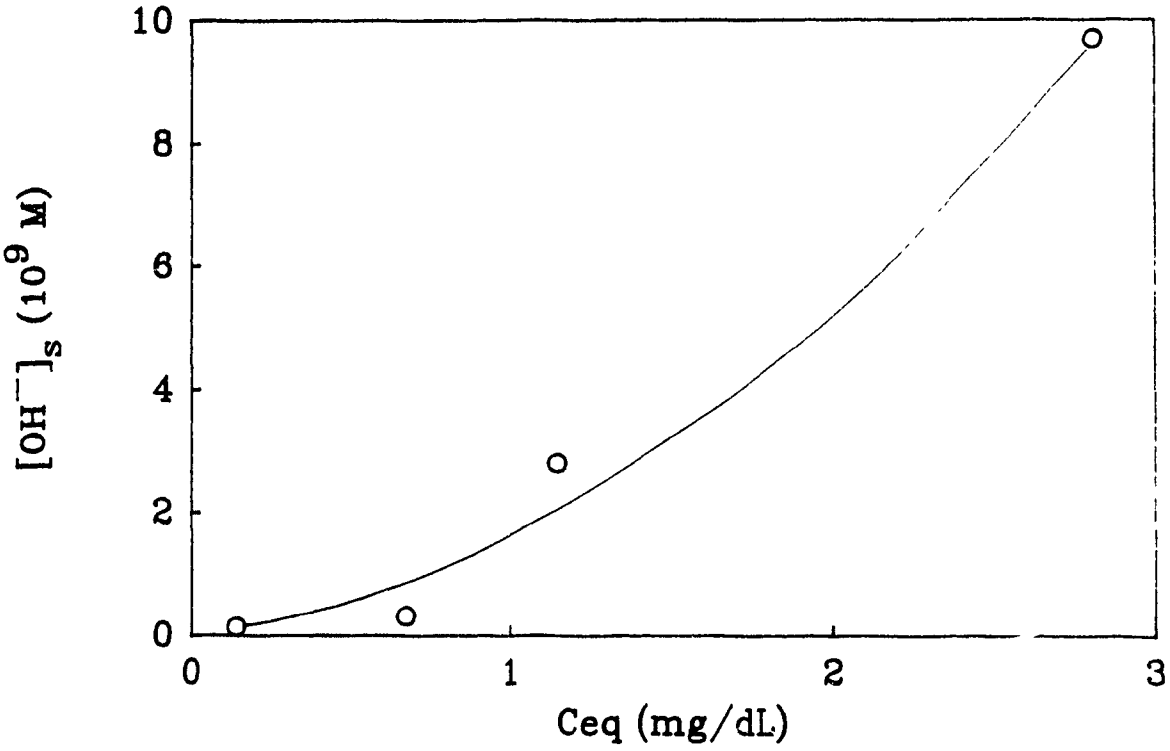

Figure 2.42 Variation of the concentration of the hydroxyl anion in the external solution, with increasing Ceq

Furthermore, as micellization takes place at higher Ceq, the resin phase becomes more hydrophobic, which could also increase the pH.

The concentration of free fixed quaternary ammonium groups, obtained from both equations 2.39 and 2.45, decreases as the concentration of bile salt in the resin phase increases (Table 2.8, Figure 2.40), reflecting the increase in bound glycocholate. As more bile acid enters the resin phase, less hydroxyl group is bound (Table 2.8, Figure 2.40) due to a displacement of the hydroxyl group by glycocholate, which is possible since large counter-ions can displace smaller ones (59).

As mentioned above, the values for the formation constant of bound glycocholate anions (K_f) and of the basicity constant (K_b) are concentration dependent; both increase with increasing equilibrium concentration of bile acid (Table 2.9, Figures 2.43, 2.44). The value of K_b changes in the direction of increased base strength, i.e., less hydroxyl groups are bound to the pendants. However, increasing K_f indicates that the binding of bile acid to the active site becomes more favoured. As pointed out above, the concentrations of bound glycocholate are well above the CMC, so that the bound bile acid molecules not only interact electrostatically with the resin pendant, but also between themselves. Therefore, as the concentration increases, the glycocholate ions will interact, thus increasing the quality of binding of the bile acid by the resin. The glycocholate ion will preferentially bind to the pendant and order itself with the adjacent bile acid ions. Therefore, although the main interaction is electrostatic, other interactions such as micelle formation by the bile salt in the resin phase and hydrophobic interactions between bound glycocholate ions can also take place.

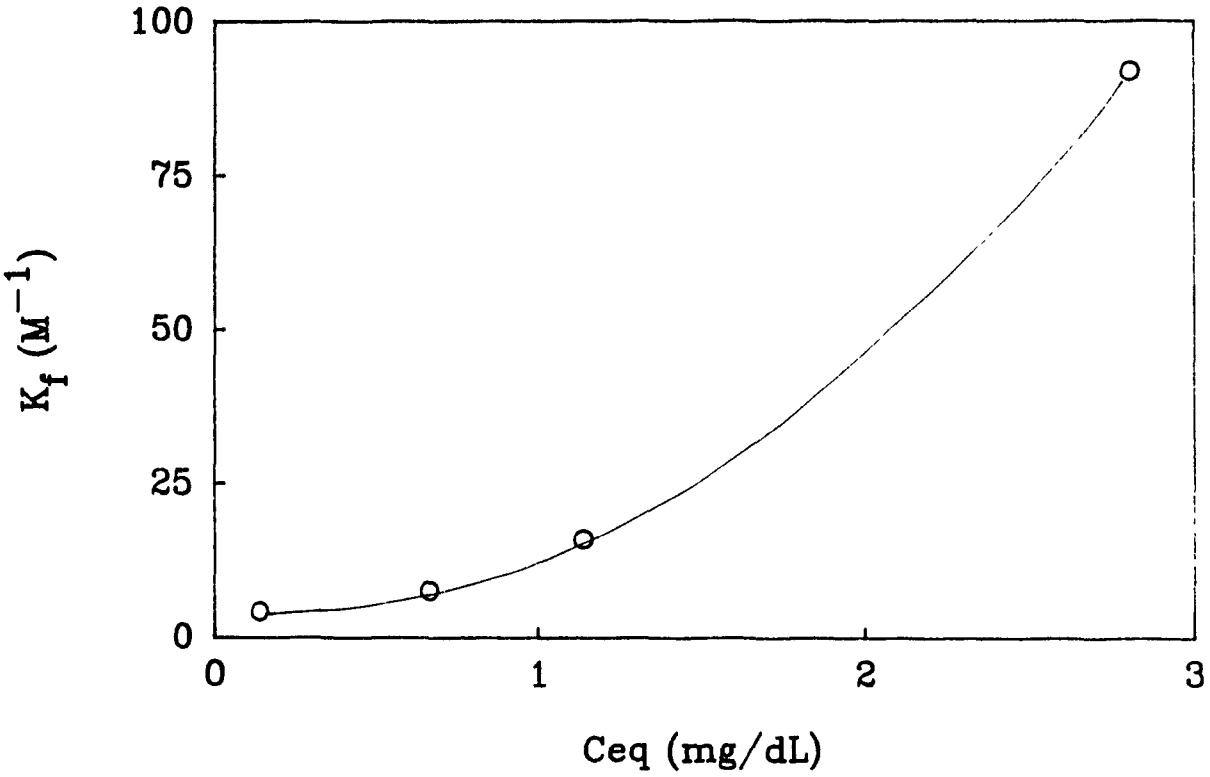

Figure 2.43 Variation of the formation constant of bound bile acid (K_f), in the resin phase, with increasing Ceq

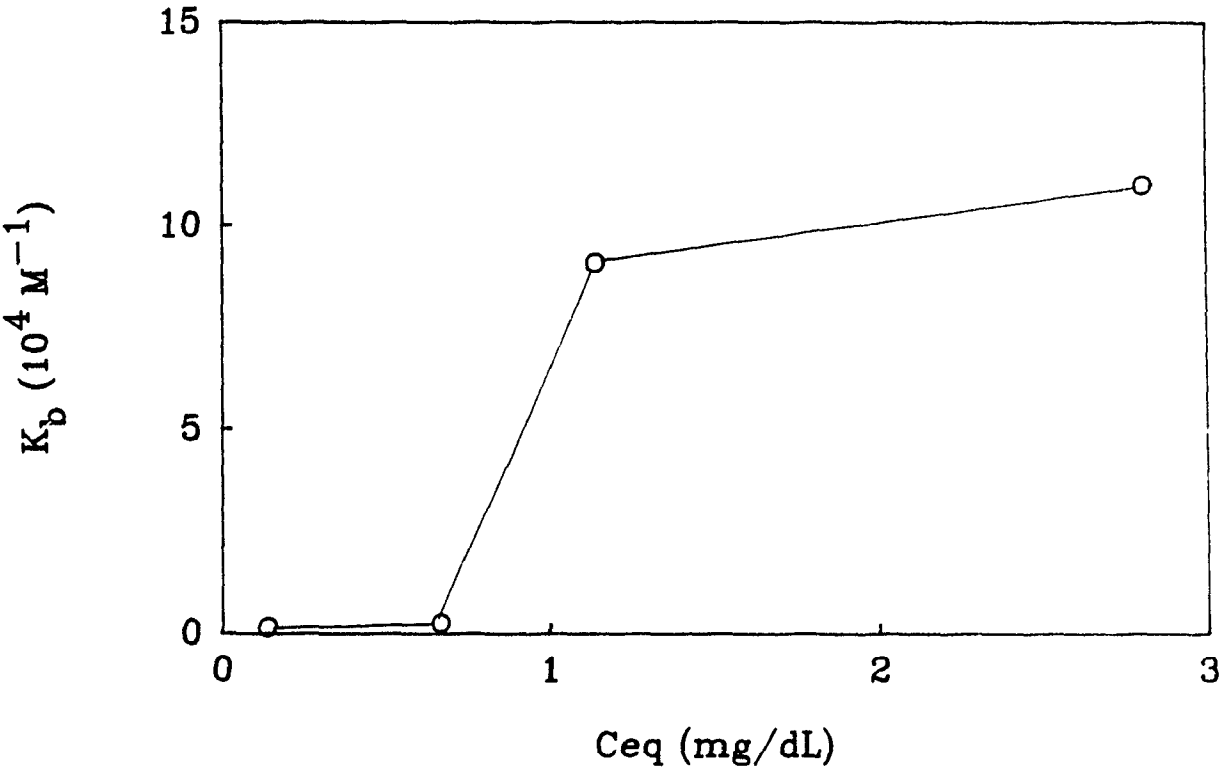

Figure 2.44 Variation of the basicity constant of the bound hydroxyl group (K_b), in the resin phase, with increasing Ceq

The importance of hydrophobic interactions between the hydrophobic parts of adsorbate and adsorbent has been proposed previously for other ion-exchange processes (25, 42-44), as well as for the adsorption by cholestyramine (1-3). The importance of the interactions between the hydrophobic faces of the bile acid anions and the pendant phenyl group is considered further in Chapter 4.

2.6.3 Challenges to the Donnan Model

The Donnan model, which is based on ion partitioning between two phases, gives valuable insight concerning adsorption of bile salt by cholestyramine. In the main, it is an ion-exchange process - the bile acid anion displaces the chloride counter-ion of cholestyramine. At low Ceq, this displacement is not stoichiometric due to the additional displacement of chloride by hydroxyl anion. However, as the concentration at equilibrium of bile acid increases, the displacement of the chloride counter-ion is due only to added bile acid anion. The bile acid in the resin phase exists in two forms, bound and unbound. Initially, the concentrations of both forms increase. However, as the Ceq increases, the bound form becomes favoured due to the strong electrostatic interaction between the pendant and the bile acid anion and to the interactions between bile acid anions on adjacent pendants. The pH of the external solution differs from that of the resin phase, the resin phase being basic compared to a slightly acidic external solution. Thus, the overall characteristics of the interaction between cholestyramine and the bile acid can be explained by the Donnan theory.

Other experimental observations can also be explained qualitatively on the basis of the Donnan theory. The lowering in the isotherm for the adsorption of glycocholic acid by cholestyramine when Tris-HCl buffer replaces water as the adsorption medium is in keeping with the presence of additional ions in the

buffered system, which will affect the partitioning between phases. Furthermore, the Tris-HCl in the resin phase also buffers the resin phase and makes it less basic.

The fact that iodide, at a given Ceq, is less displaced than chloride is consistent with an ion-exchange mechanism for the interaction between bile acid and cholestyramine. As seen earlier (section 2.4) iodide is better bound to a strong anion exchanger than chloride. Thus, the bile acid can displace the chloride counter-ion more easily. Although, the quaternary ammonium group and the chloride and iodide anions are dissociated, the latter must stay in the resin phase to maintain electroneutrality. Their displacement into the external solution becomes possible due to the entry of another anion, to maintain electroneutrality. However, this process is more favorable in the case of the chloride counter-ion than the iodide, thus explaining the lower adsorption capacity of cholestyramine having iodide as counter-ion.

Perhaps the most curious aspect of the binding of glycocholate by cholestyramine is the temperature dependence described in Section 2.2.4. From the Donnan theory it was said that the interaction between the bile acid anions and the pendant of cholestyramine is an ion-exchange process. Such a process depends, in part, on the mobilities of the ions between the different phases. At low temperature, 6°C, the movement of the ions, between the two phases, would be more difficult than at higher temperature (25-65°C). Thus, as the temperature is increased the movement of the ionic species becomes easier reaching a limiting value somewhere between 6 and 25°C.

Furthermore, positional rearrangements of backbone would also favour the ordering of bound glycocholate. Certainly these effects become more hindered as the temperature is decreased. In addition, it is now well documented that hydrophobic interactions are quite temperature dependent. For example, protein

denaturation can occur both at a high temperature and at a low temperature - the high temperature denaturation is due to an entropic contribution of the hydrophobicity and that at low temperature is due to the temperature dependence of the enthalpic term. Thus, the sudden decrease in adsorption between 25° and 6°C may reflect such a hydrophobic effect.

2.7 CONCLUSIONS

Application of the Donnan theory to the simple system for the adsorption of glycocholic acid by cholestyramine in water, affords considerable insight to this process. The ions in the system partition themselves between the two phases - the external solution and the resin phase. The concentration of bound bile acid in the resin phase is above the CMC, thus micelle-type ordering is occurring. The micellization occurs between the bound bile acid and the pendant in the form of mixed micelles. In addition, it is also possible that the unbound bile acid aggregates to form "regular" micelles. The micellization process promotes the entry of glycocholic acid into the resin phase, explaining the ability of cholestyramine to adsorb glycocholic acid significantly, ***in vitro***. The increase in both the formation constant (K_f) and the basicity constant (K_b) can also be explained. The Donnan theory leads to a better understanding of the interactions involved in this system and allows the rationalization of the experimental results.

2.8 REFERENCES

1. W.H. Johns and T.R. Bates, *J. Pharm. Sci.*, **58**, 179, 1969
2. W.H. Johns and T.R. Bates, *J. Pharm. Sci.*, **59**, 329, 1970
3. W.H. Johns and T.R. Bates, *J. Pharm. Sci.*, **59**, 789, 1970
4. L.M. Hagerman, D.A. Julow and D.L. Schneider, *Proc. Soc. Exptl. Biol. Med.*, **143**, 89, 1973
5. H.W. Florey, R.D. Wright and M.A. Jennings, *Phys. Rev.*, **21**, 36, 1941
6. W.H. Elliott, **Chap 11, Metabolism of Bile Acids in Liver and Extrahepatic Tissues**, in *Sterols and Bile Acids*, H. Danielsson and J. Sjovall eds., Elsevier, Amsterdam, 1985
7. X.X. Zhu, **Ph.D. Thesis**, McGill University, 1988
8. H.M. Burt, E.C. Cameron, H. Erber and J.D.E. Price, *J. Pharm. Sci.*, **76**, 379, 1987
9. The Dow Chemical Company, *Dowex· Ion Exchange*, The Lakeside Press, R.R. Donnelley and Sonx Co., USA, 1958
10. R. Kunin, **Chap 4 Anion Exchange Resin Characteristics**, in *Ion Exchange Resins*, 2nd edition, John Wiley and Sons Inc., New-York, 1958
11. G. Nemethy and H.A. Scheraga, *J. Phys. Chem.*, **66**, 1773, 1962
12. M.C. Carey and D.M. Small, *J. Colloid Interf. Sci.*, **31**, 382, 1969
13. M.C. Carey, *Hepatology*, **4**, 66S, 1984
14. T.A. Horbett, P.K. Weathersby and A.S. Hoffman, *J. Bioeng* , **1**, 61, 1977
15. I. Lundstrom, *Prog. Colloid Polym. Sci.*, **70**, 76, 1985
16. I.M. Klotz, F. Walker and R. Pivan, *J Am. Chem. Soc.*, **68**, 1486, 1946
17. B.R. Young, W.G. Pitt and S.L.Cooper, *J Colloid Interf. Sci.*, **124**, 28, 1988
18. R. Lee and S.W. Kim, *J. Biomed. Mater. Res.*, **8**, 251, 1974
19. H.Y.K Chuang, W.F. King and R.G. Masson, *J. Lab. Clin. Med* , **92**, 483, 1978
20. W.J. Dillman Jr. and I.F. Miller, *J. Colloid Interf. Sci.*, **44**, 221, 1973
21. J.L Brash and Q.M. Samak, *J Colloi Interf. Sci* , **65**, 495, 1978
22. H.Y. Ton, R.D. Hughes, D.B.A. Silk and R. Williams, *J Biomed Mater. Sci* , **13**, 407, 1979
23. Y. Ihara, *J. Appl. Polym Sci.*., **32**, 5665, 1986
24. Y. Ihara, *J. Appl. Polym Sci.*, **33**, 3087, 1987
25. Y. Ihara, *J. Appl. Polym. Sci.*, **36**, 891, 1988
26. I.M. Klotz and D.L. Hunston, *J. Biol Chem.*, **8**, 3001, 1975
27. I.M. Klotz and D.L. Hunston, *Arch Biochem. Biophys* , **193**, 314, 1979
28. I.M. Klotz and D.L. Hunston, *Proc Natl. Acad. Sci USA*, **74**, 4959, 1977
29. G. Scatchard, *Ann NY Acad Sci* , **51**, 660, 1949
30. I.M. Klotz, *Trends. Pharmacol. Sci.*, **4**, 253, 1983

31. B. Perlmutter-Hayman, *Acc. Chem. Res.*, **19**, 90, 1980

32. I.M. Klotz, *Arch. Biochem.*, **9**, 109, 1946

33. D.L Hunston, *Anal. Biochem.*, **63**, 99, 1975

34. W.C. Galley, M. Bouvier, S.-D. Clas, G.R. Brown and L.E. St-Pierre, *Biopolymers*, **27**, 79, 1988

35. M. Bouvier, G.R. Brown and L.E. St-Pierre, *Can. J. Chem.*, **65**, 1927, 1987

36. M. Bouvier, G.R. Brown and L.E. St-Pierre, *Can. J. Chem.*, **67**, 596, 1989

37. D. Reichenberg, **Chap. 7, Ion-Exchange Selectivity** in *Ion-Exchange. A Series of Advances* vol 1, J.A. Marinsky ed., Marcel Dekker Inc., New-York, 1966

38. R. Kunin and F.X. McGarvey, *Ind. Eng Chem.*, **41**, 1265, 1949

39. F.K. Lindsay and J.S. D'Amico, *Ind Eng. Chem.*, **43**, 1085, 1951

40. H.P Gregor, *J. Am. Chem. Soc.*, **73**, 642,1951

41. D.B. Taylor, *J. Pharmacol. Exptl. Ther.*, **186**, 537, 1973

42. F.G Donnan and A.B. Harris, *J. Chem. Soc* , **99**, 1554, 1911

43. F.G. Donnan and A.J. Allmand, *J. Chem. Soc.*, **105**, 1941, 1914

44. F.G. Donnan, *Chem. Rev* , **1**, 73, 1924

45. J.R. Barrante, **Chap.9 Electrochemistry**, in Physical Chemistry for the Life Science, Prentice-Hall, New-Jersy, 1977

46. G.E. Boyd and K. Bunzl, *J. Am. Chem Soc.*, **89**, 1776, 1967

47. R. McGregor and P. W. Harris, *J. Appl Polym Sci.*, **14**, 513, 1970

48. M.M. Reddy, S. Amdur and J.A. Marinsky, *J. Am. Chem. Soc.*, **94**, 4087, 1972

49. J. Delmenico and R.H. Peters, *Text. Res. J.*, **34**, 207, 1964

50. J. Delmenico and R.H. Peters, *Text. Res J* , **35**, 14, 1965

51. T.H. Guion and R. McGregor, *Text. Res J* , **44**, 439, 1974

52. G. Alberghina, S.-L. Chen, S. Fisichella, T. Ijima, R. McGregor, R.M. Rohner and H. Zollinger, *Text. Res. J* , **58**, 345, 1988

53. G. Alberghina, M.E. Amato, S. Fisichella and H. Zollinger, *Text. Res. J.*, **59**, 264, 1989

54. J.L. Haynes, *J. Colloid Interf Sci* , **26**, 255, 1968

55. D.B. Taylor, *J. Pharmacol. Exptl Ther* , **186**, 537, 1973

56. J. Grignon and A.M. Scallan, *J. Appl Polym. Sci.*, **25**, 2829, 1980

57. M.C. Carey, **Chap 13, Physical-Chemical Properties of Bile Acids and their Salts**, in *Sterols and Bile Acids*, H. Danielsson and J. Sjovall, eds., Elsevier, Amsterdam, 1985

58. M.C. Carey and D.M. Small, *Arch. Intern. Med.*, **130**, 506, 1972

59. F. Helfferich, **Chap 5 Equilibria**, in *Ion Exchange*, McGraw-Hill, New-york, 1962

3 ADSORPTION OF BILE ACIDS BY SYNTHESIZED RESINS

To obtain a better understanding of the binding of bile acids by cholestyramine, studies were carried out using synthesized ion-exchange resins with functional groups which chemically resemble cholestyramine in various characteristics. Schematically, cholestyramine can be viewed as a resin of the type P-R"-C_6H_4-R'-NR_3^+, where P represents the cross-linked polymer backbone, R" is a spacer (absent in cholestyramine), R' is another spacer (CH_2 in the case of cholestyramine) and R is either H or CH_3. By systematic changes of chemical structure, either the backbone, P, or the position of the methylene group, R' or R", between the benzene ring and the quaternary ammonium group, or the quaternization of the amino group, it is possible to obtain information about the interactions with bile acids and to compare their affinities to that of cholestyramine. From a knowledge of the effectiveness of these synthesized resins in binding bile acids, it should be possible to determine which functions in cholestyramine are important for effective adsorption.

The first series of resins consisted of a hydrophilic polyacrylamide backbone onto which were grafted 4-(aminomethyl)benzoic acid; it was either coupled directly to the backbone or separated from it by a spacer, R", consisting of three alanines. The effect of the presence of the spacer was studied; comparison was also made between the primary and quaternary amino groups. The effect of the degree of substitution of the resin was studied using polyacrylamide resins of different functionalities. Onto polyacrylamide was also coupled 4-aminophenylacetic acid, with and without the spacer, to determine whether the methylene group plays a role in the adsorption.

Merrifield resin, a hydrophobic styrene backbone resembling that of cholestyramine, was also used in the syntheses of some resins. Again 4-(aminomethyl)benzoic acid and 4-aminophenylacetic acid were attached to the backbone, either directly or separated by a three alanine spacer. Similar studies as for the polyacrylamide backbone were done.

The following chapter describes how these resins were prepared and characterized and reports their adsorption characteristics for bile acids. Conclusions about the important features of cholestyramine for binding bile acids are also discussed.

3.1 EXPERIMENTAL

Four polymeric backbones were utilized; two hydrophilic polyacrylamide resins and two hydrophobic Merrifield resins. The first polyacrylamide backbone was a copolymer of dimethylacrylamide and N-acryl-1,6-diaminohexane reticulated with bisacrylyl-1,2-diaminoethane (11% crosslinked, Chemalog) (Figure 3.1a). The functionality of the resin was 0.241 mmol/g resin, as determined by potentiometric titration in 0.050M potassium nitrate (KNO_3) using silver nitrate ($AgNO_3$). The second polyacrylamide resin was a copolymer of dimethyl acrylamide and the acryloyl derivative of sarcosine methyl ester reticulated with bis(acrylamido)ethane (1 mmol/g resin, Milligen) (Figure 3.1b). Before it was used as the backbone, it was reacted either with ethylene diamine (Aldrich) or tris-(2-aminoethyl)amine (Aldrich) (Figure 3.2) to produce resins with functionalities of 0.835 and 1.40 mmol of primary amino group per gram of resin, determined by acid-base titrations and by potentiometric titrations with $AgNO_3$.

a)

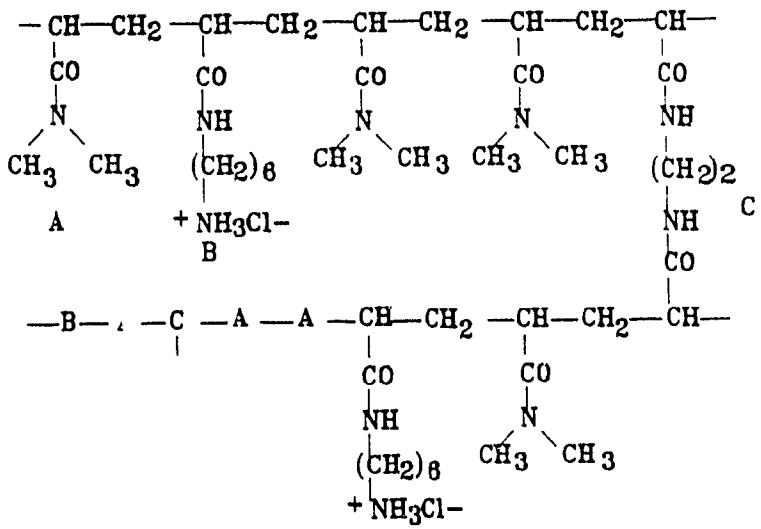

b)

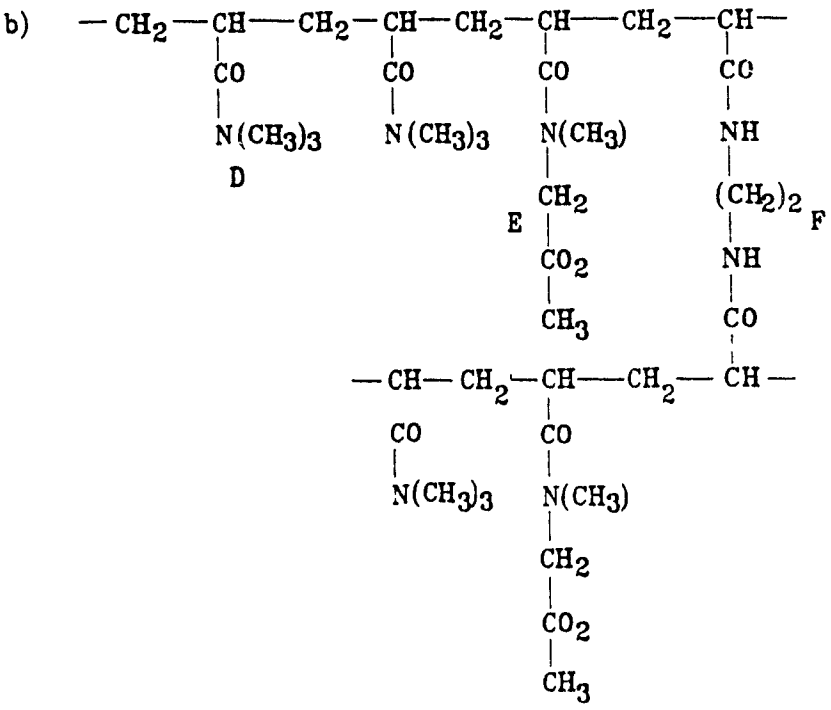

Figure 3.1 Structures of the two polyacrylamide backbones used in this study. a) Copolymer of a dimethyl acrylamide (A) and N-acryl-1,6-diaminohexane (B) reticulated with bisacrylyl-1,2-diaminoethane (C); b) copolymer of a dimethylacrylamide (D) and the acryloyl derivative of sarcosine methyl ester (E) reticulated with bis(acrylamido)ethane (F)

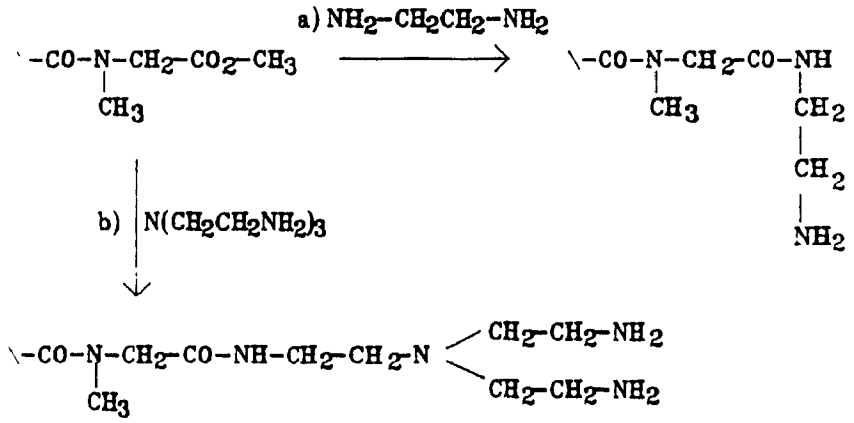

Figure 3.2 Functionalization of the polyacrylamide backbone (1 mmol/g resin) with a) ethylenediamine and b) tris-(2-aminoethyl)amine

The first Merrifield resin was a 1% crosslinked chloromethylated (1.00 mmol/g resin) styrene divinylbenzene copolymer (Sigma). The second Merrifield resin was similar to the first but with a substitution of 4.15 mmol/g resin.

3.1.1 Syntheses of the Resins

In every case the pendants were constructed by attaching the carboxylic acid function, of an appropriate amino acid, to the amino group of the polymer resin by forming the symmetrical anhydride which reacted to produce a peptide linkage.

In preparation for the coupling reaction, the amino groups of the compounds to be attached to the polymer backbone, generally amino acids, needed to be protected. The spacer t-Boc-L-Alanine (Vega Biotechnologies) was used without further purification. To protect the amino group of 4-(aminomethyl)benzoic acid (Aldrich) and 4-aminophenylacetic acid (Aldrich), di-tert-butyl-dicarbonate (t-Boc, Aldrich) (2-fold excess) was added to a solution of the acid and triethylamine (freshly distilled, 2-fold excess) (A and C) in tetrahydrofuran (THF)/water (1:1) (1). The reaction was followed by tlc. Upon completion, the THF/H_2O was distilled off, ***in vacuo***, and the residue was dissolved in ethyl acetate; the organic layer was washed with a 5% citric acid solution, followed by water. The organic layer was dried over magnesium sulfate ($MgSO_4$), evaporated ***in vacuo*** to yield the t-Boc derivative as a white powder, which was re-crystallized with methylene chloride.

All couplings were done by solid phase peptide synthesis (SPPS) techniques, using a Vega 250 synthesiser (2). Unless otherwise specified all solvents, except dichloromethane (DCM) which was dried over molecular sieves (0.4 nm), were distilled prior to use.

The polyacrylamide resin was neutralized with 40% di-isopropylethylamine (DIEA) in DCM for 20 minutes. Symmetrical anhydrides of alanine, of the protected 4-(aminomethyl)benzoic acid and 4-aminophenylacetic acid were prepared for the coupling by dissolving at 0°C six equivalents of the t-Boc derivative in DCM, for alanine, or in dimethylformamide (DMF) for the others. Stirring was continued for 20 minutes and 3 equivalents of 10% dicyclohexylcarbodiimide (DCC)/DCM were then added slowly. The mixture was allowed to stir for 30 minutes at 0°C, during which time dicyclohexylurea (DCU) precipitated (Figure 3.3). The mixture was then filtered and the filtrate was added to the resin. The reaction was left to stir until completion of the coupling, as indicated by a negative ninhydrin test (3). The t-Boc protecting groups were then removed using 40% trifluoroacetic acid (TFA) in DCM, followed by neutralization with 5% DIEA in DCM (Figure 3.4). The ninhydrin test was again used to monitor the deprotection step.

When the Merrifield resins were used as backbone, coupling of the first alanine or 4-(aminomethyl)benzoic acid or 4-aminophenylacetic acid was carried out using the cesium salt of the above (4) to form an ester linkage. Substitution of the resin was determined by a picric acid test (5). Subsequent couplings were carried out as described above. The resin was then collected, washed with DCM and finally with anhydrous diethylether. It was then dried ***in vacuo*** at room temperature (18-20°C).

3.1.2 Quaternization of the Resins

The resins were quaternized with methyl iodide (Aldrich) (16-fold excess) in methanol or DMF and potassium bicarbonate (Fisher) (10-fold excess), in the absence of light for 2-7 days (6). At the completion of the reaction, the resin was

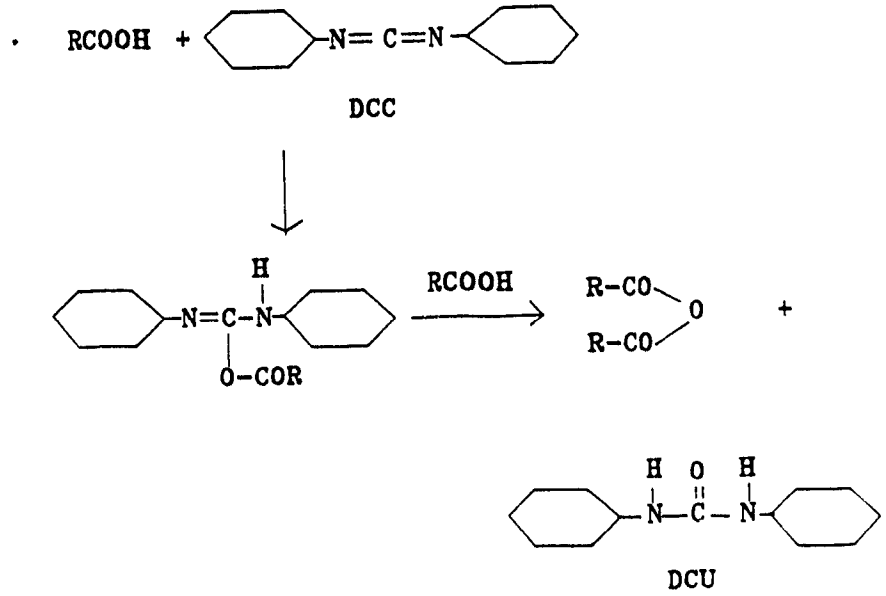

Figure 3.3 Preparation of symmetrical anhydrides of a model compound RCOOH

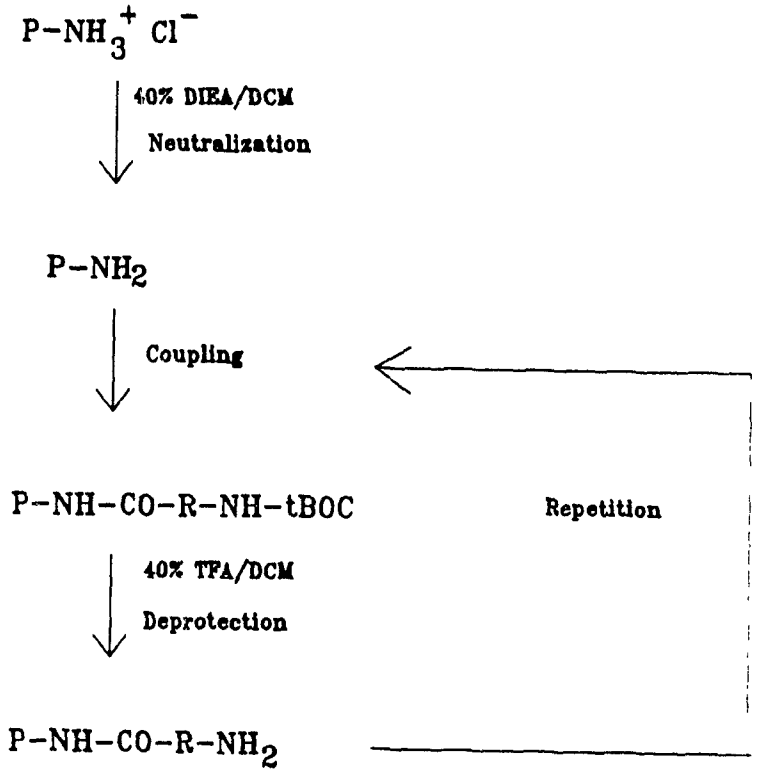

Figure 3.4 Scheme for Solid Phase Peptide Syntheses. R: -$CH(CH_3)$-, -CH_2-C_6H_4-, C_6H_4-CH_2-; P: backbone

collected, washed with methanol and finally with anhydrous diethylether. It was dried ***in vacuo*** at room temperature (18-20°C). The extent of the quaternization was determined by potentiometric titration with $AgNO_3$.

Table 3.1 lists the resins which were synthesized with their substitution and the reaction times for the quaternary reaction.

3.1.3 Adsorption Experiments

Studies of the adsorption of bile acids were done with solutions of sodium glycocholate in aqueous Tris-HCl buffer (0.0025 M), at pH 7. A stock solution of bile salt (10-20 mg/dL) was prepared, in Tris-HCl buffer, and from it a series of standard solutions were prepared by dilution. These solutions of known concentration were then added to a weighed amount of dried resin (10-15 mg). The mixtures were shaken for 20-24 hours at room temperature (18-20°C) using a mechanical shaker. The solutions containing the resin were then filtered by gravity and the peak areas of the bile salt before and after adsorption were determined by HPLC, as described previously (Section 2.1.3).

3.2 ADSORPTION OF BILE ACIDS BY SYNTHESIZED RESINS

To establish a reference point, isotherms were first determined for the adsorption of glycocholic acid by the hydrophilic polymer backbone, polyacrylamide, both in the form of a primary amine and in the quaternized form. The pendants were then added; the first series of resins were sorbents for which the active group was attached directly to the polyacrylamide backbone. A second series of resins was prepared by introducing a spacer, consisting of three alanines, between the active group and the backbone. For both series of resins, a portion was also quaternized to obtain sorbents with the corresponding quaternary

Table 3.1 List of Synthesized Resins, their Substitution and the Reaction Time for the Quaternization.

RESIN	SUBSTITUTION (mmol/g)	TIME (hours)
P_1[a]-A[b]	0.241	
P_1-Q[c]	0.232	380
P_1-C[d]-M[e]-Ph[f]-A	0.234	
P_1-C-M-Ph-Q	0.0855	193
P_1-C-Ph-M-A	0.234	
P_1-C-Ph-M-Q	0.126	243
P_1-S[g]-C-Ph-M-A	0.222	
P_1-S-C-Ph-M-Q	0.113	240
P_1-S-C-M-Ph-A	0.222	
P_1-S-C-M-Ph-Q	0.139	192
P_2[h]-D[i]	0.358	
P_2-C-Ph-M-A	0.747	
P_2-C-M-Ph-M-A	0.358	
P_2-T[j]	1.403	
M_{f1}[k]-C-Ph-M-A	0.897	
M_{f1}-S-C-Ph-M-A	0.322	
M_{f1}-S-C-M-Ph-A	0.314	
M_{f2}[l]-C-Ph-M-A	2.89	
M_{f2}-C-Ph-M-Q	1.44	171

a: P_1 = polyacrylamide (0.241 mmol/g)
b: A = primary amino group ($-NH_2$)
c: Q = quaternary ammonium group ($-N(CH_3)_3^+ I^-$)
d: C = peptide bond (-NH-CO-)
e: M = methylene group ($-CH_2-$)
f: Ph = phenyl group ($-C_6H_4-$)
g: S = spacer (3 alanine groups)
h: P_2 = polyacrylamide (1 mmol/g)
i: D = ethylene diamine ($-NH-CH_2-CH_2-NH_2$)
j: T = tris-(2-aminoethyl)amine ($-NH-CH_2-CH_2-N-(CH_2CH_2NH_2)_2$))
k: M_{f1} = Merrifield resin (1 mmol/g)
l: M_{f2} = Merrifield resin (4.15 mmol/g)

ammonium group. Isotherms were obtained to determine the effect of the quaternization, the importance of the spacer, the effect of the position of the methylene group between the phenyl group and the quaternary ammonium group on adsorption of glycocholate from Tris-HCl buffer.

The same pendants were then coupled to a hydrophobic backbone so that the adsorption capacities of resins having a hydrophilic and a hydrophobic backbones which bear the same pendant could be compared.

To see if the number of active sites per gram of resin is important in the adsorption of bile acids, hydrophilic resins of different functionalities were also tested.

Some studies were also done, using resins with the hydrophilic backbone, in which the adsorption medium and the bile acid were changed.

3.2.1 Hydrophilic Backbone with Primary Amino Groups

The commercial resin cholestyramine uses a hydrophobic, polystyrene backbone. The possibility of producing a resin with active groups similar to that of cholestyramine but on a more hydrophilic backbone was attractive. For this reason, resins were prepared using two polyacrylamide backbones, differing only in functionality.

3.2.1.1 Spacer Effects

It was of interest first to determine the isotherm for the adsorption of bile acids by the hydrophilic backbone, designated P_1-A, having a functionality of 0.241 mmol/g resin. Figure 3.5 shows the isotherm, at 20°C, for the adsorption of glycocholate by P_1-A. This isotherm has the regular Langmuir shape and indicates a low, but significant, affinity of the resin for glycocholate. This behaviour is compared with that for resins consisting of the same backbone with 4-(aminomethyl)benzoic acid coupled to the primary amine functional sites, with

and without a spacer consisting of three alanines, to produce resins of the structure P_1-C-Ph-M-A and P_1-S-C-Ph-M-A, where S is the ala_3 spacer, C is the peptide linkage, Ph is the phenyl group, M is the methylene group and A stands for the primary amino group.. For the resin without the ala_3 spacer, P_1-C-Ph-M-A, the extent of adsorption increased from 0.05 to 0.10 mol/eq pndnt, at Ceq of 15 mg/dL (Figure 3.5). Although the pendant resembles that of cholestyramine, except that it is in the primary amine form, this resin adsorbs much less glycocholate, 0.1 compared to 1.1 mol/eq pndnt for cholestyramine (Section 2.2.1), under similar experimental conditions. This startling effect, which was entirely unexpected, seems to indicate that quaternization, with the resultant increase in basicity, is of key importance.

In an attempt to improve the accessibility to the 4-(aminomethyl)benzoic acid and thus promote adsorption, a spacer consisting of three alanines was incorporated. Previous studies (2) with sorbents having pendants consisting of basic amino acids showed that the active group adsorbs bilirubin more effectively when it is separated from the hydrophilic backbone by a spacer. The choice of the amino acid, alanine, to form the spacer is justified by the fact that it contains no reactive groups in its structure other than the amide linkage, thus excluding the possibility of any reaction with the spacer either during the syntheses or during the adsorption experiment. Furthermore, this spacer should have a hydrophobic/hydrophilic ratio that is similar to that of the backbone.

The addition of the ala_3 spacer actually causes a decrease in the adsorption capacity of the resin for glycocholic acid, even when compared to the backbone. The extent of adsorption decreases from 0.08 to 0.005 mol/eq pndnt for the resin with the ala_3 spacer to which is attached 4-(aminomethyl)benzoic acid, P_1-S-C-Ph-M-A (Figure 3.5). For all intents and purposes, this resin shows no adsorption of glycocholate.

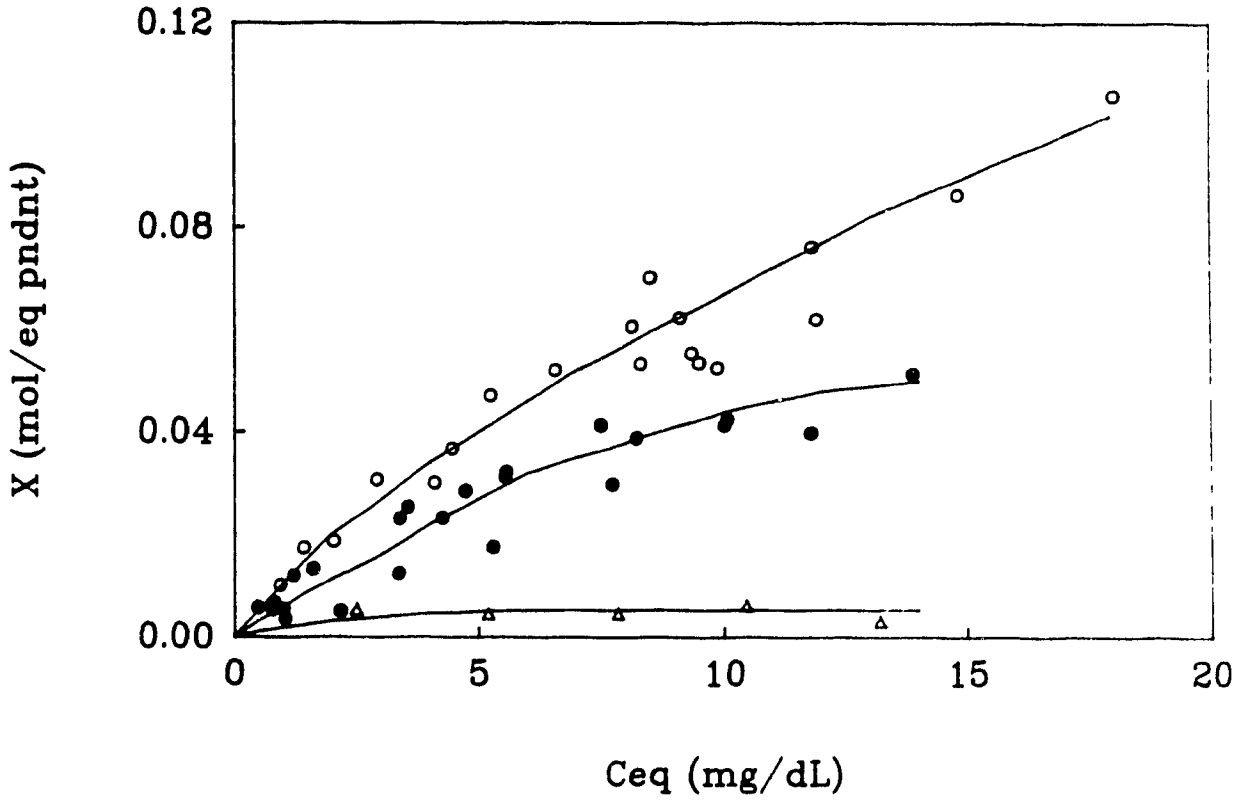

Figure 3.5 Isotherms (T = 20°C) for the adsorption of glycocholic acid by P_1-A, ●, P_1-S-C-Ph-M-A, Δ, and P_1-C-Ph-M-A, ○

Since the incorporation of the ala_3 spacer should have little effect on the basicity, other factors must also be important in determining the extent of adsorption. The decrease in adsorption may be due to a decrease in the accessible volume for the glycocholate anions when the pendant length is increased. On the other hand, a synergistic effect involving the active site and the backbone is also possible.

3.2.1.2 Effect of the Position of the Methylene Group

Figure 3.6 shows the isotherms for the adsorption of glycocholate by the polyacrylamide backbone (functionality = 0.241 mmol/g) to which is attached either 4-(aminomethyl)benzoic acid to form resin P_1-C-Ph-M-A, or 4-aminophenylacetic acid to form resin P_1-C-M-Ph-A. The composition of these resins differs only in the position of the methylene group.

The position of the methylene group will influence the basicity of the amino group significantly. When it is located between the phenyl group and the amino group, the amine will be more basic. To obtain a measure of the magnitude of this effect, benzylamine, C_6H_4-CH_2-NH_2, with pK_b= 4.67, may be compared with aniline, C_6H_4-NH_2, with pK_b= 9.37. Thus, for the pendant produced by coupling 4-aminophenylacetic acid, so that the amino group is directly attached to the benzene ring, the amine will be much less basic because the positive charge can be stabilized by the phenyl ring. Indeed, a higher adsorption capacity for glycocholic acid is seen for the resin with the methylene group between the benzene ring and the amino group.

As was seen for the resin P_1-C-Ph-M-A, the incorporation of an ala_3 spacer, S, to the resin P1-C-M-Ph-A to form P_1-S-C-M-Ph-A results in a significant decrease in adsorption capacity. However, the effect of the methylene is not as evident for the resins P_1-S-C-Ph-M-A and P_1-S-C-M-Ph-A containing the

ala_3 spacer, since both already have a very low capacity for the adsorption of glycoholate anions (Figures 3.5, 3.6).

As a further investigation of the role of the methylene spacer, adsorption isotherms were also obtained for a polyacrylamide backbone of higher functionality, 1 mmol/g resin (P_2), with pendants produced by coupling 4-(aminomethyl)benzoic acid, to yield resin P_2-C-Ph-M-A, and 4-(aminomethyl)phenylacetic acid, to produce resin, P_2-C-M-Ph-M-A. These resins differ in that, while both contain the methylene group between the phenyl group and the active amine, the 4-(aminomethyl)phenylacetic acid pendants have an additional methylene group at the 1 position, i.e., between the phenyl group and the carbonyl group attached to the backbone. The adsorption capacity of the resin having both methylene groups for glycocholate is approximately double that of the one with one methylene group (Figure 3.7). The presence of the methylene group between the carbonyl group and the phenyl group allows a greater accessibility to the binding sites. Furthermore, the increased hydrophobicity may also be of importance.

3.2.2 Hydrophilic Backbone with Quaternary Ammonium Groups

It is apparent from the previous sections that basicity plays an important role in the adsorption of bile acids. To increase the basicity of the resins they were quaternized and tested for their capacity to adsorb bile acids.

To account for incomplete quaternization, the isotherms reported for the quaternized resins have been normalized as follows: The difference between the functionality of the original resin, in the amine form, and that of quaternized form was assumed to represent un-quaternized sites. The data from the adsorption experiment were treated to obtain the total amount of bile acid bound by the pendants, both un-quaternized and quaternized. Based on the isotherm for the un-

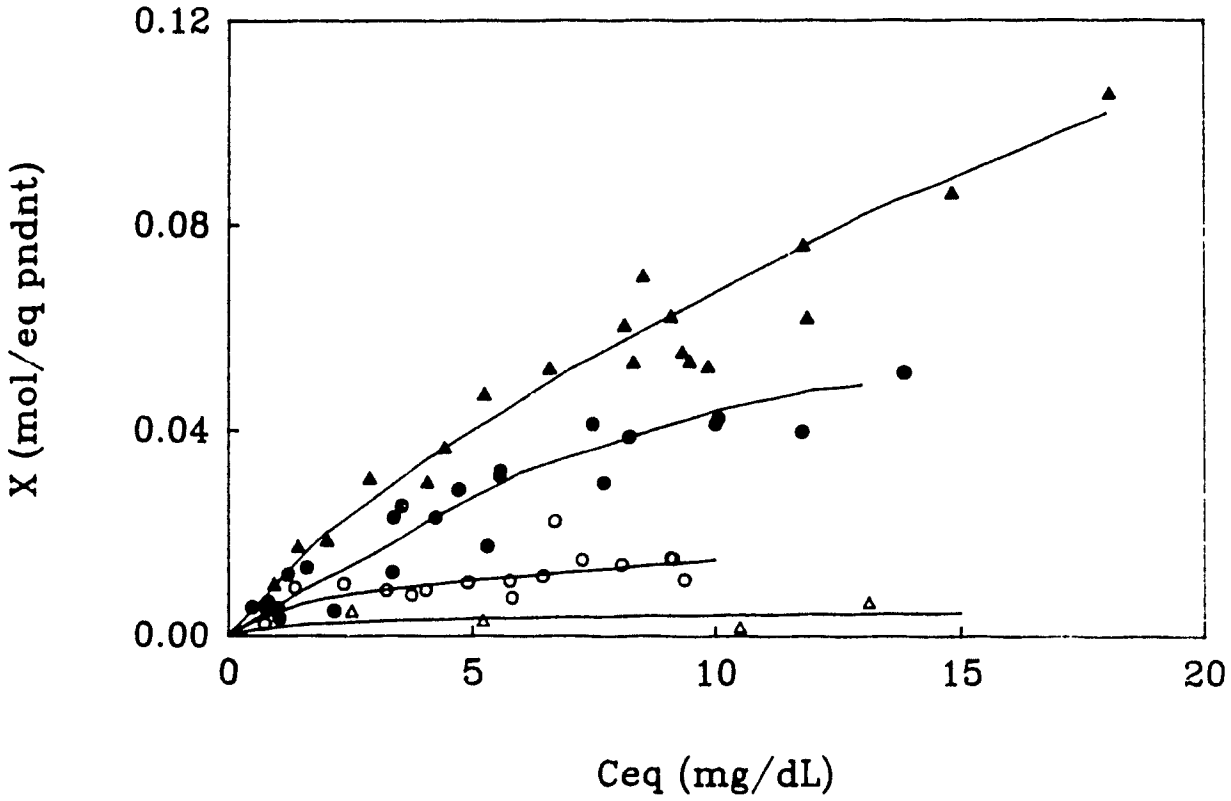

Figure 3.6 Isotherms (T = 20°C) for the adsorption of glycocholic acid by P_1-A, ●, P_1-S-C-M-Ph-A, Δ, P_1-C-M-Ph-A, ○, and P_1-C-Ph-M-A, ▲

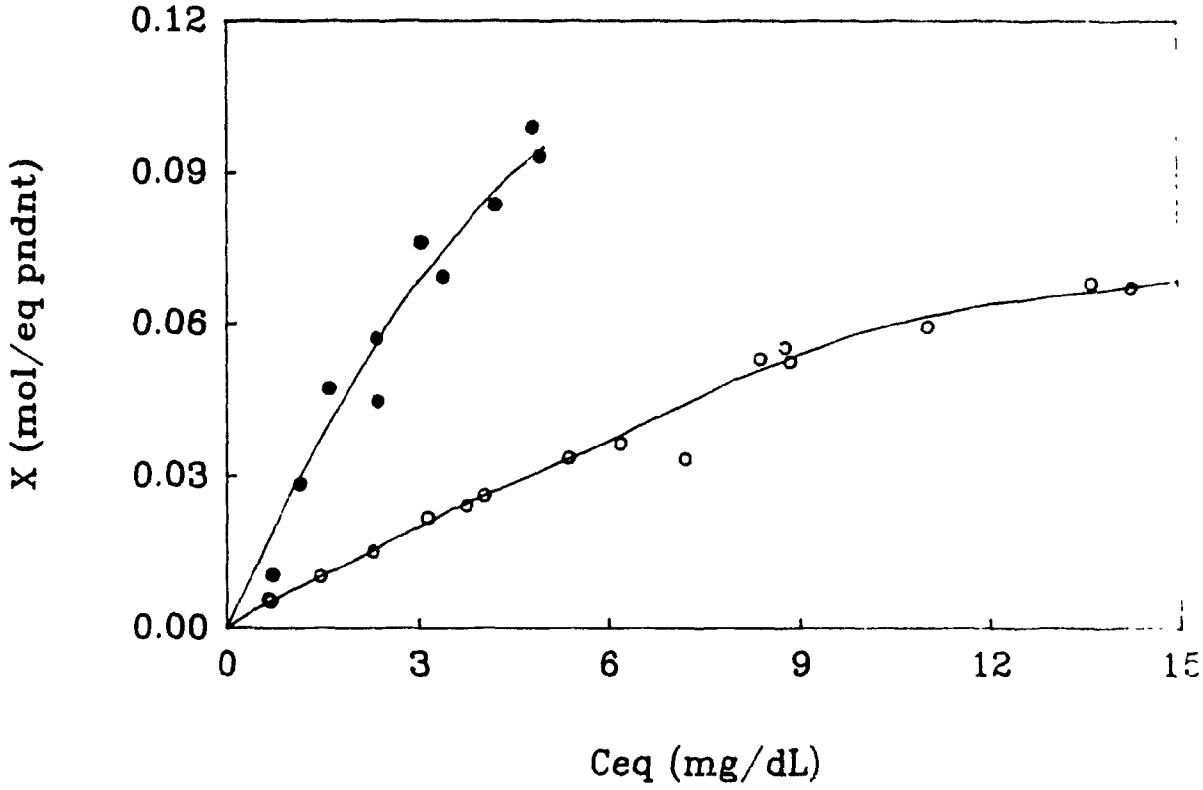

Figure 3.7 Isotherms (T = 20°C) for the adsorption of glycocholic acid by P_2-C-Ph-M-A, ○, and P_2-C-M-Ph-M-A, ●

quaternized resin and the number of un-quaternized sites, the moles of bile acid bound by the un-quaternized pendants, at a particular Ceq, was calculated. The remaining bound bile acid was considered to be bound by the quaternary pendants so that the isotherm for the adsorption of bile acid by the quaternized pendants, expressed as moles of glycocholate per equivalent of pendant, was obtained. This normalization process may somewhat oversimplify the actual adsorption behaviour since interactions between adjacent sites are completely ignored.

Figure 3.8 compares the isotherms, at 20°C, for the adsorption of glycocholate by the polyacrylamide backbone, P_1-A, with that of the quaternized analog, P_1-Q. Within the range of bile acid concentrations used in these experiments, the quaternized resin, P_1-Q, has a distinctly higher adsorption capacity (0.08 mol/eq pndnt) than the unquaternized, P_1-A, (0.05 mol/eq pndnt). However, adsorption is still relatively ineffective with binding occurring at less than 10% of the available sites. The increase in adsorption capacity as a result of quaternization is seen consistently for all of the resins (Figures 3.9-3.11), except in the case of the 4-(aminomethyl)benzoic acid coupled to the hydrophilic backbone to form P_1-C-Ph-M-Q, for which the isotherms of the quaternized and unquaternized forms are equivalent (Figure 3.13).

The higher affinity of the quaternized pendants for bile acid suggests that the primary interaction is of electrostatic nature, as shown in Chapter 2. Furthermore, hydrogen-bonding which can occur for the primary amines but not for the quaternary amines, appears to be unimportant. The primary amine resins are weaker bases than the corresponding quaternized resins so that the interaction with the bile acid anion is less favoured. At the increased pH of the resin phase, which was demonstrated in Chapter 2, the primary amine sites will be only partially protonated. Thus, the basicity of the resin is an important factor for the interaction of ion-exchange resins with bile acids.

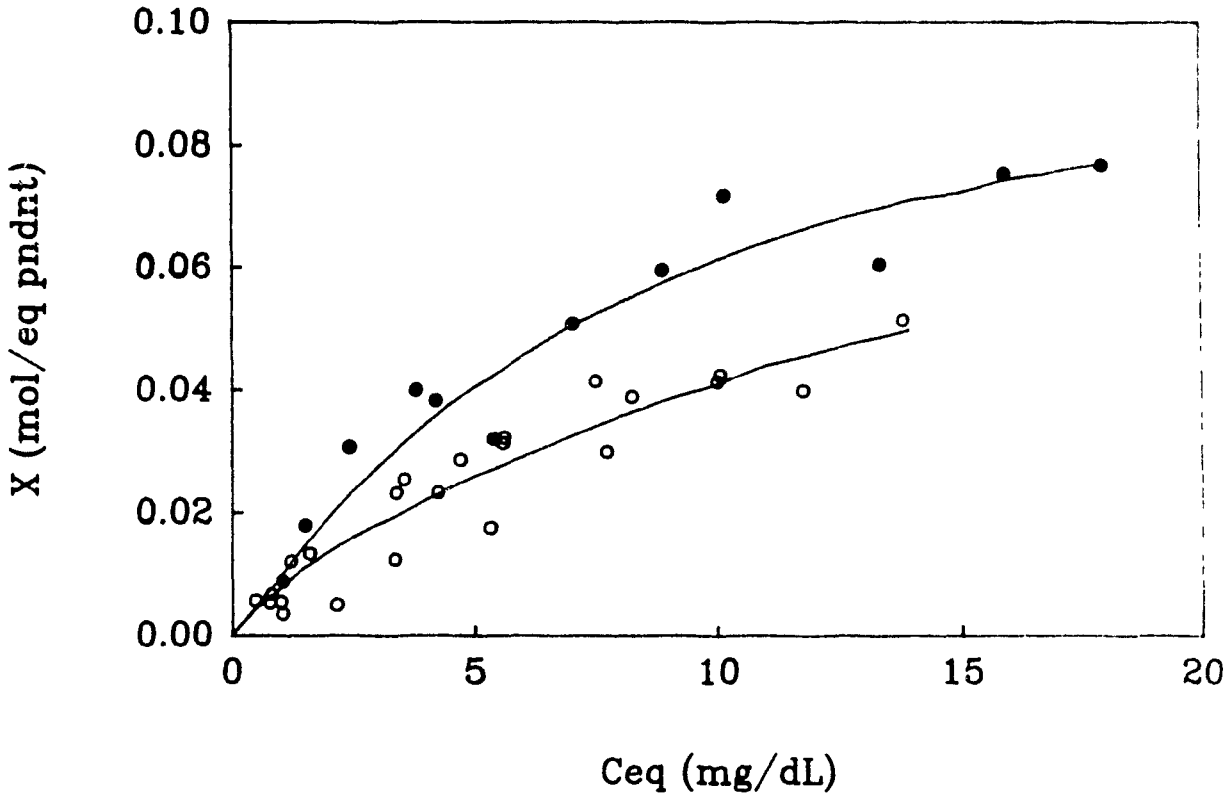

Figure 3.8 Isotherms (T = 20°C)for the adsorption of glycocholic acid by P_1-Q, ●, and P_1-A, ○

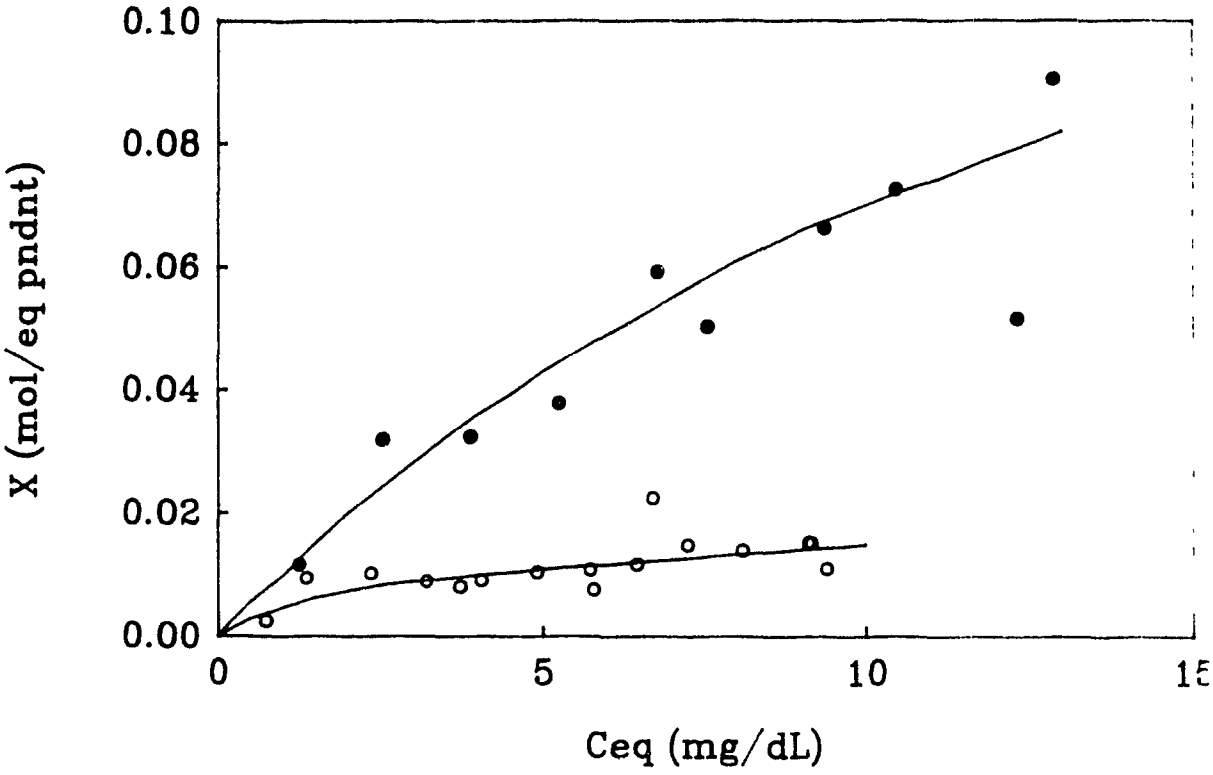

Figure 3.9 Isotherms (T = 20°C) for the adsorption of glycocholic acid by P_1-C-M-Ph-Q, ●, and P_1-C-M-Ph-A, ○

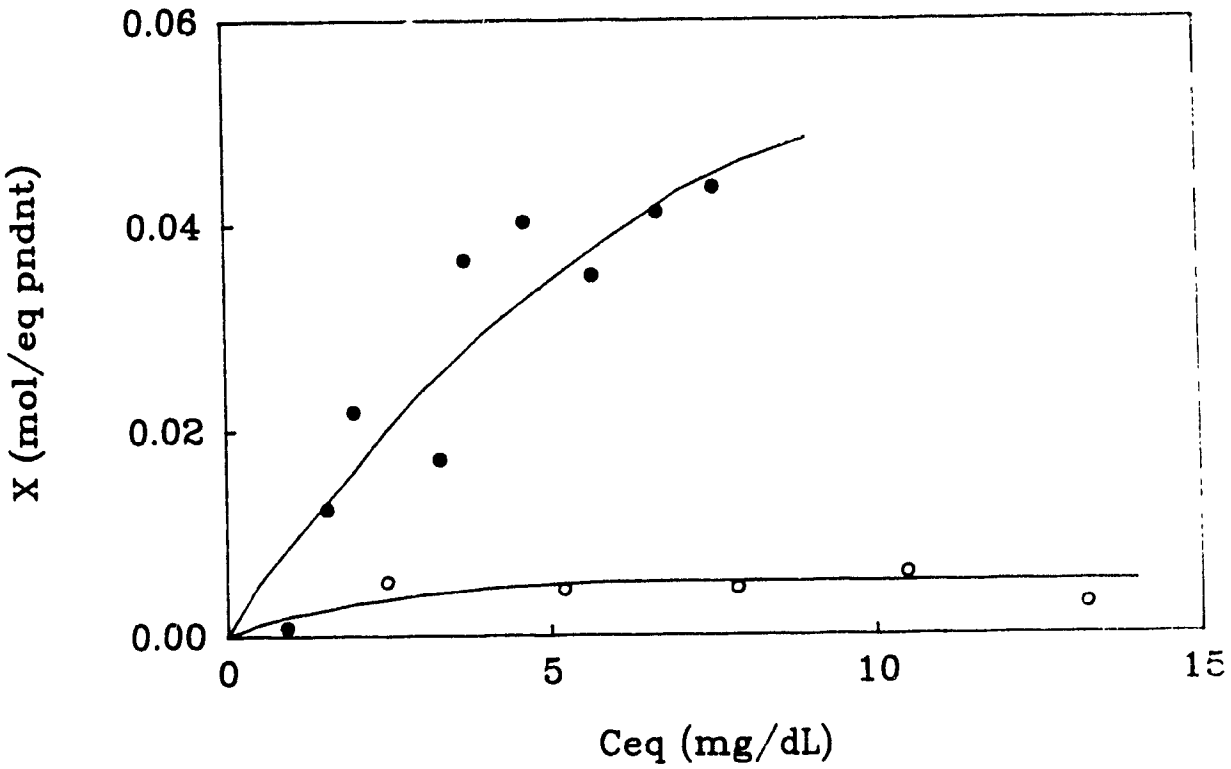

Figure 3.10 Isotherms (T = 20°C) for the adsorption of glycocholic acid by P_1-S-C-Ph-M-Q, ●, and P_1-S-C-Ph-M-A, ○

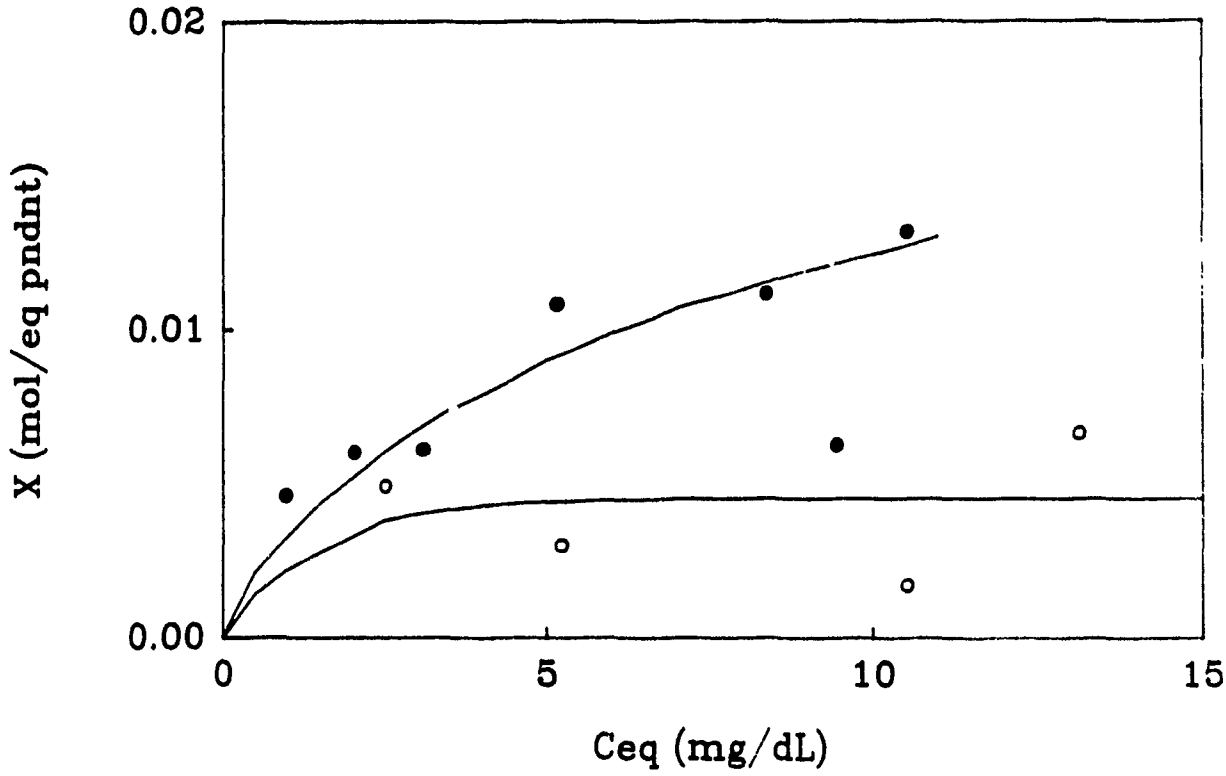

Figure 3.11 Isotherms (T = 20°C) for the adsorption of glycocholic acid by P_1-S-C-M-Ph-Q, ●, and P_1-S-C-M-Ph-A, ○

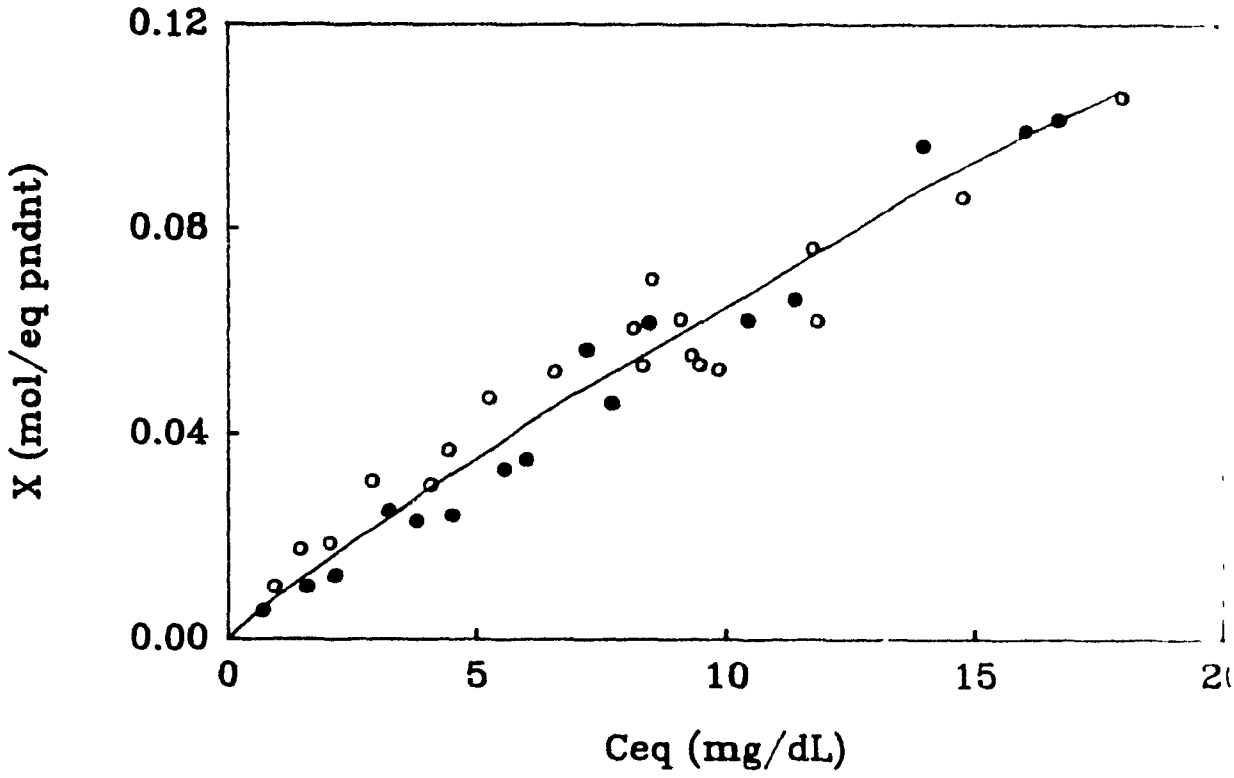

Figure 3.12 Isotherms (T = 20°C) for the adsorption of glycocholic acid by P_1-C-Ph-M-Q, ●, and P_1-C-Ph-M-A, ○

In case of P_1-C-Ph-M-A, which is the exception to the increase in adsorption capacity after quaternization, even the primary amine has a relatively high capacity for the adsorption of glycocholate, up to 0.1 mol/eq pndnt compared to about 0.01-0.02 mol/eq pndnt for the other unquaternized resins. It would appear that, in the absence of the ala_3 spacer, changes in the basicity of the amino group due to quaternization have no affect and both have the same affinity for glycocholate anions. However, when the ala_3 spacer is incorporated, this similarity disappears and the quaternized resin has a higher affinity for the bile acid than does the corresponding un-quaternized resin.

The most startling aspect of the adsorption of bile acids by these resins is that, although the quaternized 4-(aminomethyl)benzoic acid functional sites are **identical** to the pendants of cholestyramine, -Ph-M-Q, when coupled to a hydrophilic backbone the adsorption capacity for glycocholate is very much lower (Figure 3.13). Thus, the use of a water swellable backbone in the bile acid binding resin causes a decrease in the adsorption rather than increasing it. This suggests that the hydrophobic character of the backbone must be an important feature. On the hand, the lower substitution (0.241 mmol/g resin) of the hydrophilic backbone may also be important.

3.2.3 Hydrophilic Backbones of Increasing Functionality

To determine the effect of changes in density of active sites, identical polyacrylamide backbones of increased functionality were tested for their affinities for bile acids. They were tested in the primary amine form, without adding any pendants. When the amount of bile acid adsorbed was expressed as mg/g of resin, an increase in adsorption was seen with increasing substitution (Figure 3.14a). However, on a mol/eq pndnt basis, similar isotherms were obtained (Figure 3.14b).

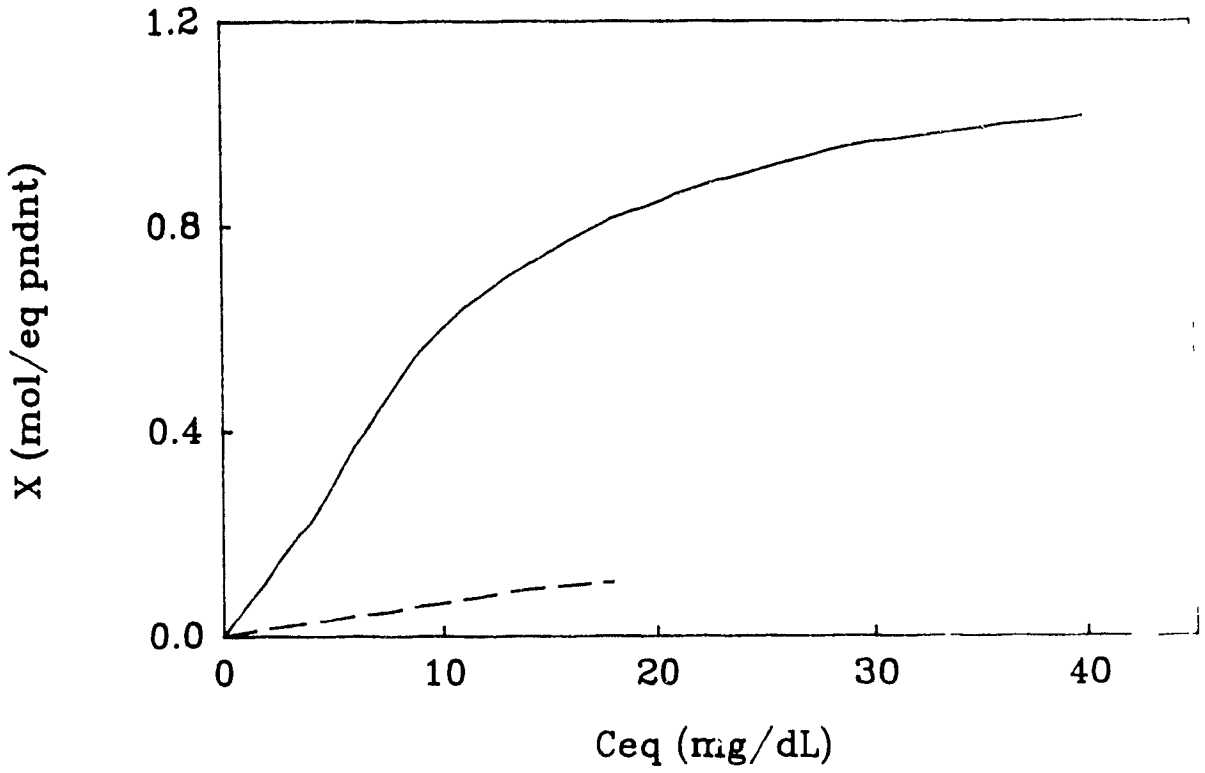

Figure 3.13 Comparison between the adsorption of glycocholic acid by cholestyramine —, and P_1-C-Ph-M-Q,

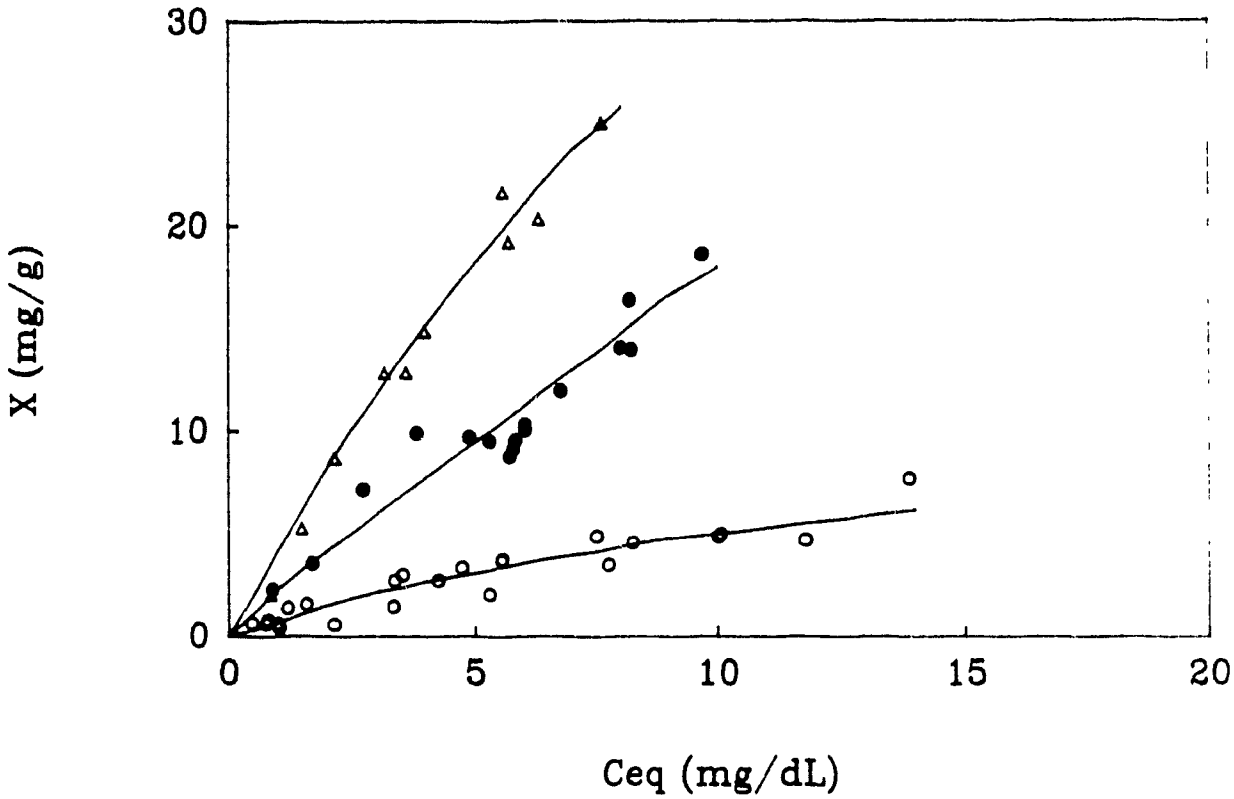

Figure 3.14a Isotherms (T = 20°C) for the adsorption of glycocholic acid by the polyacrylamide backbone of different substitution. P_2-T, Δ 1.403; P_2-A, ● 0.3580; P_1-A, ○ 0.241 mmol/g.

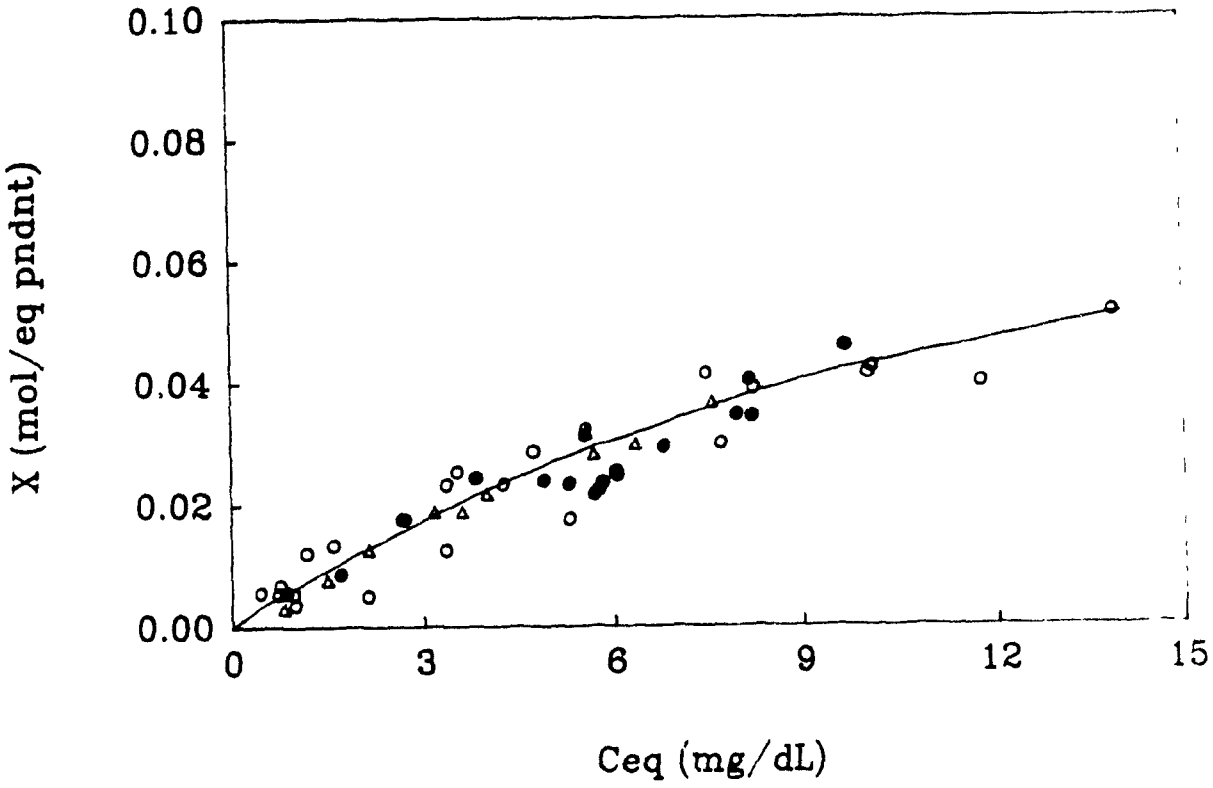

Figure 3.14b Isotherms (T = 20°C) for the adsorption of glycocholic acid by polyacrylamide backbone of different substitution. P_2-T, Δ 1.403; P_2-A ● 0.3580; P_1-A ○ 0.241 mmol/g

Therefore, as the substitution is increased the resins adsorb greater amounts of bile acids on a weight basis, but the adsorption per active site remains the same.

3.2.4 Hydrophobic Backbones

The previous results give strong evidence for the importance of hydrophobic interactions in the binding of bile acids by polymeric resins. To consider this effect further the backbone was changed from hydrophilic to hydrophobic. In these experiments, 4-(aminomethyl)benzoic acid was coupled to the Merrifield resin (polystyrene cross-linked with divinyl benzene) (1 mmol/g), to form resin M_{f1}-S-C-Ph-M-A. The extent of adsorption of sodium glycocholate by this hydrophobic resin was too small to measure. Similarly, the resin M_{f1}-S-C-M-Ph-A, produced by coupling of 4-aminophenylacetic acid, adsorbed only negligible quantities of glycocholic acid.

In the aqueous Tris-HCl, the Merrifield resin swells very little when compared to the polyacrylamide backbone; the latter swell extensively. Therefore, the decrease in the adsorption capacity may be due to poor accessibility to the binding sites, since a low swellability makes it more difficult for the bile acid anion to enter the resin.

When the Merrifield resin of higher functionality (1.44 mmol/g resin) was used as backbone, and 4-(aminomethyl)benzoic acid was coupled to it to form the resin M_{f2}-C-Ph-M-A, the primary amine form still did not adsorb measurable amounts of sodium glycocholate. However, when it was quaternized to form M_{f2}-C-Ph-M-Q, the adsorption could be quantified, but the capacity was only about 0.01 mol/eq pndnt (Figure 3.15).

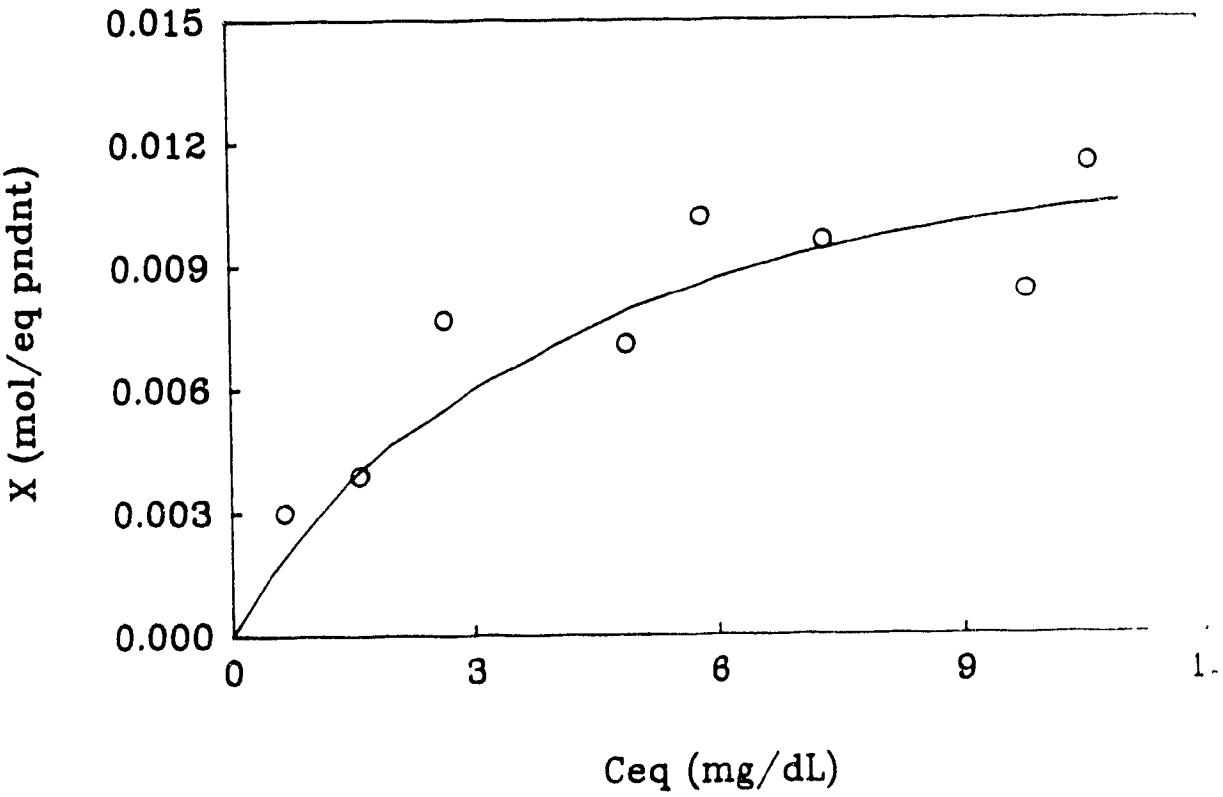

Figure 3.15 Isotherm (T = 20°C) for the adsorption of glycocholic acid by M_{f2}-C-Ph-M-Q

Therefore, it would appear that for the hydrophobic Merrifield resin, the ion-exchange occurs only with difficulty; for quantification purposes a higher number of active sites per gram of resin is required.

3.2.5 Comparison Between Buffer Solutions

The resin P_1-C-M-Ph-Q produced by coupling 4-aminophenylacetic acid to the polyacrylamide backbone (0.241 mmol/g resin), was tested for its capacity to adsorb glycocholic acid in Tris-HCl (0.0026 M, pH 7) and in phosphate buffer (0.0025M, pH 7) (Figure 3.16). There is a slight, but significant decrease in adsorption of glycocholate in the phosphate buffer. As mentioned in Section 2.2.1, this may be due to the phosphate ions competing with the bile acid anions in the interaction with the quaternary ammonium group of the pendant.

The adsorption by the resin P_1-S-C-Ph-M-Q, i.e., the polyacrylamide backbone to which is coupled ala_3 and 4-(aminomethyl)benzoic acid, was studied using glycocholic acid in Tris-HCl (0.0028 M, pH 7) and water (Figure 3.17). The adsorption of glycocholic acid from water is considerably greater than from the buffer. Again, as mentioned in Section 2.2.1, when the adsorption medium is water, no other ion interactions compete with the interaction of the glycocholic anion with the quaternary ammonium group of the resin.

3.2.6 Comparison Between Bile Acids

The isotherm for the adsorption of cholic acid by the quaternized polyacrylamide backbone, P_1-Q, is slightly higher than that for glycocholic acid (Figure 3.18). Since cholic acid is less polar, it will interact more strongly with the resin than will glycocholic acid. Furthermore, because of the higher water solubility of glycocholate less is adsorbed.

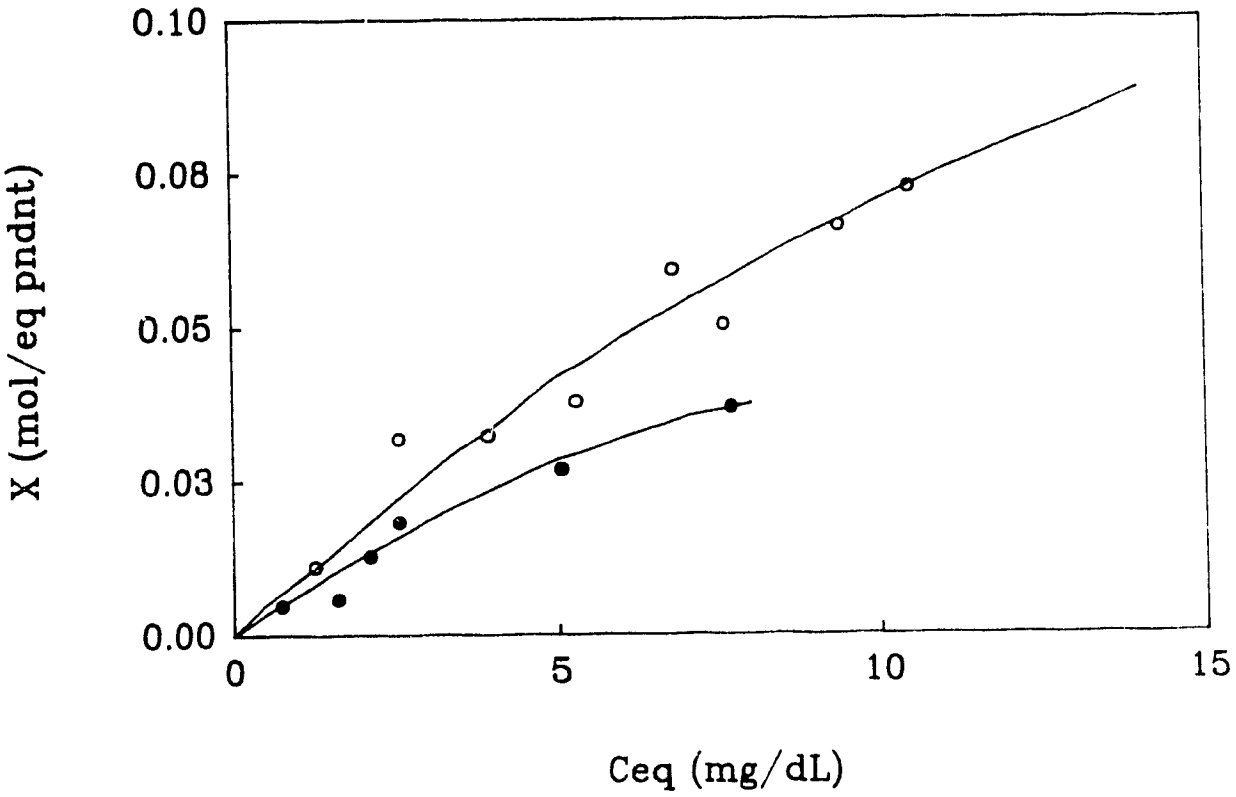

Figure 3.16 Isotherms (T = 20°C) for the adsorption of glycocholic acid by P_1-C-M-Ph-Q, in Tris-HCl (0.0026M) ○ and phosphate buffer (0.0026M) ●

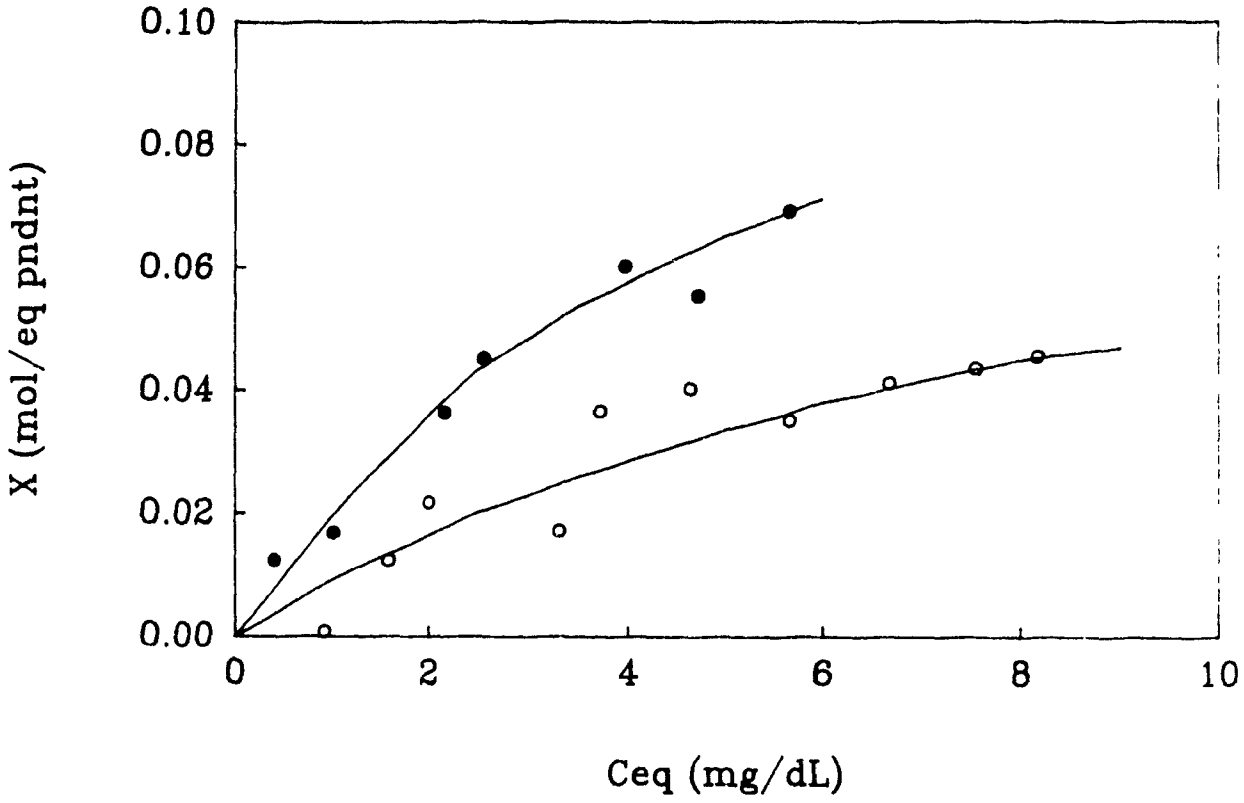

Figure 3.17 Isotherms (T = 20°C) for the adsorption of glycocholic acid by P_1-S-C-Ph-M-Q, in Tris-HCl ○ and water ●

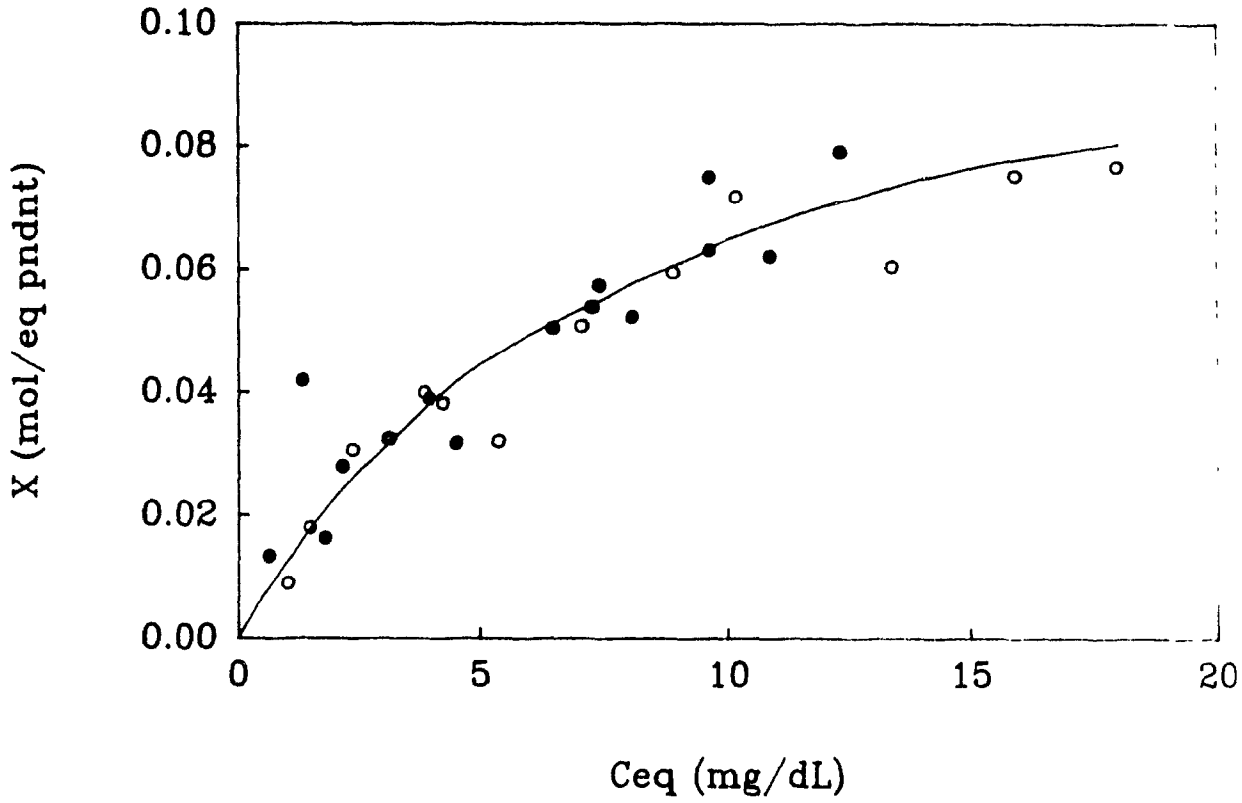

Figure 3.18 Isotherms (T = 20°C) for the adsorption of different bile acids by P_1-Q; ○ glycocholic acid; ● cholic acid

3.3 SUMMARY

The results presented in this chapter describe the effects of systematic changes of the chemical composition of cholestyramine-like sorbents on their capacity to adsorb bile acids. These changes include a change from a hydrophobic to a hydrophilic backbone; the incorporation of an ala_3 spacer between the backbone and the active site; changes in the position of the methylene group from being between the phenyl group and the amino group to being between the phenyl group and the carbonyl group, thus affecting the basicity of the amino group; and change of the primary amino group to a quaternary ammonium group, which also affects the basicity of the active group.

3.3.1 Comparison with Cholestyramine

The striking, and probably most important, result of these experiments is that all of the synthesized resins have a lower capacity for the adsorption of bile acids than does cholestyramine, under similar experimental conditions. For the synthesized resins, the most effective adsorption was obtained with resins consisting of the polyacrylamide backbone bearing the same pendant as cholestyramine, 4-(aminomethyl)benzoic acid, P_1-C-Ph-M-Q, (0.1 mol/eq pndnt). However, the extent of binding, measured on a molar basis, is only 15% that of cholestyramine.

Originally it was thought that a cholestyramine-like active site attached to a hydrophilic backbone would result in a sorbent with an increased adsorption capacity for bile acids, since the resin should be more compatible than cholestyramine with the aqueous environment. Although the polyacrylamide had a low substitution (0.241 mmol/g resin), it was thought that each active site would still adsorb a bile acid molecule. However, these resins have a much lower capacity for bile acids.

3.3.2 Experimental Results

Although the hydrophilic polyacrylamide that was used was extensively swollen in the aqueous solution, it was a highly cross-linked (11%). As cross-linking is increased, diffusion within the resin becomes more difficult (7); indeed, the diffusion paths can become so small that the entry of large ions is prohibited. Therefore, although the hydrophilic backbone may be more biocompatible, its capacity to adsorb bile acids may be limited as a result of the high degree of cross-linking, so that the bile acid anion cannot enter the resin to displace the counter-ion.

The resins with the hydrophobic Merrifield backbone might be expected to show adsorption characteritics similar to that of cholestyramine. However, in actual fact, they adsorbed only very small amounts of bile acids; too little to be quantified by HPLC. They exhibited minimal swelling in an aqueous environment, almost not being wet. Such behaviour in the aqueous adsorption medium accounts for the low adsorption capacities for the glycocholate anion.

The ion-exchange process was confirmed by the adsorption isotherms obtained for the hydrophilic resins for which the position of the methylene group was changed (Figure 3.6). The removal of the methylene group between the benzene group and the primary amino group significantly decreased the adsorption capacity. When the amino group is attached directly on the benzene ring the positive charge from the protonated amino group can be stabilized by the aromatic ring, making the amino group less basic. The lower basicity decreases the extent of the interaction with the counter-ion as well as with the bile acid anion and the ion-exchange process becomes less effective. However, when the methylene group is between the benzene ring and the primary amino group (Figure 3.9), the active site is more basic, favouring the electrostatic interaction with anions.

The addition of the ala_3 spacer between the backbone and the benzylammonium group consistently decreased the adsorption capacities of those resins (Figures 3.5, 3.6). When the structure of cholestyramine is examined it can be seen that the active group is attached directly onto the backbone. It would appear that the spacer is not required for the ion-exchange process. In fact the spacer has an inhibiting effect, perhaps due to a decrease in the space available inside the resin pores which makes it more difficult for the bile acid anion to penetrate the matrix and displace the counter-ion.

The results show that the adsorption of bile acids by the quaternary ammonium group is superior to that by primary amines. The quaternized resins have higher affinities for glycocholic acid than the corresponding unquaternized resins (Figures 3.8, 3.10-3.12), except in one case (Figure 3.9). At pH around 8-9 in the resin phase, which is a realistic value when the pH of the solution is 7, the unquaternized resins may be incompletely protonated, i.e., some of the primary amino groups, $-NH_2$, would be present. In this case, the non-protonated pendants would not be involved in the ion-exchange process, decreasing the capacity of adsorption. This would confirm that the adsorption of bile acids by cholestyramine is primarily an ion-exchange process.

When the adsorption is done with different buffers, the trends observed with the polyacrylamide resins are similar to those seen for cholestyramine. For the resin consisting of a polyacrylamide backbone with 4-aminophenylacetic acid as pendant, P1-C-M-Ph-Q, adsorption of glycocholic acid in phosphate buffer (Figure 3.16) was about half the adsorption from the Tris-HCl, a decrease similar to that observed with cholestyramine (Figure 2.2). This decrease in the extent of adsorption is due to the presence of phosphate anions which compete with the bile acid anions for the quaternary ammonium group.

The adsorption of glycocholic acid by the polyacrylamide backbone bearing the ala_3 spacer and 4-(aminomethyl)benzoic acid, P_1-S-C-Ph-M-Q, was done in water and Tris-HCl (Figure 3.17). As observed for cholestyramine (Figure 2.2) the adsorption in water increased faster with increasing Ceq than for Tris-HCl due to the absence of any ionic species other than glycocholic acid and the resin with its fixed ionic groups and the counter-ion.

When the adsorption of cholic and glycocholic acids by the quaternized polyacrylamide resin, P_1-Q, (0.241mmol/g resin) are compared, similar affinity is indicated for these two bile acids, as was also reported for cholestyramine (Figure 3.18). From a first look, it might have been expected that the hydrophilic backbone would adsorb more glycocholate since it is more hydrophilic than cholic acid. However, since the interaction between the bile acid and the resin is an ion-exchange process, interactions with the backbone are of minimal importance, which is confirmed by the present results.

From all of the above results, it can be said that cholestyramine so far appears to be the bile acid-binding resin of choice. The results confirm that the interaction between the bile acids and cholestyramine involves an ion-exchange process.

3.4 REFERENCES

1. G. Lajoie, F. Lepine. S. Lemaire, F. Jolicoeur, C. Aube, A. Turcotte and B. Belleau, *Int. J Pept. Protein Res.*, **24**, 316, 1984
2. D.S Henning, G.A. Lajoie, G.R. Brown, L.E. St-Pierre and S. St-Pierre, *Int. J. Artif. Organs*, **7**, 209, 1984
3. E. Kaiser, R.L. Colescott, C.D. Bossinger and P.I. Cook, *Anal. Biochem* , **34**, 595, 1970
4. J.M. Stewart and J.D. Young, **Chap 2, Laboratory Techniques in Solid Phase Peptide Synthesis**, p71, in *Solid Phase Peptide Synthesis*, 2nd edition, Pierce Chemical Company, Rockford, Illinois, 1984
5. B.F. Gisin, *Anal. Chim. Acta*, **58**, 248, 1972
6. F.C.M. Chen and N.L. Benoiton, *Can. J. Chem.*, **54**, 3310, 1976
7. The Dow Chemical Company, **Chap 1, Principles of Ion-Exchange**, in *Dowex:Ion-Exchange*, The Lakeside Press, R.R. Donneley and Sons Co., USA, 1958

4 MOLECULAR MODELLING OF THE INTERACTIONS BETWEEN BILE ACIDS AND ION-EXCHANGE RESINS

Recently spectacular advances have been made in interactive three-dimensional computer graphics. It allows the visualization of three dimensional structures of chemical compounds as well as the determination of the most favoured conformation as determined from energy calculations. The model can then be extended to determine how interactions take place between molecules. Using computer graphics, it becomes possible to present hypotheses concerning the modes of interaction between ligands and substrates, such as macromolecules, enzymes, proteins. Therefore, the principal use of a three-dimensional computer program is as a predictive tool.

The three-dimensional structure obtained from computer graphics can be compared with X-ray crystallography data. Programs developed recently also permit the crystallographic data to be entered directly to obtain a comparable conformation of the chemical compound.

Computer graphics programs have found widespread applications in various fields of chemistry, such as organic chemistry (1) where it is used to predict the stereochemical outcome of a reaction; in medicinal chemistry where it is used to study drug-receptor site interactions (2); and in protein chemistry where active sites of enzymes can be identified (3-5).

The most interesting aspect of computer modelling programs is the prediction of the interactions between molecules. It is this which was of interest for the present study, since it was expected that it would be possible to give a qualitative treatment to the adsorption of bile acids by ion-exchange resins and make possible the design of efficient adsorbents for bile acids. As pointed out in

Chapter 2, it is of interest to determine what are the interactions, other than electrostatic, between the bile acids and the active sites on the polymer, and between the bile acid molecules bound at adjacent sites.

4.1 ENERGY MINIMIZATION

Before describing the program used in the present study and the results, a brief survey about energy minimization is presented.

Upon entering a structure into computer graphics, it is important to obtain the "best" conformation of a particular chemical compound. When crystallographic data are available, the task of obtaining the "best" conformation is made easier because it has already been resolved. However, for chemical structures which have not been resolved previously, it tends to be more difficult.

Therefore, a chemical structure is entered and energy minimization calculations are used to obtain the molecular conformation of minimum internal energy. The chemical structure can then be modified, either by changing bond angles or torsion angles, and re-minimized to obtain another energy value. The structure with the lowest energy is considered to be the most stable conformation. Upon entering a chemical structure it is important to predict which structure could be favoured, which requires chemical intuition.

The modern computer programs for modelling are capable of calculating the energy for each conformation. The minimization process is one by which the conformation is modified and the internal energy is re calculated after each modification. Energy minimization is attained when the energy converges to a minimum.

The energy calculated for each iterative step represents the overall contribution to the potential energy ($f(x) = E_s$) as a function of molecular deformation from an arbitrary reference geometry. It can be expressed as:

$$f(x) = E_s = \sum K_b(b-b_o)^2 + \sum K_\theta(\theta-\theta_o)^2 + \sum K_\phi\{1-\cos(n\phi + \delta)\} + \sum \varepsilon\{(r_o/r)^{12} - 2(r_o/r)^6\} + \sum q_i q_j/D_r + \sum f_{HB}(r,\theta)$$

(Equation 4.1)

The terms relate to the bond length, the bond angle, the torsion angle, the non-bonded pairs, the partial charges and the hydrogen-bond contributions to the energy, respectively; b and b_o are the new bond length after deformation and the bond length at equilibrium, respectively; θ and θ_o are the new bond angle and the bond angle at equilibrium, respectively; ϕ is the torsion angle, n the periodicity and δ is the phase; r_o and r are distances between non-bonded atoms involved in Van der Waals interactions, at equilibrium and after deformation, respectively; q_i and q_j are the charges of atoms i and j, respectively, and D_r is the dielectric constant; f_{HB} is a function of the potential energy in hydrogen-bonding, which depends on the bond angle and the distance between the atoms. K_b, K_θ, K_ϕ and ε are force constants (6, 7). Therefore, to achieve an energy minimization, the computer program calculates the energy for the initial conformation, the structure is then modified and the energy is re-calculated. This sequence of operations is repeated until the conformation of minimum energy is obtained.

The most commonly used methods of energy minimization are the method of "steepest descent" and the "conjugate gradients" method (6). Each uses the energy value and the vector of the energy first derivative (the force). The second method also uses the second derivative of the energy to compute a new conformation which is expected to be of lower energy. By repeating the procedure iteratively, it is expected that eventually a structure will be obtained for which no small change of conformation leads to a lower energy.

The "steepest descent" method is based on the position of the atoms and the corresponding energy. Once the energy is quantified, the atoms are changed

to a new position and energy calculations are done again. The change in position is done according to Equation 4.2:

$$x_{i+1} = x_i - \alpha f'(x) \qquad \textbf{(Equation 4.2)}$$

where x_i is the original position of a particular atom, x_{i+1} is its new position, α is the step-length and f'(x) is the force, which can be expressed by Equation 4.3:

$$f'(x) = \partial f(x)/\partial x \qquad \textbf{(Equation 4.3)}$$

Then the energy of the molecular conformation is calculated with the coordinates corresponding to the initial trial geometry.

The "steepest descent" method calculates the energy of a particular conformation, modifies it and re-calculates the energy. This procedure is repeated until the energy minimum is obtained. As the conformation of the molecule is approaching the minimum energy, i.e., the minimum in the f(x) curve of Figure 4.1, the force, f'(x), will approach zero. When:

$$f'(x) \longrightarrow 0,$$

then from Equation 4.2:

$$x_{i+1} \longrightarrow x_i$$

Therefore, as the minimum energy is approached the two conformations will become similar and the calculations are stopped before the "true minimum" is attained, since the method is not able "to see" the difference. This represents a disadvantage of the "steepest descent" method. However, the conformation obtained by this method is close to the actual conformation of minimum energy.

For the conjugate gradients method (9), the following equation is applied:

$$x_{i+1} = x_i - \alpha_i p_i \qquad \textbf{(Equation 4.4)}$$

where α_i is chosen to get to the minimum energy along the search direction; p_i represents a specified direction along the force curve and is related to the gradient of the force $f''(x_i)$ (Figure 4.1) by Equation 4.5:

$$p_i = f''(x_i) + \beta_{i-1} p_{i-1} \qquad \textbf{(Equation 4.5)}$$

where:

$$f''(x_i) = \partial f'(x_i)/\partial x_i \qquad \textbf{(Equation 4.6)}$$

and:

$$b_{i-1} = (f''(x_i))^2/(f''(x_{i-1}))^2 \qquad \textbf{(Equation 4.7)}$$

As the energy minimum is approached, the gradient of the force $f''(x)$ (Figure 4.1) will become equal from one step to the other (Δx approaches zero), leading to $\beta_{i-1} = 1$:

$$p_i = f''(x_i) + p_{i-1} \qquad \textbf{(Equation 4.8)}$$

As the minimum is approached:

$$\Delta x = 0 \qquad \textbf{(Equation 4.9)}$$

From Equation 4.4:

$$\Delta x = -\alpha_i p_i \qquad \textbf{(Equation 4.10)}$$

and from Equation 4.8:

$$\Delta x = \alpha_i f''(x_i) - \alpha_i p_{i-1} = 0 \qquad \textbf{(Equation 4.11)}$$

Then:

$$f''(x_l) = p_{l-1} \qquad \textbf{(Equation 4.12)}$$

So it can be said that this minimization method will reach the minimum energy when the direction p down the energy gradient equals the tangent on the same energy gradient.

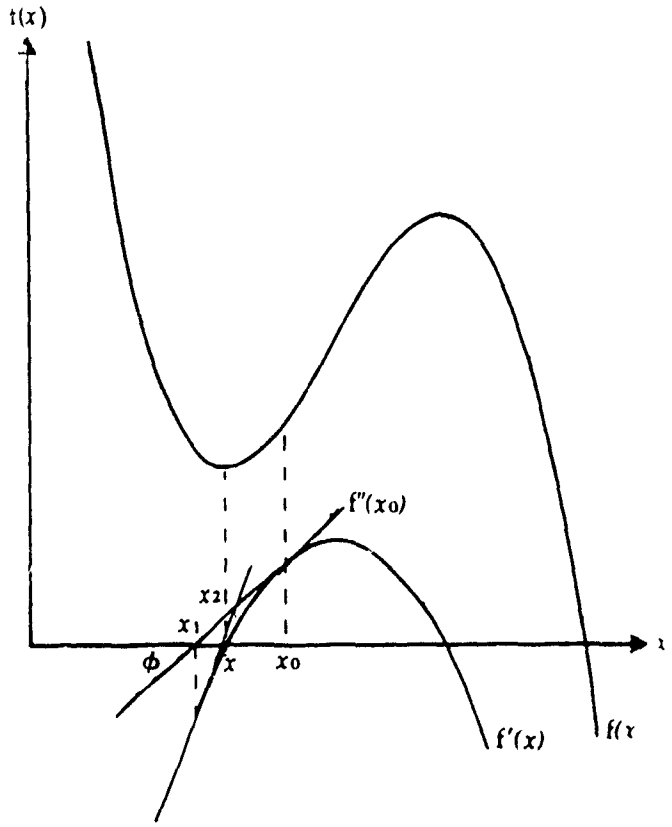

Figure 4.1 Representations of the energy plot f(x), its first (f'(x)) (force) and second (f''(x)) derivative (8)

The program which was used in the present study, Alchemy II®, uses the conjugate gradients method for minimization.

4.2 ALCHEMY II®

The molecular modelling program Alchemy II® was purchased from Tripos Associates Inc., a subsidiary of Evans and Sutherland. This program was used on a IBM-compatible AT-PC with a mathematical co-processor.

This program (11, 12) allows the construction of three-dimensional models of molecules from single atoms, chemical groups and molecular fragments, giving rise to a structure represented by the Dreiding model. A reasonable molecular conformation can be obtained with an energy minimization procedure which utilizes the conjugate gradients method. The conformation can be viewed as the Dreiding, the ball and stick, or the space-filling model. It determines the presence of chiral centers and can modify the bond length of the molecule, the bond angles and the dihedral angles. Crystallographic data can be entered directly. It can fit a series of molecules to one another with a least-squares fitting routine and then compare molecular geometries. Molecules can be moved one relative to the other to manually fit them.

For the present study, the bile acid molecules, cholic and glycocholic acids, were modelled. For cholic acid, the crystallographic data (13) were entered, and the conformation of minimum energy was obtained. The model for glycocholic acid was obtained by modifying that for cholic acid by adding the glycine group, and the conformation of minimum energy was obtained. The pendants of the polymer resins were modelled using a nine-carbon backbone, and each was minimized, modified and re-minimized so as to obtain the conformation of lowest energy. For cholestyramine, which has an active site at every second benzene ring, two pendants were also examined.

4.3 MOLECULAR MODELLING

4.3.1 Bile Acids

Figures 4.2 and 4.3 show the conformations of lowest energy for cholic and for glycocholic acid. Energy minimization results in conformations of similar energy (Table 4.1), which is expected since the only difference between the two is the glycine group on the side chain of glycocholic acid. These models clearly indicate that one "face" of the bile acid is hydrophobic, with the protruding methyl groups at position 18 and 19. The more polar groups, the hydroxyl and the carboxylic acid groups, are gathered on the other side making it more hydrophilic. From the space-filling models it is apparent that, for glycocholic acid, the hydrophilic "cavity" is more compact, i.e., more closed, due to the longer side chain which directs the carboxylic acid group towards the hydrophilic cavity. This is confirmed by the measured distances between the hydroxyl groups of the hydrophilic face of glycocholic acid and cholic acid (Table 4.2), with the distance between O_1, attached to carbon-3, and O_4, of the terminal carboxylic acid, decreasing from 9.32 Å for cholic acid to 5.66 Å for glycocholic acid.

4.3.2 Polyacrylamide Resins

Of the synthesized resins, those prepared with the polyacrylamide backbone always had greater adsorption capacity for bile acid than those with the Merrifield backbone. Therefore, for the purpose of molecular modelling, only the hydrophilic resins will be considered.

Figures 4.4 shows the conformation of lowest energy for the quaternary 4-(aminomethyl)benzoic acid attached directly to the hydrophilic polyacrylamide backbone, i.e., the model for the resin P_1-C-Ph-M-Q. The polyacrylamide backbone (P) is represented by a nine-carbon chain onto which are attached

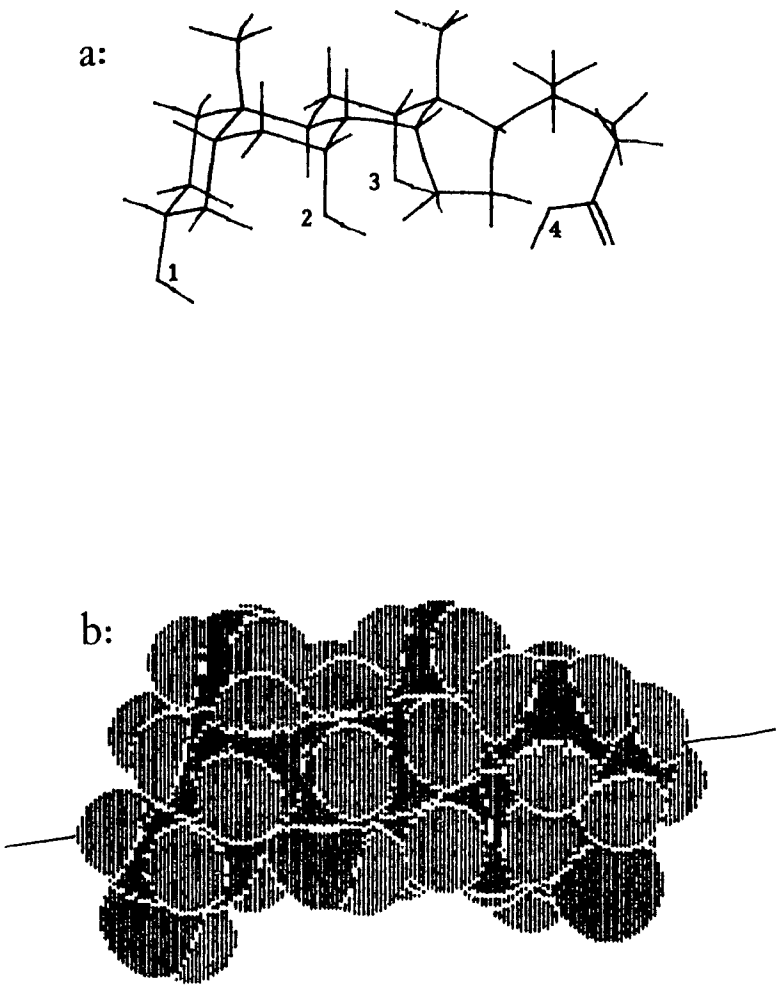

Figure 4.2 Conformation of cholic acid shown as a)the Dreiding model and b)the spacefill representation. (black:carbon, blue:hydrogen, red:oxygen)

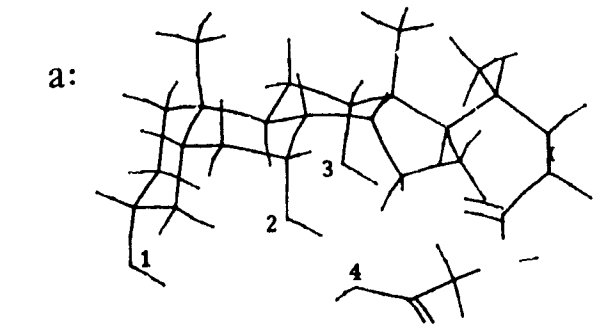

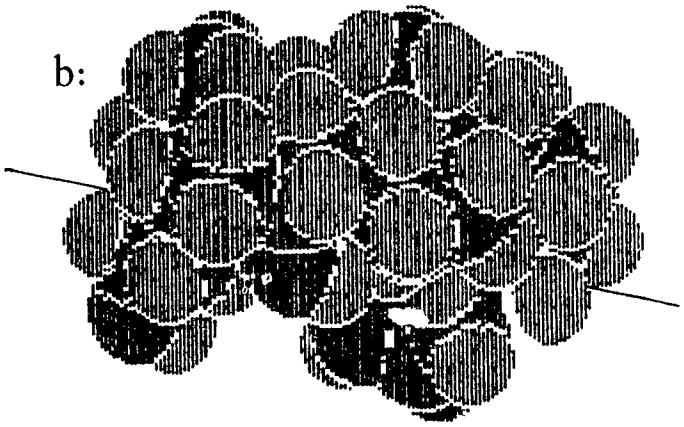

Figure 4.3 Conformation of glycocholic acid shown as a)the Dreiding model and b)the spacefill representation. (black:carbon, blue:hydrogen, red:oxygen, yellow:nitrogen)

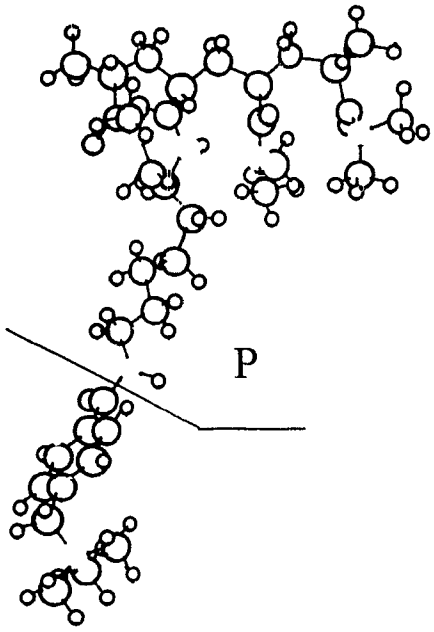

Figure 4.4 Conformation of the pendant containing the quaternary 4-(aminomethyl)benzoic acid shown as the ball and stick representation. (black:carbon, blue:hydrogen, red:oxygen, yellow:nitrogen; P: backbone)

Table 4.1 Potential Energy of the Minimized Conformations of Bile Acids and the Models for Ion-Exchange Resin Pendants

Name	Energy (kJ/mol)
Cholic Acid	-164
Glycocholic Acid	-164
\-CO-C_6H_4-$CH_2N^+(CH_3)_3$	-47.7
\-CO-CH_2-C_6H_4-$N^+(CH_3)_3$	-51.5
\-ala_3-CO-C_6H_4-$CH_2N^+(CH_3)_3$	-57.7
\-ala_3-CO-CH_2-C_6H_4-$N^+(CH_3)_3$	-59.8
Cholestyramine-1 pendant	-52.3
Cholestyramine-2 pendants	-392

Table 4.2 Distances (in Å) between the Hydroxyl Groups of Bile Acids

	Cholic Acid	Glycocholic Acid
O_1-O_2	6.03	4.79
O_1-O_3	4.80	5.76
O_1-O_4	9.32	5.66
O_2-O_3	4.69	4.36
O_2-O_4	3.68	4.82
O_3-O_4	7.39	2.95

O_1: attached to C3
O_2: attached to C7
O_3: attached to C12
O_4: attached to the carbonyl group of the side chain

acrylamide groups at C-2, C-6 and C-8. The active group is coupled to N-acryl-1,6-diaminohexane attached at C-4. The potential energies for the structures representing the various resins are also given in Table 4.1.

The quaternary 4-(aminomethyl)benzoic acid active site extends approximately 14 Å beyond the acrylamide units of the backbone. The addition of an ala_3 spacer (S) not only makes the pendant longer (to ca. 22 Å) but takes away the linearity of the pendant, i.e., it tends to become curved (Figure 4.5). Indeed the model of the ala_3 spacer alone attached to the backbone is also non-linear (Figure 4.6). As a consequence, the incorporation of the ala_3 in the resin can result in entanglements of the pendant. It may also cause the accessible volume in the resin to be diminished, thus limiting the access of bile acid to the inside of the resin. Finally, comparison of Figures 4.4 and 4.5 shows that the pendant with the ala_3 spacer has a considerably more polar nature, thus is more hydrophilic, and this may be critical. This was not anticipated, as indicated by the previous discussion (Section 3.3.2) regarding the spacer. These features may contribute to the low adsorption capacities of these resins.

The acrylamide groups and the pendant are shown as lying on the same side of the backbone. When they were alternated, i.e., as one up and one down, a conformation of higher energy (-253 as compared with -329 kJ/mol) is obtained. Thus, the preferred conformation is expected to have the acrylamide groups and the pendant on the same side of the backbone. Evidently, the lower energy results from pendant-pendant interactions which are probably disrupted on binding of bile acids. This will be considered in more detail later.

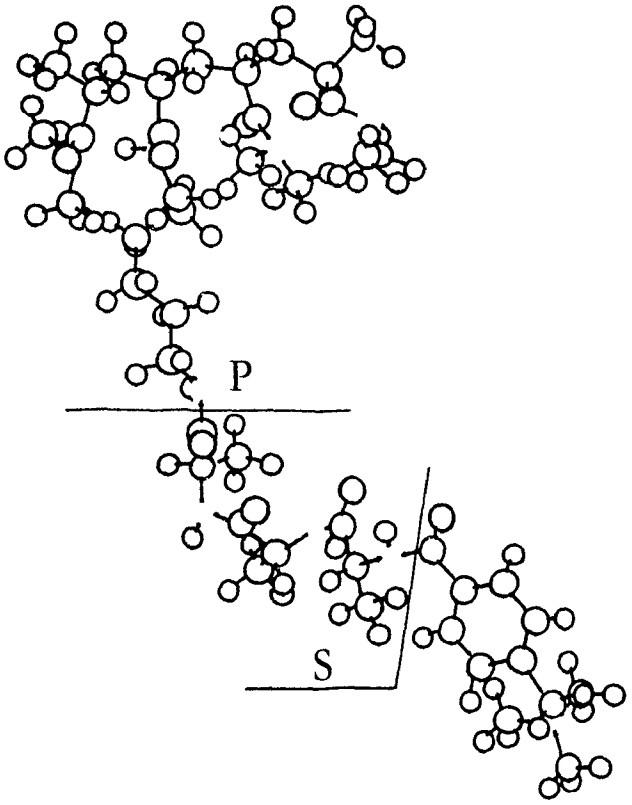

Figure 4.5 Conformation of the pendant containing the quaternary 4-(aminomethyl)benzoic acid and the ala_3 spacer shown as the ball and stick representation. (black:carbon, blue:hydrogen, red:oxygen, yellow:nitrogen; P:backbone, S:ala_3)

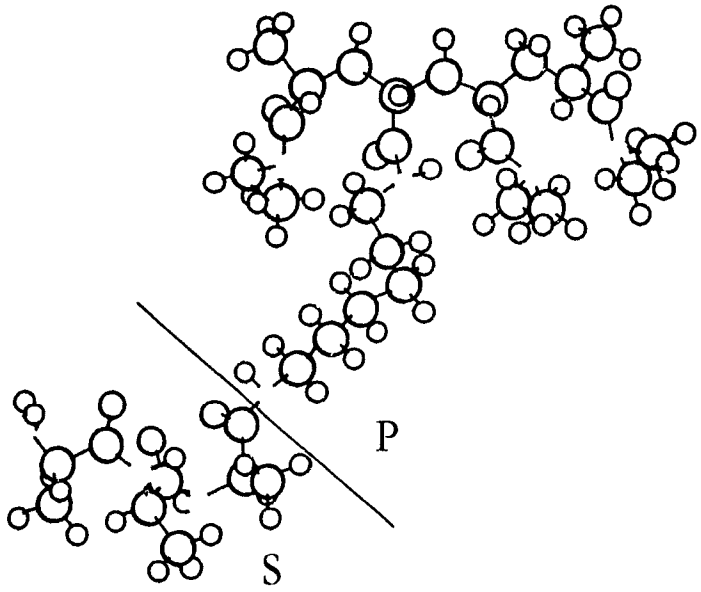

Figure 4.6 Conformation of the pendant containing the ala_3 spacer shown as the ball and stick representation. (black:carbon, blue:hydrogen, red:oxygen, yellow:nitrogen; P:backbone, S:ala_3)

4.3.3 Cholestyramine

The model of the cholestyramine adsorbent was made with a backbone consisting of eleven carbons to which is attached either one or two pendants. Figure 4.7 shows cholestyramine with two pendants. Energy minimization of the two structures indicates an energy difference of 339 kJ/mol, with the two pendant model being of lower energy (Table 4.1). For the model with two pendants the phenyl groups can align themselves, a conformation which adds extra stability. The conformation that has the two adjacent phenyl groups on opposite sides of the backbone has a higher energy, -321 kJ/mol, i.e., the alignment of the phenyl groups results in a stabilization, by 71 kJ/mol. Therefore, it would be expected that adjacent phenyl groups of cholestyramine would tend to align themselves.

This is of considerable importance since this conformation offers little space between phenyl groups for adsorbate molecules to enter and interact with the phenyl rings, especially large adsorbate molecules such as bile acids. This suggests that there is probably little interaction between the bile acid hydrophobic face and the phenyl group of the pendant. The main interaction of adsorbate with the quaternary amines is ionic, although other interactions between adsorbed molecules contribute to the binding process.

4.4 MODELLING OF THE INTERACTION BETWEEN BILE ACIDS AND ION-EXCHANGE RESIN PENDANTS

It was of interest to use the structures that resulted from energy minimization to obtain insight concerning the interactions between the bile acids and the pendants. In Chapter 2, it was proposed that an electrostatic interaction between the negatively charged carboxylic acid group of the bile acid and the

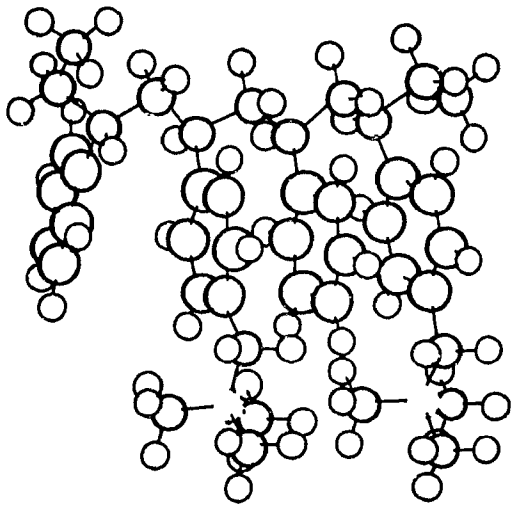

Figure 4.7 Conformation of cholestyramine with two active sites shown as the ball and stick representation. (black:carbon, blue:hydrogen, yellow:nitrogen)

positively charged quaternary ammonium group of the resin is the main driving force for binding. Unfortunately, the program used for modelling cannot make energy minimization calculations for two molecules with respect to each other or of one with respect to the other, i.e., it does not permit one molecule to be at a fixed conformation (e.g., the pendant), while energy minimization is achieved by moving the other one (e.g., the bile acid) relative to the first. Therefore, as a first approximation, calculations were made after forming a chemical bond between both the pendant and the bile acids, to determine the conformation of minimum energy for the new structure. This should allow a prediction of the probable three-dimensional position of the two molecules with respect to one another.

4.4.1 Modelling of the Interaction using a Chemical Bond between the Ion-Exchange Resin Pendant and the Bile Acid

4.4.1.1 Cholestyramine

The first set of interactions were modelled by forming a bond between the quaternary ammonium group of the cholestyramine pendant and the carboxylic acid group of the bile acid ($-N^+(CH_3)_2$-O-CO-) to represent cholestyramine interacting with cholic acid. The resulting conformation of minimum energy has the bile acid lying perpendicular to the pendant (Figures 4.8). This is a rather unexpected arrangement for these two molecules. Because cholestyramine has one active site, i.e., one quaternary amine at every second benzene ring, the bile acid molecules bound at adjacent sites would be one onto the other. However, attempts to find another minimum by rotating the bile acid and re-calculating the conformation of minimum energy, again resulted in a conformation with the bile acid perpendicular to the cholestyramine pendant. Indications are that, at least when there is sufficient space, the cholic acid molecules tend to face the polymer backbone.

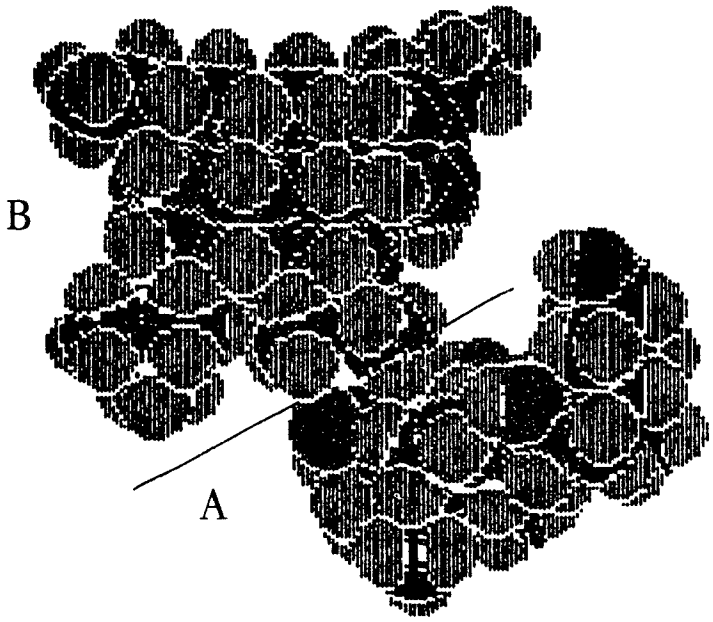

Figure 4.8 Conformation of the interaction of A)cholic acid with B)cholestyramine with two pendants shown as the spacefill representation. (black:carbon, blue:hydrogen, red:oxygen, yellow:nitrogen)

For glycocholic acid, which has a longer side-chain that is curved towards the inside of the cavity, formation of the bond between the quaternary ammonium group and the bile acid carboxylic acid group results in a conformation such that the bile acid molecule tends to be curved towards the pendant (Figure 4.9). As mentioned above, such conformation is limited to low coverage. The weakness of these calculations lies in the inability to include interactions between bile acid molecules bound at adjacent sites. As discussed in Chapter 2, these are probably of considerable importance.

4.4.1.2 Synthesized Resins

The modelling studies using bile acid chemically bonded to the quaternary amine were also made for the interactions of cholic acid with the pendant having the quaternary 4-(aminomethyl)benzoic acid. These also show that the bile acid tends to adopt a conformation perpendicular to the pendant (Figure 4.10), even after rotation of 90° of the N-O bond.

4.4.2 Modelling of the Interaction Between the Ion-Exchange Pendant and the Bile Acid

It appears that forming a bond between the bile acid and the pendant limits the position of the bile acid with respect to the pendant. Consequently, it may not give a true picture of the interactions which take place. The next set of models for the interactions between the bile acid and the ion-exchange resin pendants were obtained by manually placing the bile acid in various position with respect to the pendant.

4.4.2.1 Cholestyramine

Cholestyramine interacting with bile acid is limited by the available space in the vicinity of the active sites. At high coverage, the bile acid anion cannot lie

Figure 4.9 Conformation of the interaction of A)glycoholic acid with B)cholestyramine with two pendants shown as the spacefill representation. (black:carbon, blue:hydrogen, red:oxygen, yellow:nitrogen)

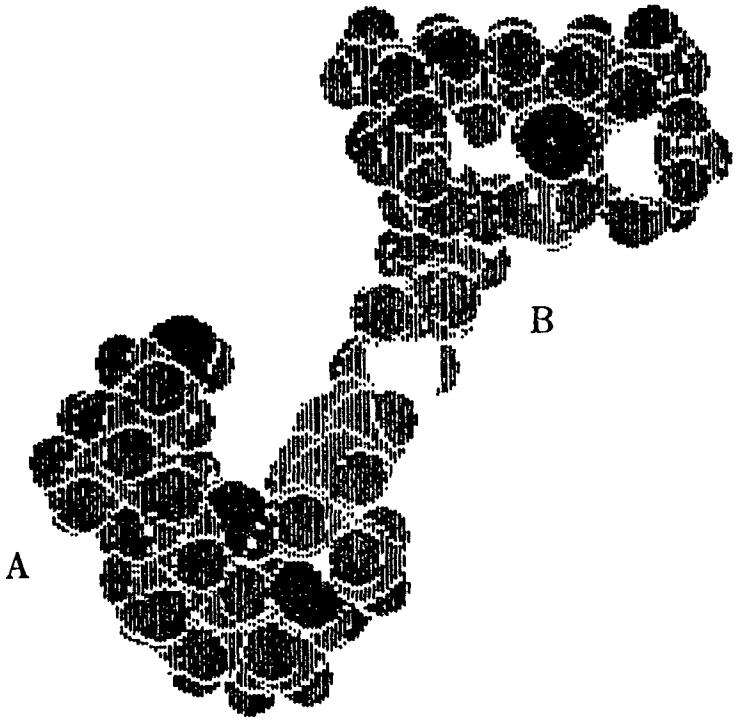

Figure 4.10 Conformation of the interaction of A)cholic acid with a B)synthesized resin pendant shown as the spacefill representation. (black:carbon, blue:hydrogen, red:oxygen, yellow:nitrogen)

perpendicular to the pendant since this would result in overcrowding of bile acid molecules on adjacent pendants. Furthermore, it cannot place itself so that the bile acid hydrophobic side interacts with the benzene group of the pendant due to the close proximity of the adjacent benzene groups (Section 4.4.1.1). Figure 4.11 shows a possible configuration for the bile acid, cholic acid, interacting with adjacent pendants of cholestyramine, at a coverage of one mole of bile acid per pendant. The two bile acid molecules can either be face to face (Figure 4.11) (hydrophilic sides) or back to back (hydrophobic sides) (Figure 4.12). The carbonyl oxygen of cholic acid are 7.59 Å apart and the hydroxyl groups at C_3 are 7.31 Å apart in Figure 4.11, giving rise to possible interactions between the bile acids, consistent with micelle formation. The same proximity is seen in Figure 4.12, the C_{18} methyl groups being separated by a distance of 4.32 Å.

It was seen earlier (Section 2.2.3) that at saturation cholestyramine (Cl) adsorbs both cholic and glycocholic acid by about 1.1 molecule per pendant. This model shows that proximity of the pendants would permit micelle formation which would favour the entry of bile acid in excess of the number of sites, agreeing with the experimental observations of the adsorption (Section 2.6.2.2). This model does not include any interaction between the benzene group of the cholestyramine pendant and the hydrophobic side of the bile acid, due to steric limitations between adjacent benzene groups of cholestyramine. Similar interactions are also expected with glycocholic acid.

4.4.2.2 Synthesized Resins

For the synthesized polyacrylamide resins, the substitution is not as high as for cholestyramine. Therefore the pendants are not as close to one another as they are for cholestyramine. Because there is more space between the pendants, interaction between the the pendant chain and the bile acid are possible. Figure 4.13 shows such an interaction between cholic acid and the pendant of the

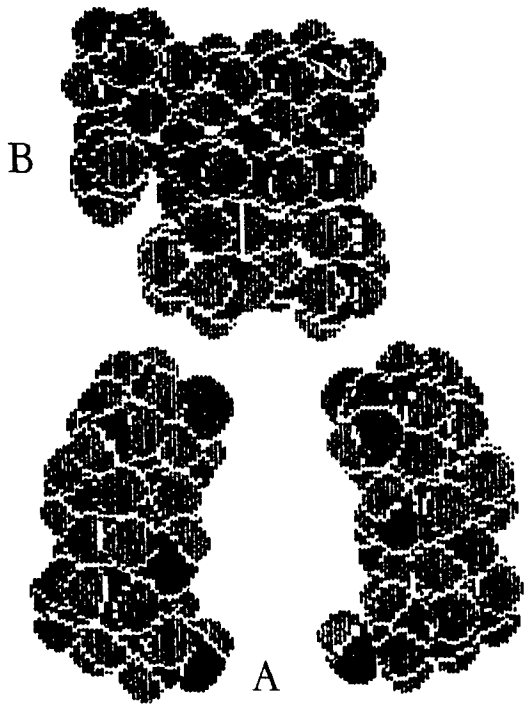

Figure 4.11 Conformation of the interaction of two A)cholic acid with B)cholestyramine with two pendants, shown as the spacefill representation. (black:carbon, blue:hydrogen, red:oxygen, yellow:nitrogen)

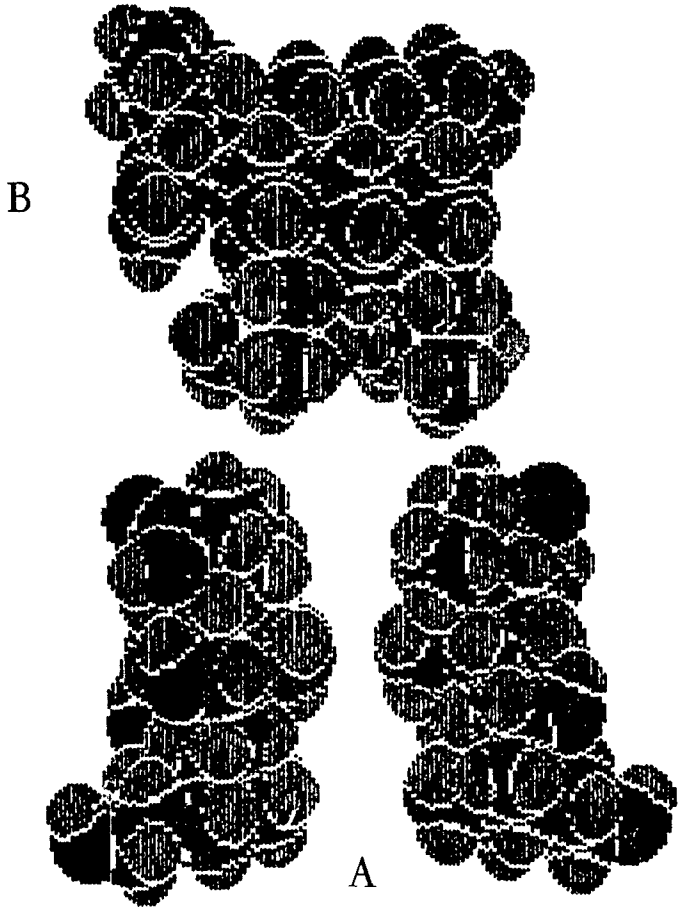

Figure 4.12 Conformation of the interaction of two A)cholic acid with B)cholestyramine with two pendants, shown as the spacefill representation. (black:carbon, blue:hydrogen, red:oxygen, yellow:nitrogen)

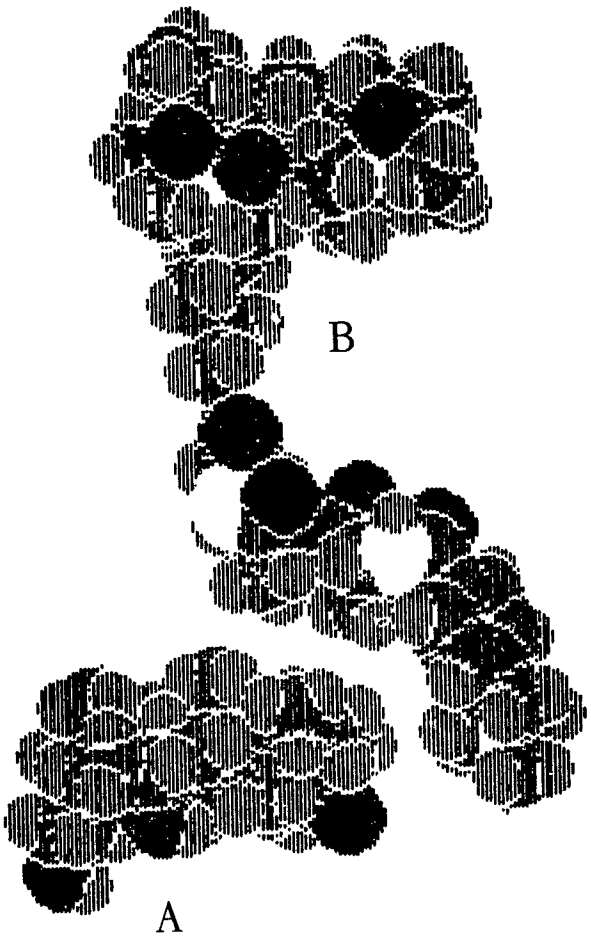

Figure 4.13 Conformation of the interaction of A)cholic acid with a B)synthesized resin pendant, shown as the spacefill representation. (black:carbon, blue:hydrogen, red:oxygen, yellow:nitrogen)

quaternary 4-(aminomethyl)benzoic acid, with the three alanine spacer. It shows the hydrophobic side of cholic acid in the vicinity of the ala_3 spacer methyl groups, giving rise to a possible hydrophobic interaction, and the quaternary ammonium group of the pendant with the carboxylic group of cholic acid, for the electrostatic interaction. Another possible conformation is shown in Figure 4.14 where the bile acid is placed perpendicular to the pendant of the quaternary 4-(aminomethyl)benzoic acid, without the ala_3 spacer. This could be possible since the pendants are not as close to one another as in cholestyramine. Figure 4.15 shows the bile acid being down the pendant, as proposed for cholestyramine.

As can be seen, for the synthesized resins the bile acid can move more freely since there is more space about the pendant. However, because of the high cross-linking, the accessibility to the active site is difficult. Similar interaction would be predicted for the other pendant. Interactions of glycocholic acid with the ion-exchange resin pendant, are also proposed to be similar to the ones for cholic acid.

4.5 SUMMARY

Proposed models for the interactions of bile acid with ion-exchange resin pendants have been presented in this chapter. First, it was noted that the cholestyramine pendants are close to one another and are separated by benzene rings, thus leaving little space between them to allow any bile acid to be interacting with the benzene rings. Therefore, the bile acid will be interacting with the quaternary ammonium group, leaving the bile acid inside the cavity. This allows the bile acid to interact with one another to form micelles. Micelle formation favours the transfer of bile acid from the external solution to the inside of the cholestyramine pores.

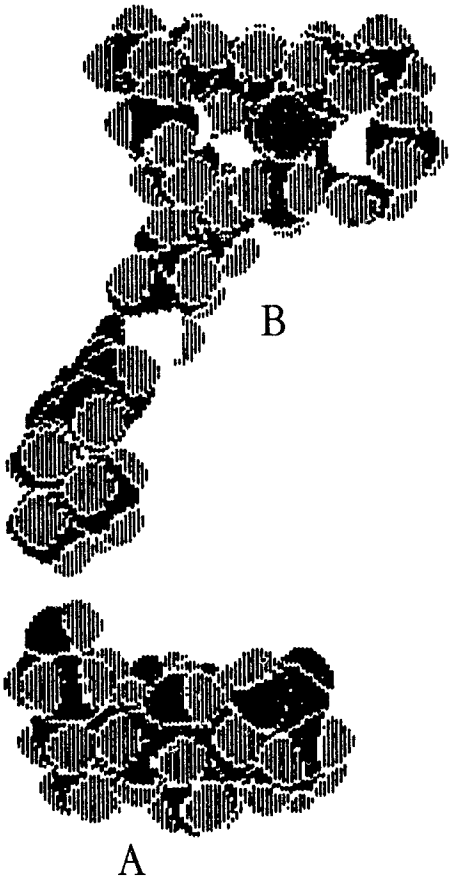

Figure 4.14 Conformation of the interaction of A)cholic acid with a B)synthesized resin pendant, shown as the spacefill representation. (black:carbon, blue:hydrogen, red:oxygen, yellow:nitrogen)

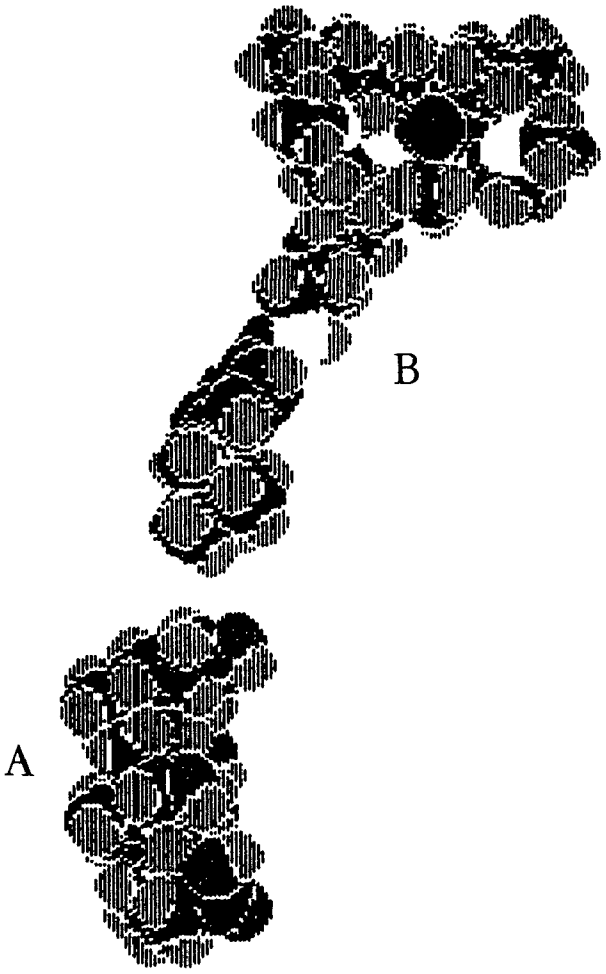

Figure 4.15 Conformation of the interaction of A)cholic acid with a B)synthesized resin pendant, shown as the spacefill representation. (black:carbon, blue:hydrogen, red:oxygen, yellow:nitrogen)

The possible interactions with the synthesized resins are more numerous since the pendants are not as close together. However, it was also seen that the longer pendants, which contain three alanine, are curved at a minimum energy conformation. This may lead to entanglements of the chain, thus reducing the availability of the active site. The pendants without the ala_3 spacer, although they are shorter and not as curved, may not be accessible to the bile acid due to other factors such as cross-linkage (Section 3.3).

In the present chapter, attempts have been made to model the interactions of bile acid with ion-exchange resin pendants. Although Alchemy II® has limitations, it yields models that can be used to show how structurally, the interactions could take place. The models show that micelle formation is possible when cholestyramine adsorbs cholic and glycocholic acid, which is in agreement with conclusions derived by use of the Donnan model. The interactions of bile acid with the synthesized resins present more possibilities but due to other factors (Chapter 3) their accessibility is more difficult.

4.6 REFERENCES

1. M Saunders, *J Am Chem Soc* , **109**, 3150, 1987
2. R.L DesJarlais, R.P. Sheridan, G.L. Seibel, J.S. Dixon, I.D. Kuntz and R. Venkataraghavan, *J. Med. Chem.*, **31**, 722, 1988
3. E. Horjales, H. Eklund and C.-I. Branden, *J. Mol. Biol.*, **197**, 685, 1987
4. G. Hangauer, A.F. Monzingo and B.W. Matthews, *Biochemistry*, **23**, 5730, 1984
5. R.H. Reid, C.A. Hooper and B.R. Brooks, *Biopolymers*, **28**, 525, 1989
6. M. Levitt, *Ann Rev Biophys Bioeng* , **11**, 251, 1982
7. N.L. Allinger, *Adv Phys Org Chem* , **13**, 1, 1976
8. V. Burkett and N.L Allinger, **Chap. 3, Methods for the Computation of Molecular Geometry**, p 65, in *Molecular Mechanics*, ACS Monograph 177, ACS Washington, 1982
9. R. Fletcher and C.M. Reeves, *Comput. J* , **7**, 149, 1964
10. R. Fletcher, *Comput J.*, **13**, 317, 1970
11. Alchemy II, Tripos Associates Inc., St-Louis, Missouri, 1988
12. G.R. Newbone, *J Am. Chem Soc.*, **110**, 325, 1988
13. L. Lessinger, *Cryst. Struct Comm.*, **11**, 1787, 1982

5 CONTRIBUTIONS TO ORIGINAL KNOWLEDGE

The object of this research was to obtain a better understanding of the interactions of bile acids with cholestyramine and novel cholestyramine-like ion-exchange resins. To this end, detailed investigation was undertaken of the adsorption of bile acids, under various conditions, by cholestyramine. In addition, cholestyramine-like sorbents were synthesized to determine the interaction of bile acids with the various chemical structures.

The Interaction of Cholestyramine with Bile Acids

A detailed investigation of the adsorption of bile acids by cholestyramine was made with different experimental conditions. Donnan theory provided a quantitative model for the interactions of bile acids with cholestyramine. From the Donnan theory, it was found that the concentration of bile acid, bound and unbound, in the resin phase is in the range where micellization can occur. Such aggregation promotes the partitioning of bile acid into the resin phase. Based on these results, it was concluded that the interaction is an ion-exchange process and that additional interaction occurs within the resin phase.

The Interaction of Synthesized Resins with Bile Acids

First, novel ion-exchange resins were prepared by solid phase peptide synthesis. Those cholestyramine-like sorbents, differing by a change in the structure, provided further insight as to why cholestyramine is such an effective bile acid sequestering agent. The structural changes were: 1. the use of a hydrophilic backbone instead of a hydrophobic one; 2. the presence of an ala_3 spacer; 3. the change in the basicity of the amino group by either removing the methylene group between the phenyl group and the amino group; 4. quaternization of the primary amine. The results from the adsorption experiments

indicated the importance of the backbone, which determines the accessibility to the active site, and the importance of the basicity of the active site. These results are consistent with an ion-exchange interaction between the resins and the bile acid.

Molecular Modelling

Molecular modelling was applied to show graphically how the interaction between cholestyramine or the synthesized resins and the bile acids occur. Due to the proximity of the active sites in cholestyramine, the bile acids interact with the quaternary ammonium group leaving the bile acids inside the cavity allowing interaction between them, which confirms the possibility of micellization. The synthesized resins, however, having pendants further apart, can interact with bile acids through the quaternary ammonium groups as well as the hydrophobic face being directed towards the hydrophobic part of the pendant. These results also confirm that the interaction between cholestyramine and bile acids is an ion-exchange process.

6 SUGGESTIONS FOR FUTURE WORK

1. Cholestyramine:

It would be of interest to study further the interaction of cholestyramine with bile acid, with respect to the Donnan theory. First, adsorption experiments, in water, should be done to obtain data at higher Ceq. It would be of interest to observe how the formation constant varies and if it reaches a constant value at a certain Ceq. The same approach should taken as to obtain data, in Tris-HCl. Exact knowledge of the concentration of buffer used in each sample would be necessary, since the chloride determination is involved (see next Section).

2. Synthesized Resins

Ion-exchange resins similar to the one prepared in this thesis should be synthesized but using a backbone of lower cross-linkage, i.e., which would be more appropriate to maximize the ion-exchange process.

A general approach could be taken to apply the Donnan theory to the adsorption of bile acids by the synthesized resins. Figure 6.1 shows a general representation of the equilibria which exist between the bile acid and the synthesized resins, in Tris-HCl. In principle, the fixed ionic group is represented by $P\text{-}NR_3^+$, where P can be any backbone, and R can either be a hydrogen or a methyl group. The fixed ionic group can either be free or bound to either iodide, chloride, hydroxide or bile acid anions to form species with respective molar concentrations of $[B^+]$, [BI], [BCl], [BOH] and [BA]. All of the other ions are also expressed as molar concentrations. The Tris-HCl cation is expressed as TNH_3^+.

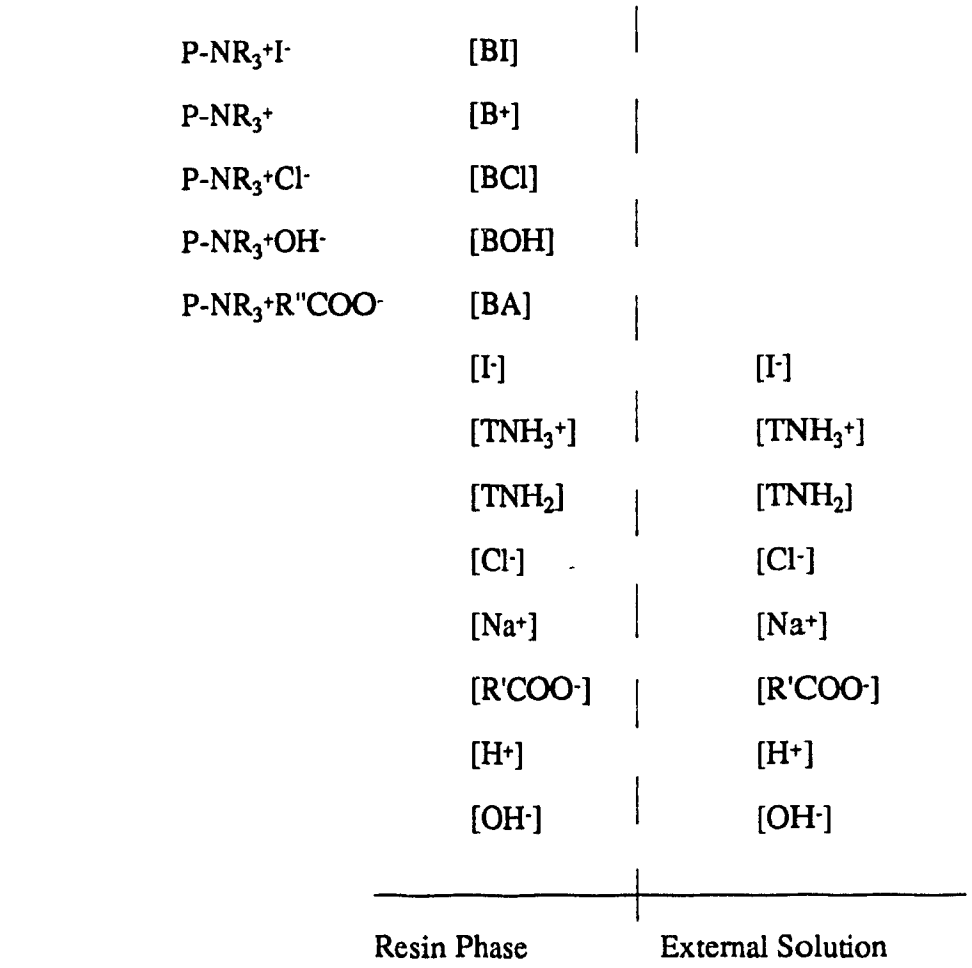

Figure 6.1 Representation of the equilibria existing between the resin and external phases, for all the adsorption of bile acids by synthesized resin

At equilibrium, electroneutrality must be preserved in both phases. Therefore, for the external solution:

$$[I^-]_s + [Cl^-]_s + [R'COO^-]_s + [OH^-]_s = [TNH_3^+]_s + [Na^+]_s + [H^+]_s$$

(Equation 6.1)

and for the resin phase:

$$[I^-]_r + [Cl^-]_r + [R'COO^-]_r + [OH^-]_r = [TNH_3^+]_r + [Na^+]_r + [H^+]_r + [B^+]_r$$

(Equation 6.2)

The total amount of moles of fixed ionic groups, (C), in the resin phase can be expressed as follows:

$$C = B^+_r + BI_r + BCl_r + BOH_r + BA_r \text{ (moles)} \qquad \textbf{(Equation 6.3)}$$

For the quaternized resins which can be considered as strong anion exchange resins, it may be assumed that the quaternary ammonium salt is completely ionized, i.e., $BI_r = BCl_r = 0$. However, for the unquaternized resins, which can be referred as weak base anion exchange resins, such assumptions cannot be made. The value of C can also be expressed as:

$$C = BI_r + I^-_r + I^-_s \text{ (moles)} \qquad \textbf{(Equation 6.4)}$$

The bile salt anion can either be found in the external solution phase or in the resin phase in the bound and unbound forms. Conservation of mass requires that:

$$(R'COONa)_i = R'COO^-_s + R'COO^-_r + BA_r \text{ (moles)} \qquad \textbf{(Equation 6.5)}$$

where $(R'COONa)_i$ is the number of moles of bile acid present in the initial solution. Furthermore, in terms of the sodium ions:

$$(R'COONa)_i = Na^+_s + Na^+_r \text{ (moles)} \qquad \textbf{(Equation 6.6)}$$

The Donnan partition coefficient can be expressed as:

$$\lambda = \frac{[TNH_3^+]_r}{[TNH_3^+]_s} = \frac{[Na^+]_r}{[Na^+]_s} = \frac{[H^+]_r}{[H^+]_s} = \frac{[I^-]_s}{[I^-]_r} = \frac{[Cl^-]_s}{[Cl^-]_r} = \frac{[R'COO^-]_s}{[R'COO^-]_r} = \frac{[OH^-]_s}{[OH^-]_r} \qquad \textbf{(Equation 6.7)}$$

and:

$$\lambda = \left(1 + \frac{[B^+]}{[Na^+]_r + [H^+]_r + [R''NH_3^+]_r}\right)^{-1/2} \qquad \textbf{(Equation 6.8)}$$

The formation constant for each bound species can be expressed by the general formula:

$$P\text{-}NR_3^+ + X^- \underset{}{\overset{K_x}{\rightleftharpoons}} P\text{-}NR_3^+X^-$$

$$K_x = \frac{[P\text{-}NR_3^+X^-]}{[P\text{-}NR_3^+][X^-]} \qquad \textbf{(Equation 6.9)}$$

where X can be the iodide, chloride, hydroxyde or bile salt anion.

To obtain these constants, the ionic species in the equilibrium would have to be evaluated. The measure of bile acid anion in solution can be done by HPLC (Section 2.1.3). It could be assumed that most of the sodium cations are present in the solution, and they can be said to equal approximately the initial concentration (Section 2.6.2.1).

For the quaternized resins, because they are strong base resins, the iodide and chloride ion would either be in the resin or the external solution phases. The total amount of both anions could be determined by potentiometry, in the solution phase, and from a knowledge of their initial concentrations, their concentrations in the resin phase could be found. Then the Donnan partition coefficient, λ, could be found from:

$$\lambda = \frac{[I^-]_s}{[I^-]_r} = \frac{[Cl^-]_s}{[Cl^-]_r} \qquad \textbf{(Equation 6.10)}$$

and:

$$\lambda = \frac{[I^-_s + Cl^-_s]}{[I^-_r + Cl^-_r]} \qquad \textbf{(Equation 6.11)}$$

For unquaternized resins, which are weak base resins, the difficulty would be in measuring the chloride anion concentration in the solution. Previously, this measurement was carried out using potentiometry. However, this method would also measure the iodide ion concentration in solution, since this method does not differentiate between these two anions. Therefore, methods to measure concentrations of iodide and chloride ions individually would be required. One method could be the potentiometric titration of the external solution. It would measure both the iodide and chloride in solution. The precipitate of silver iodide and chloride could then be collected. Because silver chloride is soluble in ammonium hydroxyde and silver iodide is insoluble, it could be added to the precipitate and the insoluble silver iodide could then be collected, dried and weighed. The amount of chloride could then be obtained by difference. The chloride ion concentrations can also be measured by using a chloride selective electrode.

The concentration of the Tris-HCl cation also must be determined. However, since the Tris-HCl cation is positively charged, the same phenomenon as the sodium cation could take place, mainly that it could be found mostly in the external solution.

Then if it is possible to determine the concentrations of the above ions in solution, from electroneutrality the hydrogen and hydroxide ions concentrations could be determined. The ionic concentrations in the resin phase could be determined from a knowledge of λ. Finally the formation constants could be determined for each bound species.

The difficulty in the application of the Donnan theory to the present system, is not in its principle but in the experimental determination of the

concentrations of the various ionic species. The synthesized resins have much lower substitution than cholestyramine, the measurement of the chloride and iodide anions in solution may be difficult. Therefore, carefully planned experiments are required to obtain results for the quantitative Donnan model.

3. Adsorption Studies

Adsorption studies should be continued ***in vitro*** using buffers which would mimic better the conditions found in the human intestine. Experiments ***in vivo*** might also be of interest. The Donnan theory could be verified as to see if it would also be applicable to other ***in vitro*** conditions and ***in vivo***.

4. Molecular Modelling

Molecular modelling should be extended further to include the study of the interaction of ion-exchange resins with bile acids. It would be of interest to try to obtain further insight as to how these two molecules interact and to see if the different possibilities proposed herein can be verified further.

APPENDIX 1

PHYSICAL PROPERTIES OF BILE ACIDS

CHOLIC ACID

3α,7α,12α-trihydroxy-5β-cholan-24-oic acid

$C_{24}H_{40}O_5$; MW = 408.56; pK_a = 4.98-5.5

monohydrate, plates from diluted acetic acid

when anhydrous, mp = 198°C

$[\alpha]_D^{20}$ + 37° (c = 0.6 in alcohol)

solubility at 15°C in water: 0.28g/L

soluble in alcohol, in acetone, in glacial acetic acid, in solutions of alkali-hydroxides or carbonate; slightly soluble in ether, in chloroform, in benzene

SODIUM SALT

$C_{24}H_{39}NaO_5$

crystals

solubility at 15°C in water: > 568.9g/L

GLYCOCHOLIC ACID

N-[3α,7α,12α-truhydroxy-24-oxo-cholan-24 -yl]glycine

$C_{26}H_{43}NO_6$; MW = 465.61; pK_a = 3.8-4.09

sesquihydrate, crystals from 5% alcohol, mp = 130°C

anhydrous form, mp = 165-168°C

$[\alpha]_D^{23}$ +30.8° (c = 7.5 in 95% ethanol)

solubility at 15°C in water: 0.33g/L, in boiling water: 8.3g/L

SODIUM SALT

$C_{26}H_{42}NNaO_6$

crystals from 95%alcohol and ether, mp = 230-240°C

$[\alpha]_D^{24}$+32 (water)

solubility at 15°C in water: > 274g/L

TAUROCHOLIC ACID

2-{[3α,7α,12α-trihydroxy-24-oxo-5β-cholan-24 -yl]amino}ethanesulfonic acid

$C_{26}H_{45}NO_7S$; MW = 515.69; pK_a = 1.85

clusters of slender, four-sided prisms from alcohol and ether, stable to air, mp = d125°C

$[\alpha]_D^{18}$+38.8° (c = 2 in alcohol)

freely soluble in water; soluble in alcohol; insoluble in ether, in ethyl acetate

SODIUM SALT

$C_{26}H_{44}NNaO_7S$

crystals with 1.5-2 moles of water, mp = d230°C

$[\alpha]_D^{20}$+24° (c = 3)

freely soluble in water and alcohol

CHENODEOXYCHOLIC ACID

3,7-dihydroxycholan-24-oic acid

$C_{24}H_{40}O_4$; MW = 392.56; pK_a = 5.88-6.53

needles from ethyl acetate and heptane, mp = 119°C

$[\alpha]_D^{20}$+11.5° (dioxane)

freely soluble in methanol, in alcohol, in acetone, in acetic acid; insoluble in water, in petroleum ether, in benzene

3α,12α-dihydroxy-5β-cholanic acid

$C_{24}H_{40}O_4$

crystals from alcohol, mp = 176-8°C

$[\alpha]_D^{20}$+55° (alcohol)

solubility at 15°C in water: 0.24g/l

soluble in alcohol, in acetone, in glacial acetic acid; slightly soluble in ether, in chloroform, in benzene

SODIUM SALT

$C_{24}H_{39}O_4Na$

solubility at 15°C in water: > 333g/L

LITHOCHOLIC ACID

3α-hydroxy-53β-cholan-24-oic acid

$C_{24}H_{40}O_3$, MW = 376.56

hexagonal leaflets from alcohol, prisms from acetic acid. mp = 184-6°C

$[\alpha]_D^{20}$+33.7° (c = 1.5 in absolute ethanol)

freely soluble in hot alcohol

CHOLESTEROL

cholest-5-en-5β-ol

$C_{27}H_{46}O$; MW = 386.64

monohydrate, pearly leaflets or plates from diluted alcohol; become anhydrous at 70-80°C, mp = 148-150°C

$[\alpha]_D^{20}$-31.5° (c = 2 in ether); [α] -39.5° (c = 2 in chloroform)

solubility at 15°C in water: 2mg/L

soluble in ether, in benzene, in chloroform, in acetic acid; slightly soluble in alcohol

REFERENCES

1. **The Merck Index**, 10th edition, M. Windholz ed., Merck and Co. Inc., Rahway, N.J. USA, 1983

2. **CRC Handbook of chemistry and physics**, 62nd edition, R.C. Weast ed., CRC Press Inc., Boca Raton, Fl., 1981

APPENDIX 2

DATA FOR FIGURES

Chapter 2

Figure 2.2

Cholestyramine (Cl)
Glycocholic acid

Ceq(mg/dL)	X (mol/eq pndnt)
a)Tris-HCl, 0.0026M	
0.63	0.03
0.84	0.0527
1.17	0.065
1.28	0.065
1.86	0.1052
1.88	0.0922
2.92	0.1439
2.99	0.1517
3.26	0.1836
3.52	0.2009
3.94	0.2007
4.13	0.2170
4.49	0.2682
4.64	0.2450
4.73	0.2538
4.97	0.2720
5.28	0.2771
5.37	0.2580
5.56	0.3619
5.76	0.3709
5.98	0.3535
6.11	0.3542
6.18	0.2926
6.26	0.4105
7.35	0.4646
7.52	0.4334
8.61	0.5950
9.68	0.5595
9.72	0.5799
11.01	0.6450
11.92	0.6250
16.84	0.8680
19.21	0.7682
19.67	0.8895
23.80	0.8975
24.53	0.9377
26.35	0.7736
30.67	0.9669
34.30	1.0010
38.86	1.0193
b)Phosphate, 0.0027M	
0.78	0.0062
1.82	0.0117
2.88	0.0213
2.98	0.0258
3.86	0.0292
3.98	0.0160
4.71	0.0428
4.91	0.0401
7.66	0.0381
7.96	0.0510
8.62	0.0472
10.35	0.0641
10.78	0.0778
10.79	0.0712
11.74	0.0499
12.63	0.1043
15.81	0.0723
15.82	0.0971
17.57	0.0715
19.40	0.1094
20.42	0.1308

c) water

Ceq (mg/dL)	X (mol/eq pndnt)
0.12	0.1702
0.14	0.1171
0.17	0.3316
0.21	0.3193
0.24	0.3080
0.29	0.1213
0.39	0.4152
0.41	0.5846
0.55	0.6248
0.57	0.2996
0.67	0.3286
0.74	0.4819
0.77	0.8261
0.92	0.6564
0.98	0.7621
0.98	0.7176
1.14	0.4995
1.26	0.7553
1.34	0.6949
1.41	0.7555
1.67	0.9014
1.92	0.7194
2.33	0.6904
2.64	0.8578
2.81	0.8012
3.74	1.0291
5.44	1.1462
6.40	1.0797
7.74	1.0106
10.09	0.9781
10.14	1.1573
10.88	1.1930
11.71	1.0621
14.69	1.1135
17.47	1.0736
18.47	1.0855
20.52	1.1029
20.76	1.0998
24.13	1.2649
24.24	1.1017
25.25	0.9878
29.72	1.0354
40.84	1.2577

d) Tris-HCl 0.005M

Ceq	X
0.7948	0.0197
1.053	0.0324
1.487	0.0421
2.097	0.0603
2.930	0.0831
3.121	0.0884

Figure 2.3

Cholestyramine (Cl)
Glycocholic acid
Water

Ceq (M)	X (mol/g)	Ceq	X
a) present results		**b) Johns and Bates**	
2.461E-6	5.387E-4	3.125E-5	9.000E-4
2.871E-6	3.706E-4	6.875E-5	1.575E-3
3.486E-6	1.050E-3	1.250E-4	1.925E-3
4.307E-6	1.010E-3	1.875E-4	2.300E-3
4.922E-6	9.748E-4	3.187E-4	2.675E-3
5.947E-6	3.839E-4	5.125E-4	2.950E-3
7.998E-6	1.314E-3	7.188E-4	3.250E-3
8.408E-6	1.850E-3		
1.128E-5	1.977E-3		
1.169E-5	9.482E-4		
1.374E-5	1.040E-3		
1.518E-5	1.525E-3		
1.579E-5	2.615E-3		
1.887E-5	2.078E-3		
2.010E-5	2.412E-3		
2.010E-5	2.271E-3		
2.338E-5	1.581E-3		
2.584E-5	2.390E-3		
2.748E-5	2.199E-3		
2.892E-5	2.391E-3		
3.425E-5	2.853E-3		
3.938E-5	2.277E-3		
4.778E-5	2.185E-3		
5.414E-5	2.715E-3		
5.763E-5	2.536E-3		
7.670E-5	3.257E-3		
1.116E-4	3.628E-3		
1.313E-4	3.417E-3		
1.587E-4	3.096E-3		
2.069E-4	3.663E-3		
2.080E-4	3.776E-3		
2.231E-4	3.362E-3		
2.402E-4	3.524E-3		
3.013E-4	3.398E-3		
3.583E-4	3.436E-3		
3.788E-4	3.491E-3		
4.208E-4	3.481E-3		
4.258E-4	4.003E-3		
4.949E-4	3.487E-3		
4.971E-4	3.126E-3		
5.178E-4	3.277E-3		
6.095E-4	3.981E-3		

Figure 2.4

Cholestyramine (Y)
Glycocholic acid
Tris-HCl, 0.0026M

Ceq (mg/dL)	X (mol/eq pndnt)
a) Y = Cl	
as Figure 2.2 a)	
b) Y = I	
2.44	0.0981
4.91	0.1797
10.93	0.3542
11.18	0.4220
13.02	0.4252
14.93	0.5036
19.76	0.4497
20.26	0.5167
25.90	0.6080
26.54	0.5469
27.89	0.5641
31.56	0.5871

Figure 2.5

Cholestyramine (Cl)

Tris-HCl, 0.0026M

Ceq	X
a)Glycocholic Acid	
as Figure 2.2 a)	
b)**Cholic Acid**, present results	
2.81	0.1401
5.25	0.3011
6.76	0.4009
12.41	0.7415
17.54	0.8781
26.67	1.0487
30.99	1.0740
32.19	1.0656
c)**Cholic Acid**, past results	
0.663	0.0263
1.016	0.0416
1.227	0.0475
1.907	0.0686
2.859	0.1004
3.643	0.1223
5.912	0.1778

Figure 2.6

Cholestyramine (Cl)
Glycocholic acid
Tris-HCl, 0.0027M

Ceq (mg/dL)	X (mol/eq pndnt)
a) 6°C	
1.35	0.0383
1.46	0.0640
2.52	0.0666
3.81	0.1163
5.01	0.1154
5.19	0.1970
7.29	0.3558
8.14	0.3400
8.39	0.2630
10.20	0.4813
15.23	0.4836
15.41	0.3099
16.50	0.4309
20.06	0.4829
b) 25°C	
0.25	0.0170
0.30	0.0264
0.61	0.0240
0.91	0.0405
1.08	0.0670
1.39	0.0578
1.85	0.1014
2.14	0.1326
3.19	0.1650
3.93	0.2243
4.36	0.2746
4.83	0.3251
4.95	0.3138
5.95	0.3797

Ceq	X
c) 37°C	
0.84	0.0409
1.06	0.0569
1.49	0.0881
2.30	0.1137
2.67	0.1160
4.15	0.2073
4.18	0.2144
4.50	0.2546
5.19	0.3384
5.42	0.2899
5.81	0.3363
5.88	0.3454
6.75	0.3944
7.26	0.3908
7.53	0.5151
13.18	0.7406
15.68	0.7494
16.37	0.8843
23.30	0.8621
28.74	0.8825
d) 65oC	
1.74	0.0768
2.15	0.0753
3.20	0.1306
3.50	0.1388
3.50	0.1652
3.69	0.1491
3.97	0.1752
4.53	0.2423
4.94	0.2297
6.37	0.4313
7.24	0.4842
10.63	0.6565
10.75	0.6610
16.45	0.8166
16.56	0.7250
19.32	0.8719

Figure 2.7

Cholestyramine (Cl)
Cholic acid
Tris-HCl, 0.0026M

Ceq (mg/dL)	X (mol/eq pndnt)	Ceq	X
a) 6°C		**d) 65°C**	
1.47	0.0425	1.20	0.0803
2.57	0.0697	1.38	0.0652
3.92	0.0966	2.92	0.1674
4.79	0.1743	4.62	0.2702
5.94	0.1641	5.37	0.2987
6.88	0.2286	6.16	0.3554
7.92	0.2982	6.32	0.3508
8.53	0.3882	6.50	0.3435
8.55	0.2503	7.34	0.4284
9.25	0.3744	7.46	0.4759
16.33	0.4689		
17.15	0.5157		
17.46	0.4606		
22.98	0.5999		

b) 25°C

as Figure 2.5 b)

c) 37°C

0.71	0.0461
1.15	0.0792
1.42	0.0951
2.45	0.1500
3.00	0.1774
3.34	0.2080
3.48	0.2357
3.91	0.2452
4.08	0.2579
5.36	0.3914
5.46	0.3460
5.81	0.3770
6.40	0.4482
6.41	0.4243
8.24	0.5455
8.41	0.5327
10.17	0.6137
11.91	0.7515
12.13	0.7167
15.03	0.7962

Figure 2.8

Cholestyramine (Cl)
Glycocholic acid
Tris-HCl, 0.0026M
Kinetics

Time (hours)	X (mol/eq pndnt)
a) 6°C	
2	0.6444
4.5	0.7106
6	0.7169
22	0.7403
b) 25°C	
2.5	0.6729
5	0.7828
7.5	0.8728
12	0.897
22	0.8988
c) 37°C	
2.5	0.5977
5.5	0.7736
7.5	0.8114
50.5	0.8643
d) 65°C	
2	0.6000
4.75	0.7398
7	0.7713
22.15	0.7821

Figure 2.9

Cholestyramine (Cl)
Cholic acid
Tris-HCl, 0.0026M
Kinetics

Time	X
a) 6°C	
2	0.6398
4.5	0.6875
8	0.7533
24	0.7858
29	0.7960
48	0.7992
b) 25°C	
2.5	0.8779
5	1.0233
7.5	1.0202
22	1.0163
c) 37°C	
2.5	0.8922
5.5	0.9400
7.5	0.9530
50.5	0.9862
d) 65°C	
2	0.5172
4.75	0.6439
7	0.6868
22.5	0.7012

Figure 2.10

Cholestyramine (Cl)
Glycocholic acid
Langmuir isotherm

1/Ceq (M^{-1}) ($\times 10^{-4}$)	1/X (g/mol) ($\times 10^{-3}$)	1/Ceq	1/X
a)Tris-HCl (0.0026M)		**b)Phosphate (0.0027M)**	
7.746	10.53	6.251	50.96
5.805	5.995	2.679	27.00
4.168	4.861	1.693	14.83
3.809	4.827	1.636	12.25
2.622	3.003	1.263	10.82
2.594	3.427	1.225	19.75
1.496	1.721	1.035	7.382
1.385	1.573	0.9931	7.879
1.238	1.574	0.6366	8.293
1.181	1.456	0.6126	6.195
1.086	1.178	0.5657	6.694
1.051	1.290	0.4711	4.929
1.031	1.245	0.4523	4.061
0.9235	1.140	0.4518	4.438
0.9080	1.225	0.4153	6.331
0.8770	0.8731	0.3861	3.029
0.8465	0.8519	0.3084	4.370
0.8154	0.8938	0.3082	3.253
0.7980	0.8920	0.2775	4.420
0.7779	0.7697	0.2513	2.888
0.6634	0.6801	0.2388	2.415
0.6484	0.7290		
0.5663	0.5310		
0.5037	0.5647		
0.5016	0.5448		
0.4429	0.4898		
0.4091	0.5055		
0.2896	0.3640		
0.2538	0.4113		
0.2479	0.3552		
0.2049	0.3520		
0.1988	0.3370		
0.1850	0.4084		
0.1590	0.3268		
0.1255	0.3100		
0.1422	0.3156		

Figure 2.10 (cont'd)

1/Ceq (M^{-1}) (x 10^{-4})	1/X (g/mol) (x 10^{-3})
c)Water	
40.63	1.856
34.83	2.698
28.68	0.9528
23.22	0.9895
20.32	1.026
16.81	2.605
12.50	0.7610
11.89	0.5405
8.865	0.5057
8.554	1.055
7.278	0.9615
6.589	0.6556
6.332	0.3825
5.300	0.4813
4.976	0.4146
4.976	0.4403
4.277	0.6325
3.870	0.4183
3.639	0.4547
3.458	0.4182
2.920	0.3505
2.540	0.4392
2.093	0.4576
1.847	0.3683
1.735	0.3944
1.304	0.3070
0.8963	0.2756
0.7619	0.2926
0.6300	0.3230
0.4832	0.2730
0.4809	0.2648
0.4482	0.2975
0.4164	0.2838
0.3319	0.2943
0.2791	0.2911
0.2640	0.2865
0.2376	0.2873
0.2349	0.2498
0.2021	0.2868
0.2012	0.3199
0.1931	0.3052
0.1641	0.2512

Figure 2.11

Cholestyramine (Y)
Glycocholic acid
Tris-HCl
Langmuir isotherms

1/Ceq (M^{-1}) ($\times 10^{-4}$)	1/X (g/mol) ($\times 10^{-3}$)
a)Y = Cl	
as Figure 2.10 a)	
b)Y = I	
1.998	3.221
0.9931	1.758
0.4461	0.8920
0.4361	0.7487
0.3745	0.7431
0.3266	0.6274
0.2468	0.7026
0.2407	0.6115
0.1883	0.5197
0.1837	0.5777
0.1748	0.5601
0.1545	0.5382

Figure 2.12

Cholestyramine (Cl)
Tris-HCl
Langmuir isotherms

1/Ceq ($\times 10^{-4}$)	1/X ($\times 10^{-3}$)
a)Glycocholic Acid	
as Figure 2.10 a)	
b)Cholic Acid	
1.532	2.255
0.8202	1.049
0.6370	0.7881
0.3470	0.4261
0.2455	0.3598
0.1614	0.3013
0.1389	0.2942
0.1338	0.2965

Figure 2.13

Cholestyramine (Cl)
Glycocholic acid
Tris-HCl

1/Ceq (M^{-1}) ($\times 10^{-3}$)	1/X (g/mol) ($\times 10^{-3}$)
a)6°C	
36.12	8.249
33.40	4.937
19.35	4.744
14.82	0.8880
12.80	2.717
9.732	2.738
9.395	1.604
5.990	0.9293
5.812	1.201
4.780	0.6565
3.202	0.6533
3.164	1.020
2.955	0.7332
2.431	0.6543
b)25°C	
195.0	18.58
162.5	11.97
79.93	13.16
53.58	7.801
45.15	4.716
35.08	5.466
26.36	3.116
27.78	2.383
15.28	1.915
12.41	1.409
11.18	1.151
10.01	0.9719
9.850	1.007
8.195	0.8321

1/Ceq ($\times 10^{-3}$)	1/X ($\times 10^{-3}$)
c)37°C	
58.05	7.725
46.00	5.553
32.72	3.586
21.20	2.778
18.26	2.724
11.75	1.524
11.66	1.474
10.84	1.241
9.395	0.9337
8.996	1.090
8.392	0.9395
8.292	0.9148
7.224	0.8011
6.716	0.8085
6.475	0.6134
3.700	0.4266
3.110	0.4216
2.979	0.3573
2.093	0.3665
1.697	0.3580
d)65°C	
28.02	4.114
22.68	4.196
15.24	2.419
13.93	2.276
13.93	1.912
13.21	2.119
12.28	1.803
10.76	1.304
9.870	1.376
7.655	0.7326
6.735	0.6525
4.587	0.4813
4.535	0.4780
2.964	0.3869
2.944	0.4358
2.523	0.3624

Figure 2.14

Cholestyramine (Cl)
Cholic acid
Tris-HCl
Langmuir isotherms

1/Ceq (M^{-1}) ($\times 10^{-3}$)	1/X (g/mol) ($\times 10^{-3}$)
a)6°C	
29.29	7.434
16.75	4.533
10.98	3.271
8.990	1.813
7.249	1.925
6.259	1.382
5.437	1.059
5.048	0.8139
5.036	1.262
4.655	0.8439
2.637	0.6738
2.511	0.6127
2.466	0.6860
1.874	0.5267
b)25°C	
as Figure 2.12 b)	

1/Ceq ($\times 10^{-3}$)	1/X ($\times 10^{-3}$)
c)37°C	
60.65	6.854
37.44	3.98
30.32	3.322
17.58	2.106
14.35	1.781
12.89	1.519
12.37	1.340
11.01	1.288
10.55	1.225
8.033	0.8072
7.886	0.9132
7.411	0.8381
6.728	0.7049
6.718	0.7446
5.226	0.5792
5.120	0.5931
4.234	0.5148
3.615	0.4204
3.550	0.4408
2.865	0.3968
d)65°C	
35.88	3.935
31.20	4.846
14.75	1.887
9.320	1.169
8.019	1.058
6.990	0.8690
6.813	0.9007
6.625	0.9198
5.866	0.7375
5.772	0.6639

Figure 2.15

Cholestyramine (Cl)
Glycocholic acid
Phosphate buffer, 0.0027M

One-binding site model

Ceq (mg/dL)	X (mol/eq pndnt)

a)Experimental data

as in Figure 2.2b)

b)Predicted data

0	0
2	0.01263
4	0.02495
6	0.03696
8	0.04868
10	0.06012
15	0.08757
20	0.1134

Figure 2.16

Cholestyramine I
Glycocholic acid
Tris-HCl, 0.0026M

One Binding Site Model

Ceq (mg/dL) X (mol/eq pndnt)

a)Experimental data

as in Figure 2.4b)

b)Predicted data

0	0
2	0.1091
4	0.1967
6	0.2682
8	0.3287
10	0.3797
15	0.4788
20	0.5505
30	0.6475

Figure 2.17

Cholestyramine Cl
Glycocholic acid
Tris-HCl, 0.0027M

One Binding Site Model

Ceq (mg/dL) X (mol/eq pndnt)

6oC

a)Experimental data

as in Figure 2.6a)

b)Predicted data

0	0
2	0.09199
4	0.1685
6	0.2331
8	0.2884
10	0.3362
15	0.4318
20	0.5033

Figure 2.18

Cholestyramine Cl
Cholic acid
Tris-HCl, 0.0026M

One Binding Site Model

Ceq X

6oC

a)Experimental data

as in Figure 2.7a)

b)Predicted data

0	0
2	0.1052
4	0.1904
6	0.2610
8	0.3201
10	0.3705
15	0.4689
20	0.5407

Figure 2.19

Cholestyramine Cl
Glycocholic acid

Two Binding Site Model

a)Tris-HCl, 0.0026M

i)Experimental data

as in Figure 2.2a)

ii)Predicted data

Ceq (mg/dL)	X (mol/eq pndnt)
0	0
2	0.1386
4	0.2547
6	0.3538
8	0.4399
10	0.5156
15	0.6712
20	0.7927
30	0.9734
35	1.043
40	1.104

b)Phosphate buffer, 0.0027M

i)Experimental data

as in Figure 2.2a)

ii)Predicted data

0	0
2	0.01371
4	0.02705
6	0.04003
8	0.05267
10	0.06498
15	0.09443
20	0.1220

c)Water

i)Experimental data

as in Figure 2.2c)

ii)Predicted data

Ceq	X
0	0
2	0.8276
4	0.9320
6	0.9827
8	1.0173
10	1.0447
15	1.0985
20	1.1419
30	1.2132
40	1.2712

Figure 2.20

Cholestyramine Cl
Cholic acid
Tris-HCl, 0.0026M

Two Binding Site Model

Ceq (mg/dL)	X (mol/eq pndnt)
a)Experimental data	
as in Figure 2.5b)	
b)Predicted data	
0	0
2	0.1474
4	0.2746
6	0.3855
8	0.4827
10	0.5690
15	0.7468
20	0.8852
25	0.9960
30	1.087
35	1.162

Figure 2.21

Cholestyramine I
Glycocholic acid
Tris-HCl, 0.0026M

Two Binding Site Model

Ceq	X
a)Experimental data	
as in Figure 2.4b)	
b)Predicted data	
0	0
2	0.1091
4	0.1967
6	0.2682
8	0.3287
10	0.3797
15	0.4788
20	0.5505
30	0.6475

Figure 2.22

Cholestyramine Cl
Glycocholic acid
Tris-HCl, 0.0027M

Two Binding Site Model

Ceq (mg/dL)	X (mol/eq pndnt)

a)60C

i)Experimental data

as in Figure 2.6a)

ii)Predicted data

0	0
2	0.1051
4	0.1902
6	0.2606
8	0.3197
10	0.3700
15	0.4684
20	0.5402

b)25, 37, 65oC

i)Experimental data

as in Figure 2.6b),c),d)

ii)Predicted data

as in Figure 2.19a ii)

Figure 2.23

Cholestyramine Cl
Cholic acid
Tris-HCl, 0.0026M

Two Binding Site Model

Ceq	X

a)60C

i)Experimental data

as in Figure 2.7a)

ii)Predicted data

0	0
2	0.08919
4	0.1687
6	0.2404
8	0.3051
10	0.3643
15	0.4919
20	0.5975

b)25, 37, 65oC

i)Experimental data

as in Figure 2.7b),c),d)

ii)Predicted data

as in Figure 2.20b)

Figure 2.24

Cholestyramine (Cl)
Glycocholic acid

Modified Scatchard model

Ceq (mg/dL)	X (mol/eq pndnt)

a) Tris-HCl, 0.0026M

i)Experimental data

as in Figure 2.2a)

ii) Predicted data

0	0
2	0.0711
4	0.2088
6	0.3572
8	0.4864
10	0.5889
15	0.7518
20	0.8364
24	0.9134
30	0.9459

b)Phosphate buffer, 0.0027M

i)Experimental data

as in Figure 2.2b)

ii)Predicted data

0	0
2	0.0137
4	0.02666
6	0.03896
8	0.0506
10	0.0617
15	0.08725
20	0.1099

Ceq	X

c)Water

i)Experimental data

as in Figure 2.2c)

ii)Predicted data

0	0
2	0.8799
4	0.9464
6	0.9662
8	0.9754
10	0.9807
15	0.9875
20	0.9908
30	0.9940
40	0.9955

Figure 2.25

Cholestyramine Cl
Cholic acid
Tris-HCl, 0.0026M

Modified Scatchard Model

Ceq (mg/dL)	X (mol/eq pndnt)
a)Experimental data	
as in Figure 2.5b)	
b)Predicted data	
0	0
2	0.08676
4	0.2486
6	0.4117
8	0.5439
10	0.6434
15	0.7917
20	0.8648
30	0.9291

Figure 2.26

Cholestyramine I
Glycocholic acid
Tris-HCl, 0.0026M

Modified Scatchard Model

Ceq	X
a)Experimental data	
as in Figure 2.4b)	
b)Predicted data	
0	0
2	0.1040
4	0.1864
6	0.2537
8	0.3098
10	0.3576
15	0.4511
20	0.5198
30	0.6150

Figure 2.27

Cholestyramine Cl
Glycocholic acid
Tris-HCl, 0.0027M

Modified Scatchard Model

Ceq (mg/dL)	X (mol/eq pndnt)
a)6oC	
i)Experimental data	
as in Figure 2.6a)	
ii)Predicted data	
0	0
2	0.1338
4	0.2112
6	0.2615
8	0.2969
10	0.3232
15	0.3664
20	0.3926
30	0.4229
b)25, 37, 65oC	
i)Experimental data	
as in Figure 2.6b),c),d)	
ii)Predicted data	
as in Figure 2.24a ii)	

Figure 2.28

Cholestyramine Cl
Cholic acid
Tris-HCl, 0.0026M

Modified Scatchard Model

Ceq	X
a)6oC	
i)Experimental data	
as in Figure 2.7a)	
b)Predicted data	
0	0
2	0.07854
4	0.1600
6	0.2380
8	0.3092
10	0.3729
15	0.5002
20	0.5916
30	0;.7081
b)25, 37, 65oC	
i)Experimental data	
as in Figure 2.7b),c),d)	
b)Predicted data	
as in Figure 2.25b)	

Figure 2.31

Cholestyramine (Cl)
Glycocholic acid
Tris-HCl (0.0026 M)

Simplified Donnan model

X/C_a (ml/g) ($\times 10^{-6}$)	X (mmol/g)	X/C_a	X
11.12	1963.5	4.122	3650.1
10.53	1354.6	3.025	2932.7
10.36	1224.0		
10.48	1194.3		
10.20	1533.2		
10.09	173.91		
9.946	866.91		
9.902	686.40		
9.620	885.06		
9.602	1913.7		
9.500	1166.6		
9.426	2128.5		
9.328	1168.9		
9.302	1846.4		
9.275	1430.2		
9.184	662.97		
9.100	347.16		
9.062	605.88		
8.938	214.50		
8.809	897.60		
8.634	837.54		
8.500	808.83		
8.454	716.10		
8.443	914.43		
8.436	2062.5		
8.310	2864.4		
8.293	787.38		
8.197	662.31		
8.171	214.50		
8.164	500.61		
7.929	474.87		
7.891	304.26		
7.733	851.40		
7.663	99.000		
7.276	2935.4		
6.762	1224.0		
6.152	3094.4		
6.068	2961.8		
5.510	4089.4		
5.074	3190.8		
4.696	3303.3		
4.408	3623.1		
4.221	3363.3		

Figure 2.32

Cholestyramine (I)
Glycocholic acid
Tris-HCl (0.0026 M)

Simplified Donnan model

X/C_a (ml/g) (x 10^{-6})	X (mmol/g)
6.462	323.73
6.071	1392.6
5.883	593.01
5.426	1661.9
4.105	1705.1
3.777	2006.4
3.316	1804.8
3.259	1861.5

Figure 2.35

Conductometry
Cholestyramine
$AgNO_3$

Vol AgNO3 (ml)	Conductance (micromho)
0	149.05
0.04	148.8
0.10	148.2
0.14	147.85
0.18	147.45
0.22	147.10
0.26	146.75
0.30	146.35
0.34	146.05
0.38	145.65
0.42	145.30
0.46	144.95
0.50	144.7
0.54	144.4
0.58	144.1
0.62	143.85
0.64	143.80
0.66	143.75
0.68	143.80
0.70	144.25
0.72	145.35
0.74	147.55
0.80	159.25
0.90	178.85
1.00	198.35

Figure 2.36

Cholestyramine (Cl)
Glycocholic acid
Water

a)original data

as Figure 2.2 c)

b)total bile acid in resin

Ceq (mg/dL)	X(mol/eq pndnt)
0.14	0.1171
0.67	0.3288
1.14	0.4995
2.81	0.8012

c)bile acid bound in resin

Ceq	X
0.14	0.1035
0.67	0.3018
1.14	0.4740
2.81	0.7830

Figure 2.37

Variation of the Donnan partition coefficient, λ, with increasing Ceq

λ (10^4)	Ceq (mg/dL)
0.973	0.14
2.33	0.67
4.21	1.14
14.7	2.81

Figure 2.38

Variation of the concentration of chloride anions in the external solution and in the resin phase, with increasing Ceq

$[Cl^-]_s$ (10^4 M)	$[Cl^-]_r$ (M)	Ceq (mg/dL)
1.70	1.75	0.14
3.23	1.38	0.67
4.54	1.08	1.14
6.30	0.43	2.81

Figure 2.39

Variation of the difference between the concentration of chloride anions in the external solution and the total bile acid concentration in the resin phase, and the variation of the concentration of unbound bile acid in the resin phase, with increasing Ceq

$[Cl^-]_s$-$((BA + R'COO^-_r)/V_r)$ (10^6 M)	$[R'COO^-]_r$ (10^2 M)	Ceq (mg/dL)
64	2.95	0.14
29	5.90	0.67
3.4	5.56	1.14
0.9	3.93	2.81

Figure 2.40

Variation of the concentration of bound bile acid, [BA], of bound hydroxyl group, [BOH], and of free fixed ionic group, [B^+], in the resin phase, with increasing Ceq

[BA] (M)	[BOH] (10^2 M)	[B^+] (M)	Ceq (mg/dL)
0.225	17	1.78	0.14
0.656	7.48	1.44	0.67
1.03	0.85	1.14	1.14
1.70	0.28	0.47	2.81

Figure 2.41

Variation of the pH in the resin phase with increasing Ceq

pH	Ceq (mg/dL)
8.18	0.14
8.15	0.67
8.83	1.14
8.82	2.81

Figure 2.42

Variation of the concentration of hydroxyl anions in the external solution, with increasing Ceq

$[OH^-]_s$ (10^9 M)	Ceq (mg/dL)
0.147	0.14
0.322	0.67
2.84	1.14
9.68	2.81

Figure 2.43

Variation of the formation constant of bound bile acid, K_f, in the resin phase, with increasing Ceq

K_f (M^{-1})	Ceq (mg/dL)
4.3	0.14
7.7	0.67
16	1.14
92	2.81

Figure 2.44

Variation of the basicity constant of the bound hydroxyl group, K_b, in the resin phase, with increasing Ceq

K_b (10^4 M^{-1})	Ceq (mg/dL)
0.16	0.14
0.27	0.67
9.1	1.14
11	2.81

CHAPTER 3

Figure 3.5

Glycocholic acid
Tris-HCl, 0.0026M

Ceq (mg/dL)	X (mol/eq pndnt)
a)\-NH_2	
0.47	0.0057
0.77	0.0054
0.80	0.0068
1.01	0.0055
1.04	0.0036
1.22	0.0121
1.62	0.0134
2.17	0.0050
3.35	0.0125
3.37	0.0232
3.54	0.0254
4.26	0.0233
4.73	0.0286
5.29	0.0176
5.54	0.0313
5.56	0.0322
7.48	0.0414
7.72	0.0299
8.24	0.0389
10.00	0.0414
10.06	0.0425
11.77	0.0399
13.87	0.0514
b)\-CO-C_6H_4-CH_2NH_2	
0.93	0.0102
1.44	0.0175
2.04	0.0187
2.90	0.0308
4.10	0.0301
4.46	0.0368
5.24	0.0471
6.59	0.0522
8.15	0.0607
8.33	0.0534
8.53	0.0702
9.11	0.0624
9.34	0.0555
9.49	0.0536

Figure 3.5 (cont'd)

9.86	0.0526
11.80	0.0762
11.88	0.0621
14.82	0.0864
18.06	0.1059

c)\-ala$_3$-CO-C_6H_4-CH_2NH_2

2.49	0.0053
5.20	0.0045
7.85	0.0046
10.47	0.0061
13.22	0.0030

Figure 3.6

Glycocholic acid
Tris-HCl, 0.0027M

Ceq (mg/dL) X (mol/eq pndnt)

a)\-NH_2

as Figure 3.5 a)

b)\-CO-CH_2-C_6H_4-NH_2

0.73	0.0025
1.37	0.0095
2.37	0.0103
3.23	0.0090
3.75	0.0081
4.06	0.0091
4.91	0.0105
5.76	0.0109
5.81	0.0076
6.45	0.0118
6.69	0.0225
7.26	0.0149
8.09	0.0140
9.10	0.0153
9.14	0.0152
9.38	0.01112

Figure 3.6 (cont'd)

c)\-ala$_3$-CO-CH_2-C_6H_4-NH_2

2.53	0.0049
5.21	0.0030
10.52	0.0017
13.15	0.00665

d)\-CO-C_6H_4-CH_2-NH_2

as Figure 3.5 b)

Figure 3.7

Glycocholic acid
Tris-HCl, 0.0025M

Ceq (mg/dL)	X (mol/eq pndnt)	Ceq	X
a) \\-CO-C_6H_4-CH_2NH_2		b) \\-CO-CH_2-C_6H_4-CH_2NH_2	
0.65	0.0058	0.72	0.0105
0.69	0.0053	1.14	0.0284
1.46	0.0103	1.59	0.0473
2.29	0.0151	2.36	0.0572
3.12	0.0218	2.37	0.0448
3.74	0.0242	3.04	0.0761
4.03	0.0262	3.36	0.0693
5.36	0.0336	4.21	0.0836
6.19	0.0365	4.81	0.0989
7.20	0.0334	4.92	0.0932
8.38	0.0531		
8.77	0.0554		
8.85	0.0525		
11.02	0.0594		
13.63	0.0680		
14.26	0.0671		

Figure 3.8

Glycocholic acid
Tris- HCl, 0.0025M

a)\-NH_2

as Figure 3.5 a)

b)\-$N(CH_3)_3^+ I^-$

Ceq (mg/dL)	X (mol/eq pndnt)
1.04	0.0090
1.52	0.0181
2.43	0.0306
3.80	0.0400
4.22	0.0382
5.37	0.0321
7.02	0.0508
8.88	0.0595
10.16	0.0718
13.37	0.0605
15.94	0.0753
17.97	0.0768

Figure 3.9

Glycocholic acid
Tris-HCl, 0.0026M

a)\-$CO\text{-}CH_2\text{-}C_6H_4\text{-}NH_2$

as Figure 3.6 b)

b)\-$CO\text{-}CH_2\text{-}C_6H_4\text{-}N(CH_3)_3^+ I^-$

Ceq (mg/dL)	X (mol/eq pndnt)
1.25	0.0112
2.55	0.0319
3.90	0.0324
5.25	0.0379
6.77	0.0593
7.56	0.0504
9.35	0.0663
10.47	0.0726
12.31	0.0517
12.87	0.0906

Figure 3.10

Glycocholic acid
Tris-HCl, 0.0028M

a)\-ala_3-CO-C_6H_4-CH_2-NH_2

as Figure 3.5 c)

b)\-ala_3-CO-C_6H_4-CH_2-$N(CH_3)_3^+$ I^-

Ceq (mg/dL)	X (mol/eq pndnt)
0.94	0.000846
1.57	0.0124
2.00	0.0218
3.31	0.0172
3.72	0.0366
4.64	0.0403
5.67	0.0351
6.67	0.0412
7.55	0.0436
8.17	0.0456

Figure 3.11

Glycocholic acid
Tris-HCl, 0.0028M

a)\-ala_3-CO-CH_2-C_6H_4-NH_2

as Figure 3.6 c)

b)\-ala_3-CO-CH_2-C_6H_4-$N(CH_3)_3^+$ I^-

Ceq (mg/dL)	X (mol/eq pndnt)
0.96	0.00458
2.01	0.00600
3.12	0.00610
5.15	0.0108
8.35	0.0112
9.46	0.00626
10.52	0.0132

Figure 3.12

Glycocholic acid
Tris-HCl, 0.0026M

a)\-CO-C_6H_4-CH_2-NH_2

as Figure 3.5 b)

b)\-CO-C_6H_4-CH_2-$N(CH_3)_3^+$ I^-

Ceq (mg/dL)	X (mol/eq pndnt)
0.70	0.00558
1.57	0.0102
2.15	0.0125
3.24	0.0250
3.81	0.0230
4.53	0.0241
5.54	0.0331
6.00	0.0350
7.22	0.0566
7.70	0.0462
8.46	0.0618
10.43	0.0623
11.42	0.0663
14.05	0.0964
16.11	0.0993
16.78	0.102

Figure 3.13

Glycocholic acid
Tris-HCl

a)Cholestyramine

as Figure 2.2 a)

b)\-CO-C_6H_4-CH_2-$N(CH_3)_3^+$ I^-

as Figure 3.12 b)

Figure 3.14 a

Glycocholic acid
Tris-HCl, 0.0025M

Ceq (mg/dL)	X (mg/g)
a)\-NH_2	
0.47	0.666
0.77	0.636
0.80	0.810
1.01	0.644
1.04	0.426
1.22	1.421
1.62	1.586
2.17	0.596
3.35	1.474
3.37	2.731
3.54	3.012
4.26	2.736
4.73	3.361
5.29	2.073
5.54	3.705
5.56	3.780
7.48	4.905
7.72	3.517
8.24	4.572
10.00	4.862
10.06	4.998
11.77	4.693
13.87	7.682
b)\\-$NH\text{-}CH_2CH_2\text{-}NH_2$	
0.90	2.320
1.74	3.562
2.71	7.163
3.83	9.913
4.88	9.716
5.29	9.539
5.71	8.773
5.78	9.130
5.83	9.575
6.03	10.327
6.04	10.078
6.78	11.966
7.97	14.096
8.17	16.397
8.21	13.985
9.69	18.642

Figure 3.14 b

Glycocholic acid
Tris-HCl, 0.0025M

X (mol/eq pndnt)
as Figure 3.5 a)
0.0057
0.0087
0.0176
0.0243
0.0239
0.0234
0.0216
0.0224
0.0235
0.0254
0.0248
0.0294
0.0346
0.0403
0.0343
0.0458

Figure 3.14a (cont'd)

c)\\-$N(CH_2CH_2NH_2)_2$

0.87	2.043
1.53	5.278
2.19	8.654
3.17	12.827
3.62	12.846
4.00	14.875
5.58	21.648
5.70	19.226
6.34	20.312
7.59	25.018

Figure 3.14b (cont'd)

0.003
0.0077
0.0126
0.0187
0.0188
0.0217
0.0316
0.0281
0.0297
0.0366

Figure 3.15

Glycocholic acid
Tris-HCl, 0.0025M

Ceq (mg/dL)	X (mol/eq pndnt)

M'-O-CO-C_6H_4-CH_2-$N(CH_3)_3^+$ I^-

0.68	0.0030
1.62	0.0039
2.63	0.0077
4.91	0.0071
5.82	0.0102
7.36	0.0096
9.82	0.0084
10.64	0.0115

Figure 3.16

\-CO-CH_2-C_6H_4-$N(CH_3)_3^+$ I^-
Glycocholic acid

Ceq (mg/dL)	X (mol/eq pndnt)
a) Tris-HCl, 0.0026M	
as Figure 3.9 b)	
b) Phosphate, 0.0025M	
0.74	0.00472
1.60	0.00578
2.09	0.0128
2.55	0.0184
5.04	0.0268
7.67	0.0369

Figure 3.17

Glycocholic acid
\-ala_3-CO-C_6H_4-$CH_2N(CH_3)_3^+$ I^-

Ceq (mg/dL)	X (mol/eq pndnt)
a)Tris-HCl, 0.0028M	
as Figure 3.10 b)	
b)Water	
0.41	0.0125
1.04	0.0169
2.17	0.0364
2.58	0.0451
3.97	0.0602
4.72	0.0554
5.67	0.0691

Figure 3.18

\-$N(CH_3)_3^+$ I^-
Tris-HCl, 0.0025M

Ceq	X
a)Glycocholic acid	
as Figure 3.8 b)	
b)Cholic acid	
0.64	0.0134
1.35	0.0191
1.85	0.0163
2.22	0.0279
3.09	0.0324
3.91	0.0390
4.50	0.0317
6.45	0.0505
7.21	0.0529
7.35	0.0574
8.04	0.0523
9.59	0.0750
9.60	0.0632
10.89	0.0622
12.33	0.0791